

FC
USGS
OFR
75-56

6000229

UNITED STATES
DEPARTMENT OF THE INTERIOR
GEOLOGICAL SURVEY

PRELIMINARY HYDROGEOLOGIC APPRAISAL
OF SELECTED HYDROTHERMAL SYSTEMS
IN NORTHERN AND CENTRAL NEVADA

By

F.H. Olmsted, P.A. Glancy, J.R. Harrill,
F.E. Rush and A.S. VanDenburgh

OPEN-FILE REPORT 75-56
Menlo Park, California

UNIVERSITY OF UTAH
RESEARCH INSTITUTE
EARTH SCIENCE LAB.

1975

CONTENTS

Page

Abstract-----	1
Introduction-----	2
Objectives of study-----	2
Acknowledgments-----	3
Numbering system for wells and springs-----	4
Regional setting-----	5
Regional geology and heat flow-----	5
Basin and Range faults and thermal springs-----	10
Regional hydrology-----	15
Selection of areas for study-----	22
Selection criteria-----	22
Areas selected-----	24
Methods of investigation-----	27
Collection of existing data-----	27
Hydrogeologic mapping-----	28
Test drilling-----	28
Borehole geophysical logging-----	32
Measurements of temperature and thermal gradient-----	37
Water-level measurements-----	40
Laboratory analyses of cores-----	43
Chemical analyses of water-----	44
Aerial photography-----	45
Conceptual models of hydrothermal systems-----	47
Model of system lacking a shallow-crustal heat source-----	49
Model of system having a shallow-crustal heat source-----	52
Discharge parts of the systems-----	53
Estimates of heat discharge-----	58
Heat discharge by springflow-----	58
Heat discharge by lateral ground-water movement-----	59
Heat discharge by steam-----	60
Heat discharge by evaporation from hot-water surfaces-----	61
Heat discharge by radiation-----	61
Heat discharge by conduction-----	62
Estimates of water discharge-----	70
Water-budget method-----	70
Heat-budget method-----	76
Carson Desert-----	77
Hydrogeologic setting-----	77
Shallow test holes-----	81
Experimental heat-flow test hole in Carson Sink-----	83
Thermal areas-----	86
Stillwater thermal area-----	87
Hydrogeologic setting-----	87
Previous information-----	88
Test drilling-----	88
Chemical character of ground water-----	89
Heat discharge-----	90
Thermal-water discharge-----	95
Hypothetical model of hydrothermal-discharge system-----	97

Soda Lakes-Upsal Hogback thermal area-----	99
Location-----	99
Previous development-----	99
Test drilling-----	99
Geology-----	103
Hydrology-----	104
Chemical character of ground water-----	109
Subsurface temperature distribution-----	111
Heat discharge-----	113
Water budget-----	115
Nature of hydrothermal system-----	117
Black Rock Desert-----	119
Hydrogeologic setting-----	119
Test holes-----	123
Heat flow outside thermal areas-----	125
Thermal areas-----	127
Gerlach thermal area-----	128
Geographic and geologic setting-----	128
Hydrologic setting-----	131
Principal hot-spring groups-----	135
Chemical character of springflow-----	138
Subsurface temperature distribution-----	138
Heat discharge-----	140
Water discharge-----	144
Inferred nature of hydrothermal system-----	147
Sulphur Hot Springs thermal area-----	149
Location-----	149
Test drilling-----	149
Geology-----	151
Hydrology-----	154
The hot springs-----	155
Chemical character of springflow-----	163
Subsurface temperature distribution-----	163
Heat discharge-----	169
Water discharge-----	173
Inferred nature of hydrothermal system-----	175
Leach Hot Springs thermal area-----	176
Location-----	176
Test drilling-----	176
Geology-----	179
Hydrology-----	184
The springs-----	187
Chemical character of springflow-----	193
Subsurface temperature distribution-----	193
Heat discharge-----	195
Water discharge-----	200
Hypothetical model of hydrothermal-discharge system-----	205
Brady's Hot Springs thermal area-----	206
Location and geologic setting-----	206
Test drilling-----	211
Hydrologic setting-----	211
Effects of initial development on hydrologic conditions-----	215

Chemical character of ground water-----	217
Subsurface temperature distribution-----	218
Heat discharge-----	218
Water discharge-----	226
Hypothetical model-----	226
Buffalo Valley Hot Springs thermal area-----	228
Location-----	228
Test drilling-----	228
Geology-----	228
Hydrology-----	234
The hot springs-----	234
Chemical character of springflow-----	236
Subsurface temperature distribution-----	238
Heat discharge-----	238
Water discharge-----	245
Inferred nature of hydrothermal system-----	248
Interpretation and evaluation of findings-----	249
Recapitulation of objectives-----	249
Delineation of areas of high heat flow-----	250
Nature of discharge parts of hydrothermal systems-----	253
Summary of heat-discharge estimates-----	254
Summary of water discharge estimates-----	256
Interpretation of estimates of regional conductive heat flow-----	258
Significance of estimates of heat and water discharge-----	259
References-----	261

ILLUSTRATIONS

Figure 1. Map of northern and central Nevada showing heat-flow measurements and exposures of Late Tertiary and Quaternary volcanic rocks-----	7
2. Map of northern and central Nevada showing Basin and Range faults, thermal springs, hot wells and fumaroles-----	12
3. Map of northern and central Nevada showing location of weather stations cited in text and average annual precipitation-----	16
4. Map of northern and central Nevada showing principal areas of ground-water recharge and discharge-----	20
5. Map of northern and central Nevada showing areas selected for study-----	25
6. Diagrammatic cross section of a hydrothermal system lacking a shallow-crustal heat source-----	50
7. Diagrammatic cross section of a hydrothermal system having a shallow-crustal heat source-----	50
8. Diagrammatic cross section of a hydrothermal system having a nonleaky discharge conduit-----	55
9. Diagrammatic cross section of a hydrothermal system having a leaky discharge conduit-----	55

Figure 10. Map of southern and central Carson Desert showing location of test holes and temperatures at a depth of 30 m-----	79
11. Temperature profile in test hole 22/31 - 10bca (USBR) Alkali Flat 1), 7 July 1973-----	85
12. Map of Stillwater thermal area showing temperature at a depth of 30 m-----	91
13. Idealized cross section of central part of Stillwater thermal area-----	92
14. Geologic map of Soda Lakes-Upsal Hogback thermal area showing location of test holes-----	100
15. Map of Soda Lake-Upsal Hogback thermal area showing configuration of confined potentiometric surface, 1973-74-----	106
16. Map of Soda Lakes-Upsal Hogback thermal area showing temperature at a depth of 30 m, December 1973-----	112
17. Map of southern Black Rock Desert showing location of test holes, wells, and thermal springs-----	124
18. Temperature profile in Cordero Black Rock 1 temperature test hole, 13 July 1973-----	126
19. Geologic map of Gerlach thermal area showing location of hot springs and test holes-----	130
20. Maps of Gerlach thermal area showing configuration of a. unconfined potentiometric surface, July 1973-----	132
b. confined potentiometric surface, July 1973-----	133
21. Map of Gerlach thermal area showing vertical potential gradients-----	134
22. Sketch map of Great Boiling Springs-----	136
23. Sketch map of Mud Springs-----	137
24. Map of Gerlach thermal area showing temperature at a depth of 30 m, October 1973-----	139
25. Geologic map of Sulphur Hot Springs thermal area showing location of test holes-----	152
26. Map of Sulphur Hot Springs thermal area showing configuration of water table, April 1973-----	156
27. Map of Sulphur Hot Springs thermal area showing distribution of vegetation types-----	157
28. Maps of Sulphur Hot Springs mound showing: a. configuration of water table-----	159
b. distribution of spring-pool overflow-----	160
c. discharge temperature at spring orifices-----	161
d. specific conductance of spring-water samples-----	162
29. Map of Sulphur Hot Springs thermal area showing temperature at depth of 30 m, Fall 1973-----	168
30. Geologic map of Leach Hot Springs thermal area showing location of test holes-----	180
31. Map of Leach Hot Springs thermal area showing configuration of water table, Fall 1973-----	186
32. Sketch of Leach Hot Springs-----	188

Figure 33.	Map of Leach Hot Springs thermal area showing temperature at a depth of 30 m, December 1973-----	194
34.	Map of Leach Hot Springs thermal area showing estimated near-surface conductive heat flow-----	198
35.	Map of Leach Hot Springs area showing distribution of phreatophytes-----	207
36.	Geologic map of Brady's Hot Springs thermal area showing location of test holes-----	208
37.	Reconnaissance surface hydrothermics of the Brady's Hot Springs thermal area-----	210
38.	Map of Brady's Hot Springs thermal area showing configuration of water table, Fall 1973-----	214
39.	Map of Brady's Hot Springs thermal area showing temperature at a depth of 30 m, 1973-----	219
40.	Map of Brady's Hot Springs thermal area showing estimated near-surface conductive heat flow-----	223
41.	Geologic map of Buffalo Valley Hot Springs thermal area showing location of test holes-----	230
42.	Map of Buffalo Valley Hot Springs thermal area showing configuration of water table, Fall 1973-----	235
43.	Sketch map of part of Buffalo Valley Hot Springs mound showing location of orifices sampled in August 1974----	237
44.	Map of Buffalo Valley Hot Springs thermal area showing temperatures at a depth of 30 m, Fall 1973-----	239
45.	Map of Buffalo Valley Hot Springs thermal area showing near-surface conductive heat flow-----	242
46.	Map of Buffalo Valley Hot Springs area showing distribution of phreatophytes-----	246

TABLES

Table 1.	Thermal springs, hot wells, and fumaroles for which geochemical data indicate a reservoir temperature of 150°C, or more or in which discharge temperature exceeds 65°C -----	14
2.	Thermal conductivity of saturated core samples from U.S. Geological Survey test holes-----	63
3.	Values of thermal conductivity assigned to lithologic categories classified in interpreted logs-----	64
4.	Data for U.S. Geological Survey test holes in Carson Desert-----	82
5.	Thermal conductivity of core samples from U.S. Bureau of Reclamation Alkali Flat 1 heat flow test hole-----	84
6.	Temperature data for Fallon, Gerlach, Winnemucca, Battle Mountain and Ruby Lake-----	93
7.	Estimate of conductive heat discharge from Stillwater hydrothermal system on the basis of method A described in test-----	94

Table 8.	Vertical potential gradients in Soda Lakes-Upsal Hogback area-----	107
9.	Chemical analyses of water samples from test holes in Soda Lakes-Upsal Hogback area-----	110
10.	Estimate of conductive heat discharge from Soda Lakes- Upsal Hogback hydrothermal system on the basis of method B described in text-----	114
11.	Ground-water budget for Soda Lakes-Upsal Hogback area-----	116
12.	Data for U.S. Geological Survey test holes in Black Rock Desert-----	124
13.	Estimate of conductive heat discharge from Gerlach hydrothermal system on the basis of method A described in text-----	142
14.	Estimate of conductive heat discharge from Gerlach hydrothermal system on the basis of method B described in text-----	142
15.	Estimate of ground-water evapotranspiration within the Gerlach thermal area-----	145
16.	Data for U.S. Geological Survey test holes in Sulphur Hot Springs thermal area-----	150
17.	Data for Sulphur Hot Springs, 1973-----	164
18.	Estimate of conductive heat discharge from Sulphur Hot Springs hydrothermal system on the basis of method A described in the text-----	170
19.	Data for U.S. Geological Survey test holes in the Leach Hot Springs thermal area-----	177
20.	Data for selected water wells near Leach Hot Springs-----	178
21.	Temperature, discharge, and chemical character of flow from individual orifices at Leach Hot Springs-----	190
22.	Total discharge of Leach Hot Springs orifices 1-29, 1947 and 1973-74-----	192
23.	Estimate of conductive heat discharge from Leach Hot Springs hydrothermal system on the basis of method A described in the text-----	197
24.	Estimate of conductive heat discharge from Leach Hot Springs hydrothermal system on the basis of method B described in the text-----	197
25.	Estimated average annual evapotranspiration of dominately thermal water at Leach Hot Springs for natural conditions-----	203
26.	Data for U.S. Geological Survey test holes in Brady's Hot Springs thermal area-----	212
27.	Estimate of conductive heat discharge from Brady's Hot Springs hydrothermal system on the basis of method A described in the test-----	221
28.	Estimate of conductive heat discharge from Brady's Hot Springs hydrothermal system on the basis of method B described in the text-----	224

Table 29	Data for U.S. Geological Survey test holes in Buffalo Valley Hot Springs thermal area-----	229
30.	Temperature, discharge, and chemical character of flow from individual orifices at Buffalo Valley Hot Springs 5 August 1974-----	237
31.	Estimate of conductive heat discharge from Buffalo Valley Hot Springs hydrothermal system on the basis of method A described in the test-----	241
32.	Estimate of conductive heat discharge from Buffalo Valley Hot Springs hydrothermal system on the basis of method B described in the text-----	243
33.	Estimated average annual evapotranspiration of dominantly thermal ground-water at Buffalo Valley Hot Springs-----	247
34.	Extent of thermal areas studied in northern and central Nevada-----	252
35.	Estimates of net heat discharge from hydrothermal systems studied in northern and central Nevada-----	255
36.	Estimates of water discharge from hydrothermal systems studied in northern and central Nevada-----	257

Conversion of units

Metric units are used throughout this report, although many of the measurements were made using English units. Thermal parameters are reported in the older, more familiar "working" units rather than in the now-standard SI (Standard International) units. The following table lists metric and equivalent English units, and "working units" and equivalent SI units for the thermal parameters

Multiply metric units	By	To obtain English units
<u>Length</u>		
millimetres (mm)	3.937×10^{-2}	inches (in)
centimetres (cm)	.3937	inches (in)
metres (m)	3.281	feet (ft)
kilometres (km)	3,281	feet (ft)
	.6214	miles (mi)
<u>Area</u>		
square metres (m ²)	10.76	square feet (ft ²)
hectares (ha)	2.471	acres (ac)
square kilometres (km ²) (10 ¹⁰ cm ²)	247.1	acres (ac)
	.3861	square miles (mi ²)
<u>Volume</u>		
cubic centimetres (cm ³)	6.10×10^{-2}	cubic inches (in ³)
litres (l)	.2642	gallons (gal)
cubic metres (m ³)	3.531×10^{-2}	cubic feet (ft ³)
	35.31	cubic feet (ft ³)
	8.107×10^{-4}	acre-feet (ac-ft)
<u>Flow</u>		
litres per second (l s ⁻¹)	15.85	gallons per minute (gal min ⁻¹)
	25.58	acre-feet per year (ac-ft yr ⁻¹)
<u>Mass</u>		
grams (g)	3.528×10^{-2}	ounces (oz)
kilograms (kg)	2.205	pounds (lb)

Temperature: degrees Celsius to degrees Fahrenheit °F = 9/5 °C + 32

THERMAL PARAMETERS

Multiply "working units" By To obtain SI units

Thermal Conductivity

millicalories per centimetre · second · degree Celsius (10^{-3} cal cm ⁻¹ s ⁻¹ °C ⁻¹)	0.4187	watts per metre · degree Kelvin (W m ⁻¹ °K ⁻¹)
--	--------	---

Thermal Diffusivity

square centimetres per second (cm ² s ⁻¹)	1.0 x 10 ⁻⁴	square meters per second (m ² s ⁻¹)
---	------------------------	---

Heat-flow (heat-flux density)

microcalories per square centimetre · second (10^{-6} cal cm ⁻² s ⁻¹) heat-flow unit (HFU)	4.187 x 10 ⁻²	watts per square metre (W m ⁻²)
---	--------------------------	--

Energy

calories (cal)	4.187	joules (J)
----------------	-------	------------

Heat Discharge

calories per second (cal s ⁻¹)	4.187	watts (W)
--	-------	-----------

PRELIMINARY HYDROGEOLOGIC APPRAISAL OF SELECTED HYDROTHERMAL SYSTEMS IN
NORTHERN AND CENTRAL NEVADA

By F.H. Olmsted, P.A. Glancy, J.R. Harrill, F.E. Rush, and A.S. Van Denburgh

ABSTRACT

Several hydrothermal systems in northern and central Nevada were explored in a hydrogeologic reconnaissance. The systems studied comprise those at Stillwater and Soda Lakes-Upsal Hogback in the Carson Desert, Gerlach, Fly Ranch-Granite Range, and Double Hot Springs in the Black Rock Desert, Brady's Hot Springs, Leach Hot Springs in Grass Valley, Buffalo Valley Hot Springs, and Sulphur Hot Springs in Ruby Valley.

The investigation focused on (1) delineating of areas of high heat flow associated with rising thermal ground water, (2) determining the nature of the discharge parts of the hydrothermal systems, (3) estimating heat discharge from the systems, (4) estimating water discharge from the systems, (5) obtaining rough estimates of conductive heat flow outside areas of hydrothermal discharge, and (6) evaluating several investigative techniques that would yield the required information quickly and at relatively low cost. The most useful techniques were shallow test drilling to obtain geologic, hydraulic, and thermal data and hydrogeologic mapping of the discharge areas.

The systems studied are in the north-central part of the Basin and Range province. Exposed volcanic rocks of latest Tertiary and Quaternary age are chiefly basaltic. Basaltic terranes are generally regarded as less favorable for geothermal resources than terranes that contain large volumes of young volcanic rocks of felsic to intermediate composition. Most of the known hydrothermal systems are associated with Basin and Range faults which are caused by crustal extension across the province. An area of high heat flow centered at Battle Mountain and possibly other areas of high heat flow may be related to crustal heat sources. However, some of the hydrothermal systems studied appear to be related to deep circulation of meteoric water in areas of "normal" regional heat flow rather than to shallow-crustal heat sources.

Discharge temperatures of thermal springs in the region range from slightly above mean annual air temperature (8° - 12° C at most places) to boiling or slightly hotter. Geochemical data indicate that, in the major systems, subsurface temperatures at which thermal waters equilibrate with reservoir rocks range from 150° to more than 200° C. These data also indicate that the major systems are of the hot-water type rather than the vapor-dominated type. Depths of thermal-water circulation probably range from 2 to 6 kilometres in areas of "normal" regional heat flow (~ 2 heat-flow units) and from 1 to 3 kilometres in areas of high heat flow (~ 3 -4 heat-flow units) such as near Battle Mountain.

Most of the heat is discharged from the hydrothermal systems studied by (1) conduction through near-surface materials heated as a consequence of thermal-water convection, (2) convection as springflow, and (3) convection

as steam discharge from spring pools, vents, fumaroles, and cracks. The rate of heat discharge by radiation from warm ground and by convection as lateral ground-water outflow is believed to be small in most systems and is not estimated.

Estimates of net heat discharge from the systems studied range from about 0.8×10^6 calories per second at Buffalo Valley Hot Springs to about 14×10^6 calories per second at Stillwater. These estimates represent the approximate magnitude of the excess heat discharge from the thermal areas that results from the upward convection of hot water from deep sources.

Water discharges from the hydrothermal systems by springflow, evapotranspiration, steam discharge, and lateral ground-water outflow. Estimated discharges range from about 0.2×10^6 cubic metres per year from the Buffalo Valley Hot Springs system to about 3×10^6 cubic metres per year from the Stillwater system.

In most of the hydrothermal systems studied and, by inference, in other similar systems in northern and central Nevada, the scale for potential commercial development for production of electricity or for other uses may be constrained by the natural discharge of heat and water. Greater rates of production of fluid generally would result in decreases in both temperature and pressure in the system. Exceptions to this limitation might occur at favorable sites within broad areas of high heat flow such as the Battle Mountain heat-flow high. At Buffalo Valley Hot Springs, for example, the natural discharge of heat and water is small, but, because of the high conductive heat flow and the low thermal conductivity of the valley fill, a thermal reservoir might lie within economic drilling depths.

INTRODUCTION

Objectives of Study

The abundance and wide distribution of hot springs in northern and central Nevada make this region a promising target for geothermal exploration. Sporadic test drilling has been done at several thermal areas during the past 10-15 years, but few advances have been made in the techniques of exploration or in the delineation of geothermal systems. The U.S. Geological Survey has selected northern and central Nevada as one of the first regions in which to make reconnaissance studies designed as first stages in the exploration and evaluation of geothermal resources on public lands in the western States.

The broad objectives of the reconnaissance studies are to develop and test geologic, geophysical, geochemical, and hydrologic techniques that will find geothermal systems, determine the nature and magnitude of the systems and their contained fluids, and determine the flux of heat and fluid through the systems. The ultimate goal is to formulate conceptual and mathematical models that will describe the system dynamics, both before and after development.

Many kinds of data are required for the formulation of the models. These kinds of data may be grouped into three principal categories: (1) reservoir parameters; (2) fluid and temperature parameters; and (3) system dynamics.

Reservoir parameters include the three-dimensional distribution of flow boundaries, effective porosity, intrinsic permeability, specific storage, specific heat, thermal conductivity, and rock chemical and mineralogical composition. Some of these parameters may be inferred from surface geologic and geophysical evidence, but useful quantitative data generally must be obtained by costly deep drilling into the geothermal reservoir.

Fluid and temperature parameters include the three-dimensional distribution of temperature, fluid pressure, and fluid quality, both chemical and physical. As with the reservoir parameters, drilling of numerous wells into the reservoir is required for the acquisition of useful fluid and temperature data.

System dynamics concerns the input to, movement through, and discharge from, the system of heat and fluid. The last part of the cycle, the discharge, is the part most easily studied in the early stages of a hydrologic reconnaissance. Moreover, in the types of systems inferred from preliminary geologic studies of northern and central Nevada by Hose and Taylor (1974), the natural rates of discharge of both heat and fluid may place severe constraints on the scale of economic development.

Accordingly, this study was designed to (1) delineate areas of high heat flow associated with rising thermal ground water, (2) determine the nature of the discharge from the hydrothermal systems, (4) estimate thermal-water discharge from the hydrothermal systems, and (5) obtain rough estimates of conductive heat flow outside areas of hydrothermal discharge, and (6) evaluate several investigative techniques that would yield the required information quickly and at relatively low cost.

Parallel investigations of northern and central Nevada by the U.S. Geological Survey are those of the geology (Hose and Taylor, 1974), the geochemistry of the principal hot springs (Mariner and others, 1974), the regional heat flow (Sass and others, 1971), and the geophysical studies.

Acknowledgements

The writers express their appreciation to the private landowners who permitted access to their properties for purposes of this study. Organizations that furnished information include the Southern Pacific Co.; Cordero Mining Co.; the U.S. Bureau of Reclamation; Lawrence Berkeley Laboratory of the University of California, Berkeley; the city of Fallon; O'Neill-Oliphant; and Standard Oil Co. of California. The writers benefited from discussions with Donald E. White, Richard K. Hose, L.J. Patrick Muffler, John Sass, Manuel Nathenson, Robert Mariner, Alfred Clebsch, Jr., Lee C. Dutcher, G.F. Worts, Jr., and Michael L. Sorey of the U.S. Geological Survey, and Hibbard E. Richardson, Lyle Tomlin, John Gallagher and Robert Green of the U.S. Bureau of Reclamation. The Bureau of Reclamation also furnished assistance in the investigation of the Carson Desert area and in drilling of some of the test holes.

Numbering System for Wells and Springs

In this investigation wells and springs are assigned numbers according to the rectangular system of subdividing public lands, referred to the Mount Diablo baseline and meridian. The first two elements of the number, separated by a slash, are, respectively, the township (north) and range (east); the third element, separated from the second by a hyphen, indicates the section number; and the lowercase letters following the section number indicate the successive quadrant subdivisions of the section. The letters, a, b, c, and d designate, respectively, the northeast, northwest, southwest, and southeast quadrants. Where more than one well or spring is catalogued within the smallest designated quadrant, the last lowercase letter is followed by a numeral that designates the order in which the feature was catalogued during the investigation. For example, well number 32/23-14ccd 2 designates the second well recorded in the SE $\frac{1}{4}$ SW $\frac{1}{4}$ SW $\frac{1}{4}$ section 14, T. 32 N., R. 23 E., Mount Diablo baseline and meridian. In unsurveyed areas, a land net is projected from the nearest adjacent surveyed land corners, and location numbers of wells and springs are assigned accordingly.

In addition to the location number based on the public-land net, all these wells and many other wells are assigned chronological numbers within each area of study. The numbers are preceded by letters which indicate the agency (or company) that drilled the well, the area of study, and the method of drilling. Where more than one well was installed at a single site, the chronological number is followed by a capital letter which designates the order of installation. The letters USBR refer to the U. S. Bureau of Reclamation; USGS, to the U. S. Geological Survey. DH indicates a drill hole (usually hydraulic-rotary method); AH, an auger hole. For

example USGS BR AH-3B refers to the second augered well at the third site in the Black Rock Desert area (BR), by the U. S. Geological Survey. Area designations are as follows: BH, Brady's Hot Springs area; BR, Black Rock Desert area; BV, Buffalo Valley area; CD, Carson Desert area; GV, Grass Valley area; RV, Ruby Valley area.

REGIONAL SETTING

Regional Geology and Heat Flow

The following summary of the regional geology of northern and central Nevada is based in large part on a recent paper by Hose and Taylor (1974). Heat-flow data are chiefly from Sass and others (1971).

The area of study lies within the north-central part of the Basin and Range province. The province is characterized by elongate north-trending fault-block mountain ranges and intervening basins. Exposed rocks are exceedingly varied and range in age from Precambrian to Holocene. Major rock groups include Paleozoic and Mesozoic sedimentary and volcanic rocks; intrusive rocks, chiefly of Mesozoic age; Tertiary volcanic and sedimentary rocks; and late Tertiary and Quaternary sedimentary and minor volcanic rocks.

The Paleozoic and Mesozoic rocks consist of both miogeosynclinal and eugeosynclinal facies and include diverse types such as limestone, dolomite, shale, quartzite, graywacke, chert, evaporites, lavas, and their metamorphic correlatives. These rocks were intruded at different times, chiefly during the Mesozoic, by magmas that range in composition from granite to gabbro.

The Tertiary Period was marked by widespread volcanism, interspersed with the deposition of smaller amounts of nonmarine sediments. The volcanic rocks consist chiefly of lava flows and ash flows of felsic to intermediate composition which now comprise almost one-fourth of the outcrops of northern Nevada. The earliest eruptions began during the Oligocene, and the most intensive activity ended about 10 million years ago.

Minor volcanism in the province persisted into the Pleistocene. The late volcanic rocks consist chiefly of flows and cinder cones of basalt, which are widely scattered throughout northwestern Nevada (fig.1). Flows and pyroclastic rocks of intermediate composition are much less abundant than basalt, and silicic rocks younger than middle Tertiary are absent in most of the region. However, White (written commun., 1974) and Silberman (oral communication, 1974) report rhyolite domes of Pleistocene age (1.1, 1.2, and 3.0 m.y. old in the Steamboat Hills and west flank of the Virginia Range near Virginia City), and a dome on the east flank of the Virginia Range is 1.5 m.y. old.

Generally north-trending grabens, separated from the mountain blocks by Basin and Range high-angle normal faults, are filled with late Tertiary and Quaternary nonmarine sedimentary deposits. The thickness of the basin fill in most valleys is poorly known but probably exceeds 1 km at many places. In the northwestern part of the region, the upper part of the fill includes predominantly fine-grained strata of late Pleistocene Lake Lahontan.

Pre-Tertiary structural features are numerous and varied and include major thrust faults. On some of the thrust faults eugeosynclinal rocks moved many tens of kilometres relatively eastward over miogeosynclinal rocks. Movement on many of the faults has persisted to the present. Present topography began to be outlined during the early or middle Tertiary by Basin and Range faulting. Total throw on some of these high-angle normal faults may be more than 2 km. The Basin and Range structural features result from crustal extension, which Thompson and Burke (1973) have estimated amounts to a total of about 100 km across the province. As a consequence, the present crust is notably thinner than that in adjacent regions and may be underlain by a plastic substrate (Stewart, 1971).

Probably as a consequence of the relatively thin crust and a high-temperature upper mantle, the northern Basin and Range province is characterized by heat flows substantially higher than the average for continental areas (Sass and others, 1971). Data are not yet abundant and are mostly restricted to mountainous areas, commonly in mining districts. Therefore, generalizations should be made with caution and with the understanding that they may be modified when more data become available.

Most of the heat-flow values in the northern Basin and Range province range from about 1.5 to 2.5 HFU ($\text{cal cm}^{-2} \text{s}^{-1} \times 10^{-6}$) (See fig. 1.) Higher values have been measured at a few scattered test holes and a sizable area of uncertain extent, centered near Battle Mountain, has heat flow values that range from about 2.5 to 3.8 HFU. The localized highs may, in part at least, reflect upward-convecting thermal ground water, but the high heat flow in the Battle Mountain area of, at least several hundred square kilometres extent may be related to crustal heat sources (Sass and others, 1971, p. 6409).

However, significant magmatic sources of heat in the upper crust, such as characterize most of the known geothermal systems of the world, are not known to be present in most of northern and central Nevada. There are large volumes of silicic to intermediate volcanic rocks in the region, but most are more than 10 m.y. old and, according to calculations by A. H. Lachenbruch (oral commun., 1974), have long since cooled to temperatures characteristic of other rocks of the province. Younger volcanic rocks, of latest Tertiary and Quaternary age, are widely distributed throughout the western part of the province (fig. 1). In places, these rocks might be associated with shallow-crustal sources of heat. However, most of the exposures are basalt, which is generally believed to be derived from the upper mantle rather than from shallow-crustal magma chambers.

Basin and Range Faults and Thermal Springs

According to Hose and Taylor (1974), most, if not all, the hydrothermal systems of northern and central Nevada are probably related to deep circulation of meteoric water along Basin and Range faults rather than to shallow crustal sources of heat. Knowledge of the distribution of Basin and Range faults is therefore useful in prospecting for geothermal resources. The known distribution of the Basin and Range faults on which movement has occurred in Pleistocene or Holocene time, based on a compilation from county geologic maps by Hose and Taylor (1974), is shown on figure 2.

Figure 2 also shows the distribution of the major thermal springs in northern and central Nevada. Most thermal springs are either on or near Basin and Range faults, although the relation of some springs to faults is ambiguous. However, mapping of several hot spring areas during this study revealed that not all the Basin and Range faults are shown on the county geologic maps from which figure 2 was compiled. Most thermal springs not on exposed fault traces probably are nonetheless controlled by Basin and Range faults that are concealed by unaffected valley fills. Significantly, many faults have only nonthermal springs, or no springs at all.

Thermal springs may occur singly, in more or less equant clusters, in long, linear arrays, or in irregular groups. Single orifices within a hydrothermal-discharge area are uncommon; some spring areas contain dozens or even hundreds of separate orifices. Discharges from individual orifices range from a trickle to several tens of litres per second. Many thermal springs are depositing silica, calcium carbonate, or both; other spring areas contain only fossil spring deposits, which indicates a change with time of temperature, discharge rate, water chemistry, or a combination of these factors.

Discharge temperatures of thermal springs range from slightly above mean annual air temperature (8° - 12°C) to slightly above boiling temperature at atmospheric pressure (superheated). On figure 2, only those springs are shown for which geochemical data indicate a reservoir temperature of at least 150°C or in which the maximum temperature of the discharge is at least 65°C . Also shown are a few hot wells and fumaroles; all these features are listed in table 1.

Subsurface temperatures at which thermal waters are in equilibrium with reservoir rocks may be inferred from hydrochemical data. Silica concentration of the discharge water is a commonly used index of subsurface temperature; other geothermometers include the ratio of sodium to potassium (Na/K) and more complex ratios of sodium to potassium plus calcium to sodium ($\text{Na}/\text{K} + 1/3 \log \sqrt{\text{Ca}/\text{Na}}$; and $\text{Na}/\text{K} + 4/3 \log \sqrt{\text{Ca}/\text{Na}}$) (Fournier and Rowe, 1966; White, 1965; Ellis, 1970; Fournier and Truesdell, 1973; Fournier, White and Truesdell, 1974).

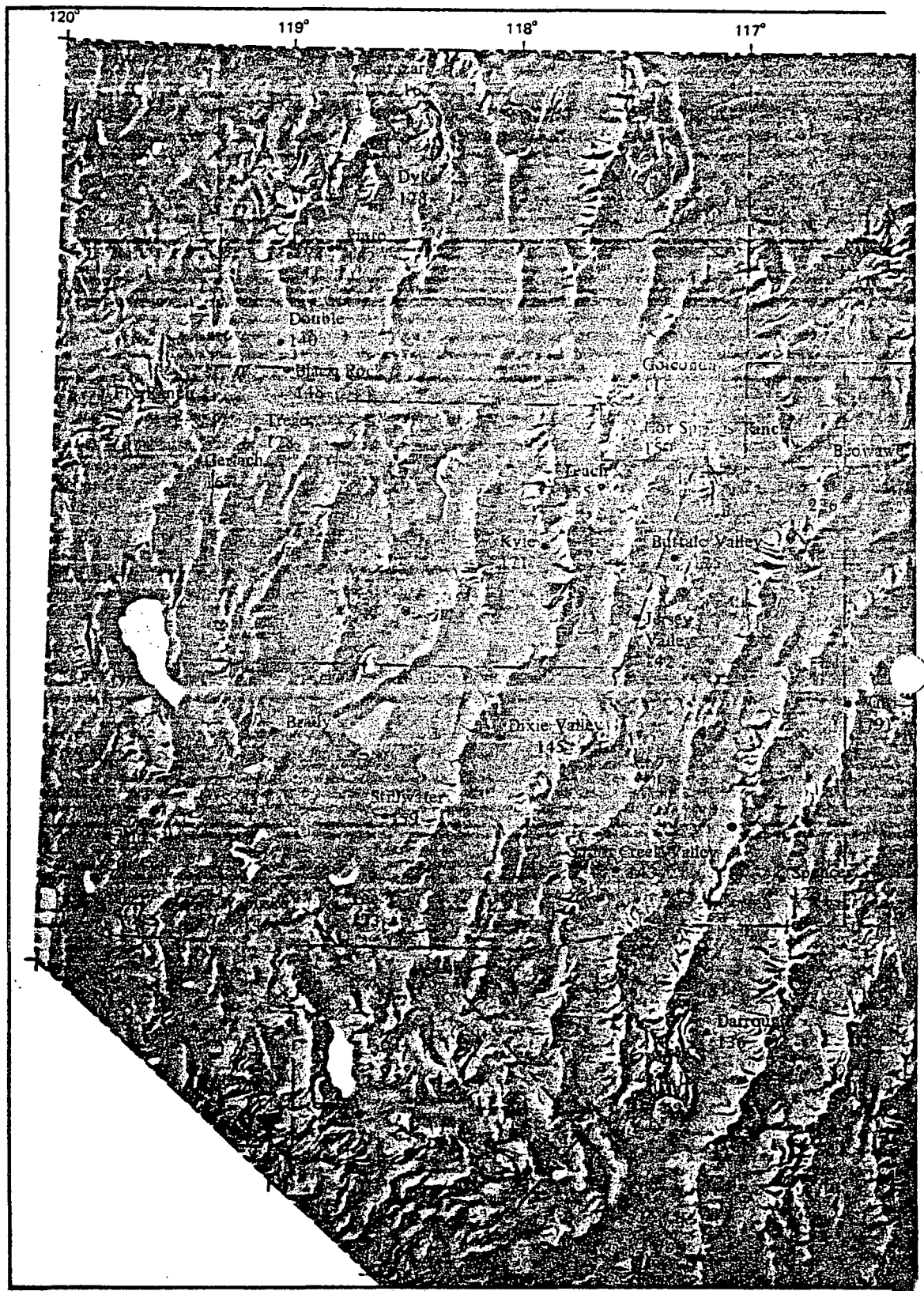
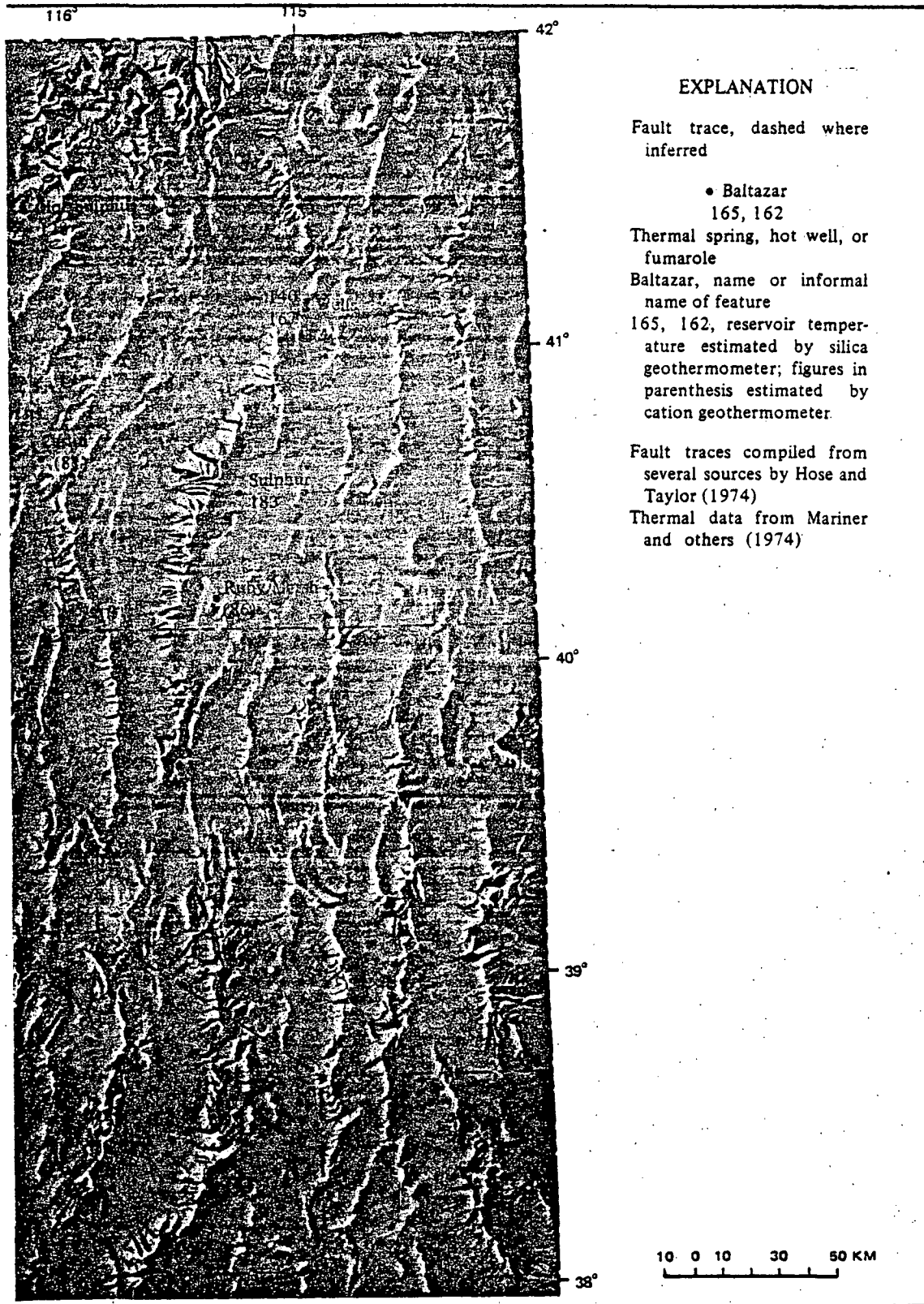


Figure 2.-- Map of northern and central Nevada showing Basin and Range faults, thermal springs, hot wells, and fumaroles.



EXPLANATION

Fault trace, dashed where inferred

• Baltazar

165, 162

Thermal spring, hot well, or fumarole

Baltazar, name or informal name of feature

165, 162, reservoir temperature estimated by silica geothermometer; figures in parenthesis estimated by cation geothermometer.

Fault traces compiled from several sources by Hose and Taylor (1974)

Thermal data from Mariner and others (1974)

10 0 10 30 50 KM

Table 1.—Fumaroles, hot wells, and fumaroles for which geochemical data indicate a reservoir temperature of 150°C or more or in which discharge temperature exceeds 95°C.

[Data from Mariner and others, 1974, except as footnoted]

Spring, well, or fumarole	Location	Discharge temperature (°C)	Estimated reservoir temperature (°C)			
			Silica	Na-K	Na-K-1/3 Ca	Na-K-A/3 Ca
Lee Hot Springs	16/21-24b (p)	98	173		162	
Dixie Valley Hot Springs	22/35-8a,d	72	145		144	
Flowing well in Stillwater	19/31-7c		159		140	
Fumarole at Brady's Hot Springs.	22/26-12	96	183 ^{1/}		170 ^{1/}	
Fumarole northeast of Soda Lake.	20/28-28c	96				
Sulphur Hot Springs	31/59-11b	93	183		181	
Hot Sulphur Spring	41/52- 8a	90	190		178	
Unnamed hot spring near Wells	38/62-20	50	121			
Unnamed hot spring near Wells	38/62-17a	61	167		184	
Unnamed hot spring near Carlin	33/52-33	79				81
Unnamed hot spring near Ruby Marsh.	27/58- 2b	65				86
Walti Hot Spring	24/48-33c	72				79
Beowawe Hot Springs	31/48- 8d	98	196		194	
Beowawe "steam" well	31/48-17b	96	226	238		
Unnamed hot spring at Hot Springs Ranch.	33/40- 5d	85	150		180	
Unnamed hot spring near Golconda.	36/40-29d	74	115			
Double Hot Springs	36/26- 4b	80	140		127	
West Pinto Hot Spring (well)	40/28-30a (p)	92	165	157		
East Pinto Hot Spring	40/28-29a (p)	93	162	145		
Dyke Hot Spring	43/30-25d	66	128		137	
Flowing well near Beltazor Hot Spring.	46/28-13b	90	162		148	
Beltazor Hot Springs	46/28-13b	80	165		152	
Spencer Hot Springs	17/45-24a	72	123			
Unnamed hot spring in Smith Creek Valley.	17/39-11	86	143		157	
Buffalo Valley Hot Springs	29/41-23d	79 ^{2/}	125			
Wabuska Hot Springs	15/25-16d	97	145		152	
Darrrough "steam" well	11/43-17b	94	135		131	
Darrrough Hot Springs	11/43-17b	95	136		127	
Unnamed hot spring in Jersey Valley.	27/40-29c	29	142		182	
Kyle Hot Springs	29/36- 1c	77	171		194	
Unnamed hot spring near Trego	34/25-35b (p)	86	128		120	
Unnamed hot spring near Black Rock.	35/26- 2b (p)	90	148		117	
Leach Hot Springs	32/38-36d	92	155		176	
Great Boiling Springs (Goriach)	32/33-15b	81	167	175		
"Geyser" at Fly Ranch	34/23- 2	80	125			
Steamboat Springs	18/20-33a	94	201		208	

1/ White, 1970, table 4. 2/ Temperature of hottest orifice, measured by F. H. Olmsted in August 1974.

All these geothermometers must be used with caution; sources of error and limitations of the methods are discussed by Fournier, White, and Truesdell (1974) and by Mariner and others (1974). Temperatures listed in table 1 are those judged by Mariner and others (1974), who did most of the sampling and all the analyses, as being most reliable.

Regional Hydrology

Virtually all ground water in northern and central Nevada is derived from precipitation within the region. Generally eastward-moving storms impinge on the mountain ranges and produce orographic precipitation--mountain summits may receive yearly totals of more than 500 mm, whereas valley floors, particularly the lower, western valleys, receive less than 150 mm. Annual precipitation shown on figure 3 is based on maps by Hardman (1936) and Hardman and Mason (1949). These workers had scanty data for the higher, mountainous areas; their estimates for these areas are based chiefly on indirect methods and are therefore less accurate than the estimates for the valleys and lowlands, which are based on weather-station records. Seasonal variations in precipitation are not large, except that less precipitation occurs in the summer than during the rest of the year. Most of the winter precipitation is snow.

In ground-water reconnaissance studies in Nevada by the U. S. Geological Survey, estimates of ground-water recharge from precipitation have been made on the basis of percentages of different ranges of precipitation derived empirically by Eakin and others (1951) from studies

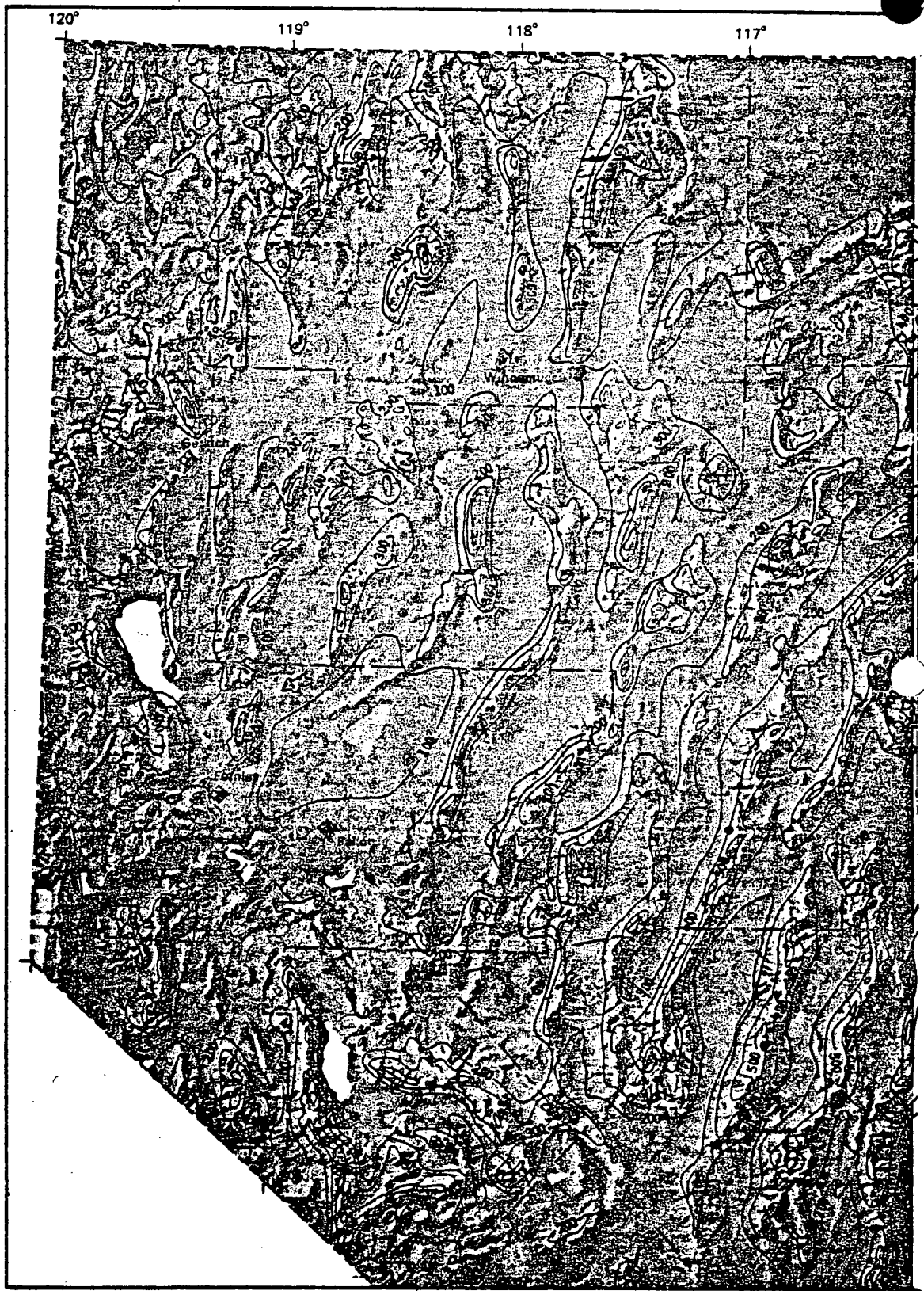
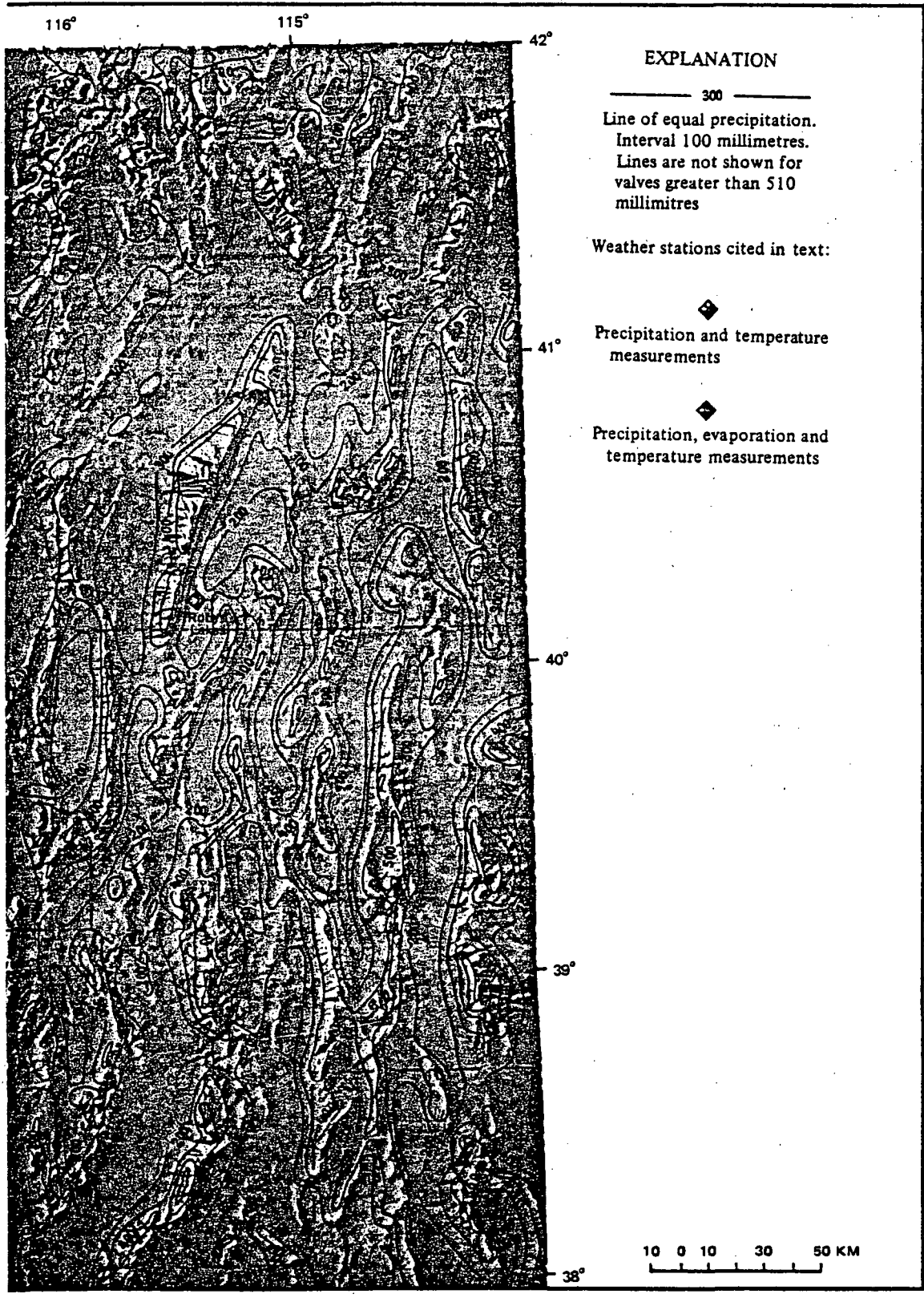


Figure 3.--Map of northern and central Nevada showing location of weather stations cited in text and average annual precipitation.



116°

115°

42°

EXPLANATION

300

Line of equal precipitation.
Interval 100 millimetres.
Lines are not shown for
values greater than 510
millimetres

Weather stations cited in text:



Precipitation and temperature
measurements



Precipitation, evaporation and
temperature measurements

41°

40°

39°

38°

10 0 10 30 50 KM

in eastern Nevada. These authors used the following figures:

Estimated annual precipitation		Estimated recharge ÷ precipitation
(mm)	(in)	(percent)
> 510	> 20	25
380-510	15-20	20
300-380	12-15	7
200-300	8-12	3
< 200	< 8	0

Estimates based on these figures are, of course, uncertain; recharge rates are probably highly variable from place to place.

Estimates of recharge to the shallow ground water system have been made for the areas of the present study, using the figures cited above, by Sinclair (1963), Harrill (1970), Eakin and Maxey (1951), and Cohen (1964). All these estimates, as well as estimates for the rest of the state, are summarized by Scott and others (1971). The amount of recharge water that reaches the deep, hydrothermal system which is of particular interest in the present study, is unknown.

Because of the high rates of potential evapotranspiration at low altitudes (8 - 10 times the annual precipitation), little or no water from precipitation infiltrates to the saturated zone in the valleys and low mountains, except where the water table is shallow (less than about 1 m depth) and the capillary fringe extends to the land surface. However, some of the runoff infiltrates to the saturated zone near the apexes of alluvial fans, where the streams debouch from the mountains onto the valley slopes, especially where the deposits are coarse grained and highly permeable. In addition, recharge takes place in the higher parts of the mountains, particularly through highly fractured or faulted zones. A mantle of coarse colluvium or talus also facilitates recharge in areas of relatively abundant precipitation.

In general, ground water moves in the direction of the potential gradient from areas of recharge to areas of discharge, usually in the lowest parts of the basins. The pattern of flow may be complex, and direction and rate of flow may vary markedly with depth as well as areally. Ground-water movement in the shallow zone, not far below the water table, commonly is related closely to the topography--unconfined potentiometric divides and topographic divides are coincident or nearly so. However, flow in deeper zones may diverge substantially from the flow in the shallow zone, especially where permeable rocks or permeable zones, such as faults, fractures, and solution channels extend to considerable depth in older rocks beneath unconsolidated valley fill. Examples of interbasin ground-water movement have been recorded in several regions in Nevada where mountains and interbasin divides are underlain by permeable rocks such as some of the Tertiary tuffs and pre-Tertiary miogeosynclinal carbonate rocks. (See Eakin, 1966; Hunt and Robinson, 1960; Winograd, 1962; Mifflin, 1968.) Dinwiddie and Schroder (1971) have documented subsurface flow in greatly different directions between depths above 300 m and depths of 1,500 - 2,100 m in Little Fish Lake, Monitor, Hot Creek, and Little Smoky Valleys in central Nevada.

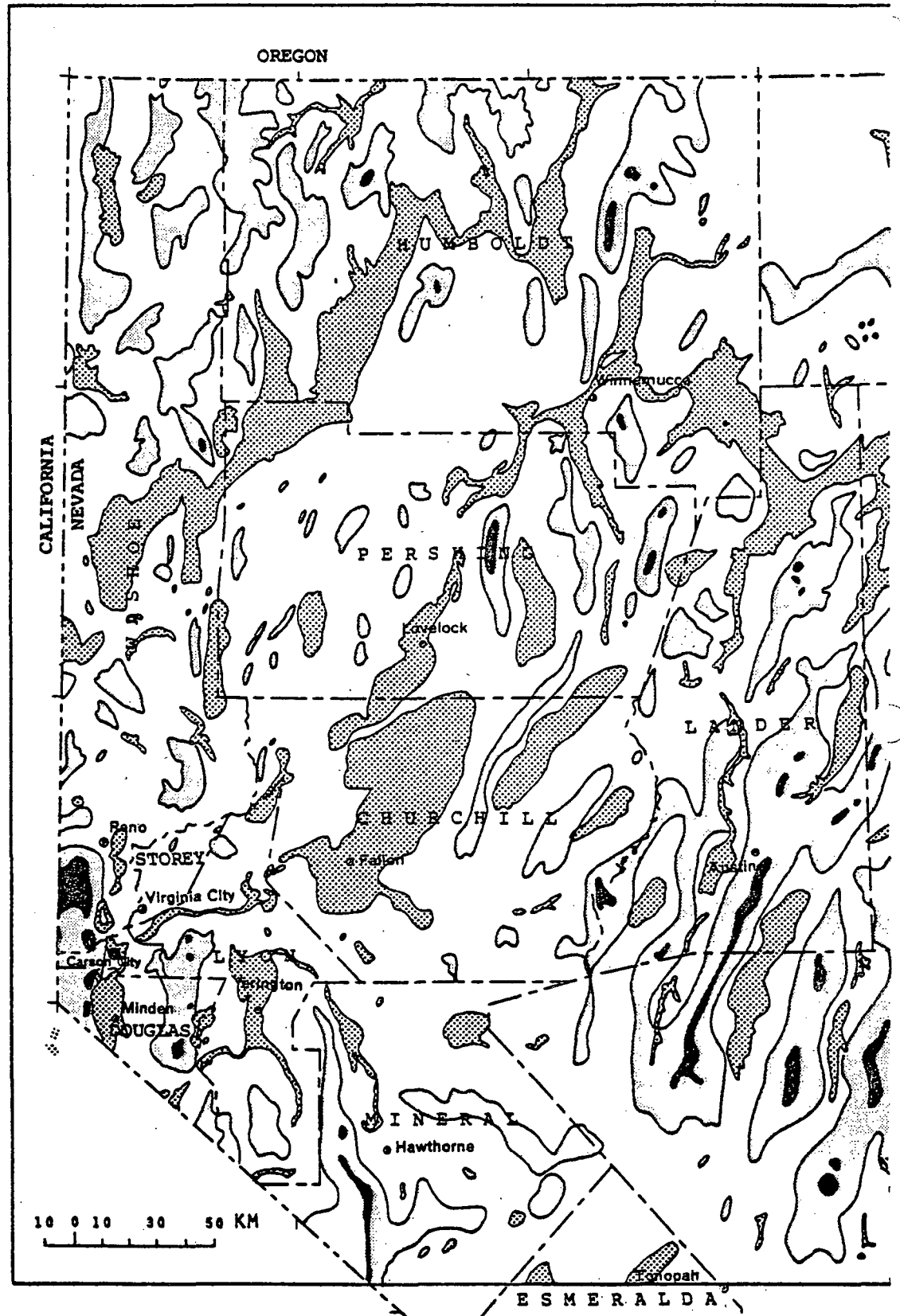


Figure 4.--Map of northern and central Nevada showing principal areas of ground-water recharge and discharge



EXPLANATION



Area of ground-water discharge. Includes area of phreatophytes and area of bare soil (playas) where ground water is discharged by direct evaporation. Depth to water is generally less than 15 m.



Area where most ground-water recharge is generated. Patterned area represents average annual precipitation greater than 305 mm and less than 510 mm. Solid area represents average annual precipitation greater than 510 mm.

Thermal ground water generally circulates at great depths and therefore probably diverges substantially from shallow ground water in directions and rates of movement, at least in places. Regional ground-water flow at depth also may significantly affect heat flow. Sass and others (1971) attribute abnormally low heat-flow values in a large region in south-central Nevada to transport of heat by water moving through carbonate rocks. Conversely, areas of abnormally high heat flow are at least in part related to upward convection of thermal ground water. The areas described later in this report belong to the latter category.

Ground-water generally discharges in the lower parts of the basins (fig. 4). Natural discharge takes place from springs and seeps, as transpiration by phreatophytes where the water table is within about 20 m of the land surface, as evaporation from the soil where the water table is within about 2 m of the land surface, and as inflow to perennial streams such as the Humboldt River. Artificial discharge consists of water pumped from wells, especially in irrigated areas. Some of the pumped water percolates back to the water table; the remainder is lost by evapotranspiration. None of the region drains to the ocean, so all water eventually is discharged by evapotranspiration.

SELECTION OF AREAS FOR STUDY

Selection Criteria

Several criteria were used in the preliminary selection of areas for study:

(1) The area contains hot springs having high rates of flow, high discharge temperature, and high source temperature.

(2) Subsurface data (test wells or geophysical data) suggest high temperature, moderate to high permeability of reservoir rocks, or both.

(3) The area constitutes a hydrologic system that has well-defined boundaries.

(4) The area is suitable for shallow test drilling.

(5) The area is reasonably accessible from paved roads or settlements.

(6) Relatively abundant hydrologic data are available.

(7) Relatively abundant geologic data are available.

As an overall guiding principle, an attempt was made to choose areas in which a maximum amount of information would be yielded at minimum cost and time. Another criterion was used by the U. S. Bureau of Reclamation, with whom the U. S. Geological Survey worked in the Carson Desert, one of the major areas of study: The area is near a present or planned electric-power transmission line, a market for electric power, or a market for desalted water.

As time went on, emphasis on the various criteria changed. Logistical problems (criteria 4 and 5) became important, and two promising areas that seemed to satisfy criteria 1 and 2 were omitted. Beowawe, a very promising system in the Whirlwind-Crescent Valley area, was omitted because part of the area was not suitable for shallow test drilling. Steamboat Springs, between Reno and Carson City, was omitted because the area already had been studied extensively by White (1968) and others.

Areas Selected

The location of the areas finally selected for study is shown on figure 5. The first two major areas were the southern Black Rock Desert, especially the Gerlach KGRA (Known Geothermal Resources Area) where hydrothermal discharge is indicated at the land surface by hot springs; and the Carson Desert, particularly the Stillwater-Soda Lake KGRA, where two known principal hydrothermal systems do not include hot springs but are indicated by wells and other indirect evidence. Initial fieldwork in the southern Black Rock Desert involved test drilling in the Gerlach, Fly Ranch-Granite Ranch, and Double Hot Springs areas, but virtually all later work was done in the Gerlach area. Likewise, emphasis in the later phases of the investigation of the Carson Desert was focused on the Soda Lakes-Upsal Hogback area--the western one of the two known principal hydrothermal systems.

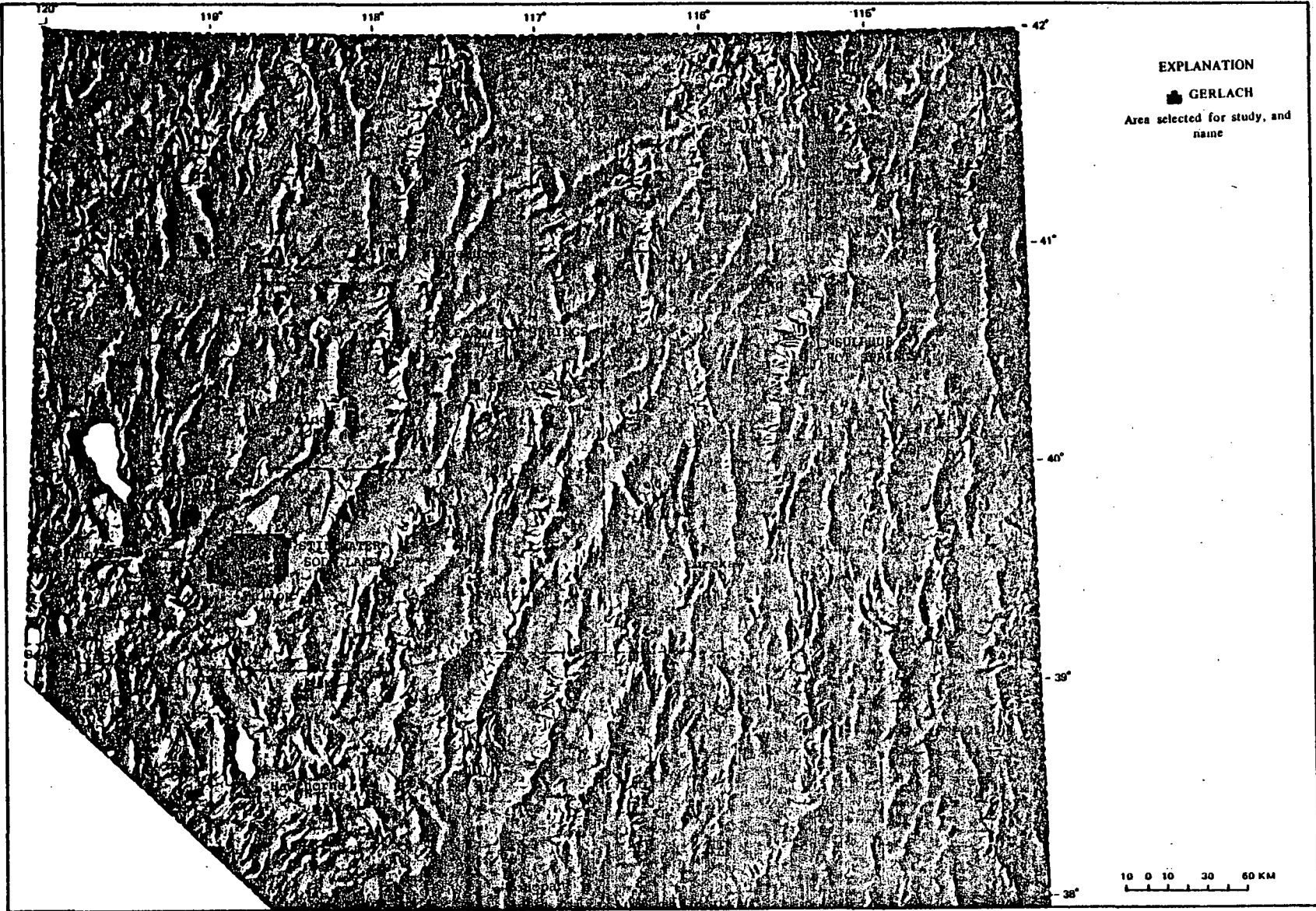


Figure 5.--Map of northern and central Nevada showing areas selected for study.

Four other areas were added after the investigation was underway. Brady's Hot Springs, Leach Hot Springs (Grass Valley), Buffalo Valley Hot Springs (Buffalo Valley), and Sulphur Hot Springs (Ruby Valley) (fig. 5). Test-well data were available for Brady's Hot Springs, and early production tests indicated high reservoir temperatures ($>200^{\circ}\text{C}$) in comparison with most other geothermal areas in northern and central Nevada. Leach Hot Springs, in Grass Valley, 44 km south of Winnemucca, was selected primarily because of high subsurface temperature indicated by several lines of evidence, accessibility, and suitability for shallow test drilling. Buffalo Valley Hot Springs, 46 km south of Battle Mountain, is near a chain of late Tertiary or Quaternary basaltic cinder cones and associated lava flows along the southeast margin of Buffalo Valley. This hydrothermal system is the only one of the present study in obvious proximity to relatively young volcanic rocks. Although the rate of water discharge is small and indicated reservoir temperature is only moderate, the system is within the broad area of high heat flow centered at Battle Mountain. Other factors favorable for the selection of Buffalo Valley Hot Springs included easy accessibility, moderate suitability for shallow test drilling, and concurrent geophysical investigations by Lawrence Berkeley Laboratory. Finally, Sulphur Hot Springs, in northern Ruby Valley, 91 km by road southeast of Elko, was selected because of high indicated reservoir temperature, accessibility, and suitability for shallow test drilling.

METHODS OF INVESTIGATION

In this study, the primary emphasis was on the development and evaluation of various reconnaissance methods of studying hydrothermal systems of the types found in northern and central Nevada. The following sections summarize the activities in approximate chronological sequence. A possible sequence for an actual exploration program would be somewhat different, as will be explained later.

Collection of Existing Data

The first step in the present investigation, and the logical first step in most geothermal exploration programs, is to collect existing data. Public agencies and private companies were canvassed for reports and information on surface and subsurface geology, temperature and heat flow, surface or airborne geophysical surveys, seismic activity, borehole geophysics, geochemistry, meteorology, botany, hydraulics, and water budgets. Available sources of this information for 19 hydrographic areas or groups of areas in northern and central Nevada are presented by Olmsted and others (1973). The 19 areas include all the hydrothermal systems described in the present report.

Hydrogeologic Mapping

Several kinds of maps were made of hydrothermal discharge areas and surrounding lands at a scale of 1:24,000 or larger, and measurements were made of the discharge, temperature, and specific conductance of hot springs. Mapping included geology, especially of structural features and rock types related to hydrothermal activity; vegetation, with emphasis on classification and description of phreatophytes; soils; and detailed mapping of spring orifices. The chief purposes of the geologic mapping were to determine whether volcanic rocks young enough to be possible sources of heat were present, to assist in delineation of the hydrothermal-discharge system, and to provide a basis for relating chemical character of the discharge to rock types with which the thermal water has been in contact. Vegetation and soils were mapped primarily to provide data needed for estimating hydrothermal discharge by evapotranspiration. In deriving the estimates, empirical annual rates of evapotranspiration were assigned to several categories of phreatophytic vegetation on the basis of earlier reconnaissance ground-water studies of hydrographic areas throughout Nevada by the U. S. Geological Survey.

Test Drilling

Thermal and hydraulic data from shallow (10 - 50 m) test holes were used to determine the extent of areas of hydrothermal discharge. In the Carson Desert, test-hole data were also used to prospect for possible near-surface thermal anomalies between two known anomalies and to estimate conductive heat flow at a site underlain by fine-grained deposits of low permeability.

Wherever possible, test holes were completed at depths of at least 30 m in order to avoid significant seasonal fluctuations in temperature. Unlike test holes used to determine crustal heat flow, however, test holes of depths sufficient to minimize the effects of heat transport by groundwater flow were not required. Accordingly, most holes were drilled or bored to depths within easy reach of light-weight drilling or augering equipment, generally 50 m or less.

The first U.S. Geological Survey test holes were bored with a truck mounted power auger. The holes were bored to depths of 10-45 m with solid-stem auger flights 1.5 m in length and about 10 cm in diameter. The U.S. Bureau of Reclamation drilled early temperature test holes in the Carson Desert with hydraulic-rotary drilling equipment. Four of the holes were drilled and completed to a depth of 50 m; an experimental heat-flow test hole in the Carson Sink was drilled and completed to 153.9 m.

In the first of the auger holes, galvanized-steel pipes of 3.8 cm nominal inside diameter, fitted at the bottom with well points or well screens, were installed to the bottom of the hole, or as close to the bottom as possible. At many places, soft, caving materials prevented penetration of the pipe and screen or point to the bottom, and a few holes had to be completed at depths of less than 10 m. Owing to the stability of the hydraulic-rotary drill holes maintained by the mud cake, it was possible to complete all the early U.S. Bureau of Reclamation test holes to the total drilled depth, using pipes that were capped at the bottom and filled with water. The pipes therefore were hydraulically isolated from the adjacent materials and provided only geologic and thermal information instead of the

hydrologic information also provided by the U. S. Geological Survey test holes. With the exception of the experimental heat-flow test hole in the Carson Sink, which was completed with a black-iron pipe of 5.1 cm (2 in) nominal inside diameter, all the U. S. Bureau of Reclamation test holes in the Carson Desert were completed with black-iron pipe of 3.2 cm (1¼ in) nominal inside diameter. The small diameter is an asset in determining precise thermal gradients because thermal convection within the pipe is minimized (Sammel, 1968). However, the pipes are not accessible to most borehole-geophysical-logging tools.

Drilling techniques improved with experience. As a result, most of the later test holes were completed to total drilled depths and better geologic information was obtained. Use of the hollowstem auger permitted installation of pipe to the bottom of the hole before the auger flights were removed. Hydraulic-rotary drilling was used more often and cores were obtained of representative geologic materials in the hydro-thermal-discharge areas.

In a test hole used for precise measurements of potentiometric head or thermal gradient, the annulus between the pipe and the walls of the hole is usually filled with cement or other impervious material. The cement prevents a hydraulic "short-circuit" of the natural system through the annulus. However, for several reasons, the test holes were not cemented. First, cementing each test hole would have increased cost and completion time substantially. The number of holes completed or the average depth might thereby have been reduced by as much as one-half. The hydraulic and thermal data obtained from an individual hole was not quite as precise as it could have been, however, data was obtained from many more holes from greater depths. Second, an envelope of cement around the pipe would have precluded obtaining several kinds of borehole geophysical logs that were

needed for a reliable interpretation of the materials penetrated by the test hole. Virtually all the radiation logs, which are the most severely affected by a cement-filled annulus, were made through the pipes rather than in the open holes. Finally, the exothermic effect of curing cement probably would have delayed thermal equilibration of the test hole with its surroundings for many days or weeks after completion. Because many sites were selected as drilling proceeded on the basis of temperatures and thermal gradients measured in recently completed test holes, time was not available for thermal equilibration of a cemented test hole.

As a compromise solution, the annulus outside the pipe in most test holes was backfilled with drill cuttings or surface materials at the site. Where the backfill was well sorted, not in lumps, and fairly dry, a reasonably effective seal was obtained. However, in some holes, especially those where the available materials were clayey, cohesive, or wet, the backfill tended to bridge in the annulus and to leave zones in which water moves upward or downward in response to vertical potential gradients. These zones are indicated by abnormally low thermal gradient (commonly straddled by intervals of high thermal gradient) and by abnormally low density and high water content on, respectively, the gamma-gamma and the neutron borehole geophysical logs.

Borehole Geophysical logging

After the test holes were drilled, various types of borehole geophysical logs were made, primarily in order to better define the physical characteristics of the materials penetrated. During the early stages of the investigation, natural-gamma logs (hereinafter referred to as gamma logs) and a few temperature logs were made in the cased holes, usually several days or weeks after the wells were completed. It soon became apparent, however, that gamma logs, by themselves, were not sufficient to define the lithologic characteristics and other important physical characteristics of the materials. Accordingly, other logging techniques were used, and, during the later stages of the logging program, single-point resistivity, spontaneous potential, caliper, gamma, gamma-gamma, neutron, and temperature logs all were routinely made of the test wells. Logging was done chiefly by R.A. McCullough of the U.S. Geological Survey, Denver, Colorado, using truck-mounted equipment; some logs were made in open holes with a portable "suitcase" logger. The following paragraphs briefly describe the logging techniques in the approximate sequence in which they were used in the last test holes drilled during the present investigation. It should be emphasized that none of the techniques, by itself, is as useful as an interpretive tool as several techniques used conjunctively.

Single-point resistivity logs.---Single-point resistivity logs were made in fluid-filled holes drilled by the mud-rotary method, commonly at the same time the spontaneous potential logs were made. Unlike multiple-electrode resistivity logs, single-electrode resistivity logs do not provide information about the chemical character of the formation fluid. They do, however, indicate strata of contrasting electrical properties. These logs are perhaps the most useful of all the logs in identifying the position of tops and bottoms of strata. The single-point resistivity log is regarded primarily as a stratigraphic or lithologic tool. In general, water-filled clay and silt strata are indicated by zones of low resistivity; sand and gravel are indicated by zones of high resistivity.

Spontaneous-potential logs.---Spontaneous-potential logs were made in conjunction with single-point resistivity logs in a few of the last test holes. These logs, which record the natural electric potentials between fluid in the borehole and adjacent earth materials, were used primarily as a supplement to the resistivity logs in defining lithologic boundaries. As with the resistivity log, an uncased fluid-filled hole is required.

Caliper logs.---Caliper logs record the average diameter of the hole, as measured by expandable arms or feelers mounted near the bottom of the logging tool. Like the single-point resistivity and spontaneous-potential logs, caliper logs were used only during the late stages of the drilling program. They are useful as a supplement to other logs in interpreting lithology and also in correcting some of the other logs for effects of variations in hole diameter. Although quantitative interpretations of the gamma-gamma and neutron logs were not attempted, the caliper would be required if such interpretations were made.

effect of
caliper on
gamma +
neutron logs.

Gamma logs.-- Gamma logs, record the natural gamma radiation emitted by the earth materials penetrated by the test hole. During the study, almost all the gamma logs were made in cased holes, but these logs can also be made in fluid- or air-filled holes. The effectiveness of the gamma log as a tool in lithologic interpretation depends on the differences in abundance of gamma-emitting minerals among the common earth materials. If the differences between sand and clay, for example, are consistent, these materials can be differentiated on the gamma logs. At most places, however, interpretations made from gamma logs alone are ambiguous; and other kinds of logs must be used in conjunction with the gamma log for reliable analysis. This proved to be true in most of the areas drilled. Clean, quartzose sands are relatively low in natural gamma radiation and clays tend to be relatively high. Unfortunately, many sands contain abundant potassium feldspar, micas, and other high-gamma-emitting minerals and commonly are higher in natural gamma emission than the interbedded clay and silt. At a few localities, the gamma logs were useful in helping to identify beds of silicic ash or tuff (very high gamma count) and basalt flows or sediments made up chiefly of basalt detritus (very low gamma count).

Gamma-gamma logs.--Gamma-gamma logs are made with a probe that contains a source of gamma radiation, separated by shielding from a detector that measures the backscattered, attenuated radiation from the borehole and surrounding materials. The intensity of the radiation measured by the detector is related to the bulk density of the materials, and the gamma-gamma log is sometimes referred to as a density log. In all the areas of the present study, gamma-gamma logs, which were made in the cased holes, were useful in identifying lithologic types and also in determining the top of the saturated zone (or, more correctly, the top of the saturated part of the capillary fringe). In the water-filled unconsolidated deposits penetrated by most of the test holes, sand and gravel are characterized by relatively high density, clay and silt by relatively low density, owing to the lower porosity of the coarse-grained materials in comparison with the fine-grained materials. In the unsaturated zone, the relation is generally reversed because of the higher water content of the fine-grained materials. Some difficulty is encountered in interpreting the gamma-gamma log where the diameter of the hole is variable, where the backfill in the annulus between the pipe and the wall of the hole is nonuniform, or where the backfill material differs greatly from the adjacent materials. In a few holes, it is possible to identify zones of incomplete backfill or enlarged (washed-out or caved) hole by intervals of abnormally low density indicated by the gamma-gamma log.

Neutron logs.-- Neutron logs indicate the water content (actually the hydrogen content) of the borehole environment. In the saturated zone, the water content is a function of the porosity of the material; clay and silt usually have higher porosity and higher water content than sand and gravel. In the unsaturated zone, the relation of water content to lithologic type is the same as it is in the saturated zone, so that the response of the neutron log to the different materials is not reversed above the water table as it is in the gamma-gamma log. The neutron logs proved very useful in supplementing the gamma-gamma and other logs in lithologic interpretations and, particularly, in identifying the water table or top of the capillary zone. Like the gamma-gamma log, the neutron log also indicates zones of washed-out hole or incomplete backfill in the annulus between pipe and hole wall.

Temperature logs.-- Although most of the temperature data used for interpretive purposes was obtained using equipment that does not record continuously, temperature logs were made in many test holes in order to supplement the other data. The primary value of the temperature log lies in its continuous record of change in temperature with depth. The other temperature measurements, discussed in the next section, are generally more accurate but are made only at discrete points and thus may fail to reveal thin zones of abnormal temperature or thermal gradient.

Measurements of Temperature and Thermal Gradient

Measurements of subsurface temperature and thermal gradient were made in order to identify possible thermal areas, to determine the extent of hydrothermal-discharge systems, and to obtain the data needed to estimate heat flow from the hydrothermal-discharge areas and from a few points outside the discharge areas. In addition, temperatures were measured of discharging springs and of a few flowing or pumping wells.

Maximum-recording mercury-in-glass thermometers 15 cm in length were used to measure temperature of discharge from most springs and wells, for early measurements of subsurface temperatures in test holes, and for measurements of subsurface temperatures higher than 100°C. Thermometers were calibrated with a laboratory standard mercury-glass thermometer, and most measurements are probably accurate to $\pm 0.5^{\circ}\text{C}$. Temperatures in test holes were measured by lowering a maximum thermometer attached by wire to the end of a steel tape to the desired depth, allowing time for equilibration (usually about 1 minute), then retrieving the thermometer, immersing it in a water bath kept at about 10° - 20°C, and reading it with hand lens to the nearest 0.2°C or 0.5°F (about 0.3°C).

Most of the measurements of temperature and thermal gradient in the test holes were made using a portable reel with 152 m of three-conductor cable, fitted at the bottom with a weighted probe containing a two-bead thermistor, and attached to a miniaturized wheatstone-bridge circuit having a digital readout of temperature. The range of the instrument is 0-100°C; the accuracy of the measurements within this range probably is well within $\pm 0.5^{\circ}\text{C}$. However, temperatures were read to 0.01°C, and the relative error in measurements at adjacent depths probably is no more than about 0.05°C. Temperatures and gradients were measured by

lowering the probe in the pipe in 0.6 or 1.2 m increments from a point just below the water level in the pipe to the bottom or to some other desired depth. The time required for stabilization or equilibration of the temperature reading was about 1 minute, except where the thermal gradient exceeded about 1°C m^{-1} , when as much as 3 minutes was required.

Temperatures and gradients in some test holes, including the experimental heat-flow test in the Carson Sink, were measured by Paul Twichell and John Sass of the U.S. Geological Survey, using both portable and truck-mounted equipment having thermistors as sensors. Temperatures measured with this equipment are more accurate than those measured with the digital thermometer and maximum thermometer, and readings were recorded to 0.001°C . This equipment is capable of measuring temperatures well above 100°C .

Temperatures at a depth of about 1 m were measured in the hottest part of the Soda Lake-Upsal Hogback thermal anomaly in the Carson Desert in order to better define the configuration of the anomaly. Measurements were made with a thermistor mounted at the bottom of an aluminum wand 1 m in length, which was inserted in holes made with either a hand driver or a soil auger. The thermistor probe was attached by way of a three-conductor cable to the digital thermometer used for the measurements in the test holes. Readings were made at regular time intervals for periods as much as 40 min and temperatures were extrapolated to equilibrium temperature by a method described by Parasnis (1971).

In order to avoid the effects of seasonal fluctuations in temperature, thermal gradients at depths of less than 10-15 m below land-surface datum, were not generally used in calculations of heat flow. Temperatures at depths of 30 m below the land surface and thermal gradients within the depth interval 15-45 m are the parameters most commonly used in the analysis of the temperature and heat-flow patterns of the hydrothermal-discharge areas. Temperatures used in the analysis were measured several weeks to several months after completion of most wells in order to minimize the thermal disequilibrium caused by drilling. However, during the later stages of the field studies, it was learned that temperatures measured only 2 or 3 weeks after drilling could be used without introducing significant error. Temperatures measured at depths less than 10-15 m did provide useful information, especially if measurements were repeated at different times of the year. For example, average thermal diffusivity of the near-surface materials can be computed, using the shallow temperature data to define the depth of the seasonal (winter-minimum or summer-maximum) temperature wave. The temperatures at a depth of only 1 m obviously have a sizable amplitude of seasonal fluctuation. Therefore, measurements made in a given area at this depth had to be made within as short a time as possible, and even so, the observed temperatures had to be adjusted to allow for changes during the survey.

Water-level Measurements

In addition to obtaining geologic and temperature information, the other principal objective of the test-drilling program was to determine potentiometric heads and directions of ground-water movement. Depths to water in the test holes were measured by the wetted-tape method and recorded to the nearest 0.003 m or, in a few less accurate measurements, to the nearest 0.03 m. At many sites, the water-bearing zone at the bottom of the hole is confined and an upward or downward potential gradient exists between that zone and the water table. Where time permitted and the water table was not too deep, companion test holes or piezometers were installed by hand or power auger to a depth slightly below the water table in order to define the difference in depth or altitude between the water table (unconfined potentiometric surface) and the artesian water level (confined potentiometric surface). The difference in water level, divided by the depth of the well point of the deeper well below the water table, equals the vertical potential gradient, which is customarily expressed as a dimensionless ratio. If the water table is higher than the artesian water level in the deeper hole, the gradient is downward (negative); if the reverse is true, the gradient is upward (positive). If the annulus between the pipe and the wall of the hole is not tightly sealed or is filled with material having higher vertical hydraulic conductivity than the adjacent natural materials, the system is short-circuited hydraulically and the measured vertical potential gradient is less than the true gradient. This situation probably exists at several of the test-hole sites, but the magnitude of the difference has not been determined.

For many sites where water-table test holes (shallow piezometers) were not installed, an attempt was made to determine the position of the water table from the neutron or gamma-gamma log of the test hole. Primary reliance was placed on the neutron log, which generally shows a large change in water content of the materials at the water table (actually the top of the saturated part of the capillary fringe). The gamma-gamma log usually indicates a similarly large change in density at about the same depth. However, in a few test holes, the depths indicated by the two logs are substantially different, and interpretation of the position of the water table is highly uncertain. Another source of uncertainty is the thick capillary zone that is present above the water table in fine-grained materials (clay and fine silt). Where such a thick capillary zone exists, the neutron and gamma-gamma logs probably indicate the top of the saturated part of this zone rather than the water table. For these reasons, water-table depths and altitudes interpreted from the neutron and gamma-gamma logs are much less precise and reliable than those measured with a tape in shallow piezometers. In most holes where the water table is in sand or other coarse material, the range of uncertainty may amount to only a few tenths of a metre, and where the unconfined and confined water levels differ by several metres, as they do in part of the Soda Lakes-Upsal Hogback area in the Carson Desert, a reasonably reliable estimate of the vertical potential gradient may be made. However, where the water table is in a fine-grained material or where head differences between confined and unconfined zones are small, usable data on vertical potential gradients must await the installation of shallow piezometers.

In many of the test holes, the well points or well screens become clogged with silt or clay during installation. As a result, several weeks or months were required for water levels in the pipes to equilibrate with the water levels in the aquifers opposite the points or screens in these test holes. The time required for equilibration can be shortened with development by air-lift pumping, surging, backflushing or other means.

Laboratory Analyses of Cores

During the last stage of test drilling, cores were taken of different materials to provide a representative range of geologic, hydrologic, and thermal properties of the rocks within the several areas of study. Most of the cores were obtained by driving a brass tube into previously undisturbed material below the bottom of the drill hole; the cores were contained in aluminum sleeves 15 cm in length and 6.4 cm in diameter inside the drive tube. Upon removal from the tube, the cores were capped top and bottom and sealed with water-proof, air-impermeable tape. Generally, two 15-cm-long cores were taken from each 30 cm cored interval. One of the cores was sent to the laboratory of the U.S. Geological Survey, Denver Colorado, for geologic, mineralogic, hydrologic, and thermal-conductivity analysis.

Analyses by the Denver laboratory included mineral identification and clay-mineral identification, both by X-ray diffraction method; carbonate content, by CO_2 absorption method; particle size; pore-size distribution; vertical hydraulic conductivity; and thermal conductivity. Bulk density and grain density also were determined.

Thermal conductivity was measured with a needle probe by both the Denver and Menlo Park laboratories.

The purposes of the core analyses were to assist in the definition of the subsurface geology, to determine physical properties which can be correlated with thermal conductivity so that the thermal-conductivity data can be extrapolated on the basis of the physical properties inferred from the borehole geophysical logs, to obtain thermal-conductivity data needed for heat-flow estimates, and to obtain hydraulic parameters required for estimates of ground-water-flow rates.

Chemical Analysis of Water

The major sampling and chemical analyses of the hot springs and wells were done by Mariner and others (1974). During the present study, supplemental samples from numerous spring orifices were collected and analyzed in order to determine gross variations in water chemistry in relation to flow rates and temperatures. In addition, samples were obtained by bailing from several test holes in the Soda Lake-Upsal Hogback area in the Carson Desert. The purpose of the sampling and analysis was to determine whether the thermal water could be distinguished from shallow nonthermal ground water on the basis of chemical differences, and if so, the amount and mechanism of mixing of the two waters. Specific conductance was measured for all the samples of spring and well waters; a few analyses included chloride and dissolved solids.

Aerial Photography

During the final stages of the field studies, aerial-photography was tested as a method of identifying and outlining thermal areas. The Soda Lakes-Upsal Hogback area and the Brady's Hot Springs area were selected for the tests because the most detailed information about temperatures at shallow depths and near-surface geologic conditions such as zone of hydrothermal alteration was available for those areas. Although the aerial photography was done at the end of the investigation, it would ordinarily be used during the initial stages of exploration as means of selecting target areas for further study and of selecting optimum sites for test drilling and geophysical exploration.

The first technique, tested in January 1974, was oblique aerial photography of snowmelt patterns. About a year earlier, a tract surrounding a fumarole and an abandoned shallow steam well between Soda Lakes and Upsal Hogback was bare of snow a day after a snowfall of 10 cm. The pictures, taken from a U.S. Navy helicopter at altitudes of about 100-200 m above ground level, clearly revealed this area and also two other nearby patches of bare ground. Photographs taken the same day at Brady's Hot Springs showed long narrow areas of snowmelt along the fault that controls the discharge of the hydrothermal system. Depth of snow outside the snowmelt areas was about 8 cm at Brady's Hot Springs and 5 cm in the Soda Lakes-Upsal Hogback area. In all the areas, the snowmelt was caused by very high rates of heat flow, probably at least 300 times the rates outside the thermal areas, according to estimates by D. E. White (written commun., 1974) for localities in Yellowstone National Park. It is concluded that, given the optimum amount of snowfall and favorable weather

conditions a day or so after the storm, snowmelt photography is a valuable and comparatively inexpensive method of defining areas of high heat flow. Similar success has been reported by Koenig and others (1972) at Coso Hot Springs in east-central California. White (1969) has used snowmelt at hydrothermal areas in Yellowstone National Park to derive quantitative estimates of heat flow; his methods could be combined with aerial photography to yield heat-flow estimates of sizable areas at low cost, provided factors such as topography, vegetation, and geology were favorable.

Vertical color aerial photographs of the same two areas were taken in February 1974. The photographs overlap about 60 percent along the flight paths so that stereoscopic viewing is possible; the scale is about 1:6,000. As expected from earlier visual aerial reconnaissance, areas of hydrothermal alteration are revealed clearly on the photographs, and detailed geologic mapping of the hydrothermal-discharge areas is greatly facilitated. An unexpected bonus, however, is the correlation of a subtle vegetation pattern and color with warm ground in the Soda Lakes-Upsal Hogback area. The warm anomalies are those determined by the very shallow (1 m depth) temperature survey and by the oblique snowmelt photography. Inspection of the vegetation on the ground soon after the color photographs were taken indicated that the anomalous pattern and color resulted from an unusually dense and luxuriant stand of Russian thistle (Salsòla Kàli L. var. tenufòlia Fausch).

CONCEPTUAL MODELS OF HYDROTHERMAL SYSTEMS

Although information is not yet sufficient to reach firm conclusions as to the nature of the known hydrothermal systems in northern and central Nevada, simplified conceptual models may be formulated on the basis of available geological, geophysical, and geochemical data. From evidence discussed briefly in the section, "Regional setting," it is inferred that most, if not all, the systems are related to the deep circulation of meteoric water in permeable zones associated with Basin and Range faults. Chemical characteristics of the thermal waters indicate that the systems are of the hot-water type rather than of the vapor-dominated type (White, Muffler, and Truesdell, 1971; Mariner and others, 1974, p. 27). Sources of heat for the deeply circulating water are believed to be a hot mantle beneath a relatively thin (~30 km) crust or, possibly in some places, local heat sources within the upper part of the crust.

On the basis of the nature of the heat source, two conceptual models of the hydrothermal systems in northern and central Nevada are postulated. Because of the severe limitations of the available information about the real systems, each model is highly simplified and generalized and is regarded mainly as a guide to methods of further study. The first model postulates a system in an area of "normal" regional heat flow--that is, an area in which the source of heat is a hot mantle beneath a relatively thin crust and a local heat source in the upper crust is absent. In the second model a local heat source in the upper crust is superimposed on the regional heat flow.

Each model has two variants which depend on the characteristics of the discharge of the system. Before discussing the features that distinguish the two conceptual models, the features common to both are described briefly in the following paragraphs.

In both models, the thermal water is assumed to be entirely or predominantly of meteoric origin. Runoff from mountainous areas, and in a few places, irrigation water, moves downward through permeable zones in consolidated rocks or through primary pore spaces in unconsolidated deposits. Indirect evidence, cited later, indicates that the thermal water may circulate to depths ranging from less than 1 km, to more than 5 km. At greater depths, the excess of lithostatic over hydrostatic pressure is sufficiently large to close all fractures or other openings, and no appreciable permeability or flow of water exists.

At some depth, or perhaps at several depths, water moves laterally beneath zones of less permeable rock and is heated by conductive heat flow through the underlying impermeable rocks. The nature of the permeable zone or zones through which the water moves laterally probably varies from place to place. In part the zone may be fault-controlled conduit system: either the same fault through which the water moved downward from the recharge area or a connected fault. The zone or zones also might consist of highly fractured competent rocks, sandy aquifers in clastic-rocks, or solution openings in soluble rocks such as limestone or dolomite.

The laterally moving heated water eventually encounters a conduit or conduit system, generally associated with a Basin and Range fault, through which it rises to a zone of discharge at or near the land surface.

The flow of water in these systems is controlled by the hydraulic gradient and the intrinsic permeability of the rocks. Generally, but not always, the hydraulic gradient has two components: 1) the gradient caused by the higher altitude of the recharge area in relation to the discharge area, and 2) the gradient caused by the greater density of the cold recharge water in relation to the hot discharge water. The first component is predominant in shallow, nonthermal ground-water systems, but the second component may be predominant in many hydrothermal systems. In fact, as White (1968, p. C11) has pointed out, the area of recharge to a hydrothermal system can have a lower altitude than the area of discharge. In this instance, the potential gradient is dominated by the second component .

Flow of water through the deep, hot parts of the hydrothermal systems is enhanced by the decrease in viscosity with increasing temperature and also by the increase in solubility of some common minerals and mineraloids with increasing temperature, especially those composed of silica. On the other hand, flow may decrease, owing to the precipitation of other minerals, such as calcite, and silica also may precipitate in the cooler, discharge parts of the system.

Model of System Lacking a Shallow-Crustal Heat Source

The first conceptual model postulates a hydrothermal system in an area of "normal" regional heat flow, about 1.5 - 2.5 HFU. Figure 6 is a diagrammatic cross section which shows the inferred flow of ground water through the system and its effect on the distribution of temperature with depth. As shown by the spacing of the isotherms in the

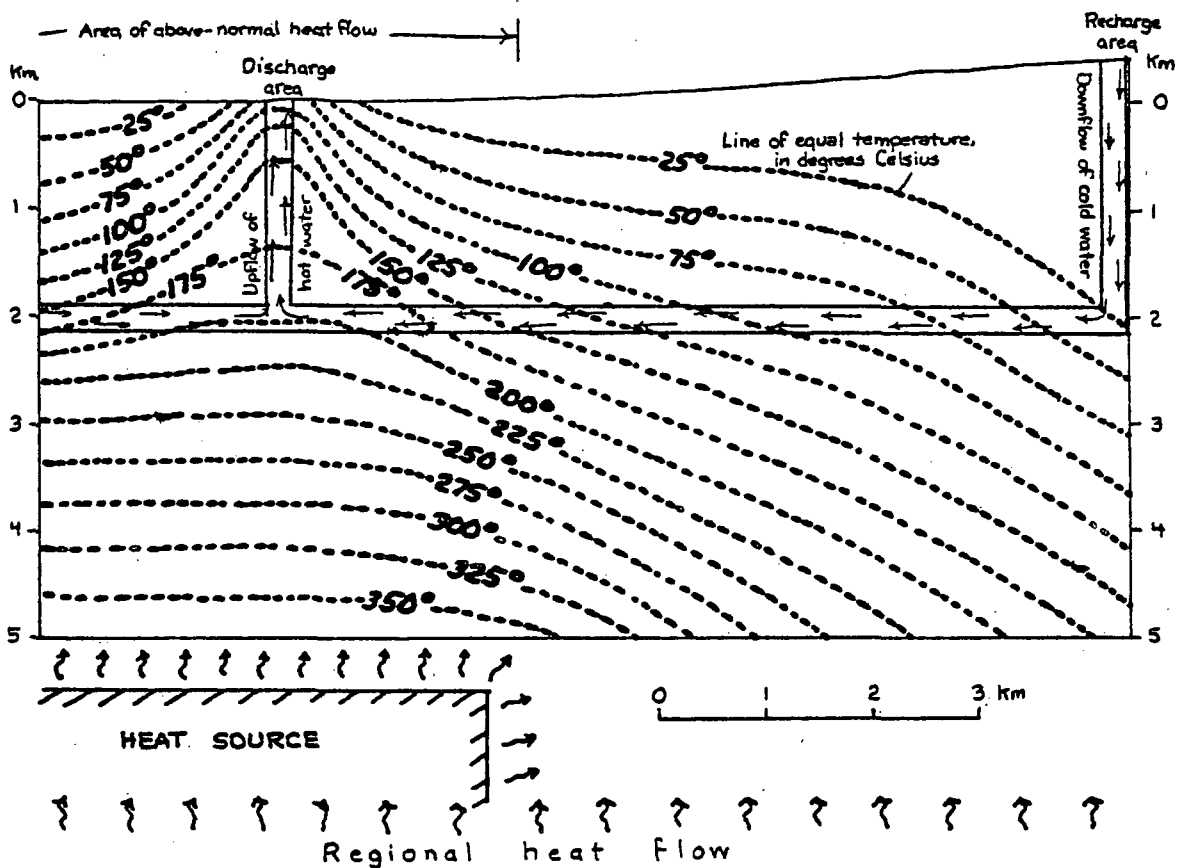
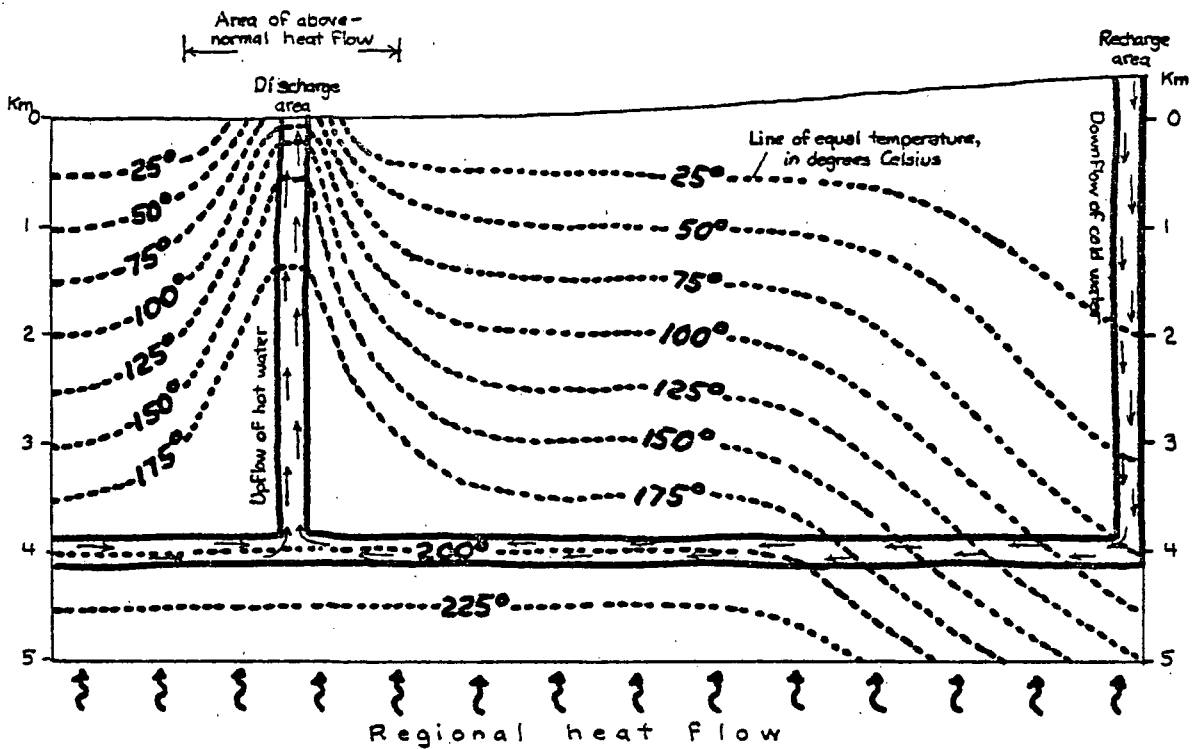


Figure 6.-- (top) Diagrammatic cross section of hydrothermal system lacking a shallow-crustal heat source.

Figure 7.-- (bottom) Diagrammatic cross section of hydrothermal system having a shallow-crustal heat source.

diagram, the near-surface thermal gradient and heat flow are less than "normal" (regional conductive values) in and near the area of downflowing cold recharge water and substantially above "normal" in and near the area of upflowing hot water. The thermal gradients in the downflowing and upflowing sections, indicated by the spacing of the isotherms, depend in part on the velocities and magnitudes of flow. Where the velocity is high the gradient is small, and the converse is true. Where the velocity of upflow is sufficiently high, little decrease in temperature occurs in the conduit until boiling begins at the hydrostatic depth at which the vapor pressure of the water equals the fluid pressure caused by the overlying column of water. From this depth to the land surface, the temperature decreases along the curve of boiling point versus hydrostatic depth.

Depths to which the water circulates are large because of the postulated absence of a local heat source in the upper crust. The depths may be estimated roughly on the basis of the regional heat flow, assumed thermal conductivities of the rocks, and the rock-water equilibrium temperatures indicated by the various chemical geothermometers. For example, if the regional heat flow is 2 HFU, the average thermal conductivity of the rock is $6.0 \times 10^{-3} \text{ cal cm}^{-1} \text{ s}^{-1} \text{ }^{\circ}\text{C}^{-1}$ (a reasonable value for granite), and the mean annual temperature at the land surface is 10°C , the water would have to circulate to a depth of 4.5 km in order to attain a temperature of 160°C and to a depth of 5.7 km to attain a temperature of 200°C . If the materials through which the water circulated were unconsolidated alluvial or lacustrine deposits having a low thermal conductivity, say $2.5 \times 10^{-3} \text{ cal cm}^{-1} \text{ s}^{-1} \text{ }^{\circ}\text{C}^{-1}$, the depths of circulation would be 1.9 km for 160°C and 2.4 km for 200°C . Actual depths of circulation in the systems where the regional heat flow is "normal" for the northern Basin and Range province probably range from about 2 to about 6 km.

At shallow depths (less than about 50 m), a system lacking a shallow-crustal heat source is characterized by a comparatively small area surrounding the points of water discharge (usually hot springs) where the heat flow is greatly above "normal." Outside this area, heat flow tends to approximate "normal" values for the region except near places where downflow of cold recharge water occurs, where heat flow is less than "normal." Extent of the area where heat flow greatly exceeds "normal" depends in part on the temperature and flow rate of the rising thermal water and in part on whether some of the rising water leaks from the conduit into shallow aquifers, as is explained in the section, "Discharge parts of the systems."

Model of System Having a Shallow-Crustal Heat Source

The second conceptual model differs from the first model in that a local heat source in the upper crust is superimposed on the regional heat flow postulated in the first model. The dimensions and nature of the local heat source are unspecified; the body of hot rock might be only a few square kilometres in extent, or it might underlie an area of several hundred square kilometres, like the Battle Mountain high described earlier. The general features of such a system are shown in a diagrammatic cross section on figure 7.

The important differences between the two models are the depths of water circulation and the extent of the area of above-"normal" heat flow. In the second model, the water does not have to circulate as deep to attain a given temperature as it does in the first model, owing to the greater heat flow resulting from the local heat source. For example, consider a system within the Battle Mountain high where the conductive heat flow might be 4 HFU instead of the "normal" regional value of 2 HFU. Depths of circulation would be only about one half as great as those cited for the first model, perhaps on the order of 1-3 km. The area of above-normal heat flow is considerably greater in the second model than in the first, because the area of high heat flow near the discharge outlets merges gradually with the surrounding area of above-normal heat flow which overlies the local heat source.

Discharge Parts of the Systems

In addition to the classification described above, which is based on the nature of the heat source, the hydrothermal systems may be grouped according to the nature of their discharge parts. Two models of the discharge systems are considered: (1) a system having a nonleaky discharge conduit, and (2) a system having a leaky discharge conduit.

The essential features of the nonleaky system are shown diagrammatically on figure 8. The vertical or nearly vertical conduit system is isolated hydraulically from the adjacent deposits or rocks by impermeable walls formed by minerals precipitated from the thermal fluid, or the conduit system may consist of fractures in impermeable rocks which are isolated from other fracture systems. All or nearly all the rising water therefore discharges at the land surface as springflow.

As shown on figure 8, heat is discharged laterally from the conduit system by conduction through the conduit walls. Relatively large thermal gradients are maintained through the conductive zone. The surrounding nonthermal ground water is heated, and the heat may be transported laterally by convection in the direction of the local hydraulic gradients. If the upper part of the conduit system is surrounded by unsaturated rocks, heat flow away from the system is almost entirely by conduction. The thermal area surrounding the conduit system, where conductive heat flow through near-surface materials is above "normal," is of the order of 0.5-5 km² on the basis of model studies by M. L. Sorey (oral commun., 1974) and data obtained during this study.

Systems in which leakage from the upper part of the conduits is zero probably are rare or absent. The model described above is idealized and is only approached by some real systems.

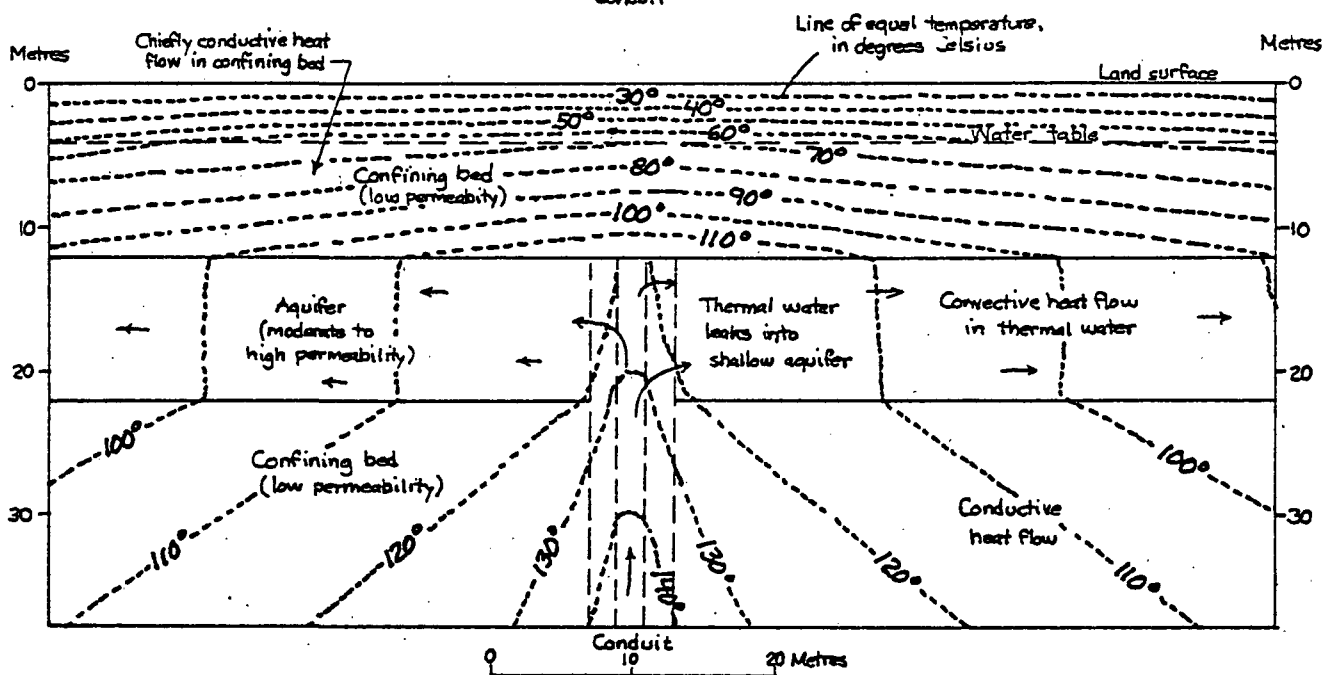
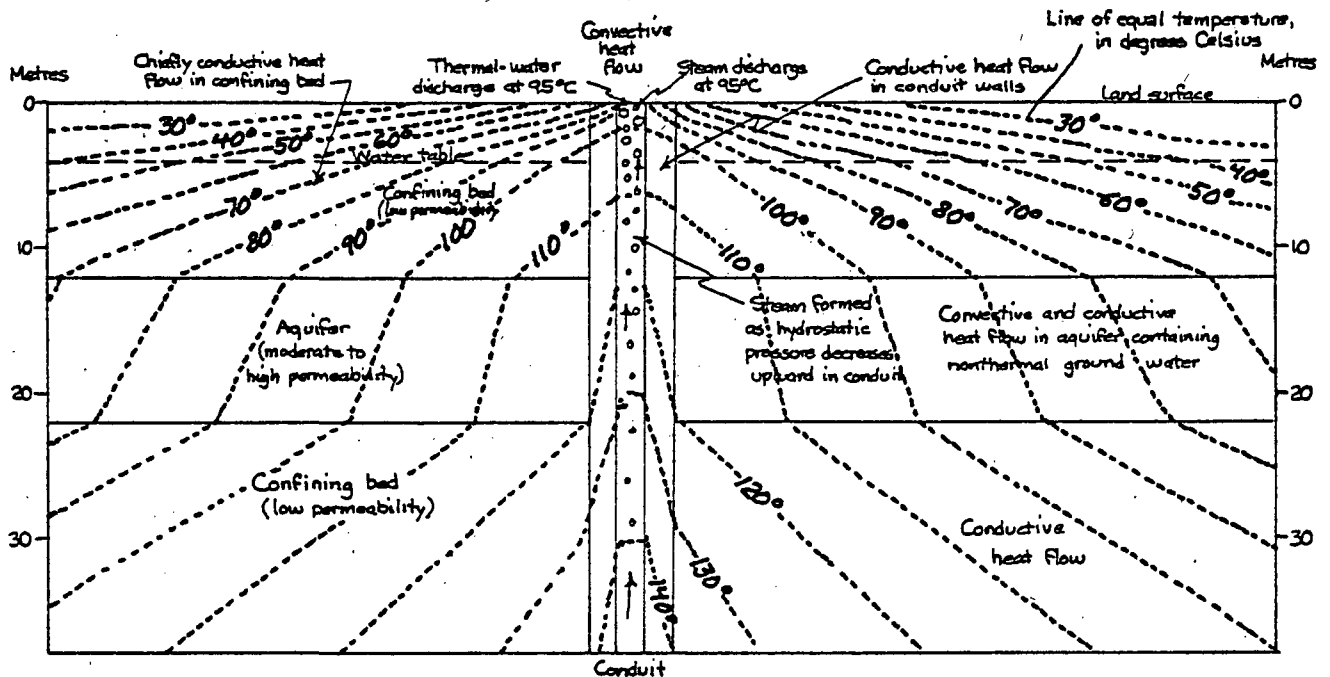


Figure 8.--(top) Diagrammatic cross section of a hydrothermal discharge system having a nonleaky discharge conduit.

Figure 9.--(bottom) Diagrammatic cross section of a hydrothermal discharge system having a leaky discharge conduit.

A special case of a system having a leaky discharge conduit is one where the leakage is into relatively deep aquifers, that is, aquifers at depths of hundreds of metres below the land surface. The near-surface temperature distribution associated with such a system in an area of "normal" regional heat flow may closely resemble that associated with a nonleaky discharge in an area having a local crustal heat source. That is, the near-surface temperature anomaly would be extensive, but temperatures, thermal gradients, and heat flow would not greatly exceed "normal" values.

Another special case is a system in which shallow, nonthermal water is not isolated hydraulically from the thermal water but mixes with it as the thermal water rises to discharge at spring outlets. Such a system is leaky in the sense that the conduit is not isolated hydraulically, but the near-surface distribution of temperature tends to resemble that of a system having a nonleaky discharge conduit. Identification of this type of system requires more abundant and detailed chemical and hydraulic data than were obtained during this study.

Figure 9 illustrates the essential features of a system having a leaky discharge conduit. In this type of system, some of the rising thermal water leaks laterally into aquifers. The amount of leakage may vary from a small proportion of the upward flow from the thermal reservoir to all the flow, so that no water discharges as liquid at the land surface. Where the leakage is small, little heat is transported laterally from the conduit system by convection, and the near-surface distribution of temperature is similar to that in the nonleaky-conduit system. Where the leakage is large, as shown on figure 9, the near-surface distribution of temperature is modified greatly because of lateral convective heat transport by the movement of thermal water through the aquifers intersected by the conduit system. As a result, the extent of the thermal area defined by above-"normal" temperatures and thermal gradients in the near-surface materials is much greater than that in the nonleaky system.

ESTIMATES OF HEAT DISCHARGE

Two of the primary objectives of this study are to estimate the discharge of heat and the discharge of water from the hydrothermal systems. The estimates are based on an assumption implicit in the conceptual models described in the preceding section: All hydrothermal discharge takes place within a thermal area delineated by temperatures and thermal gradients above normal at shallow depths. The thermal area may or may not contain hot springs or fumaroles in its central part.

There are several modes of heat discharge from a thermal area: (1) by hot-spring discharge; (2) by lateral movement of warm ground water beyond the margin of the thermal area; (3) by steam discharged from vents or fumaroles or by heated air that escapes from the soil surface; (4) by evaporation from hot-water surfaces; (5) by radiation to the atmosphere from warm soil and water surfaces; (6) by conduction through near-surface materials. Each of these modes is discussed briefly in the following sections.

Heat Discharge by Springflow

In some of the systems studied, a sizable fraction of the heat discharge is by convection as springflow. All this heat eventually is lost by other processes, such as radiation to the atmosphere from hot pool surfaces and by heat of vaporization (evaporation). However, the net quantity of heat discharged from a spring or spring system is most readily computed as the product of the volume rate or mass rate of springflow and the enthalpy or heat content of the water in the spring orifice in excess

of that remaining at ambient temperature. For example, consider the springflow at Sulphur Hot Springs in Ruby Valley, one of the systems studied:

Weighted-average temperature of springflow: 63°C. Enthalpy: 63 cal g⁻¹

Mean annual temperature at land surface: 8°C. Enthalpy: 8 cal g⁻¹

Net enthalpy of springflow: 55 cal g⁻¹

Springflow: 8.9 l s⁻¹ (8.9 x 10³ cm³s⁻¹)

Density of water at 63°C: 0.982 g cm⁻³

$$\begin{aligned} \text{Heat discharge} &= (55 \text{ cal g}^{-1})(0.982 \text{ g cm}^{-3})(8.9 \times 10^3 \text{ cm}^3\text{s}^{-1}) \\ &= 0.48 \times 10^6 \text{ cal s}^{-1} \end{aligned}$$

The actual rate of heat discharge fluctuates in response to fluctuations in springflow, temperature of discharge, and ambient air temperature; the type of computation above is useful mainly for deriving rough estimates of heat discharge for long periods, such as a year.

Heat Discharge by Lateral Ground-Water Movement

Convective discharge by lateral movement of warm ground water may be significant in hydrothermal systems having leaky discharge conduits or in systems having nonleaky conduits where shallow ground water of nonthermal origin is heated adjacent to the conduit. However, in this study, the margins of the thermal areas are defined so as to include only ground water significantly warmer than normal for the depth considered. Therefore, discharge of heat by lateral movement of ground water beyond the margins of the thermal area is generally small and is neglected.

Heat Discharge by Steam

Convective heat discharge by steam occurs where the temperature of the thermal water in the deep reservoir substantially exceeds boiling temperature at 1 atmosphere and where the upward flow in the discharge conduit is sufficiently rapid so that the rising water boils in the upper part of the conduit. As an example, consider once again the Sulphur Hot Springs system, where the reservoir temperature indicated by the silica-quartz geothermometer is 186°C (table 1) and the surface boiling temperature is 94°C. If all the heat loss from the reservoir to the surface were in the steam discharge (no conductive heat loss), the percentage of the total heat loss discharged as steam would be computed as follows:

Reservoir temperature:	186°C	Enthalpy of water:	188 cal g ⁻¹
Surface boiling temperature:	94°C	Enthalpy of water:	94 cal g ⁻¹
Ambient surface temperature:	8°C	Enthalpy of water:	8 cal g ⁻¹

$$\frac{(188 - 94) \text{ cal g}^{-1}}{(188 - 8) \text{ cal g}^{-1}} = 52 \text{ percent}$$

The percentage in the above example undoubtedly exceeds the actual percentage of heat discharged as steam at Sulphur Hot Springs and represents an upper limit probably not approached in most systems in northern and central Nevada. At Sulphur Hot Springs and the other spring areas investigated, most of the springs discharge water at less than boiling temperature. A substantial proportion of the heat loss between the deep reservoir and the discharge outlets probably results from conduction and mixing of thermal and nonthermal water rather than discharge of steam from boiling pools, vents, or fumaroles. In the systems containing boiling springs, the percentage of the convective heat discharged as steam is estimated on the basis of the computed equivalent volume of water discharged as steam, as discussed later in the section, "Estimates of water discharge," and the enthalpy of the steam.

Heat Discharge by Evaporation from Hot-Water Surfaces

The quantity of heat discharged by evaporation from spring pools and other hot-water surfaces is significant in many systems. However, most of this heat is included in that measured as heat discharge by springflow a small amount is not included, owing to the reduction in the measured springflow resulting from evaporation.

Heat Discharge by Radiation

Heat discharge by radiation to the atmosphere from warm soil and water surfaces may be significant near active outlets of fluid discharge, such as boiling springs or fumaroles, or at other places where ground temperatures are substantially higher than ambient air temperatures most of the time. Radiative heat discharge can be determined with an infrared radiation thermometer (Sekioka and Yuhara, 1974) or by snowfall calorimetry (White, 1969). In most of the systems studied, the areas of high radiative heat discharge are believed to be small, and the discharge by this means is not estimated.

Heat Discharge by Conduction

Conductive heat flow is indicated by linear thermal gradients in zones or beds of uniform thermal conductivity. Such gradients are characteristic of many depth intervals penetrated by most of the test holes bored or drilled during this investigation. The thermal gradients, together with the estimated thermal conductivities of the materials in the corresponding depth intervals, form the basis for estimates of conductive heat discharge from the thermal areas. Thermal gradients and thermal conductivities were measured by methods described in the section "Methods of investigation."

Results of all laboratory measurements of thermal conductivity of core samples are given in table 2. The cores obviously represent only a very small sample of the materials in which thermal gradients were measured. Fortunately, however, thermal conductivities of porous granular materials of the types penetrated by most of the test holes do not have nearly as wide a range as the hydraulic conductivities of the same materials. For this reason, the data from the cores can be used to infer thermal conductivities of materials having similar properties such as bulk density, porosity, and mineral composition. The errors that result from such an extrapolation are much less than those that would result from a similar extrapolation of hydraulic properties. Accordingly, the values of thermal conductivity listed in table 3 are assigned to various categories of water-saturated unconsolidated and semi-consolidated to consolidated clastic sediments. If a reasonably accurate description of the materials is made on the interpreted log, the error of most estimates of the thermal conductivity probably will be well within plus or minus 50 percent.

Table 2.--Thermal conductivity of saturated core samples from U. S. Geological Survey test holes.

[Measurements made with a needle probe by Robert Munroe, U.S. Geological Survey, Menlo Park, California]

Test hole	Depth of sample (m)	Material	Thermal conductivity (x 10 ⁻³ cal cm ⁻¹ s ⁻¹ °C ⁻¹)
BR DH-14	10.06-10.21	Lacustrine clay	1.86; 1.87
BR DH-15	14.63-14.78	Lacustrine sandy clay	2.05; 2.05; 2.03
BH DH-16	3.81-3.96	Alluvial gravel; silt and clay matrix.	2.44; 2.62
BH DH-17	8.53-8.66	Alluvial silty sand	2.83; 2.69
GV DH-8	28.10-28.25	Alluvial silty sand and gravel ^{1/} .	0.50
GV DH-11	37.19-37.34	Tertiary mudstone	4.86; 3.84; 4.12
BV DH-5	14.63-14.78	Lacustrine sand, silt, and clay.	2.93; 2.83
RV DH-8	2.29-2.44	Alluvial sandy clay	3.74; 3.94; 3.92
	3.66-3.81	Alluvial sand	3.45; 3.58; 3.34
BV DH-1	32.77-32.92	Vesicular basalt ^{2/}	3.54
CD STH-1	0.70-0.75	Sandy clay (hydro- thermally altered fluvial or eolian sand.	2.29
CD STH-42	0.60-0.65	Sand ^{1/}	0.50; 0.47

^{1/} Sample nearly dry

^{2/} Porosity = 10 percent

Table 3.--Values of thermal conductivity assigned to lithologic categories classified in interpreted logs.
 [All materials assumed to be saturated with water]

<u>Lithologic category</u>	<u>Thermal conductivity</u> (mcal cm ⁻¹ s ⁻¹ °C ⁻¹)
<u>Unconsolidated deposits</u>	
Gravel; coarse gravel; clean gravel; gravel and sand; sandy gravel.	5.0
Sand and gravel; gravelly sand	4.0
Sand and scattered gravel; coarse sand; sand; coarse sand with thin beds of clay and silt.	3.5
Sand and silt; silty sand; fine sand	3.0
Silt, sand, and clay; sandy clay; clay and sand; silt; clay and gravel; clay, sand, and gravel.	2.5
Clay; silty clay; clay and silt	2.0
<u>Semiconsolidated to consolidated deposits</u>	
Cemented gravel; conglomerate	6.0
Cemented sand; sandstone; sandstone and siltstone; siltstone and sandstone.	5.0
Claystone and siltstone; mudstone	4.5

Most thermal gradients used in computations of heat flow are measured or estimated for depth intervals that include more than one kind of material. Virtually all these intervals are in horizontally stratified materials, so that, with vertical (upward) heat flow, the situation is analogous to the flow of electric current through resistors in series. Therefore, the heat flow through a series of beds of different thermal conductivity is equal to the thermal gradient from top to bottom of the series of beds, multiplied by the harmonic mean of their thermal conductivities. The harmonic mean (k_m) for a sequence of n layers is computed as

$$k_m = \frac{\sum_{i=1}^n z_i}{\sum_{i=1}^n (z_i/k_i)}$$

where z_i = thickness of layer i and k_i = thermal conductivity of layer i . In application, the harmonic-mean thermal conductivity is computed from the lithologic log of the well, using the thermal-conductivity values given in table 3. On the basis of thermal gradients observed in test holes in several areas of study, thermal conductivities of the unsaturated materials above the water table are estimated to be 0.6 times the thermal conductivities of corresponding saturated materials listed in table 3. An exception is made for materials in the depth range 0-1 m, which are ordinarily drier and therefore poorer conductors of heat than the underlying unsaturated materials, owing to the removal of moisture by evapotranspiration. On the basis of scanty core data, values of thermal conductivity assigned to three general categories of material in the depth range 0-1 m are:

<u>Material</u>	<u>Thermal conductivity ($\times 10^{-3}$ cal cm^{-1} s^{-1} $^{\circ}\text{C}^{-1}$)</u>
Clay	1.0
Silt; sand and clay	.8
Silty sand; sand and silt	.7
Sand	.5

Temperatures 30 m below the land surface and thermal gradients in the test holes are tabulated for the measurements believed to be most reliable-- that is, those measurements unaffected or only slightly affected by thermal disequilibrium from drilling, seasonal temperature fluctuations, convection by upward or downward ground-water flow across bedding, or convection by upward or downward flow of water in the annulus between the pipe and the wall of the borehole. Heat discharge is then calculated by one or both of two methods, for convenience designated as methods A and B, which are described below.

Method A.--In method A, the simpler but generally less accurate procedure, the following assumptions are made:

- (1) All heat discharge from the area of the thermal anomaly is measured as conductive heat flow in the top 30 m of materials, except for heat discharged by springflow and steam discharge.
- (2) The thermal anomaly is delimited by the isotherm at 30 m depth for which heat flow computed by the method is approximately equal to the average for the region--generally the 15°C or 20°C isotherm and an estimated heat flow ranging from about 2 to 5 HFU.
- (3) The heat flow at any point is equal to the thermal gradient computed from the temperature difference between the 30 m isotherm and the land surface, multiplied by the harmonic mean of the thermal conductivities of horizontally stratified materials in the same depth range.
- (4) The mean annual temperature at the land surface throughout the area of the thermal anomaly, which is used in computing the thermal gradient for 0-30 m, is equal to the mean annual air temperature at the nearest weather station.

(5) The harmonic-mean thermal conductivity of the materials from 0 to 30 m depth is constant throughout the area of the thermal anomaly and is equal to the average of the computed harmonic-mean conductivities at all the test-well sites within the area.

Because of the simplified assumptions and the uncertainty of the values of some of the parameters, method A yields only crude, approximate answers for most of the hydrothermal-discharge systems described in this report. For example, the assumption that all heat discharge from the area of the thermal anomaly is measured as conductive heat flow in the top 30 m of materials, except for heat discharged by springflow and steam discharge, introduces significant errors where thermal gradients are modified by upward or downward convection or by boiling, or where heat is transported beyond the area of the thermal anomaly by lateral ground-water flow. Another significant source of error is the estimate of the harmonic-mean thermal conductivity of the materials 0-30 m below the land surface. The error of the estimate is relatively large where the water table is deeper than a few metres below the land surface, because the uncertainty of the values of thermal conductivity assigned to the unsaturated materials is greater than that of the values assigned to the saturated materials. It is believed that, in most of the estimates, the true heat discharge is within the range of 1/2 to 2 times the estimated value.

Method B.---Method B differs from method A in that heat-flow rates are computed using thermal gradients measured in the test holes below the water table and below the depth of significant seasonal fluctuation of temperature instead of using average thermal gradients from 0 to 30 m depth computed from temperatures at 30 m and land surface. Method B is inherently more accurate than method A, for three principal reasons. First, the thermal conductivities of the saturated materials used in method B can be estimated within much narrower limits than the thermal conductivities

of unsaturated materials, which at most places constitute a significant proportion of the 0-30 m depth interval used in method A. Second, in method B, only those depth intervals are selected for which the thermal gradients appear to be essentially linear and conductive. In method A, however, the computed gradient from 0 to 30 m probably reflects convection as well as conduction at many places and therefore does not necessarily yield valid estimates of conductive heat flow. Third, method B does not use a constant thermal conductivity for the entire area of the thermal anomaly as does method A. Instead, in method B, the conductivity is assumed to vary laterally and is defined by the values calculated for each test hole.

The computation procedure in method B is similar in several respects to that in method A. The major difference is that, in method B, measured thermal gradient and computed harmonic-mean thermal conductivity for the corresponding interval are multiplied to give heat flow at each test-hole site. Heat-flow isograms are then drawn from the test-hole data, and the heat discharge from the area between two isograms is computed as the product of the area and the geometric mean of the two heat-flow isograms. The heat discharges of the areas between the pairs of heat-flow isograms are then added to obtain the total heat discharge from the thermal area. The boundary of the thermal area is placed at the heat-flow isogram that is believed to represent the conductive heat flow of the larger area surrounding the hydrothermal-discharge system.

The procedures in both methods described above provide estimates of the total conductive heat discharge from a hydrothermal-discharge system. For the purpose of estimating water discharge from the system by the heat-budget method, described later, it is necessary to compute the

amount of conductive heat discharge that results from rising thermal water, for convenience called the "net conductive heat discharge." The net conductive heat discharge is computed as the total conductive heat discharge minus the so-called "normal conductive heat discharge," which is defined as the heat discharge from the thermal area that would have occurred without the upflow of thermal water.

ESTIMATES OF WATER DISCHARGE

Water may discharge from a hydrothermal system as flow from springs and wells, lateral ground-water outflow, evaporation from soil and water surfaces, and transpiration by phreatophytes. In water budgets, evaporation and transpiration are usually grouped under the term evapotranspiration. Evapotranspiration is the dominant mode of water discharge from each of the hydrothermal systems studied; if a sufficiently large area surrounding a thermal anomaly is included, all water is ultimately discharged by this process. In general, not all the water discharge from a thermal area is deep, thermal water; some of it is shallow, nonthermal water of local derivation, which may mix with the thermal water in variable proportions. In this study, two methods are used to estimate the discharge of thermal and nonthermal water from the hydrothermal systems: the water-budget method and the heat-budget method. The assumptions and procedures used in computing water discharge by each of these methods are reviewed below.

Water-Budget Method

In the water-budget method, it is assumed that the shallow part of the hydrothermal system is in hydrologic equilibrium, where inflow equals outflow. Inflow items include recharge from local precipitation and runoff, thermal-water upflow from the deep part of the system, and imported water (generally insignificant). Outflow items are evapotranspiration, lateral ground-water outflow, and springflow that leaves the budget area. Upflow of thermal water is considered the unknown in the budget, and the hydrologic equation is solved for this unknown.

Springflow.--In the systems studied, none of the springflow leaves the budget area as liquid outflow; all the water is ultimately discharged by evapotranspiration. However, for some purposes, it is useful to estimate the discharge from spring orifices. (Discharge from flowing or pumping wells is either zero or very small and is neglected in the budget estimates.) Most of the spring-discharge rates are based on visual estimates. Wherever possible, the estimates were made at channel sections where the flow velocity was fairly uniform and where the areas of the channel cross sections could be determined within narrow limits. Accuracy of the visual estimates is believed to be within about \pm 30 percent for discharges of several litres per second, but the percentage errors for smaller discharge rates probably are larger. A few measurements of spring discharge were made with a pygmy current meter. The accuracy of these measurements exceeds that of the visual estimates and is believed to be within about \pm 15 percent.

Evapotranspiration.--Evapotranspiration includes evaporation from soil and water surfaces and transpiration by plants. Except for playas and other non-vegetated areas, evaporation from ground surfaces is not estimated as a separate budget item but is grouped with transpiration.

Evaporation from water surfaces, mostly spring pools, represents only a small percentage of the total evapotranspiration discharge in the areas of study and is not estimated separately, except for the Gerlach and the Sulphur Hot Springs thermal areas. Evaporation rates from thermal pools at these two sites are estimated using a quasi-empirical mass-transfer equation of Harbeck (1962). The data used in the equation are average monthly temperature, humidity, and wind velocity, as measured

at the Winnemucca WBO AP weather station. The following rates are computed and used in this report:

Pool-surface temperature (°C)	Estimated annual evaporation (metres)
10	1.3
20	3.4
40	13
60	36
80	88

An estimated rate of evaporation from playa deposits, 9 cm yr^{-1} , is based in part on a study of rates of upward ground-water flow in near-surface deposits beneath Smith Creek Playa in central Nevada by M. L. Sorey (written commun., 1971) and in part on published and unpublished estimates made in other parts of Nevada by the U.S. Geological Survey. Sorey's estimate is derived from the degree of curvature of the thermal gradient, which depends on the rate of vertical ground-water flow (Bredenhoeft and Papadopoulos, 1965; Stallman, 1960; Sorey, 1971). Depth to water at the Smith Creek Playa sites averaged about 3.6 m below land surface (Sorey, written commun., 1971), whereas the depth to water at the sites in this study ranges from about 0.3 to 1.5 m below land surface. Evaporation rates for the playa deposits considered in this study therefore would be greater than that at Smith Creek Playa on the basis of the smaller depth to water. However, Smith Creek Playa lacks the salt crust present at the surface of the playa deposits considered in this study. The salt crust is believed to inhibit evaporation. For this reason, the evaporation rate for the playas in this study is assumed to be no greater than that at Smith Creek Playa, despite the lesser depth to water in the former playas.

Actual rates of evaporation from playa surfaces probably are highly variable and depend on several factors, among which are depth to the water table, salinity of the water, temperature, and nature of the near-surface materials. Although the rate for a given location is uncertain, the total volume of evaporation from playa surfaces within the thermal areas studied is small in comparison with the volume of evapotranspiration from vegetated area. For this reason, large errors in the estimate do not greatly affect the estimates of total evapotranspiration.

Ground water is discharged by evapotranspiration where the roots of phreatophytes penetrate to the capillary fringe or the underlying water table, or where the capillary fringe extends to or near the land surface. Rough estimates of ground-water evapotranspiration were obtained by mapping types of phreatophytic vegetation, multiplying the area covered by each type by an estimated annual rate of water discharge by that type, and summing the products. Estimates of annual rates are based on data from several sources, including Lee (1912), White (1932), Young and Blaney (1942), Houston (1950), Robinson (1958, 1965), Blaney and Hanson (1965), and Han and Price (1972).

The estimated rates of evapotranspiration are regarded as approximate; the actual rates may vary by a factor of 2 or 3, depending on depth to water, soil type, salinity of the water, and other variables.

Lateral ground-water outflow.---Lateral ground-water outflow from the budget area is a significant item in most of the systems studied but is difficult to estimate accurately. The computation procedure is as follows. First, the isotherm that delineates the thermal anomaly is used as the position of the transmitting section. From available subsurface geological data, supplemented by a reasonable guess as to thickness and character of the materials transmitting water below the depths for which the data are available, the intrinsic permeability and thickness of the transmitting section are inferred. Next, the average horizontal potential gradient normal to the transmitting section is estimated using water-level data from the test holes. Finally, the outflow is computed as the average potential gradient normal to the transmitting section multiplied by the product of the area of the transmitting section, its average intrinsic permeability, and the kinematic viscosity of the water.

Water discharge as steam.--An unmeasured amount of water is discharged as steam in those systems containing boiling springs. The actual discharge is difficult to estimate. However, for purposes of this study, an approximate estimate is derived as follows. The example is taken from Sulphur Hot Springs, one of the systems studied.

Total springflow, including evaporation from pool surface: $0.28 \times 10^6 \text{ m}^3 \text{ yr}^{-1}$

Springflow at boiling temperature (from table 16): $0.03 \times 10^6 \text{ m}^3 \text{ yr}^{-1}$

Reservoir temperature (table 1): 186°C Enthalpy of water: 188 cal g^{-1}

Boiling temperature at surface: 94°C Enthalpy of water: 94 cal g^{-1}

Net enthalpy available for steam: 94 cal g^{-1}

Enthalpy of steam-water mixture at 94°C : 543 cal g^{-1}

Weight percent of steam at 94°C : $94/543 = 17.3 \text{ percent}$

Discharge of steam and boiling water (as equivalent water)

$$= \left(\frac{1}{1 - 0.173} \right) (0.03 \times 10^6 \text{ m}^3 \text{ yr}^{-1})$$

$$= 0.036 \times 10^6 \text{ m}^3 \text{ yr}^{-1}$$

Discharge of steam (as equivalent water) = $(0.036 - 0.03) \times 10^6 \text{ m}^3 \text{ yr}^{-1}$

$$= 0.006 \times 10^6 \text{ m}^3 \text{ yr}^{-1}$$

This discharge is a very small percentage of the total water discharge and is neglected. However, as discussed in the preceding section, the heat discharged as steam is a much more significant fraction of the total heat discharge that results from convective upflow of thermal water, owing to the high enthalpy of the steam.

Heat-Budget Method

In the heat-budget method, it is assumed that the shallow part of the hydrothermal system is in both hydrologic and thermal equilibrium-- that is, the inflow of both water and heat equals outflow. The method yields an estimate of thermal-water discharge, provided that the source temperature of the water indicated by the chemical geothermometers reflects only the deep thermal water and not an admixture of the deep thermal water and shallow nonthermal water. Information required to differentiate thermal water from a mixture of thermal and nonthermal water was not obtained in this study. In the absence of such information, it is assumed that the chemical (silica and cation) geothermometers indicate the temperature of a deep source or sources.

In order to compute the discharge of thermal water, it is assumed that the net heat discharge from the system is derived from rising thermal water, which leaves the deep source or sources at the temperature indicated by the silica or cation geothermometers. (The net heat discharge equals the total heat discharge minus the discharge that represents "normal" heat flow from the thermal area.) The net heat discharge is based on an estimate derived by one of the methods described earlier in the section, "heat discharge." The net heat content of the water is computed as the difference between the temperature of the water at the deep source or sources and the mean annual temperature at the land surface, multiplied by the heat capacity of water, approximately $1.0 \text{ cal g}^{-1} \text{ } ^\circ\text{C}^{-1}$. The discharge of thermal water is computed as the net heat discharge from the thermal area, divided by the net heat content of the thermal water at the deep source or sources.

CARSON DESERT

Hydrogeologic Setting

The Carson Desert is a large basin in west-central Nevada (fig. 10).

Fallon, the principal center of population and trading, is 90 airline km east of Reno. The Stillwater-Soda Lake KGRA occupies a roughly rectangular area of 91,140 ha in the south-central part of the basin. The basin floor, which lies at altitudes of 1,170 - 1,250 m above mean sea level, is immediately underlain by deposits of late Pleistocene Lake Lahontan and by Holocene fluvial and eolian deposits. Bordering mountains, as much as 1,500 m higher than the basin floor, are formed of a variety of consolidated to semiconsolidated rocks of Paleozoic, Mesozoic, and Cenozoic ages. Tertiary lavas and pyroclastic rocks of mafic to felsic composition are widespread in the mountains and have been penetrated in test wells beneath the basin fill. Maximum thickness of the unconsolidated basin fill overlying the Tertiary volcanic or older rocks is not accurately known but probably is at least 2 km.

Basaltic rocks of Quaternary age are exposed at several places within the basin. Lone Rock, an isolated outcrop of basalt, possibly a remnant of a volcanic plug or neck, rises about 27 m above the surrounding floor of east-central Carson Sink. Rattlesnake Hill is a similar outcrop of basalt about 1.5 km northeast of Fallon. Upsal Hogback is a cluster of several cones of basaltic tuff 16 km north of Fallon. The eruptions that formed the cones occurred chiefly during an interpluvial time in the late Pleistocene, when Lake Lahontan was dry (Morrison, 1964, p. 100). Soda and Little Soda Lakes, 10 km northwest of Fallon, are within, respectively, elliptical and circular craters, 1.6 and 0.3 km in diameter, which are rimmed by a mixture of basaltic and nonvolcanic debris blown out by repeated gaseous eruptions. According to Morrison (1964, p. 72), the

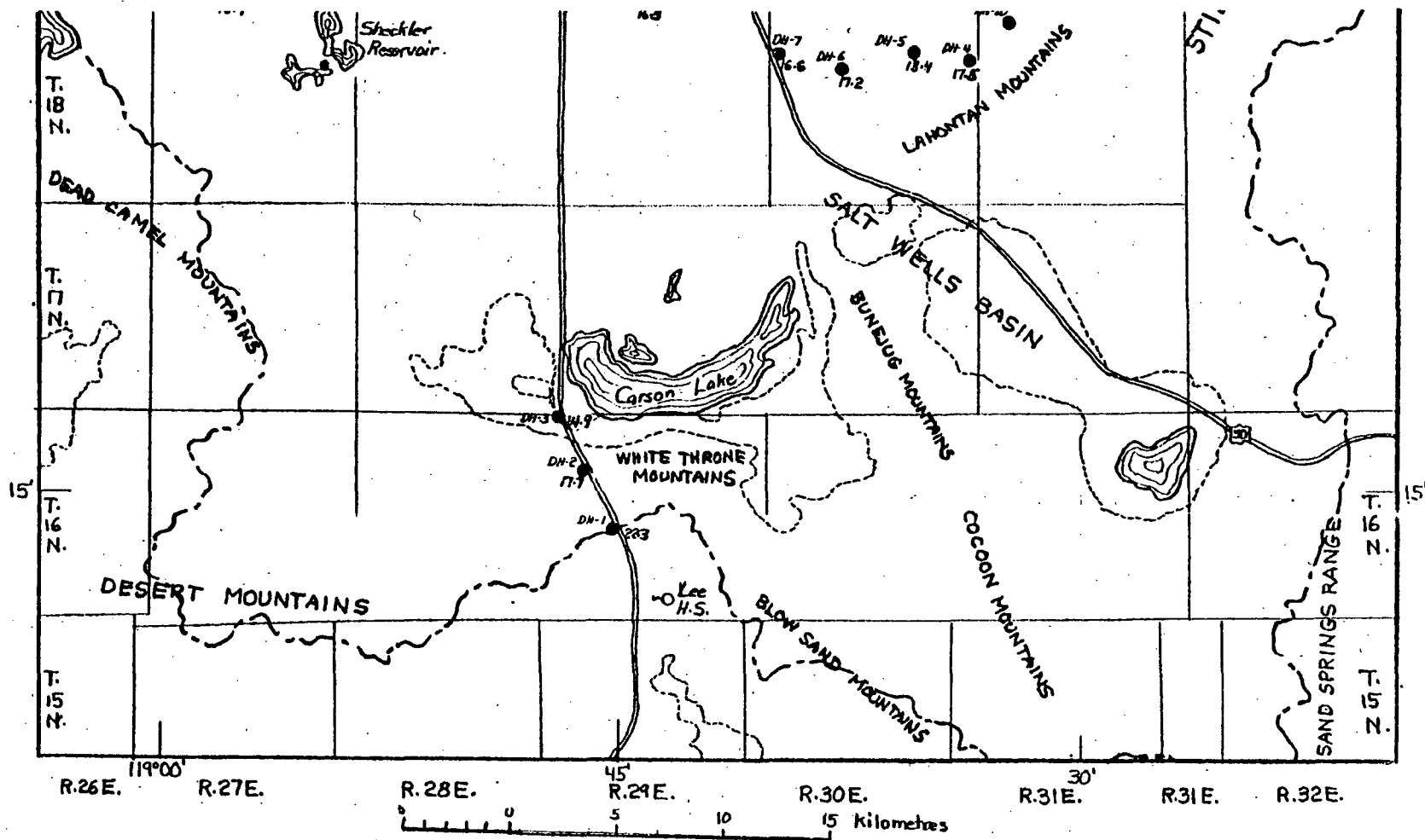


Figure 10.--Map of southern and central Carson Desert showing location of holes and temperatures at a depth of 30 m.

earliest eruptions may have been as early as or earlier than the first eruptions at Upsal Hogback, 14 km to the north-northeast, but the latest eruptions apparently were later than those at the Hogback.

The lowest part of the Carson Desert is occupied by the Carson Sink, a large bare playa, mostly dry, which is the sump for the Carson River and, at times, overflow from Humboldt Sink. (See fig.10) Before development of irrigated agriculture in the southern part of the basin in the early 1900's, the Carson River was the chief source of water supply and ground-water recharge. Irrigation, partly with diverted water from the Truckee River as well as with Carson River water, all stored at Lahontan Reservoir near the southwest corner of the basin, is now the important source of ground-water recharge. Recharge takes place by penetration to the saturated zone of both applied irrigation water and leakage of irrigation-supply water from unlined canals. Only a very small amount of recharge to ground water in the basin is derived from local precipitation and runoff. Average annual river releases from Lahontan Reservoir are about $4,700 \times 10^6 \text{ m}^3$. All this water eventually is discharged by evapotranspiration, but a large fraction, probably more than one half, penetrates to the saturated zone before it is discharged. In contrast, the estimated potential ground-water recharge from the surrounding mountains is only $1.6 \times 10^6 \text{ m}^3 \text{ yr}^{-1}$ (Glancy and Katzer, 1974).

Local patterns of ground-water circulation are complex, but the large-scale lateral movement is generally northeast and north toward the Carson Sink. Sandy aquifers within a few tens of metres of the land surface probably transmit most of the water. Confined ground water at greater depths moves more slowly and, in the vicinity of the Carson Sink, moves mainly upward across confining beds of lacustrine clay and silt.

Shallow Test Holes

Test drilling related to the present study began in 1972. The U.S. Bureau of Reclamation installed iron pipes of 3.2 cm inside diameter, capped at the bottom and filled with water, in several seismic-exploration holes drilled by Standard Oil Co. of California at scattered sites in the southern part of the basin. Most of the holes are 33.5 m in depth and were used to determine temperatures and thermal gradients. During the fall of 1972, these holes were supplemented by four additional test holes, drilled with a U.S. Bureau of Reclamation hydraulic-rotary drill rig to a depth of 50 m and similarly completed with water-filled 3.2 cm iron pipes.

During 1972 and 1973, the U.S. Geological Survey completed 34 test holes in the Carson Desert. Data for these test holes are summarized in table 4. The first drilling was done in an area surrounding the steam well north-northeast of Soda Lakes (20/28-28ccb). The purpose was to determine the extent of the thermal area associated with the steam well and believed to be also associated with Soda Lakes and Upsal Hogback. Later, holes were drilled in the marginal parts of the Stillwater thermal area in order to better delineate that feature. Test holes were also drilled between the Stillwater and Soda Lakes-Upsal Hogback areas to supplement temperature information obtained from earlier U. S. Bureau of Reclamation test holes.

Table 4.--Data for U.S. Geological Survey test holes in Carson Desert

Type of completion: Casing type is indicated by "St" (steel) or "P" (PVC).

Wells capped and filled with water are indicated by "C". Wells with well-point screens at bottom are indicated by "Sc".

Depth to water table: Obtained from neutron (N) and (or) gamma gamma (G²) log. Accuracy variable.

Static water level: Depth below land-surface datum.

Geophysical logs available: Gamma ("G"), gamma-gamma ("G²"), neutron ("N"), resistivity ("R"), Caliper ("Ca"), Conductivity ("Co"), and temperature ("T").

Well number	Location	Depth metres below land surface	Casing		Land-surface altitude (m)	Depth to water table			Static confined water level		Geophysical logs available
			Inside diameter (cm)	Type of completion		Metres below land surface	Source of data	Date	Metres below land surface	Date	
CDM-1	19/25-9dda	0.77	3.8	St, Sc	1,216.5	0.3	N		2.33	74 03 28	
AM-2	20/28-22ba	26.2	3.8	St, Sc	1,212.4	9.3	N	74 04 04	9.26	74 02 26	G, G ² , N
AM-3	20/28-11bbb	14.04	3.8	St, Sc	1,199	2.1	N	73 05 15	2.17	74 02 26	G, G ² , N
AM-4	19/27-1aad	20.7	3.8	St, Sc	1,219.78	1.5	N	73 05 18	3.72	74 03 06	G, G ² , N
AM-5	19/28-17bhd	39.6	3.8	St, Sc	1,224.96	8.0	N	73 05 18	11.89	74 02 17	T, Co, G, G ² , N
AM-6	19/27-13ceb	43.6	3.8	St, Sc	1,223.31	2.3	N	73 05 18	6.76	74 02 17	T, Co, G, G ² , N
AM-7	20/28-21cbb	27.7	3.8	St, C	1,213.26	7.3	G ²	74 03 28			G, G ² , N
AM-8	20/28-12ead	39.0	3.8	St, Sc	1,216.27	2.7	N	73 05 14	5.26	74 03 06	G, G ² , N
AM-9	20/28-21bhd	39.9	3.8	St, Sc	1,209	8.6	N	73 05 16	8.50	74 02 26	T, Co, G, G ² , N
AM-10	21/28-21bba	32.9	3.8	St, Sc	1,190	2.7	N	73 05 15	2.61	74 02 26	G, G ² , N
AM-11	21/28-14dda	9.4	3.8	St, C	1,204	-	-	-	-	-	G
AM-12	20/28-11aaa	22.3	3.8	St, Sc	1,207	10.0	N	74 04 04	10.75	74 04 04	G, G ² , N
AM-13	21/29-7baa	22.3	3.8	St, Sc	1,189	2.5	N	73 05 16	2.45	74 02 26	T, Co, G, G ² , N
AM-14	19/29-11aeb	45.20	3.8	St, Sc	1,194.2	1.7	N	73 05 16	2.60	73 06 02	T, G, G ² , N
AM-15	19/30-10cdd	45.20	3.8	St, Sc	1,190.5	1.3	N	73 05 16	>=0.24	73 04 12	G, G ² , N
AM-16	17abb	15.48	3.8	St, Sc	1,192.1	< 1	N	73 05 16	>=0.30	73 04 12	G, G ² , N
AM-17	20/28-12aad	9.8	3.8	St, Sc	1,212.07	5.1	G ²	73 05 15	2.63	74 03 06	T, Co, G, G ²
AM-18	20/28-12ade	41.8	3.8	St, Sc	1,214.72	3.6	N	73 05 14	4.80	74 03 06	T, G, G ² , N
AM-19	19/31-29cca	32.9	3.8	St, Sc	1,196	6.7	N	73 11 27	6.81	73 04 13	T, G, G ² , N
AM-20	18/31-6dad	20.79	3.8	St, C	1,201	3.6	N	73 11 27	-	-	T, G, G ² , N
AM-21	19/31-9aba	45.48	3.8	St, Sc	1,191	2.6	N	73 11 27	.58	73 04 13	T, G, G ² , N
AM-22	20/31-30ced	41.18	3.8	St, Sc	1,183.5	< 2.8	N	73 05 17	>=0.16	73 04 14	T, G, G ² , N
AM-23	19/30-25bbb	39.14	3.8	St, Sc	1,191.8	< 1.8	G ²	73 11 17	>=0.24	73 07 10	T, G, G ²
AM-24	19/31-30bhd	45.42	3.8	St, Sc	1,190	< 1.6	G ²	73 11 17	.64	73 07 10	G, G ²
AM-25	20/31-18bhd	45.26	3.8	St, Sc	1,182.0	< .8	N	73 11 17	>=1.22	72 12 16	G, G ² , N
AM-26	19/31-17cbb	45.4	3.8	St, Sc	1,188.4	< 1.6	G ²	73 11 17	>=0.10	73 07 10	T, G, G ²
CDM-27	20/28-11abe	44.5	5.1	P, Sc	1,211.87	1.8	N	74 03 27	3.23	74 03 27	T, G, G ² , N
AM-28	19/27-12aca	18.3	3.8	St, Sc	1,220.05	0.64	N	73 11 27	1.73	74 04 05	G, G ² , N
DM-29	20/28-27cca	44.8	3.8	St, Sc	1,211.08	7.5	N	74 03 27	5.18	74 03 27	T, G, G ² , N
DM-30	20/28-26cde	40.2	3.8	St, Sc	1,209.60	1.3	N	73 11 15	0.73	74 02 20	G
DM-31	20/28-11aab	38.7	3.8	St, Sc	1,214.60	3.0	N	74 03 28	5.59	74 03 28	G, G ² , N
DM-32	20/28-28beb	45.1	3.8	St, Sc	1,213.68	6.2	N	74 03 27	6.91(?)	74 03 27	Co, R, G, G ² , N
DM-33	20/28-28aad	44.8	3.8	St, Sc	1,212.34	6.7	G ²	74 03 28	5.25	74 03 28	R, G, G ²
DM-34	20/28-13beb	45.1	3.8	St, Sc	1,215.97	4.0	N	74 03 28	6.78	74 03 27	Co, R, G, G ² , N

Experimental Heat-Flow Test Hole in Carson Sink

Using hydraulic-rotary drilling equipment, the Bureau of Reclamation drilled an experimental heat-flow test hole near the middle of the Carson Sink, 43 km northeast of Fallon. The purpose of the experiment was to determine the feasibility of obtaining a heat-flow measurement in a relative shallow test hole in fine-grained lacustrine and playa deposits.

It was hoped that upward ground-water movement in the poorly permeable deposits would be so slow that convective heat transfer would be minimal

The test hole was drilled to a depth of 153.9 m and completed at the same depth with 5.1 cm iron pipe, capped and filled with water for temperature measurements. Cores were obtained at depths of 61.0 - 62.5 m, 91.4 - 93.0 m, 123.4 - 124.7 m, and 150.9 - 152.4 m. Recovery of the upper two cored intervals was incomplete, and the samples may represent only the most cohesive, clay-rich deposits within those intervals.

However, on the basis of the borehole geophysical logs, especially the gamma-gamma and the neutron logs, the cores are believed to be representative of the average materials penetrated by the drill hole. Thermal conductivity of the core samples was measured with a needle probe by the Geothermal Laboratory of the U.S. Geological Survey in Menlo Park, Calif., the results are given in table 5. The average thermal gradient, measured in July 1973 with truckmounted equipment and 17-bead thermistor probe, is $76.4^{\circ}\text{C km}^{-1}$ (fig. 11).

The heat flow calculated from this gradient and an average thermal conductivity of $2.07 \times 10^{-3} \text{ cal cm}^{-1} \text{ s}^{-1} \text{ }^{\circ}\text{C}^{-1}$ is 1.57 HFU. The corrected heat flow, using an assumed rate of deposition of the lacustrine and playa sediments of 1 mm yr^{-1} , is about 1.9 HFU (John Sass, oral commun., 1974).

Table 5.--Thermal conductivity of core samples from U.S. Bureau of Reclamation heat-flow test hole Alkali Flat 1 in Carson Sink

(Data from John Sass and Robert Munroe, US Geol. Survey, Menlo Park, California)

Thermal conductivities ($\times 10^{-3}$ cal cm^{-1} s^{-1} $^{\circ}\text{C}^{-1}$)

Depth (m)	Position				Average
	A	B	C	D	
60.96 - 62.48	2.44	1.67	2.06	1.97	2.04
91.44	2.27	2.15	2.08		2.17
123.44	2.06	2.15	2.06		2.09
124.66	1.91	2.04	1.94		1.96
150.88 - 152.40	(1) 2.33	2.16	1.91	1.97	2.09
	(2) 2.03	2.00			2.02
151.03	2.05	2.03	2.14		2.07
151.79	2.10	2.02	2.11	2.16	2.10
Average from 8 samples					2.07 \pm 0.02

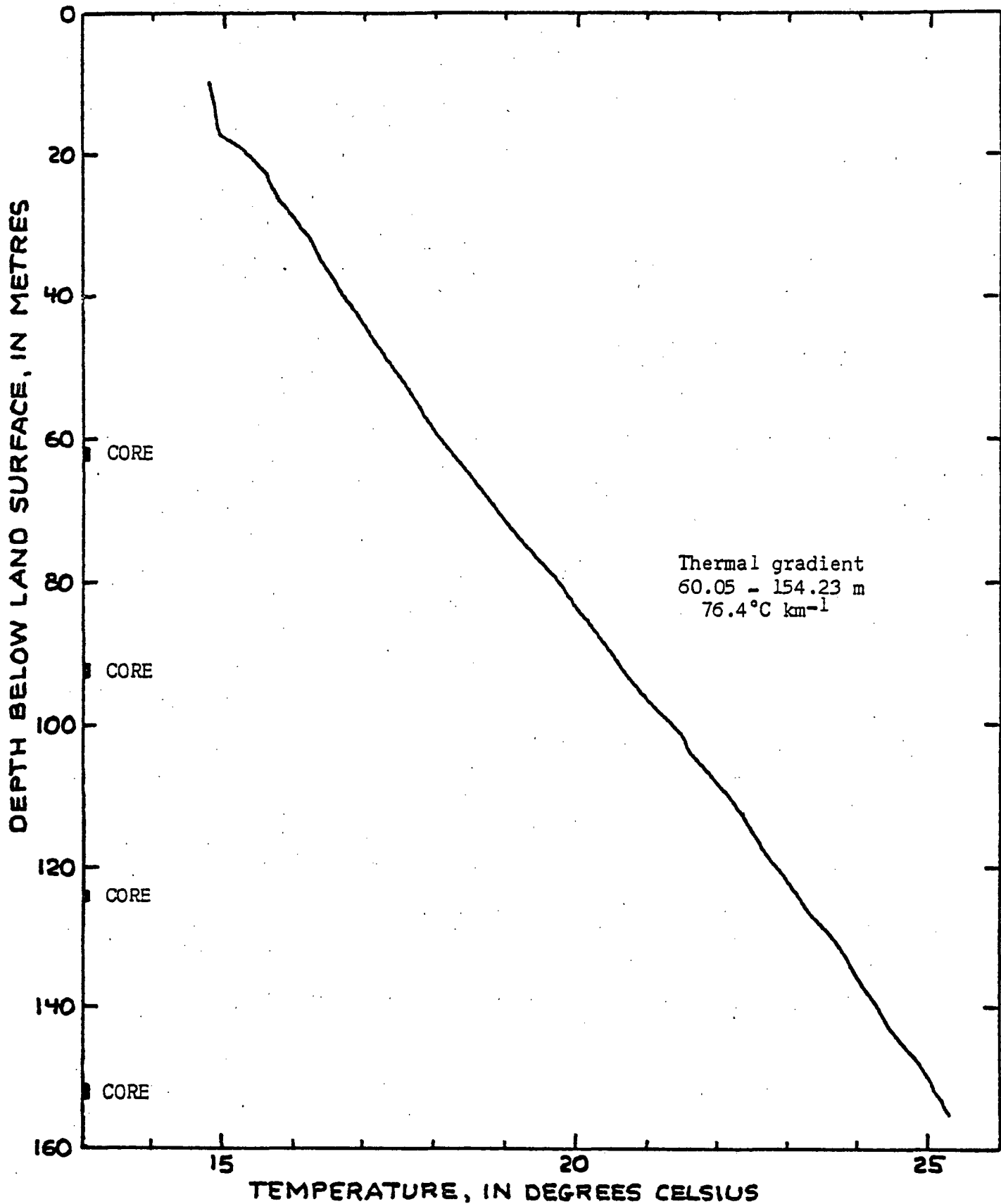


Figure 11—Temperature profile in test-hole 22/31 - 10bca (USBR Alkali Flat 1), 10 July 1973

[Temperatures measured by P. Twichell and S. Chicoine, U. S. Geological Survey]

Thermal Areas

The Carson Desert contains two known thermal areas where temperatures at a depth of 30m exceed 20°C: the first, centered near Stillwater in the eastern part of the Stillwater-Soda Lake KGRA; the second, between Soda Lakes and Upsal Hogback in the western part of the KGRA (fig. 10). Other thermal areas likely are present, but test-hole data available during this study are not sufficient to define their location or extent.

Temperature data obtained in test holes between the Stillwater and the Soda Lakes-Upsal Hogback thermal areas suggest that the two systems are not connected, at least at the depths of most of the test holes (about 45 m). However, in a few deeper holes (about 150 m), thermal gradients generally increase below depths of about 50 to 100 m. Drillers' logs do not indicate that the deeper materials are finer grained. Instead, the downward increase in thermal gradient is believed to be caused in part by the effects of circulation of ground water derived from irrigation-water and river-water seepage in the near-surface deposits. The downward increase in thermal gradient also results from the warming of the near-surface environment to temperatures above the mean annual air temperature by large applications of relatively warm irrigation water during the growing season. It is possible that thermal systems exist outside the two known areas but are concealed by the effects of ground-water flow and infiltration of irrigation water in the overlying deposits.

STILLWATER THERMAL AREA

Hydrogeologic Setting

The Stillwater thermal area is centered near the small community of Stillwater, about 20 km east-northeast of Fallon. The area enclosed by the 20°C isotherm at a depth of 30 m forms an ellipse about 11 km long (north-south) and 7 km wide. Most of the land is farmed and is traversed by both irrigation canals and drains. Stillwater Point Reservoir lies along the southeast margin of the area; a large tract of marshes and shallow lakes lies to the northeast. The eastern and northern parts of the thermal area are within the Stillwater Wildlife Management Area.

The top of the saturated zone is within 2 m of the land surface throughout most of the area. Deposits within the upper few hundred metres are chiefly lacustrine clay and silt; interbedded fine to medium sand contains water under artesian pressure. Artesian-pressure levels (confined potentiometric surfaces) in sand strata within 50 m of the land surface are above the land surface, and the dominant potential gradient is upward. The lateral component of the gradient is northward, toward the Carson Sink. Ground water is discharged from the area by underflow toward the north and by evapotranspiration; the latter undoubtedly is predominant.

Previous Information

General dimensions and near-surface temperatures of the Stillwater thermal area were unknown many years ago from numerous domestic and farm wells. Deeper subsurface information was obtained in 1964 from the O'Neill-Oliphant Reynolds 1 geothermal test well, drilled to a depth of 1,292 m near the center of the area. The information from the test well was supplemented by unpublished detailed gravity and magnetic surveys of an area of 60 km² which includes most of the thermal feature. Areal geology was mapped by Morrison (1964); his maps (pls. 3 and 4) show the traces of several faults formed during earthquakes in the summer of 1954. A report by Stabler (1904) gives areal variations in salinity and in several dissolved constituents of ground water, as well as depths to the water table.

Test Drilling

Nine shallow test holes were bored by the U.S. Geological Survey during the fall of 1972 in order to define the limits of the thermal area and to obtain geologic, hydrologic, and thermal data. Two additional holes (USGS CD AH's 14 and 16) were bored west of the thermal area to supplement information from U.S. Bureau of Reclamation test holes and other wells bearing on the possible presence of other thermal areas between Stillwater and Soda Lakes. Data for the U.S. Geological Survey test holes are given in table 4. All the test holes were bored by power auger and 3.8 cm diameter galvanized-steel pipes fitted with well points or well screens were installed for subsequent borehole geophysical logging, temperature measurements, and water-level measurements. Completed depths range from 20.8 to 45.5 m.

Chemical Character of Ground Water

Water samples were analyzed from the U.S. Geological Survey test holes near the margins of the thermal area, and Mariner and others (1974) analyzed a sample from a well in Stillwater, near the center of the thermal area, which was discharging a small amount of boiling water and steam. The samples from the test holes (CD AH's 15, 23, and 24) represent chiefly infiltrated irrigation water of local origin; the sample from the well (19/31-7cda) probably represents deep thermal water. Depths of the samples from the test holes range from 39 to 45 m; the depth and construction of well 19/31-7cda are unknown.

All four samples of water are similar in gross chemical characteristics, although there are significant differences in some constituents between the thermal water and the nonthermal water from the three test holes. Dissolved solids range from about 4,500 to 6,500 mg l⁻¹ in the samples of nonthermal water and are about 4,300 mg l⁻¹ in the thermal water. Sodium and chloride are the dominant constituents in both waters. The thermal water, however, is relatively high in silica, calcium, and fluoride, whereas the nonthermal water is relatively high in bicarbonate. More sampling is needed to establish clearly the criteria for distinguishing thermal from nonthermal water and to provide an index for the amount of mixing of the two waters.

The reservoir temperatures of the thermal water indicated by the silica-quartz and the sodium-potassium-calcium geothermometers were, respectively, 159°C and 140°C (table 1; Mariner and others, 1974, table 3).

Heat Discharge

Only the general configuration of the isotherms at a depth of 30 m is known (see fig.12). Also, reliable data on shallow thermal gradients in the central part of the thermal area are not available. For these reasons, only a crude estimate of heat discharge is possible, using method A described in the section "Estimates of heat discharge".

A mean annual temperature at land surface of 11°C is used in the computation of average thermal gradients. This is the approximate average of the mean annual temperatures at Fallon and Lahontan Dam, the two weather stations within the Carson Desert. (See table 6 for temperature data for Fallon). The harmonic-mean thermal conductivity for the depth interval 0-30m is estimated to be $2.5 \times 10^{-3} \text{ cal cm}^{-1}\text{s}^{-1}\text{°C}^{-1}$ on the basis of the means computed from the logs of test holes CH AH's 15 and 22-26. This estimate is believed to be more reliable than those made in this study for the other thermal areas for two reasons. First, the strata beneath the thermal area appear to be less variable in thickness and character than those beneath other areas. Strata several metres thick may be traced for several kilometres, using their characteristic "signatures" on the gamma-gamma and neutron logs. Second, the deposits throughout the entire thermal area are saturated or nearly saturated to the land surface. Thus, there is less uncertainty as to the value of the harmonic-mean thermal conductivity than in the other thermal areas, where the water table is generally deeper.

The estimated total discharge of heat from the thermal area is $15 \times 10^6 \text{ cal s}^{-1}$. The derivation of the estimate is given in table 7. "Normal" heat discharge from an equivalent area would be $1.1 \times 10^6 \text{ cal s}^{-1}$ on the basis of an average corrected heat flow of $1.9 \times 10^{-6} \text{ cal cm}^{-2}\text{s}^{-1}$ estimated at the Alkali Flat 1 experimental heat-flow test hole in the Carson Sink, 29 km to the north. The excess heat discharge, $14 \times 10^6 \text{ cal s}^{-1}$, is interpreted as resulting from convective upflow of deep thermal water as depicted in figure 13.

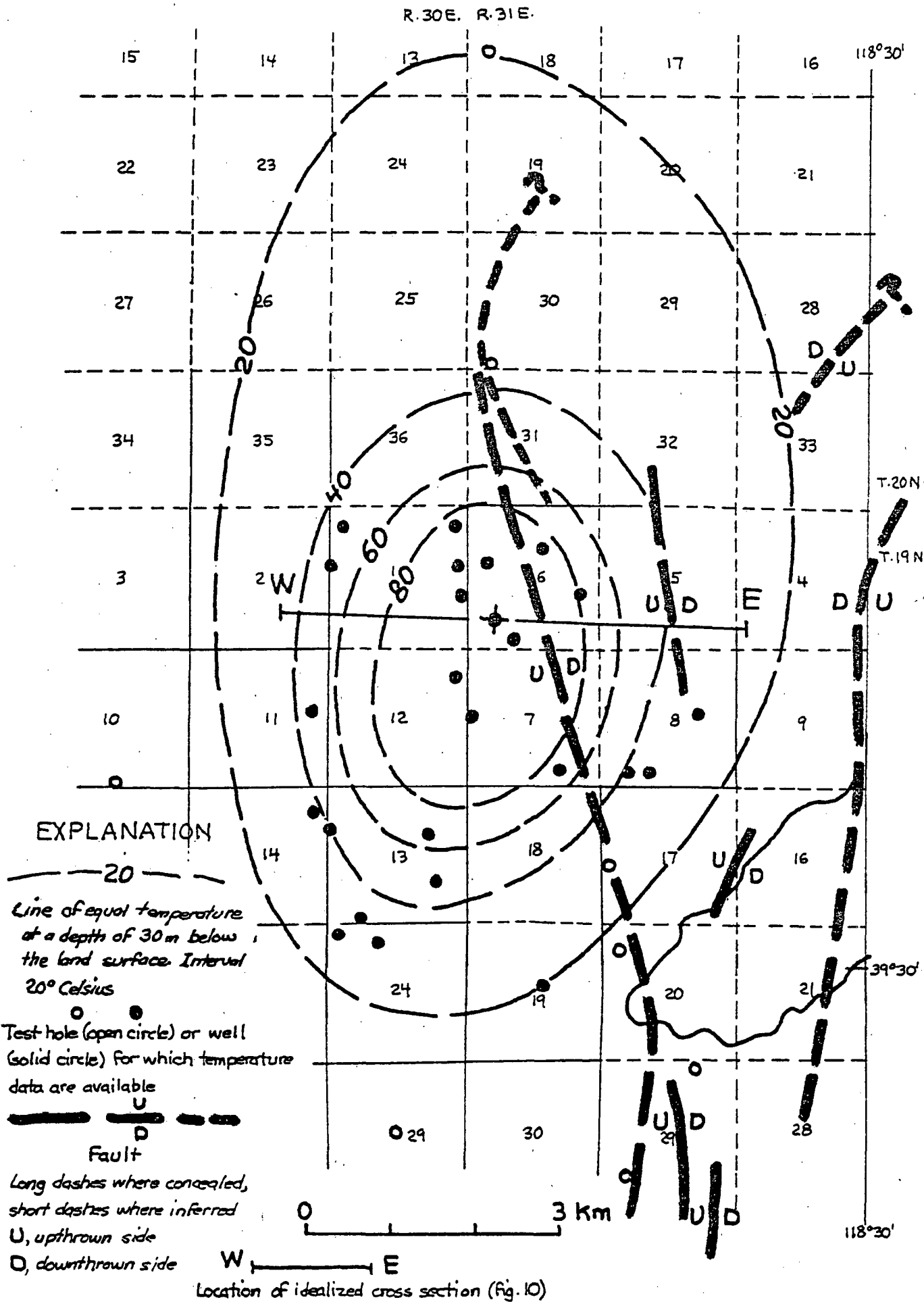
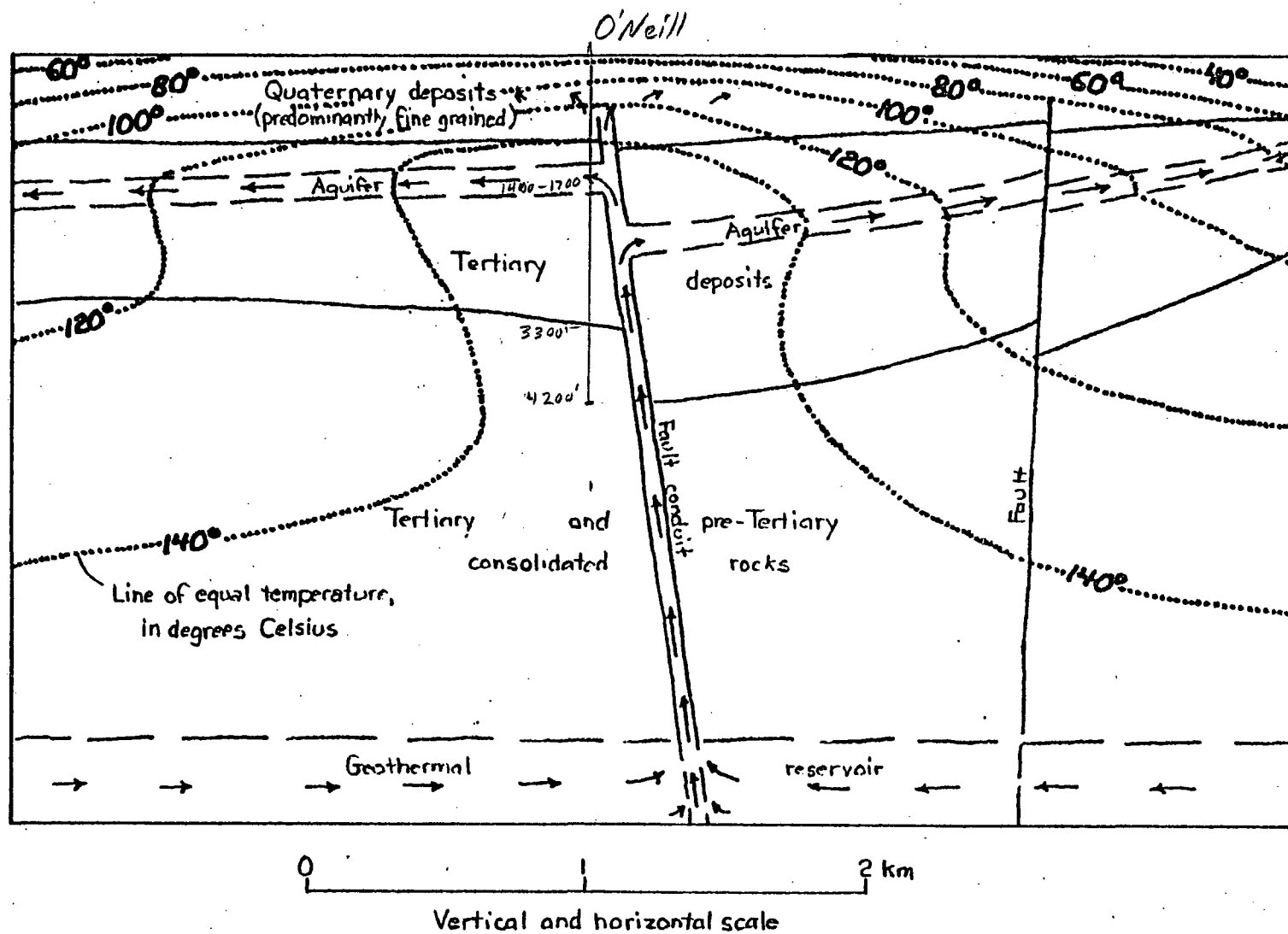


Figure 12. — Map of the Stillwater thermal area showing temperature at a depth of 30 m

WEST

EAST



92

Figure 13.— Idealized cross section of central part of Stillwater thermal anomaly.

Table 6.--Temperature data for Fallon, Gerlach, Winnemucca, Battle Mountain, and Ruby Lake.

[Source of data: U. S. Department of Commerce, 1973, Climatological data, Nevada, Annual Summary, 1973].

Average temperatures, in °C

Month	Fallon Experiment Station (1931-60)	Gerlach (1931-56)	Winnemucca (1931-60)	Battle Mountain Airport (1945-60)	Ruby Lake (1941-60)
January	-0.8	-0.9	-2.7	-3.4	-3.6
February	2.2	1.7	.2	.3	-1.3
March	5.8	5.6	3.3	3.1	1.8
April	10.2	10.6	7.7	7.8	6.6
May	14.2	13.6	12.1	12.3	11.0
June	18.3	18.8	16.4	16.7	15.2
July	22.6	24.5	21.7	21.8	20.3
August	21.2	23.3	19.8	19.9	19.2
September	16.9	18.8	14.8	14.9	14.6
October	11.1	12.3	8.7	9.1	9.0
November	4.2	4.6	2.1	2.2	2.2
December	.4	.1	-1.2	-2.1	-2.0
Annual	10.5	11.1	8.6	8.6	7.7

Table 7.---Estimate of conductive heat discharge from Stillwater hydrothermal system on the basis of method A described in the text.

Temperature range (°C)	Geometric mean temperature (°C)	Thermal gradient ^{1/} ($\times 10^{-3}$ °C cm ⁻¹)	Heat flow ^{2/} ($\times 10^{-6}$ cal cm ⁻² s ⁻¹)	Area ($\times 10^{10}$ cm ²)	Heat discharge ($\times 10^6$ cal s ⁻¹)
20-40	28.3	5.8	14	38.7	5.4
40-60	49.0	13	32	8.9	2.8
60-80	69.3	19	48	4.7	2.3
>80	90.0	26	65	6.8	4.4
Totals				59.1	15

(1) Based on 11°C mean annual temperature at the land surface.

(2) Based on harmonic-mean thermal conductivity of 2.5×10^{-3} cal cm⁻¹ s⁻¹ °C⁻¹.

The above estimate is regarded as approximate because of the paucity of data and the errors introduced by the simplified assumptions of method A. Convective heat transfer by ground-water upflow probably affects thermal gradients in the uppermost 30 m of deposits, so that the assumption of linear conductive gradients in the depth range 0-30 m tends to yield computed heat-flow values that are too small. In addition, the thermal area undoubtedly extends beyond the 20°C isotherm at 30 m depth, which is used in the computation of heat discharge. Therefore, it is believed that the actual net heat discharge is substantially greater than the computed value and probably is within the range of 15 to 25 x 10⁶ cal s⁻¹.

Thermal-Water Discharge

Ground water discharges from the Stillwater thermal area by evapotranspiration, lateral ground-water outflow (chiefly northward), and discharge from domestic and farm wells (of which the net discharge is by evapotranspiration and is relatively small). An unknown proportion of the total discharge is shallow nonthermal water of local derivation. Because of the difficulty in determining the proportions of thermal and nonthermal water in the total discharge, and because the magnitudes and directions of ground-water flow are poorly known, thermal-water discharge is not estimated by the water budget method. Instead, a more reliable estimate is made by the heat-budget method.

The heat carried by the thermal water is assumed to be the excess over normal conductive heat discharge from the thermal area, as derived in the preceding section. Temperature at the deep source of the thermal water is based on the silica-quartz geothermometer. (See table 1 and

Mariner and others, 1974, table 3.) The computation is as follows:

$$\text{Net heat discharge} = 14 \times 10^6 \text{ cal s}^{-1} = 4.4 \times 10^{14} \text{ cal yr}^{-1}$$

$$\text{Net heat content of thermal water} = (159^\circ\text{C} - 11^\circ\text{C})(1.0 \text{ cal g}^{-1}\text{C}^{-1}) =$$

$$\text{Thermal-water discharge} = \frac{4.4 \times 10^{14} \text{ cal yr}^{-1}}{1.48 \times 10^2 \text{ cal g}^{-1}} = 3.0 \times 10^{12} \text{ g yr}^{-1}$$

This is equivalent to a discharge of $3.1 \times 10^6 \text{ m}^3 \text{ yr}^{-1}$ of water at 80°C (the approximate near-surface temperature), or to $3.3 \times 10^6 \text{ m}^3 \text{ yr}^{-1}$ at 159°C (the inferred reservoir temperature).

Thus, $3.3 \times 10^6 \text{ m}^3 \text{ yr}^{-1}$ of water leaving the geothermal reservoir at 159°C would carry $4.4 \times 10^{14} \text{ cal yr}^{-1}$ of heat, all of which is assumed to be discharged by conduction through the near-surface deposits within the thermal area. An additional 1 million cal s^{-1} or $3.2 \times 10^{13} \text{ cal yr}^{-1}$ of heat is discharged as so-called "normal" conductive heat flow from the area.

Hypothetical Model of Hydrothermal-Discharge System

Alinement of the Stillwater thermal area with high-angle Basin and Range faults at Rainbow Mountain 8-10 km to the south and unpublished magnetic and gravity data (O'Neill-Oliphant) suggest that the near-surface high temperatures result from rising thermal water along a north-trending concealed fault or fault zone, as shown on figure 13. The rising thermal water causes a mushrooming of the isotherms near the fault. The velocity of the upflow is sufficient to maintain the temperature of the water near the temperature of the deep source, which is inferred to be close to 160°C on the basis of geochemical data (Mariner and others, 1974). (See table 1.)

The depth and nature of the deep thermal reservoir and the source of recharge for the thermal water are unknown. On the basis of the "normal" regional heat flow at the experimental heat-flow test hole in the Carson Sink, 29 km to the north and temperatures reported from the O'Neill-Oliphant test well, the hydrothermal system appears to be related to deep circulation of meteoric water in an area of "normal" regional heat flow (the first conceptual model described in the section, "Conceptual models of hydrothermal systems") rather than to a shallow-crustal heat source (the second conceptual model). The source of the thermal water probably lies at a depth of several kilometres, well within the pre-Tertiary basement. Admittedly, however, the available data are inconclusive. The sizable extent of the thermal area--which is considerably larger than the other thermal areas studied--suggests that a local heat source of restricted extent, perhaps of the order of several tens of square kilometres, may be present.

Bottom-hole temperatures observed during drilling of the O'Neill-Oliphant geothermal test well, which is about 0.7 km west of the inferred fault that carries the thermal-water upflow, indicate a reversal in thermal gradient below a permeable sand aquifer of probable Tertiary age at a depth of about 430 m. The temperature in the sand aquifer was reported to be 156°C (Beuck, written commun., 1964), only slightly less than the reservoir temperature of 159°C indicated by the silica-quartz geothermometer (table 1). This information suggests that much of the thermal water that rises along the inferred fault discharges laterally into the sand aquifer, in which lateral flow is sufficiently rapid to maintain high temperatures for considerable distances from the fault, as indicated diagrammatically on figure 13.

High temperatures at shallow depths in domestic and farm wells in the central part of the Stillwater thermal area suggest that not all the rising thermal water moves laterally into the prominent sand aquifer of probable Tertiary age; some of the water rises into the predominantly fine-grained Quaternary deposits and discharges laterally into sands within these deposits. Temperatures at a depth of 30 m exceed 80°C in the central part of the thermal area (figs. 12 and 13). The high temperatures at this depth probably result from both upflow of water across the bedding of the predominantly fine-grained lacustrine deposits and lateral flow in the relatively permeable sands. However, none of the upflowing water discharges at the land surface except by evapotranspiration.

SODA LAKES-UPSAL HOGBACK THERMAL AREA

Location

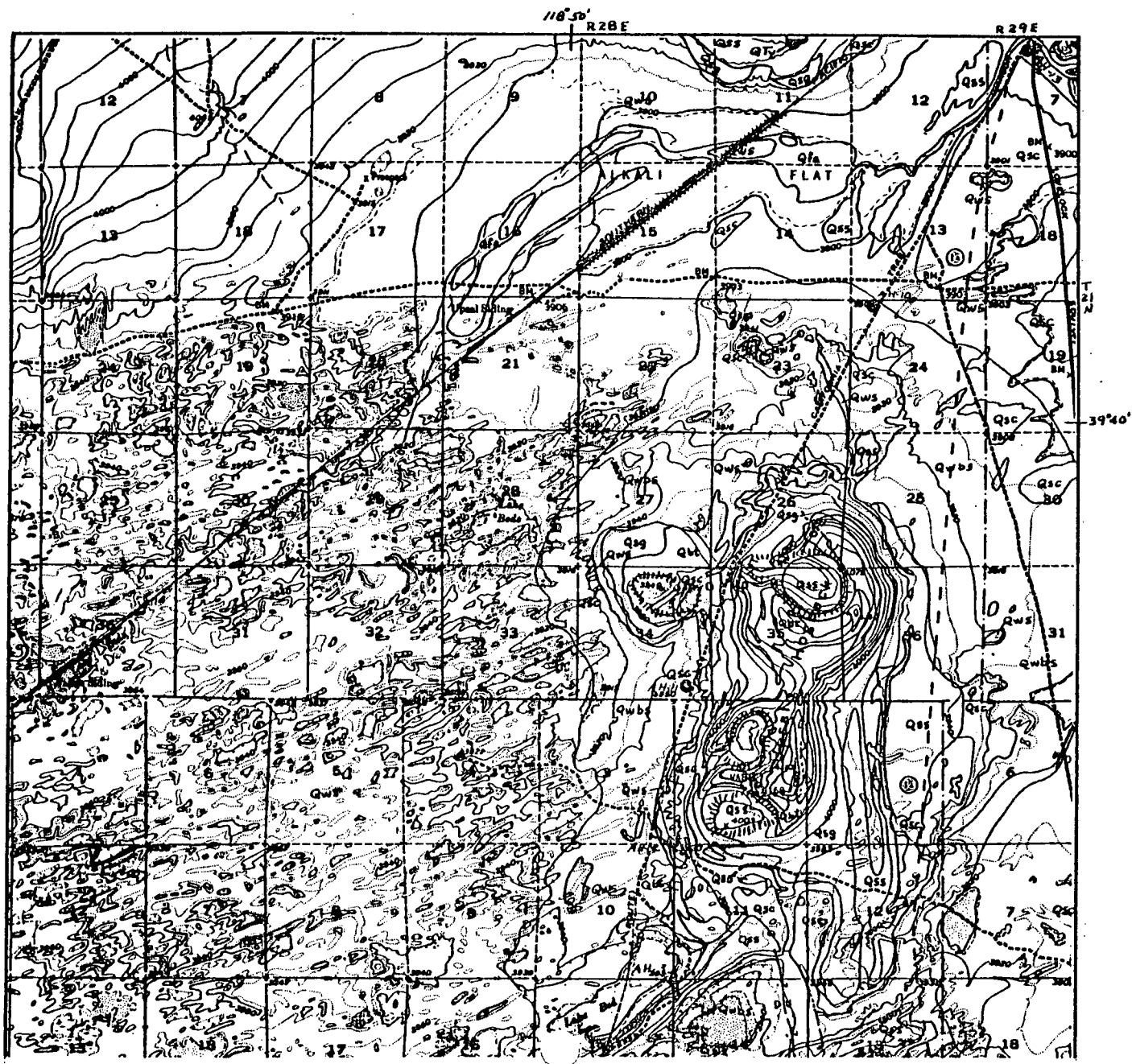
The Soda Lakes-Upsal Hogback thermal area is in the west-central part of the Carson Desert, 12 km northwest of Fallon. The thermal area is elongated toward the north-northeast and lies between two centers of late Quaternary basaltic eruptions, Soda Lakes and Upsal Hogback (fig. 10).

Previous Development

The thermal area is undeveloped except for intermittent cattle grazing. Adjacent lands to the south are irrigated with water from Lahontan Reservoir. The hydrothermal system is undeveloped at present, although a steam well (20/28-28ccb) was used in the past for steam baths. No information about the construction of the steam well is known to be available, except that the well is reported to have been 18 m deep.

Test Drilling

During 1972 and 1973, the U. S. Geological Survey drilled 23 test holes as a part of this study in order to evaluate the near-surface geologic, hydrologic, and thermal characteristics of the area. An additional test hole was drilled by the U. S. Bureau of Reclamation for similar purposes. Data for the U. S. Geological Survey test holes are summarized in table 4. Locations of the test holes are shown on figure 14.



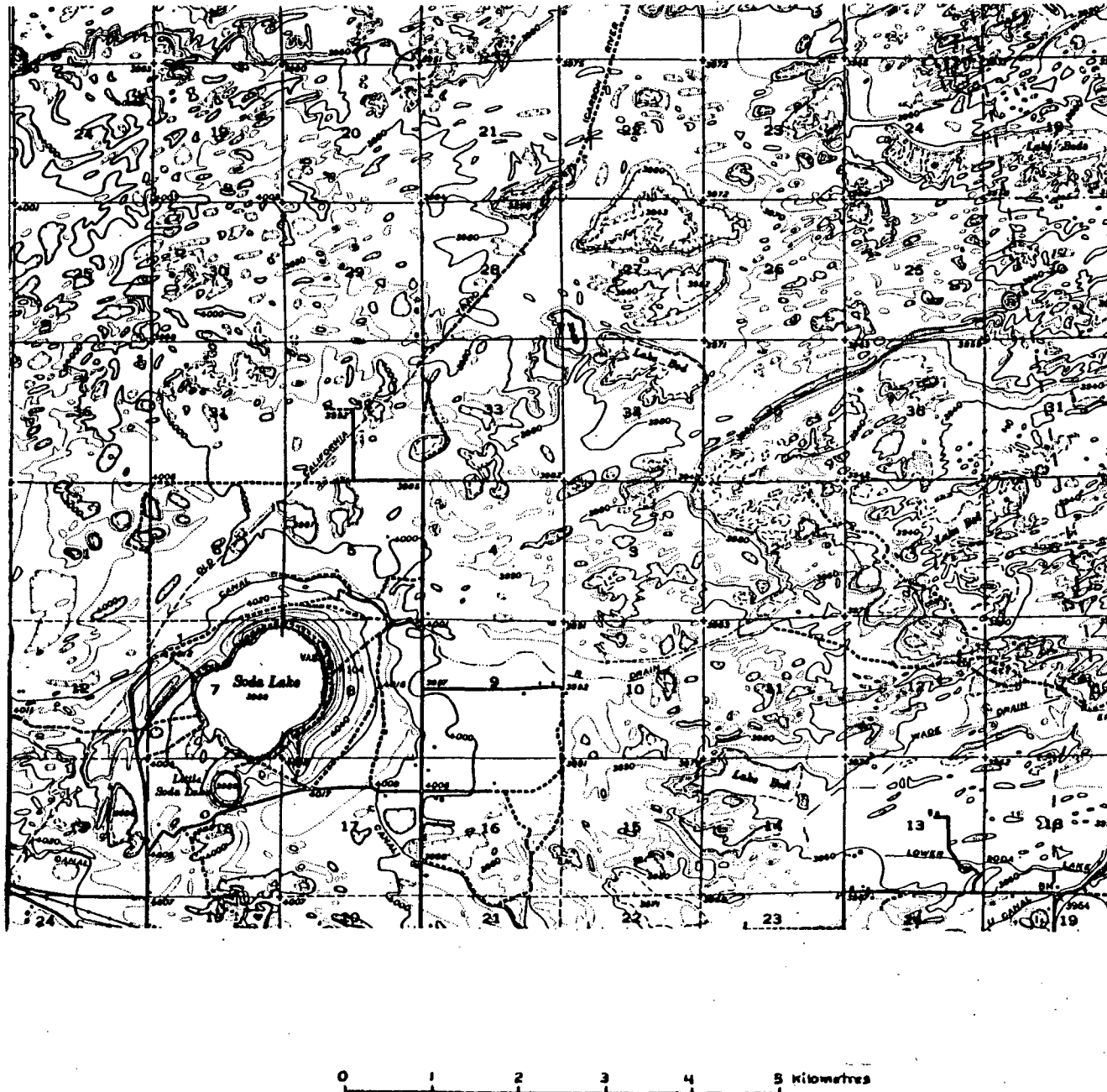
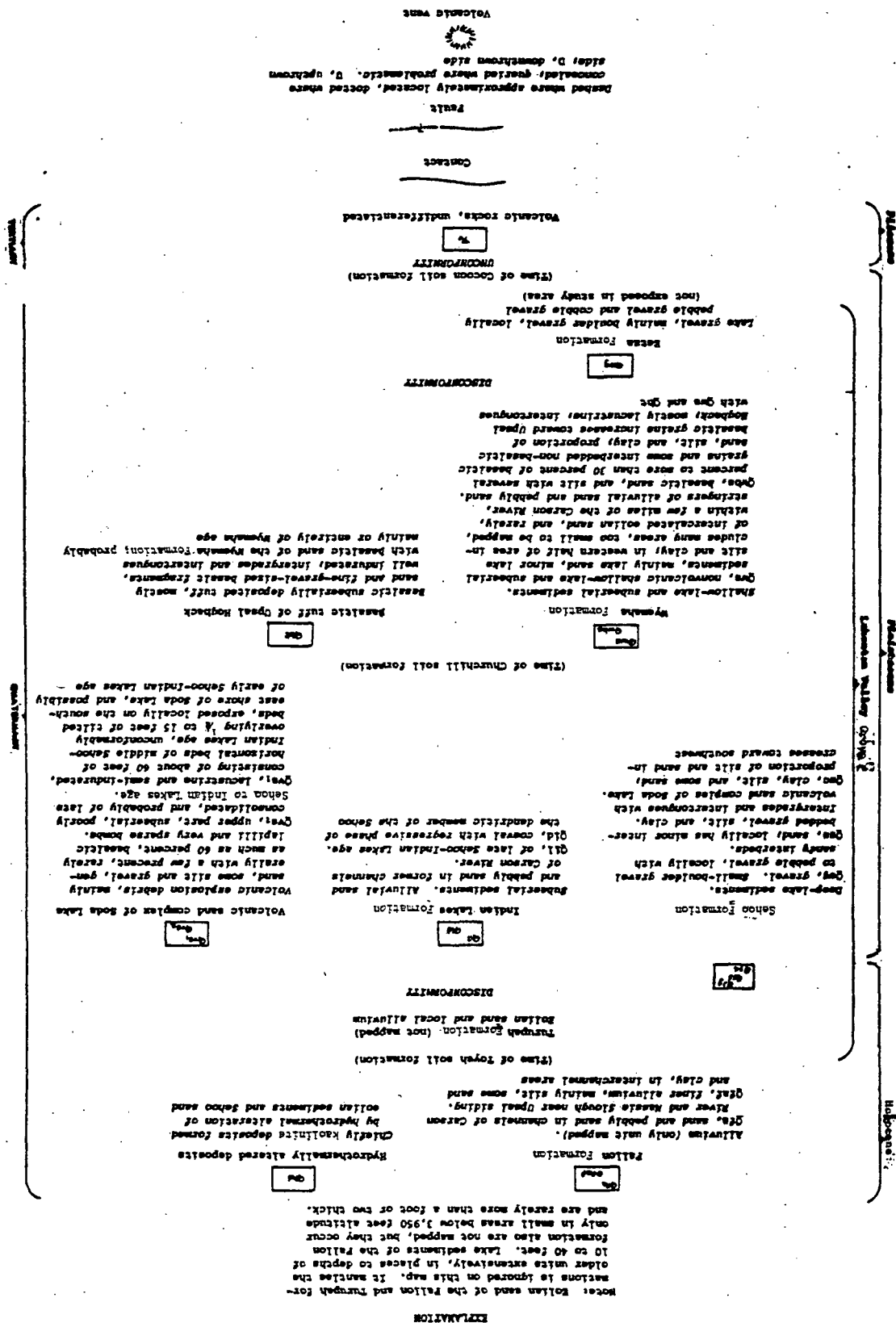


Figure 14.--Geologic map of Soda Lakes-Upsal Hogback thermal area showing

Geology mainly from Morrison, N. B., 1964, Plate 6.



Geology

Exposed and near-surface materials in the thermal area are unconsolidated of late Pleistocene Lake Lahontan and a discontinuous capping of eolian and minor fluvial sediments, largely reworked from the Lake Lahontan deposits. The areal geology shown on figure 14 is based on mapping by Morrison (1964, pl.6), modified during the present study in a small area surrounding the old steam well.

The eolian and minor fluvial sediments, chiefly sand, were assigned by Morrison (1964) to the Turupah Formation of latest Pleistocene age. Birkeland and others (1971) revised its age to Holocene. However, on Morrison's geologic map of the area (1964, pl.6), these sediments are grouped with an upper sand of the Sehoo Formation of Pleistocene age. The Sehoo's age was revised by Birkeland and others (1971) to Pleistocene and Holocene. The sand overlies a clay member of the Sehoo on a surface of moderate local relief, as revealed by data from the U.S. Geological Survey test holes and by exposures on the sides of wind-scoured depressions. Within the thermal area, the capping sand ranges in thickness from 0 to 5 m, and the underlying clay of the Sehoo Formation, from 9 to 10m. In the vicinity of the steam well, the capping sand has been altered in part to kaolinite and various iron oxides or hydroxides by hydrothermal activity, probably chiefly vapor.

Beneath the Sehoo Formation clay is the Wyemaha Formation, of Pleistocene age, generally sandy in the upper part, but containing interbeds of clay and silt. The predominantly nonvolcanic deposits inter-tongue with basaltic sands and lapilli tuff derived from the cinder cones at Upsal Hogback. The basaltic tuff and cinders at Upsal Hogback are the oldest exposed deposits near the thermal anomaly; they are probably coeval with the lower part of the Wyemaha Formation.

Within the depth range of the test holes, probably all the lower deposits belong to the Wyemaha Formation. Morrison (1964) does not specify the age or stratigraphic assignment of the beds underlying the Wyemaha Formation within the thermal area. Presumably some of the deposits represent early stages of Lake Lahontan.

Bedding in the area is nearly horizontal. Present topography is the result chiefly of wind scour during Turupah time (Morrison, 1964). Exposed faults or local flexures are rare. Morrison (1964) mapped two small northeast-striking faults at the Soda Lakes and two north-trending faults south of Upsal Hogback. The latter two faults bound an upthrown block of basaltic tuff of Upsal Hogback, flanked by generally nonvolcanic deposits of the Wyemaha Formation.

Although few faults are exposed, the generally north-northeasterly alignment of Soda Lakes, Upsal Hogback, and the intervening thermal area suggest faults at depth, possibly along a zone of rupture in the consolidated rocks of Tertiary and (or) pre-Tertiary age.

Hydrology

Ground water moves both laterally and vertically through the unconsolidated lacustrine, fluvial, and eolian deposits beneath the area. Nonthermal water derived from infiltrated irrigation water and Carson River water to the south-southwest moves generally north-northeast, toward the western Carson Sink. Thermal water rises from unknown depths, probably through open fractures or faults, into the near-surface deposits, where it also moves laterally toward the north-northeast, in the direction of the potential gradient. The deep, thermal water probably mixes with the

much shallower nonthermal water, but the extent of the zone of mixing or diffusion is not known. Since the early 1900's irrigation and controlled river flow have raised the water table throughout broad areas and have greatly modified the natural flow pattern.

Throughout the thermal area, the water table is 1.5 to 10.7 m below land surface. Seasonal fluctuations range from a few centimetres to about 1 m. At many places, confined conditions exist at depths greater than a few metres below the water table, and the confined potentiometric surface is either above or below the water table. Configuration of the confined potentiometric surface representing a zone 30 m beneath the land surface is shown on figure 15.

The map indicates a dominantly north-northeastward lateral potential gradient of about 0.0017. The altitude of the confined potentiometric surface representing a depth of 30 m beneath the land surface was computed by adjusting the measured water level in the test hole for the difference in potentiometric head between the depth of the well screen and a depth of 30 m, using the vertical potential gradient listed in table 8.

Vertical potential gradients between the water table and screened aquifer zones and depths to confined and unconfined water levels in the test holes are given in table 8. These data indicate the following conditions in the study area:

1. Downward potential gradients in the southwestern part of the study area reflect downward movement of irrigation recharge water from the water table to deeper aquifers.

EXPLANATION

---1202

Potentiometric contour

Shows attitude of confined potentiometric surface. Contour interval 2 metres.

Datum is mean sea level

● AH-4
1215.2

Test hole. Number is altitude of confined potentiometric surface, in metres above mean sea level

N

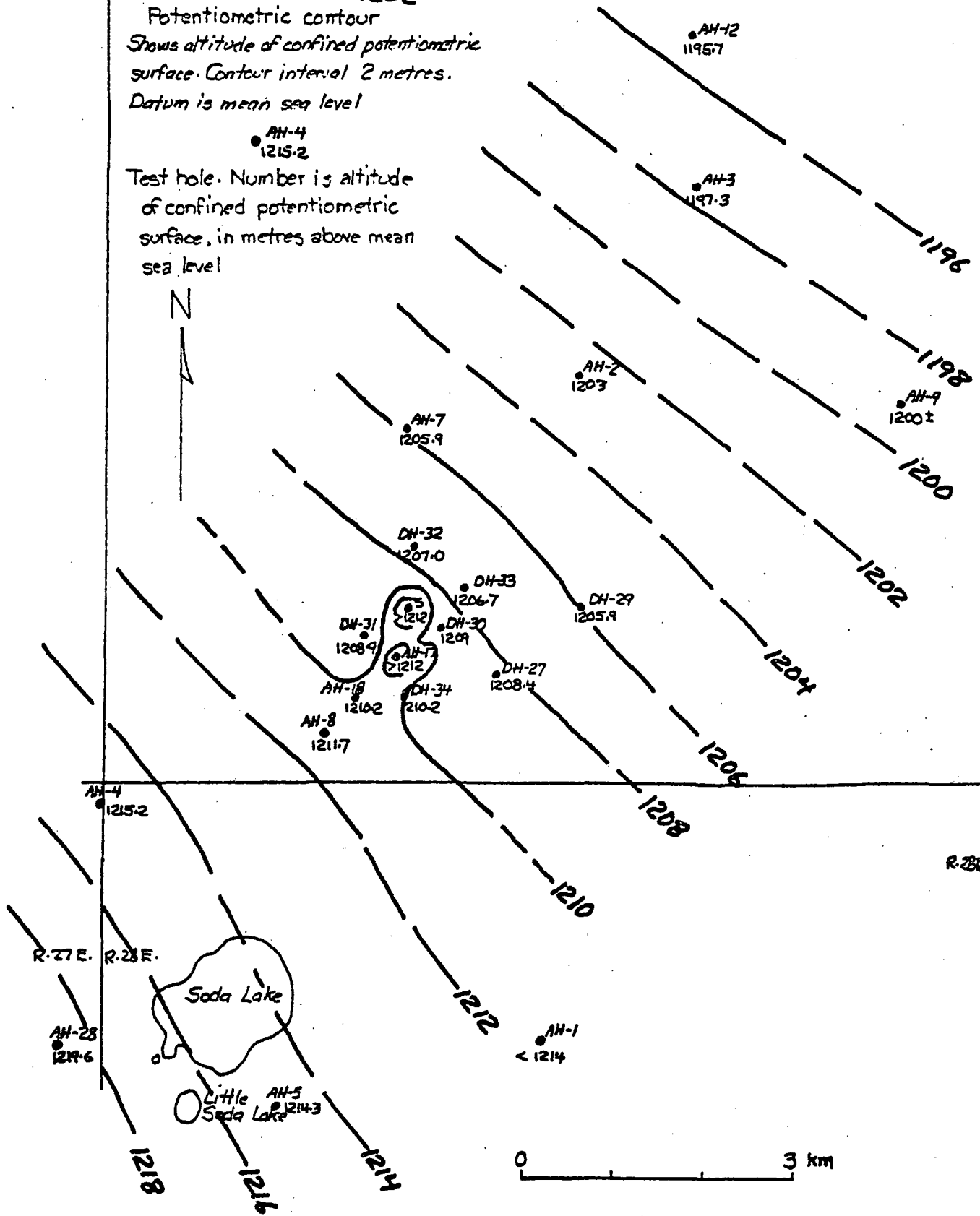


Figure 15. — Map of Soda Lakes - Upsal Hogback thermal area showing configuration of confined potentiometric surface, 1973-74

Table 8.--Vertical potential gradients in Soda Lakes-Upsal Hogback area

Well	Date	Depth to top of screen (m)	Depth to water table (m)		Depth to confluvial potentiometric (m)	Vertical potential gradient
			from Neutron log	from Gamma-gamma log		
CDAH-2	74 04 04	25.91	9.3	9.4	9.28	0
AH-3	73 05 15	43.56	2.1	2.4	2.08	0
AH-4	73 05 18	20.12	1.5	-	3.50	- .11
AH-5	73 05 18	38.71	8.0	8.7	11.83	- .13±
AH-6	73 05 18	42.98	2.3	2.1	6.57	- .11
AH-7	74 03 28	27.7± ²⁾	-	7.3	(?)	(?)
AH-8	73 05 14	37.95	2.7	2.7	5.15	- .071
AH-9	73 05 16	39.32	8.6	8.7	8.65	0
AH-10	73 05 15	32.31	2.7	2.3	2.42	(?)
AH-12	74 04 04	21.46	10.0	10.4	10.75	- .03±
AH-13	73 05 16	21.18	2.5	2.5	2.3	+ .01
AH-17	73 05 15	8.99	-	5.1	2.6	+ .64 ¹⁾
AH-18	73 05 14	41.15	3.6	3.7	4.88	- .034
DH-27	74 03 27	44.07	1.8(?)	7.3(?)	3.23	(?)
AH-28	73 11 27	17.9	0.6±	-	0.74	- .007
DH-29	74 03 27	43.95	2.5(?)	6.0(?)	5.18	(?)
DH-30	73 11 15	39.93	1.3	-	0.45	>+ .02
DH-31	74 03 28	38.01	3.0(?)	6.2(?)	5.59	(?)
DH-32	74 03 27	44.53	6.2	6.2	6.91	- .019
DH-33	74 03 28	43.95	-	6.7	5.25	+ .038 ¹⁾
DH-34	74 03 28	44.44	4.0	5.0	6.78	- .070±

1. Based on gamma-gamma log.

2. Approximate depth to thick mud in pipe.

2. Upward gradients at a few well sites near the hottest parts of the thermal area reflect the rise of thermal water into near-surface aquifers. A part of the upward movement probably reflects thermo-artesian conditions--that is, thermal convection in response to the lower density of the hotter water. Data are not available to estimate the relative magnitude of thermo-artesian and true artesian effects.

3. Vertical potential gradients are nearly zero at a few sites northeast of the hottest part of the area.

4. Upward leakage, probably in response to discharge of ground water by evapotranspiration, is indicated by the vertical gradients in wells in the northeastern part of the area, near Upsal Hogback.

Although vertical potential gradients greatly exceed the lateral gradients at most places, rates of vertical ground-water flow are generally less than rates of lateral flow. The contrast results from the extremely low vertical hydraulic conductivity of the confining beds of clay and silt as compared to the high horizontal hydraulic conductivity of the sand aquifers. Most of the large potential gradients are in the confining beds rather than the aquifers; the observed vertical gradient is the harmonic mean of very high gradients through the confining beds and very low gradients through the aquifers.

Chemical Character of Ground Water

Water samples were collected by bailing from nine test holes in the area. Before bailing, the test holes were developed by air-lift pumping so that samples representative of water in the formation adjacent to the well point or well screen could be obtained. The gross characteristics of the water, as indicated by the specific conductance, concentration of dissolved solids, and concentration of chloride, are summarized in table 9. The results indicate substantial variation in salinity; concentration of dissolved solids ranges from about 600 to about 6,000 mg l⁻¹, a tenfold variation. This variation may be caused by uneven mixing from place to place of infiltrated dilute (?) river water and irrigation water with more saline ground water.

Reasonably complete chemical analyses are available for only three samples, from test holes CD AH-4, 8, and 9. These data (not shown in table 9) disclose the following chemical characteristics: (1) sodium is the dominant cation in all three samples; (2) cation proportions are variable; and (3) water from test hole AH-4 is extremely hard, whereas the samples from test holes AH-8 and 9 are very soft.

No chemical data have been collected thus far that would allow characterization of the upflowing thermal water. Because of the evident variability of the shallow nonthermal water in the system, it may be difficult to select chemical parameters that would distinguish the thermal from the nonthermal water.

Table 9.--Chemical analyses of water samples from test holes in Soda
Lakes-Upsal Hogback Area.

Test hole	Depth to top of well screen (m)	Specific conductance (micromhos cm^{-1} at 25°C)	Concentration of Dissolved Solids (mg l^{-1})		Concentration of chloride (mg l^{-1})
			Determined	Computed ^{1/}	
CDAH-2	25.91	4,720		2,830	1,440
AH-3	43.56	2,370		1,420	507
AH-4	20.12		5,890		490
AH-8	37.95		612		160
AH-9	39.32		2,140		990
AH-10	32.31	4,150		2,490	1,020
AH-12	21.46	9,730		5,840	3,140
AH-18	41.15	1,030		618	124

^{1/} Computed by multiplying specific conductance by 0.6.

Subsurface Temperature Distribution

The distribution of temperature at a depth of 30 m below land surface is shown on figure 16. Except for the hottest part of the area, the isotherms are based on temperatures measured in the test holes shown on the map. On the basis of the test-hole data, only one hot center, in the vicinity of the old steam well, is indicated. However, measurements made at 1 m depth at 100 sites during the later stages of the fieldwork indicated two separate thermal highs, as shown on figure 16. Both highs are elongated toward the northeast and are separated by a similar-trending area of lower temperature between the northwestern high centered at the steam well and the southeastern high centered about 70 m west of test hole CD AH-17. The same pattern is shown on oblique snow-melt photographs taken in January 1974. The southeastern thermal high is indicated by a dense growth of Russian thistle, which is apparent on vertical color aerial photographs taken in February 1974. The pattern strongly suggests that thermal water rises into near-surface aquifers through somewhat elongate parallel or en echelon conduits, possibly along concealed faults. That at least a part of the rising water is boiling is indicated by discharge of steam from the steam well and a fumarole a few metres away and by high temperatures (up to more than 90°C) at depths of 1 m in nearby shallow temperature holes.

The most striking feature of the thermal area is its asymmetry. The isotherms are elongated strongly toward the north-northeast, in the direction of the lateral ground-water gradient. The hottest areas are near the south-southwest margin so that horizontal thermal gradients are large toward the south-southwest and small toward the north-northeast. The pattern suggests dispersion of thermal water in the direction of

regional ground-water flow from two sources of restricted extent. In none of the other thermal areas studied is the effect of lateral heat transport by ground-water flow so striking.^{1/}

Heat Discharge

The heat carried by lateral flow of thermal water through shallow sand aquifers is discharged by conduction through the near-surface deposits. Thermal gradients measured in most of the test holes are affected by vertical ground-water flow, however, so that reasonably accurate estimates of the conductive heat discharge from the thermal area cannot be made. In addition, data are insufficient to define accurately the positions of the cooler isotherms, especially in the eastern and southeastern parts of the area. For these reasons, only a crude estimate of the heat discharge is made, using method A described earlier. As in the Stillwater thermal area, the 20°C isotherm at a depth of 30 m is used as the boundary of the hydrothermal-discharge area, and the mean annual temperature at the land surface is assumed to be 11°C. The harmonic-mean thermal conductivity of the materials in the depth range 0-30 m is estimated to be $2.3 \times 10^{-3} \text{ cal cm}^{-1} \text{ s}^{-1} \text{ }^\circ\text{C}^{-1}$ on the basis of the procedure described in the section "Estimates of heat discharge"

^{1/} Recent data not publicly available from proprietary sources suggest that not all the asymmetry of the thermal area is due to lateral transport of heat by north-northeastward ground-water flow; a part of the asymmetry may be due to leakage of rising thermal water into progressively deeper aquifers toward the north-northeast. The recent data also indicate that the conduits may be more elongate than is suggested by the temperature pattern shown on figure 16.

Table 10.--Estimate of conductive heat discharge from Soda Lakes-Upsal Hogback hydrothermal system on the basis of method A described in text.

Temperature range (°C)	Geometric-mean temperature	Thermal gradient ^{1/} (x 10 ⁻³ C cm ⁻¹)	Heat flow ^{2/} (x 10 ⁻⁶ cal cm ⁻² s ⁻¹)	Area (x 10 ¹⁰ cm ²)	Heat discharge (x 10 ⁶ cal s ⁻¹)
20 - 30	24.5	4.5	10	13.05	1.3
30 - 40	34.5	7.9	18	4.00	.72
40 - 60	49.0	13	30	2.40	.72
60 - 80	69.3	19	44	.83	.37
80 - 100	89.4	26	60	.64	.38
100 - 120	109.5	33	76	.17	.13
120	121.0	37	85	.04	.03
Totals				21.13	3.6

^{1/} Based on 11°C mean annual temperature at the land surface

^{2/} Based on harmonic-mean thermal conductivity of 2.3×10^{-3} cal cm⁻¹ s⁻¹ °C⁻¹.

The total near-surface conductive heat discharge, estimated by method A, is $3.6 \times 10^6 \text{ cal s}^{-1}$. Derivation of the estimate is given in table 10. "Normal" conductive heat discharge from the area enclosed by the 20°C isotherm at a depth of 30 m is computed on the basis of a "normal" heat flow of 2 HFU:

$$(21.13 \times 10^{10} \text{ cm}^2)(2 \times 10^{-6} \text{ cal cm}^{-2}\text{s}^{-1}) = 0.42 \times 10^6 \text{ cal s}^{-1}$$

Net conductive heat discharge is then

$$(3.6 - 0.42) \times 10^6 \text{ cal s}^{-1} = 3.2 \times 10^6 \text{ cal s}^{-1}$$

This estimate is considered closer to a minimum than to an average within the probable range of values. Further studies, presently underway, will result in an improved estimate, using method B described in this report.

Water Budget

Data required for an estimate of thermal-water discharge from the Soda Lakes-Upsal Hogback system are not available. Instead, a generalized ground-water budget for the tract that includes the irrigated land surrounding Soda Lakes as well as the thermal area to the north-northeast is presented in table 11.

The magnitude of the outflow in the budget can be estimated within narrower limits than the magnitude of the inflow. Lake-surface evaporation is computed as the product of the free (non-vegetated) water-surface area (3.1 km^2) and a net rate of annual evaporation 120 cm based on estimates by Rush (1972) and Kohler and others (1959). Lateral ground-water outflow toward the north-northeast is computed on the basis of an average horizontal potential gradient of 0.0017 determined from figure 15 an effective width of flow cross section of 10 km, and transmissivity of $1,200 \text{ m}^2 \text{ day}^{-1}$ at a prevailing temperature of 20°C . Discharge by ground-water evapotranspiration is computed on the basis of an area of 20 km^2 and an assumed average rate of 6 cm per year.

Table 11.--Ground-water budget for Soda Lakes-Upsal Hogback Area

Budget item	Annual volume of water ($\times 10^6 \text{ m}^3$)
OUTFLOW:	
Evaporation from lake surfaces	3.7
Lateral ground-water outflow	7.5
Ground-water evapotranspiration	1.2
TOTAL OUTFLOW (ROUNDED)	12
INFLOW:	
Seepage losses from irrigation canals	12
Infiltration to saturated zone from irrigated fields	Unknown
Seepage loss from Carson River	Unknown
TOTAL INFLOW (ROUNDED)	>12

The inflow items in the budget are difficult to estimate within reasonable limits. The only item for which a reliable estimate has been made is seepage losses from irrigation canals. By a series of tests to determine effectiveness of chemical sealants in reducing seepage losses, the U. S. Bureau of Reclamation has estimated the leakage from major canals in the present study area at roughly $12 \times 10^6 \text{ m}^3 \text{ yr}^{-1}$ (10,000 ac-ft yr^{-1}) (John Gallagher, written commun., 1974). This item, by itself, equals the estimated total outflow. Water lost from the Carson River by seepage probably does not enter the Soda Lakes area during at least half the year, owing to the high ground-water levels maintained by leakage from major canals (Lee and Clark, 1916, p. 683). Underflow of water that has infiltrated to the saturated zone from irrigated fields also may be similarly restricted. However, present data are too scarce and incomplete to evaluate these two items of ground-water inflow to the study area. The budget items most likely to introduce large errors in the overall budget, if sizable percentage errors exist in their evaluation, are the estimates of lateral ground-water outflow and seepage losses from irrigation canals because they are the major items of outflow and inflow.

Nature of Hydrothermal System

Data obtained in this study permits only a sketchy and tentative inference as to the nature of the Soda Lakes-Upsal Hogback hydrothermal system.

The depth and extent of the thermal reservoir and the source of the recharge are unknown, although the most likely source would appear to be the Carson River and the irrigation system to the south. Temperature of the source of the rising thermal water is not known but it is probably much greater than 105°C , the highest temperature observed in the test holes.

Sparse and somewhat equivocal data from test holes and wells less than 200 m in depth throughout the Carson Desert suggest that heat flow outside the known convective hydrothermal systems, Stillwater and Soda Lakes-Upsal Hogback, probably is not much greater than average for the northern Great Basin region--perhaps on the order of 2 HFU. However, local shallow heat sources of restricted extent cannot be ruled out with present information. Thus, it seems most likely that the thermal water in the Soda Lakes-Upsal Hogback system has circulated to depths of several kilometres, but depths of circulation would be less if a local heat source is present.

The distribution of temperature observed in the shallow test holes in this study suggests that the thermal water rises along steeply inclined, perhaps vertical, fault-controlled conduits and discharges into sand aquifers between confining beds of lacustrine clay and silt. Some of the thermal water nearly reaches the land surface, but none presently discharges in hot springs. The thermal water flows laterally in the sand aquifers toward the northeast or north-northeast, in the direction of the horizontal component of the potential gradient, but also moves more slowly upward across the confining beds to discharge ultimately by evapotranspiration.

Mixing of thermal and nonthermal waters probably occurs along the margins of the thermal-water upflow and in the shallow aquifers. However, the mechanisms of the mixing process are poorly understood, and the width of the zone of mixing is unknown.

BLACK ROCK DESERT

Hydrogeologic Setting

The southern and central parts of the Black Rock Desert include several groups of hot springs and surrounding thermal areas. Three of the areas have been classified as Known Geothermal Resources Areas (KGRA's): Gerlach, Fly Ranch, and Double Hot Springs (fig. 17-). Except for Hualapai Flat, which includes Fly Ranch KGRA, the water resources of the region are largely undeveloped. Ground water is pumped for irrigation use at Hualapai Flat. The hot springs are undeveloped except for bathing and minor stock water supply. Gerlach and Empire, the only communities, are in the southwestern part of the area, about 145 km by road north of Reno, Nevada.

The Black Rock Desert consists of a large playa having several arms or embayments and rimmed by rugged mountain ranges. The playa is nearly flat and has an altitude of about 1,190 m above mean sea level. Piedmont slopes between the playa and the mountains are generally narrow and occupy only a minor part of the total area. The mountains are largely of fault-block origin and rise to altitudes as much as 2,740 m above sea level in the Granite Range, 16 km north of Gerlach. The mountains and bordering Basin and Range faults generally trend north, but there are local departures from the dominant pattern.

The mountains are composed of a variety of consolidated to semi-consolidated rocks which range in age from Paleozoic to Cenozoic (middle Tertiary). Volcanic rocks of Tertiary age are extensive, but none are known to be younger than about 15 m.y. (McKee and Marvin, 1974). The intervening basins are underlain to unknown depths by unconsolidated to semiconsolidated deposits of late Tertiary and Quaternary age. The upper part of this fill consists of predominantly fine-grained deposits of Lake Lahontan (late Pleistocene), overlain by similar

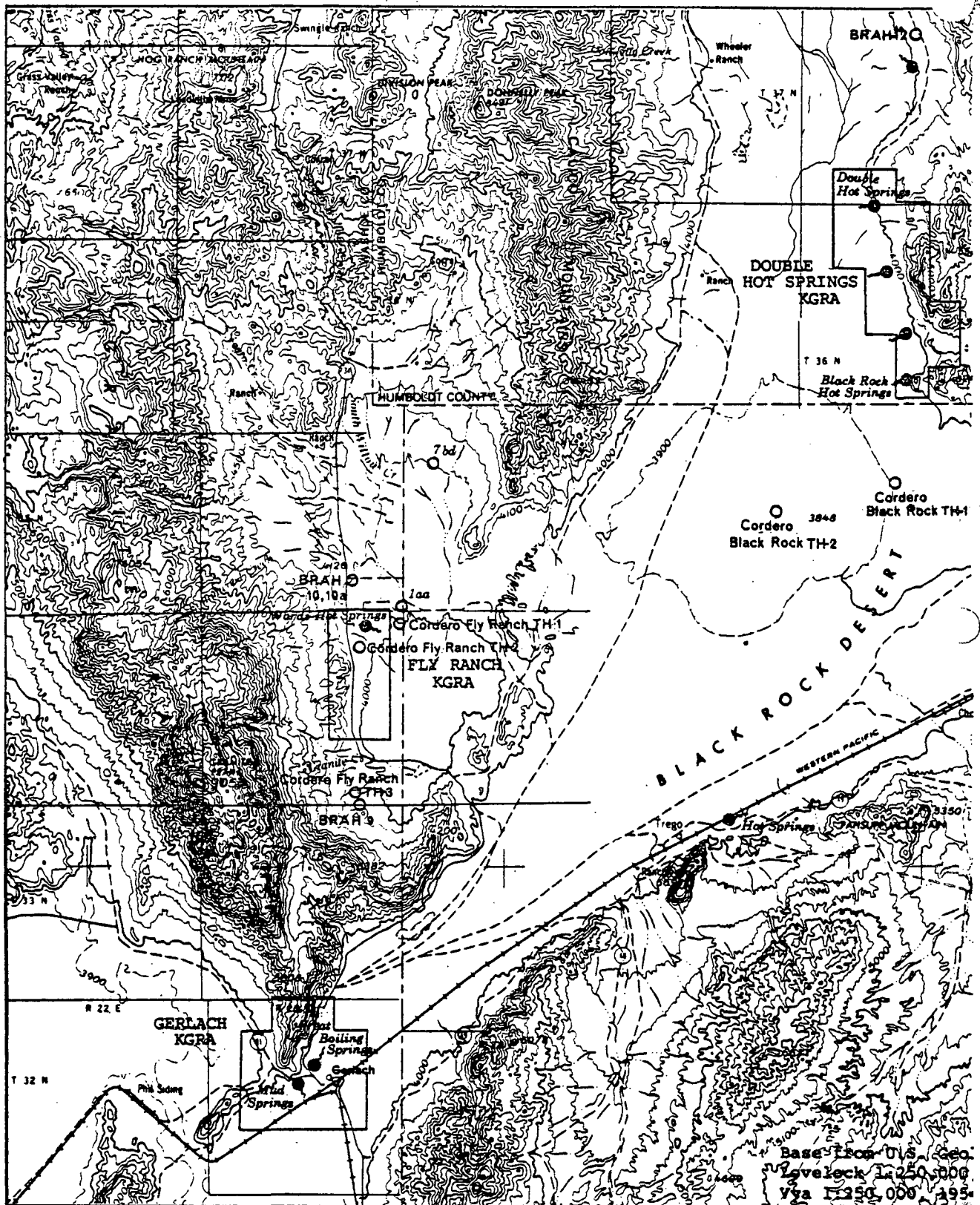
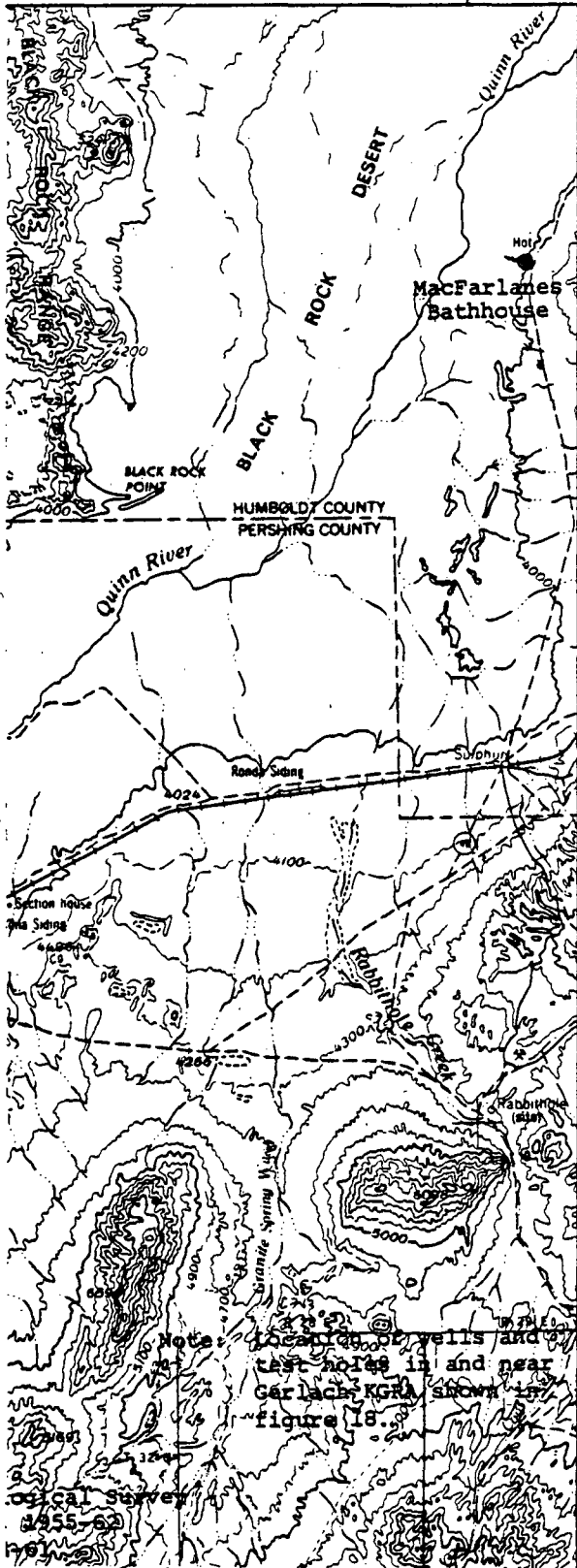


Figure 17.--Map of southern Black Rock Desert showing location of test holes, wells, and thermal springs

118°45'



EXPLANATION

● Thermal spring

○ Cordero Black Rock TH-2

Cordero Mining Co.
test hole and name

○ BRAH-120

U.S. Geological Survey
test hole and name

○ 7bd

Well used as data point,
and location number



Boundary of KGRA
(known geothermal resource area)

40°45'

playa deposits of Holocene age. Coarse-grained near-shore deposits are locally abundant, as near Gerlach, and wave-cut shorelines are prominent throughout the area on mountain slopes below an altitude of 1,335 m.

The playa floor of the Black Rock Desert serves as a sump for the Quinn River and local runoff from the bordering mountain ranges. Ground water also discharges by evaporation from the playa and by evapotranspiration from the adjacent piedmont slopes, where the water table is within reach of the roots of phreatophytes. Ground-water discharge has increased in Hualapai Flat since the advent of irrigated agriculture in the early 1960's (Harrill, 1969).

Recharge to the ground-water system in the southern and central Black Rock Desert occurs chiefly in the Granite Range and to a lesser degree in the northern Black Rock Range and the Selenite Range (fig.17). The highest part of the Granite Range, about 16 km north of Gerlach, receives more than 500 mm average annual precipitation (fig.3), in large part as snow. This area probably is the main source of recharge for the southern Black Rock Desert.

Some recharge takes place where storm runoff and snowmelt runoff crosses the small alluvial fans and piedmont slopes, but a significant part also takes place directly through fractured, weathered, and colluvial-mantled bedrock in the higher mountain areas. It is likely that most of the recharge to the deep, thermal ground-water system, is through the bedrock of the high mountain areas.

Test Holes

The U. S. Geological Survey bored or drilled 23 test holes in the central and southern Black Rock Desert as a part of this study. The test holes range in depth from 1.7 to 45.7 m. All are finished with 3.8-cm or 5.1-cm pipes fitted with screens or well points to permit acquisition of hydrologic as well as temperature data. Test-hole data are summarized in table 12; locations are shown on figures 17 and 19.

In 1972 the Cordero Mining Company drilled eight temperature test holes in the same area. These holes were finished with 3.2-cm black-iron pipes, capped at the bottom and filled with water. The holes range in depth from 111.3 to 274.3 m. Locations are shown on figures 17 and 19.

Table 12.--Data for U.S. Geological Survey test holes in Black Rock Desert

Type of completion: Casing type indicated by "St" (steel) or "P" (PVC).

Wells capped and filled with water are indicated by "C". Wells with well-point screens or perforations at bottom are indicated by "Sc".

Depth to water table: Depth below land-surface datum. Obtained from neutron log. Accuracy about ± 0.5 metre except in clay where capillary fringe may cause larger errors.

Static water level: Depth below land-surface datum.

Geophysical logs available: Gamma ("G"), gamma-gamma ("G²"), neutron ("N"), resistivity ("R"), and temperature ("T").

Well number	Location	Depth (metres below land surface)	Casing		Land-surface altitude (m)	Depth to water table			Static confined water level		Geophysical logs available	Remarks
			Inside diameter (cm)	Type of completion		Metres below land surface	Source of data	Date	Metres below land surface	Date		
BRAN-1A	32/23-3dcb1	44.2	3.8	St, Sc	1,194.8	-	-	-	+1.87	73 10 04	G, T	
AR-1B	32/23-3dcb2	1.8	5.1	P, Sc	1,194.8	1.19	N	73 10 04	-	-	-	Water-table
AR-2A	32/23-21bbb1	45.1	3.8	St, Sc	1,197.9	-	-	-	.44	73 10 04	G, G ² , N, T	
AR-2B	32/23-21bbb2	2.7	5.1	P, Sc	1,197.9	2.46	N	73 10 04	-	-	-	Water-table well
AR-3A	32/23-1hced1	6.6	3.8	St, Sc	1,193.3	-	-	-	.97	73 10 04	G, G ² , N, T	
AR-3B	32/23-1hced2	45.1	3.8	St, Sc	1,193.3	-	-	-	>2.04	73 10 04	G, G ² , N, T	
AR-3C	32/23-1hced3	2.0	5.1	P, Sc	1,193.3	.86	N	73 10 04	-	-	-	Water-table well
AR-4A	32/23-21aad1	45.1	3.8	St, Sc	1,196.6	-	-	-	>1.96	73 10 04	G, G ² , N, T	
AR-4B	32/23-21aad2	1.7	5.1	P, Sc	1,196.6	>1.44 (dry)	N	73 10 04	-	-	-	Water-table well; bottom filled with silt.
AR-5	32/23-16aab1	13.1	3.8	St, Sc	1,214.6	7.3	N	73 05 08	-	-	G, G ² , N, T	
AR-6	32/23-16aab2	44.8	3.8	St, Sc	1,205.5	4.6	N	73 05 08	8.32	73 10 04	G, G ² , N, T	
AR-7	32/23-19aab1	45.1	3.8	St, Sc	1,196.3	5.8	N	73 05 08	6.61	73 10 04	G, G ² , N, T	
AR-8A	32/23-3aab1	45.1	3.8	St, Sc	1,192.4	-	-	-	>3.55	73 10 04	-	
AR-8B	32/23-3aab2	1.8	5.1	P, Sc	1,192.4	1.26	N	73 10 04	-	-	-	Water-table well filled with mud to 60 cm.
AR-9	33/23-2a	31.1	3.8	St, Sc	1,240 ±	-	-	-	.68	72 10 31	G, G ² , N, T	
AR-10A	35/23-35ba1	20.1	3.8	St, Sc	1,250 ±	-	-	-	11.48	73 05 10	G, G ² , N, T	
AR-10B	-35ba2	27.4	3.8	St, Sc	1,250 ±	11.0	N	73 05 10	11.24	73 05 10	G, G ² , N, T	
AR-11	-35ba	41.1	3.8	St, Sc	1,250 ±	6.2	N	73 05 10	6.36	73 05 10	G, G ² , N, T	
AR-12	37/26-3c	45.1	3.8	St, Sc	1,230 ±	-	-	-	-	-	-	
AR-13A	33/23-35cab1	45.7	3.8	St, Sc	1,190.2	-	-	-	3.55	73 10 04	G, G ²	
AR-13B	33/23-35cab2	3.1	5.1	P, Sc	1,190.2	1.13	N	73 10 04	-	-	-	Water-table well
BR-14	32/23-15caa	45.6	3.8	St, Sc	1,201.5	-	-	-	>1.22	73 10 07	R	
BR-15	32/23-10cab	30.8	3.8	St, Sc	1,210.7	6.1	-	-	2.85	73 10 07	R	

Heat Flow Outside Thermal Areas

In July 1973, John Sass and R.K. Hose of the U.S. Geological Survey, Menlo Park, Calif., made temperature measurements in the Cordero Mining Co. test holes in support of this study. Six of the eight holes are within areas affected by convection of thermal water and provide data to supplement information from the U.S. Geological Survey test holes. However, two of the holes are in the central part of the Black Rock Desert, at places apparently unaffected by local convection of thermal water. The temperature measurements in these two holes furnish general information on regional heat flow similar to that obtained from the U.S. Bureau of Reclamation experimental heat-flow test hole in the Carson Sink described earlier.

The temperature profile in Cordero Black Rock test hole 1, 2 km south of Black Rock, is presented in figure 18. The thermal gradient for the depth interval 54.9 to 204.2 m is $75.8^{\circ}\text{C km}^{-1}$, about the same as that measured in the heat-flow test hole in the Carson Sink. The driller's log of the Cordero test hole reports predominantly clay (probably lacustrine) throughout the measured interval. The average thermal conductivity of the lacustrine clay is likely about the same as that measured in the cores from the test hole in the Carson Sink, that is, about $2 \times 10^{-3} \text{ cal cm}^{-1} \text{ s}^{-1} \text{ }^{\circ}\text{C}^{-1}$. (See table 2.) The corrected heat flow, therefore, is probably not more than 2 HFU--not unusually high for the northern Basin and Range province.

The thermal gradient in Cordero Black Rock TH-2, 2.5 km west-southwest of TH-1, is $61.6^{\circ}\text{C km}^{-1}$ for the depth interval 68.6 - 274.3 m, even less than that in TH-1. The corrected heat flow at the site of TH-2 may be no more than about 1.5 HFU.

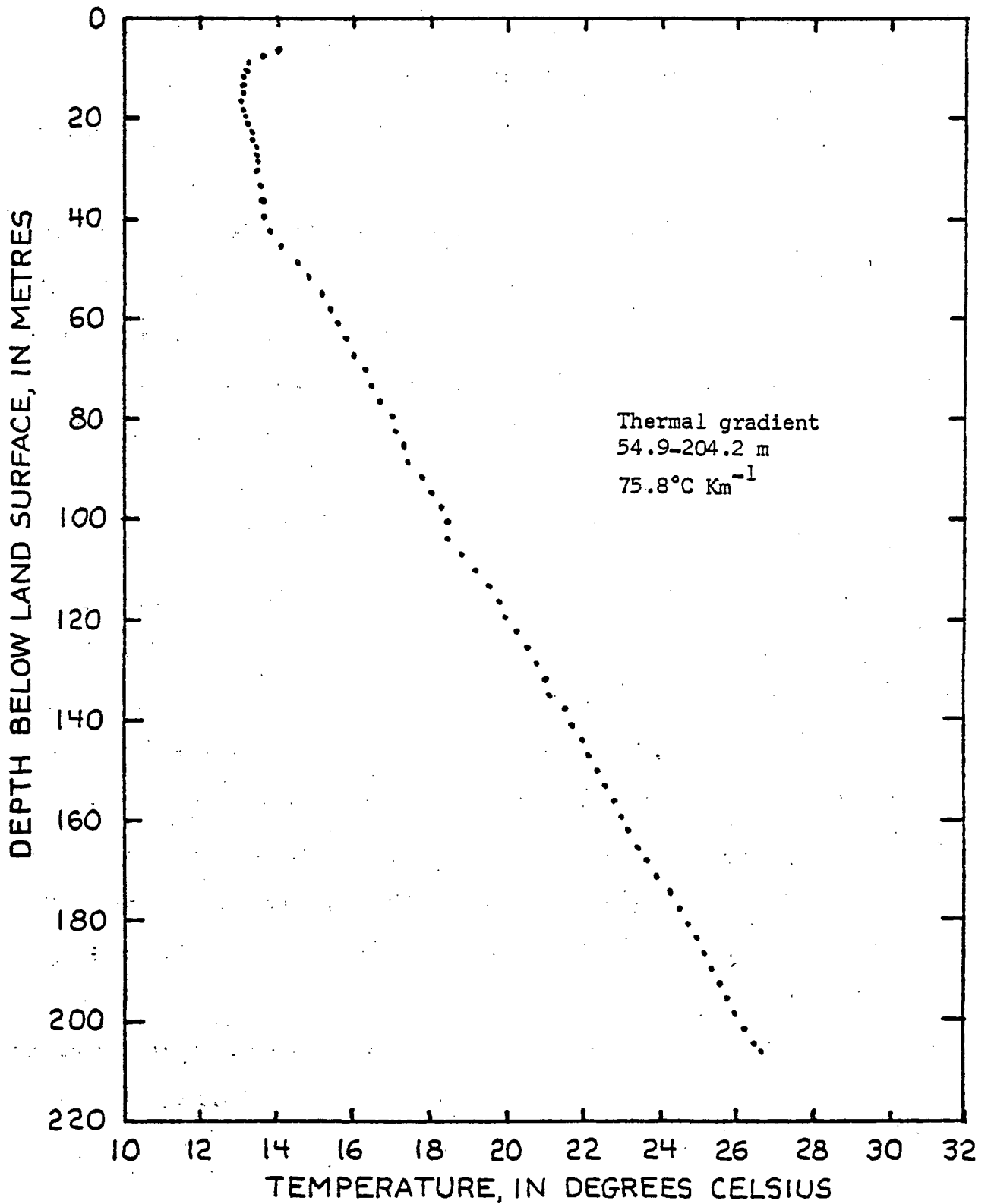


Figure 18.—Temperature profile in Cordero Black Rock 1 temperature test hole, 13 July, 1973

[Temperatures measured with thermistor equipment by John Sass and R. K. Hose, U. S. Geological Survey]

Thermal Areas

There are several known thermal areas within the southern and central Black Rock Desert area. Three of these have been classified as Gerlach, Fly Ranch, and Double Hot Springs KGRA's. All three areas have been explored by test drilling during this study, although in only the Gerlach area were sufficient holes drilled to define the extent of the near-surface thermal anomaly. In addition to the above three areas, thermal areas of unknown extent surround the hot springs near Trigo, 25 km northeast of Gerlach, and West Pinto and East Pinto Springs, 90 km northeast of Gerlach.

Double Hot Springs form two large orifice pools at the north end of a chain of hot springs some 11 km in length. The springs are probably along a Basin and Range fault on the west side of a range of low hills which constitutes the southern Black Rock Range. U. S. Geological Survey test hole BR AH-9, 9 km north of Double Hot Springs, encountered warm ground (although no temperatures were measured in this test hole subsequent to completion), which suggests that the thermal area associated with the Double Hot Springs fault extends at least 9 km north of those springs.

The hot springs at Fly Ranch, in the Hualapai Flat area (Wards Hot Springs on fig. 17), appear to be a part of only one of several localized hydrothermal systems, although available information is insufficient to define the extent and nature of these systems. Test holes BR AH-10A, B, and 11, 2.6-3.1 km northwest of the springs, and flowing thermal wells penetrate warm ground, but an unused farm well 33 m in depth only 1 km east of the springs contains water of near-normal temperature. The thermal areas near Fly Ranch may be related to a series of subparallel faults that cross Hualapai Flat in a northeasterly direction (Harrill, 1969, p. 1).

A thermal area of unknown extent is present near the south end of Hualapai Flat; about 1.5 km south of Granite Ranch and 10 km south of Fly Ranch. No thermal water discharges at the land surface. The presence of the thermal area was first detected in a farm well, now abandoned and filled in. Later, Cordero Fly No. 3 test hole near the old well also penetrated thermal water, as did U.S. Geological Survey test hole BR AH-9, 0.5 km southwest of the Cordero Test hole. The temperature profile in the Cordero test hole indicates a reversal in thermal gradient below a depth of 45 m, which suggests lateral flow of thermal water through an aquifer at that depth. The thermal water presumably moves into the aquifer from much greater depth along a concealed conduit, probably of fault origin.

The thermal area at Gerlach was explored with 18 shallow test holes of the U. S. Geological Survey and 3 deeper test holes of the Cordero Mining Company. Much more intensive study was made of this thermal area than of the aforementioned areas; the results are described in some detail in the following section.

GERLACH THERMAL AREA

Geographic and Geologic Setting

The Gerlach thermal area is at the south end of the Granite Range in southern Black Rock Desert (fig.17). Most of the thermal area is within the Gerlach KGRA, which encompasses 3,631 ha and includes the town of Gerlach.

The thermal area includes two major groups of springs and four individual springs. The larger group, Great Boiling Springs, 1.4 km northwest of Gerlach, is used for bathing and was the site of a small borax works many years ago. Mud Springs, 1.9 km west of Gerlach, is the source of water for livestock and irrigation of pasture.

The hot springs issue from unconsolidated lacustrine and alluvial deposits, but the thermal water probably has been in contact with granodiorite and related plutonic rocks of the Granite Range throughout most of its paths from probable recharge areas high in the range to where it rises into the unconsolidated deposits beneath the springs. The distribution of exposed rocks and deposits near the thermal area is shown on figure 19. Both the unconsolidated deposits and the granodiorite are altered hydrothermally along a fault west of Great Boiling Springs and in places are difficult to distinguish from each other.

Basin and Range faults are prominent, as shown on figure 19. Deposits as young as Holocene are offset. Some faults in lacustrine and alluvial fan deposits near the hot springs may represent rupture of incompetent materials in response to movement along a single fault zone in the underlying granodiorite.

The granodiorite is highly jointed within the area shown on figure 19. Spacing of joints ranges from a few centimetres to several metres. Approximate strikes and dips of the most prominent sets are listed below:

<u>Strike</u>	<u>Dip</u>
N. 42° - 50° W.	90° - 70° S.W.
N. 82° - 86° W.	45° - 50° S.
N. 18° - 22° E.	40° - 45° N.W.
N. 0 - 2° W.	40° - 45° E.
N. 68° - 72° E.	85° N. - 85° S.

Figure 19 also shows lineaments apparent in the field or on aerial photographs but of undetermined origin. Lineaments in the Granite Range may be traces of joints or faults; those in the unconsolidated deposits may be fault traces.

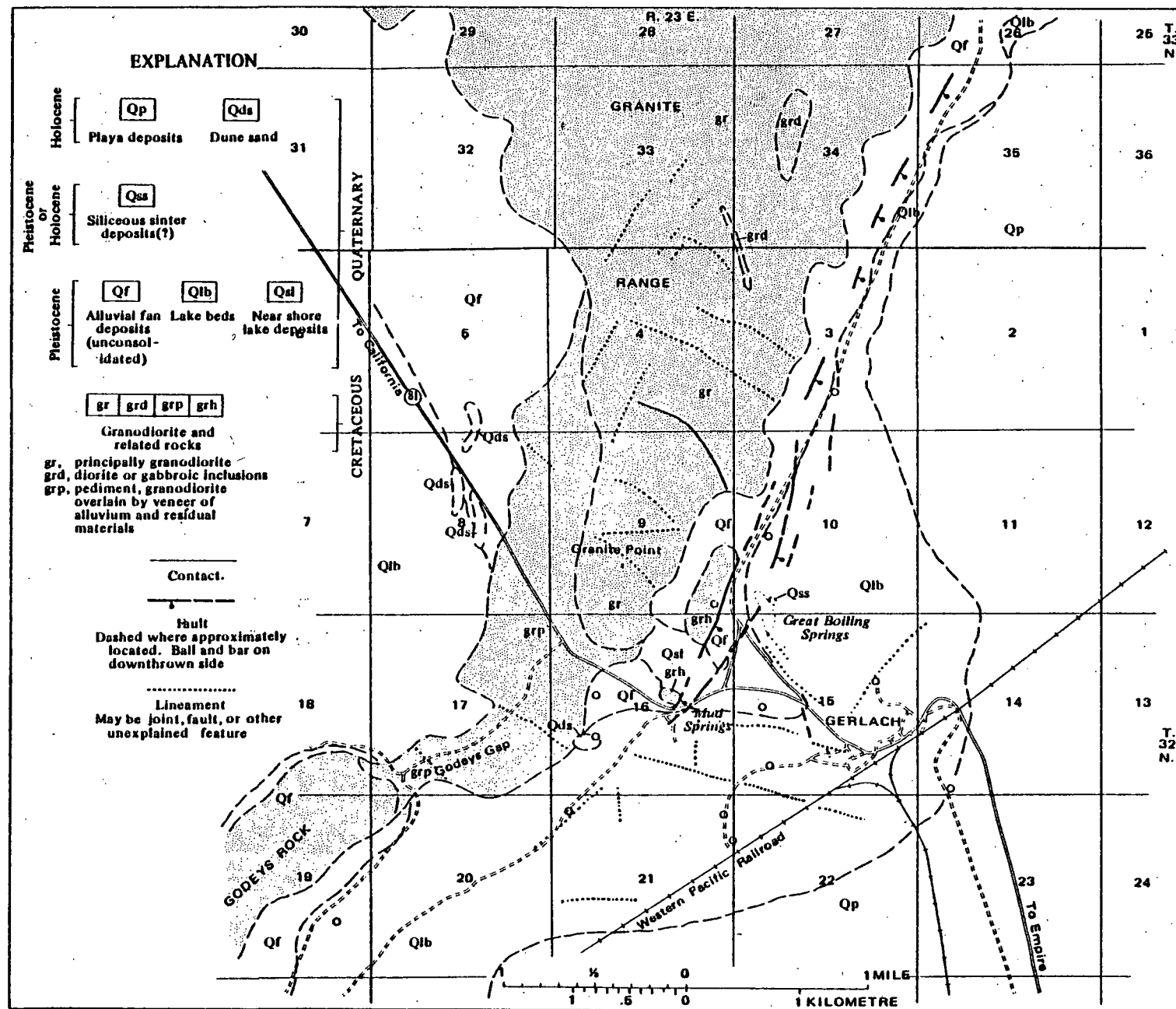


Figure 19.--Geologic map of Gerlach thermal area showing location of hot springs and test holes.

Hydrologic Setting

The unconsolidated deposits are saturated at shallow depths throughout most of the Gerlach area. Ground water also occurs in open joints, fractures, and faults in the granodiorite and related plutonic rocks. Recharge in the contiguous drainage area is insufficient to sustain the discharge of thermal water. Likely source areas for the deep-circulating thermal water have not been delineated precisely but are believed to be in the higher parts of the Granite Range, 10-20 km north of the area of hydrothermal discharge.

Shallow ground water locally is unconfined, but, because of the abundance of clay and silt in the lacustrine deposits, ground water in these deposits generally is confined at depths of only a few metres below the water table. Because of the generally shallow depths to water, the configuration of the unconfined potentiometric surface (water table) is similar to that of the land surface. (See fig. 20a). This suggests that in much of the thermal area the water table is analogous to a surface of seepage, except that the water discharges by evapotranspiration instead of by seepage. Both unconfined and confined potentiometric surfaces (figs. 20a and b) indicate mounding of ground water near springs and movement from the Granite Range toward the playa.

Vertical potential gradients (fig. 21) are computed from water-level measurements in paired test holes, geophysical logs which indicate the water table or top of the saturated part of the capillary zone in single test holes, and interpolated differences in altitude between unconfined and confined potentiometric surfaces (figs. 20a and b). The gradients indicate downward movement of ground water in a narrow band of coarse-grained deposits adjacent to the mountains and upward movement in most of the remaining area. The largest upward gradients are near the hot springs and probably are due to temperature-induced differences in density of the water.

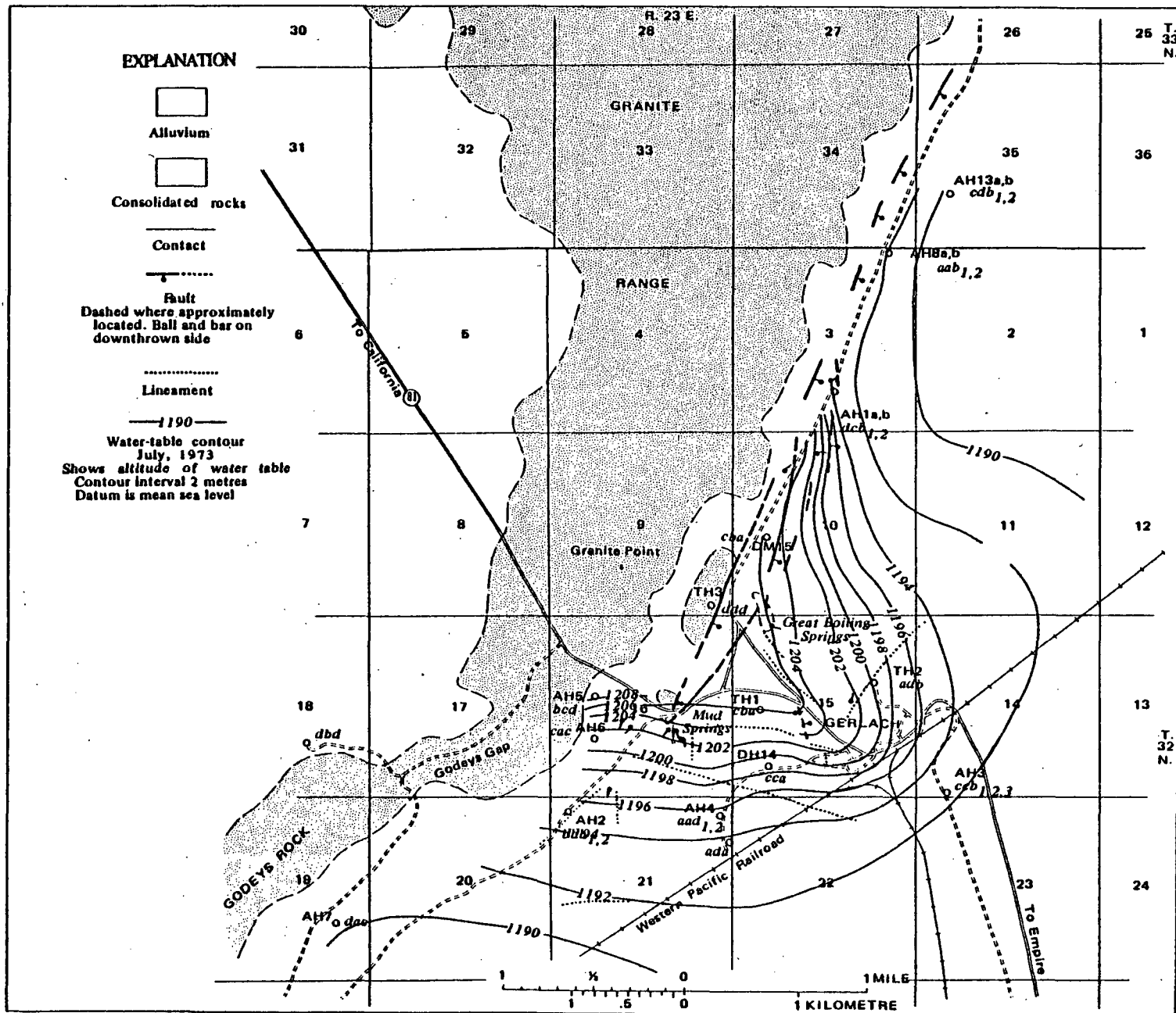


Figure 20a.--Map of Gerlach thermal area showing configuration of unconfined potentiometric surface, July 1973.

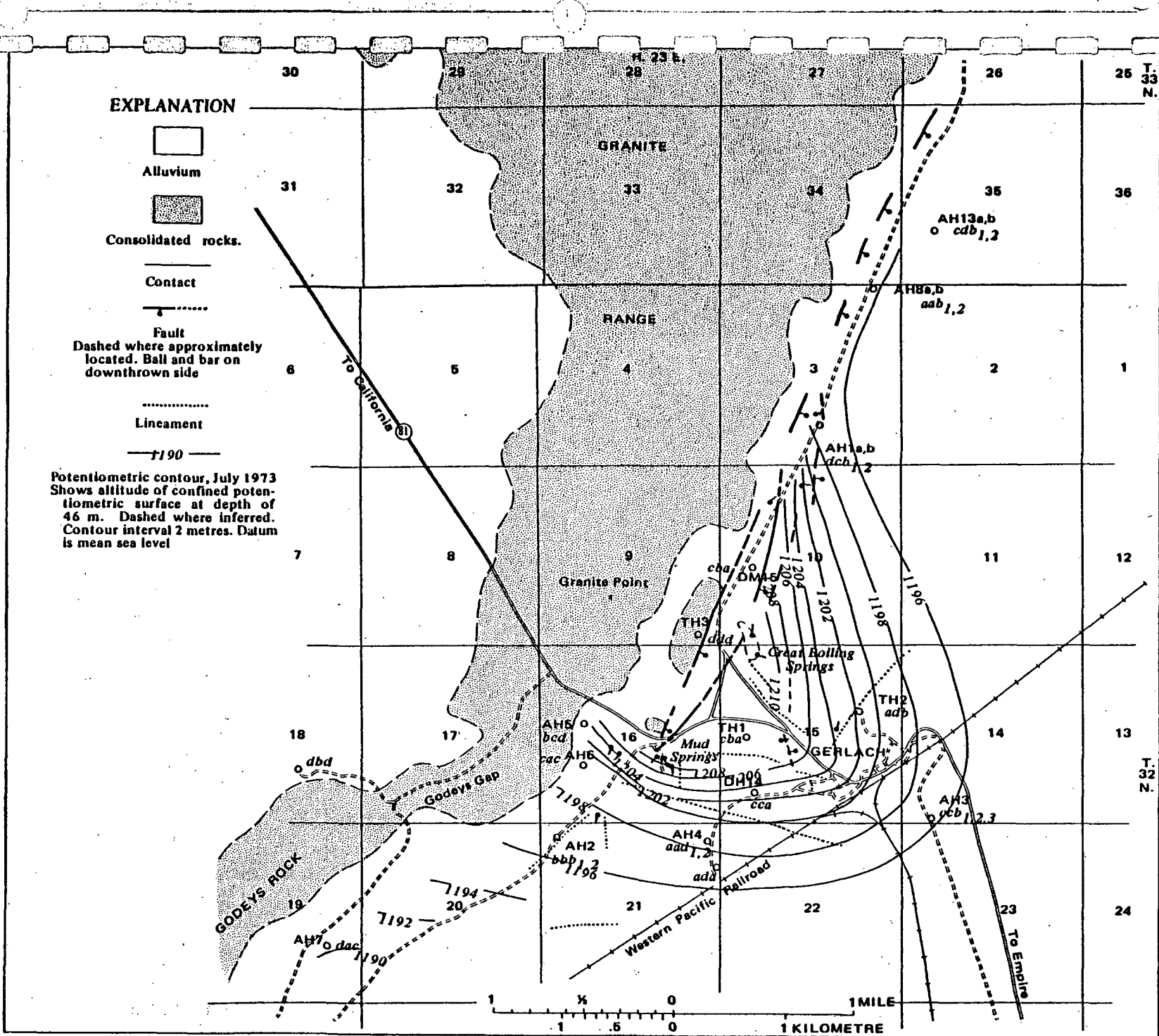


Figure 20b.--Map of Gerlach thermal area showing configuration of confined potentiometric surface, July 1973.

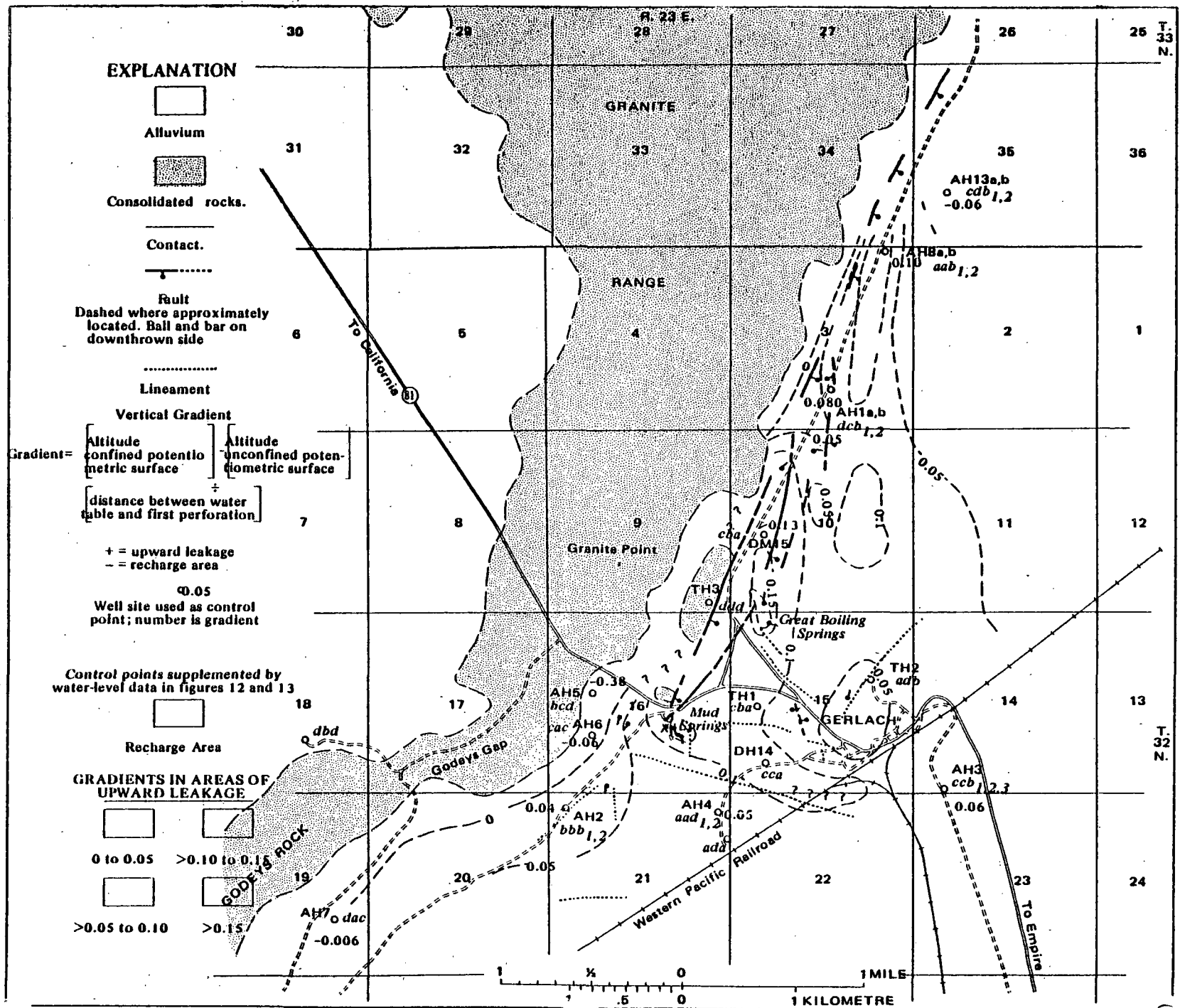


Figure 21.--Map of Gerlach thermal area showing vertical potential gradients, July 1973.

134

Principal Hot Spring Groups

The principal hot spring areas consist of 4 small individual springs and two major spring areas, Great Boiling Springs and Mud Springs.

Significant features of the four individual springs are listed below:

<u>Location</u>	<u>Discharge ($l\ s^{-1}$)</u>	<u>Temperature ($^{\circ}C$)</u>	<u>Remarks</u>
32/23-10baa	0.19 est.	54.4	Orifice in alluvium on the up- thrown side of a fault scarp.
32/23-10bac	1.0 est.	boiling	Orifice in alluvium on upthrown side of fault. Is near out- crop of altered granitic rocks. Prior to development by ditch- ing, flow was only about 0.19 $l\ s^{-1}$.
32/23-15acd	1.4 est.	67.8	Orifice in alluvium. Linear feature that may be fault.
32/23-15cab	.06 est.	49.4	Orifice in alluvium along 0.7- metre-high scarp.

The most prominent features of the Great Boiling Springs area are shown in figure 22. Figure 23 shows the most prominent features of the Mud Springs area. Springflow may fluctuate above and below quantities listed in the figures but insufficient data are available to document the magnitude of any fluctuations.

Orifice number	Temperature (°C)	Orifice number	Temperature (°C)
1	60.6	35	27.2
2	40.0	36	50.6
3	49.4	37	48.9
4	42.2	38	64.4
5	50.0	39	52.2
6	33.3	40	35.6
7	36.7	41	58.9
8	43.3	42	28.9
9	72.2	43	43.3
10	50.5	44	56.7
11	31.7	45	59.4
12	33.9	46	86.7
13	70.0	47	51.1
14	36.7	48	92.2
15	35.6	49	51.1
16	36.7	50	61.1
17	57.8	51	60.0
18	50.6	52	44.4
19	96.1 (Boiling)	53	34.4
20	48.3	54	70.0
21	59.4	55	77.8
22	40.6	56	58.9
23	48.3	57	86.7
24	33.3	58	47.8
25	48.3	59	43.3
26	61.7	60	55.6
27	33.3	61	66.1
28	42.8	62	73.3
29	47.8	63	67.8
30	63.3	64	57.7
31	74.4	65	57.7
32	29.4	66	61.1
33	48.9	67	32.2
34	53.3	68	58.3

Note: Area very dynamic; distribution of smaller vents differs slightly from that mapped in 1966 and will probably continue to change in the future.

Estimated discharge (litres per second)

Borax Works Area:

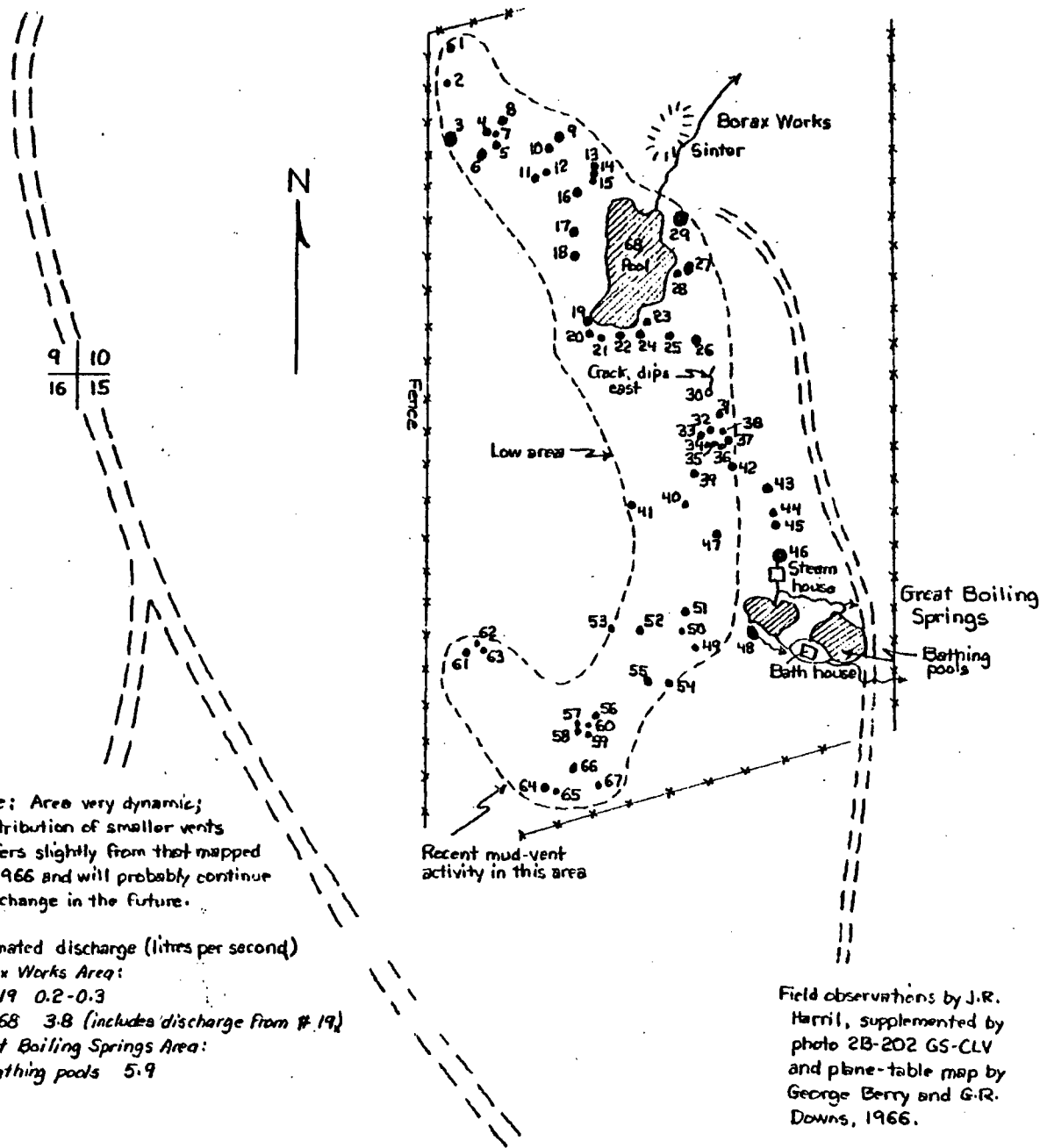
#19 0.2-0.3

#68 3.8 (includes discharge from #19)

Great Boiling Springs Area:

Bathing pools 5.9

0 50 100 Metres



Field observations by J.R. Harril, supplemented by photo 2B-202 GS-CLV and plane-table map by George Berry and G.R. Downs, 1966.

Figure 22.--Sketch map of Great Boiling Springs

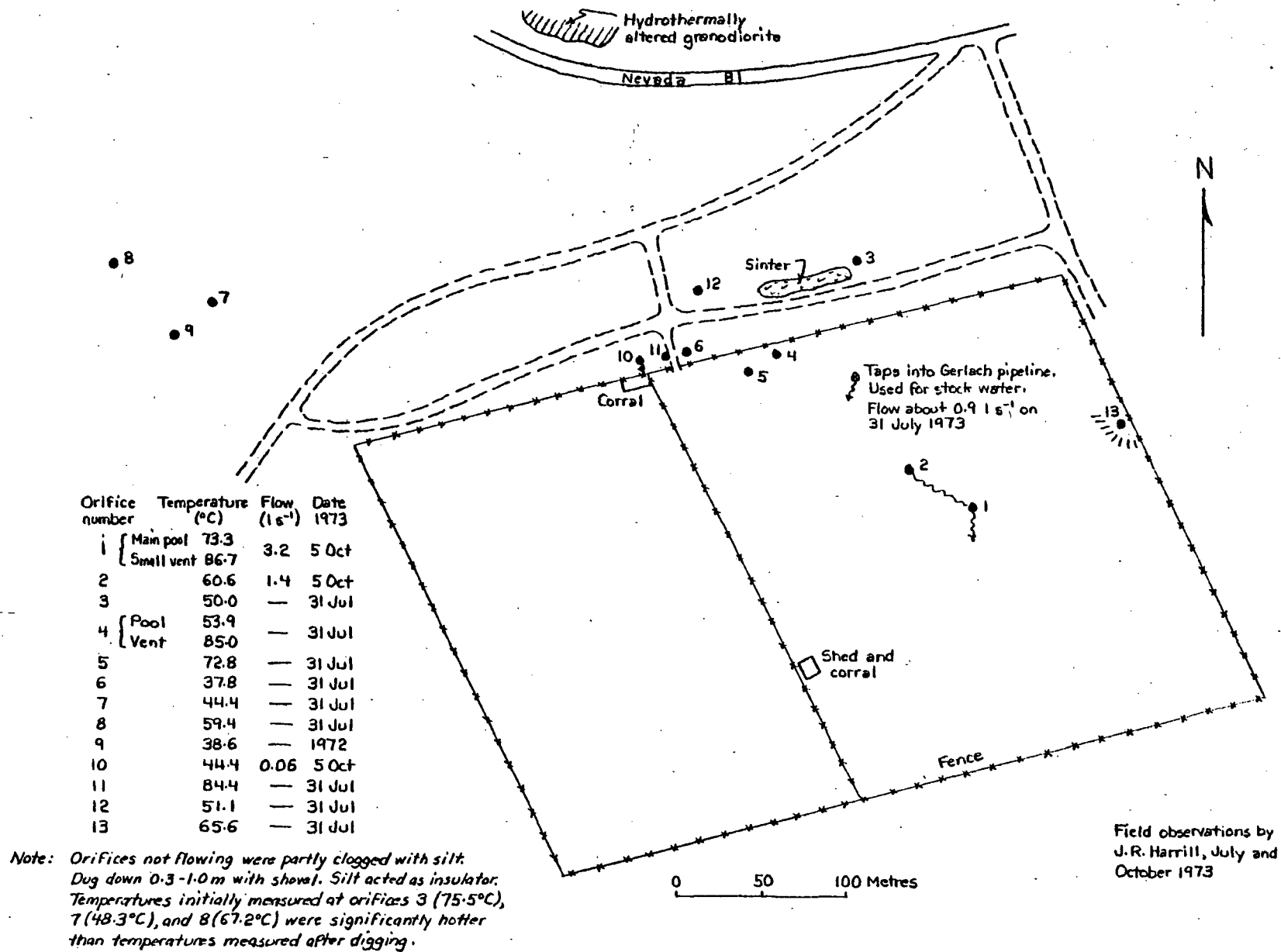


Figure 23.--Sketch map of Mud Springs

Subsurface Temperature Distribution

The general configuration of the Gerlach thermal area is indicated by the distribution of temperature at a depth of 30 m below land surface, as shown on figure 24. The map is based chiefly on temperature measurements made in July and October 1973 in test holes of the U. S. Geological Survey and the Cordero Mining Company. Temperatures measured in hot-spring orifices are extrapolated to temperatures at 30 m by using thermal gradients in nearby wells or, where the springs are boiling, by using the relation of boiling temperature to hydrostatic depth at the altitude of Gerlach ($\sim 1,200$ m). Control for the temperature distribution in the basement rocks in the western and northern parts of the thermal area is lacking; the position of the isotherms shown on figure 24 is based on the assumption that the thermal area is bilaterally symmetrical.

The thermal area is elongated toward the north-northeast and southwest, and the hottest parts surround the major hot springs. The elongation is obviously related to the faults that control the positions of the hot springs. Close similarity of the temperature pattern to the configuration of the unconfined and confined potentiometric surface (compare figs. 20a, 20b, and 24) also suggests convective heat transport by lateral as well as vertical ground-water movement. The approximate limits of the thermal area are defined by the 15°C isotherm; "normal" temperatures at 30 m for the region are about $13^{\circ} - 15^{\circ}\text{C}$.

Chemical Character of Springflow

Discharge water from one of the hottest orifices at Great Boiling Springs was analyzed by Mariner and others (1974). Concentration of dissolved solids is high in comparison with most other hot-spring waters sampled in northern and central Nevada. Sodium and chloride are the dominant constituents. Specific conductance determined by Mariner and others (1974, table 2) is $7,610 \mu\text{mhos cm}^{-1}$. Reservoir temperature is 167°C by the silica-quartz geothermometer, 175°C by the sodium-potassium geothermometer (Mariner and others, 1974, table 3).

Heat Discharge

Heat is discharged from the Gerlach hydrothermal system principally by conduction through near-surface material, by springflow, and by discharge of steam or heated air. Heat discharge by lateral ground-water movement is not considered significant, because the boundary of the thermal area is placed at the 15°C isotherm at a depth of 30 m, where the temperature of the ground-water outflow is only slightly above the "normal" temperature for the area. Heat discharge by evaporation from hot-water surfaces is not estimated as a separate item. Almost all this discharge is included in the springflow, because temperatures of the flow were measured in the throats of the orifices, before significant cooling had occurred. Heat discharge by radiation from warm soil or water surfaces also is not estimated; data on which to base an estimate are not available. However, it is believed that the radiative heat discharge is small in comparison to the conductive and convective discharges.

Conductive heat discharge.--Discharge of heat by conduction through near-surface materials in the Gerlach hydrothermal system is estimated by methods A and B described in the section, "Estimates of heat discharge." As in most of the other thermal areas, method B is believed to provide the more reliable estimate.

The conductive heat discharge is estimated by method A, using the following assumptions:

- (1) Mean annual temperature at the land surface is 11°C, the approximate long-term mean annual temperature at Gerlach (table 6).
- (2) The 15°C isotherm at 30 m depth encloses the area of excess heat flow related to the hydrothermal-discharge system.

(3) The average thermal conductivity of the materials in the depth range 0-30 m throughout the thermal area is $2.6 \times 10^{-3} \text{ cal cm}^{-1} \text{ s}^{-1} \text{ }^{\circ}\text{C}^{-1}$, the average of the computed harmonic-mean thermal conductivities of the deposits penetrated by test holes BR AH 1-8, 13, and DH 14 and 15.

Using these values, the estimate of conductive heat discharge by method A is $5.7 \times 10^6 \text{ cal s}^{-1}$. Derivation of the estimate is given in table 13.

The estimate of conductive heat discharge by method B is $4.4 \times 10^6 \text{ cal s}^{-1}$, significantly less than the estimate by method A. The derivation of the estimate is given in table 14.

Heat discharge by springflow.--Heat discharge by springflow is computed on the basis of an average springflow of $5.6 \times 10^5 \text{ m}^3 \text{ yr}^{-1}$ at an average temperature of 80°C as

$$\begin{aligned} & [(80 - 11) \text{ cal g}^{-1}] [(0.972 \times 10^6 \text{ g m}^{-3})(5.6 \times 10^5 \text{ m}^3 \text{ yr}^{-1})] \\ & = 3.8 \times 10^{13} \text{ cal yr}^{-1} \\ & = 1.2 \times 10^6 \text{ cal s}^{-1} \end{aligned}$$

Heat discharge by steam or heated air.--The large difference in temperature between the source of the thermal water (about 171°C , as indicated by the chemical geothermometers) and the discharge at land surface (96°C or less), together with the substantial rate of springflow, suggests the possibility that much of the heat carried by the upflowing thermal water is discharged as vapor (steam) or as heated air. Theoretically, as discussed in the section "Estimates of heat discharge" as much as one half the total heat carried by the thermal water as it leaves the deep source might be discharged in this manner. However, the evidence at Gerlach suggests a much smaller discharge. Instead of appearing in a single boiling spring, most of the springflow is dispersed

Table 13.—Estimate of conductive heat discharge from Gerlach hydrothermal system on the basis of method A described in text.

Temperature range (°C)	Geometric mean temperature (°C)	Thermal gradient $\frac{1}{2}$ ($\times 10^{-3}$ °C cm ⁻¹)	Heat flow $\frac{1}{2}$ ($\times 10^{-3}$ cal cm ⁻² s ⁻¹)	Area ($\times 10^{10}$ cm ²)	Heat discharge ($\times 10^6$ cal s ⁻¹)
15-20	17.3	2.1	5.5	9.0	0.50
20-30	24.5	4.5	12	3.3	.40
30-40	34.6	7.9	21	1.4	.29
40-60	49.0	13	34	1.5	.51
60-80	69.3	19	49	1.4	.69
80-100	89.4	26	68	1.5	1.0
100-120	109.5	33	86	2.1	1.8
> 120	121	37	96	.5	.48
Totals				20.7	5.7

(1) Based on 11°C mean annual temperature at the land surface.

(2) Based on harmonic-mean thermal conductivity of 2.6×10^{-3} cal cm⁻¹ s⁻¹ °C⁻¹.

Table 14.—Estimate of conductive heat discharge from Gerlach hydrothermal system on the basis of method B described in the text.

Range in heat flow (MFU)	Geometric-mean heat flow (MFU)	Area ($\times 10^{10}$ cm ²)	Heat discharge ($\times 10^6$ cal s ⁻¹)
2-10	4.5	11.2	0.50
10-50	22	5.7	1.3
50-100	71	2.7	1.9
>100	110	.68	.75
Totals		20.3	4.4

throughout numerous orifice pools in which the temperatures are generally less than boiling (figs. 22 and 23). It seems likely, therefore, that most of the steam produced by boiling in the conduit system as the thermal water rises to the surface condenses before discharging to the atmosphere. The heat released by condensation probably is discharged by conduction through near-surface deposits or by augmented springflow.

Data are not available from which to base an estimate of heat discharge as vapor. Some heat doubtless does escape as steam from the few boiling pools or as heated air or steam from vents or cracks, but it is believed that this discharge amounts to less than 20 percent of that by springflow--perhaps about $0.2 \times 10^6 \text{ cal s}^{-1}$.

Total heat discharge--The estimated total heat discharge from the Gerlach hydrothermal system is the sum of the conductive heat discharge, as estimated by methods A and B, the heat discharge by springflow, and the heat discharge by steam or heated air:

	Heat discharge ($\times 10^6 \text{ cal s}^{-1}$)	
	Method A	Method B
Conduction through near-surface materials	5.7	4.4
Convection by springflow	1.2	1.2
Convection by steam or heated air	.2	.2
	Total	
	7.1	5.8

Net heat discharge---The net heat discharge from the system is the total heat discharge minus the so-called "normal" heat discharge--the heat discharge that would have occurred from the thermal area without the effects of the upflow of thermal water.

On the basis of method A, the "normal" heat flow at the 15°C isotherm at 30 m depth is $3.4 \times 10^{-6} \text{ cal cm}^{-2} \text{ s}^{-1}$. Thus, the "normal" conductive heat discharge from the area enclosed by the 15°C isotherm (see table 13) is:

$$(20.7 \times 10^{10} \text{ cm}^2) (3.4 \times 10^{-6} \text{ cal cm}^{-2} \text{ s}^{-1}) = 0.70 \times 10^6 \text{ cal s}^{-1}$$

The estimate of net heat discharge by method A is therefore equal to the total heat discharge, $7.1 \times 10^6 \text{ cal s}^{-1}$, minus the "normal" conductive heat discharge, $0.70 \times 10^6 \text{ cal s}^{-1}$, or $6.4 \times 10^6 \text{ cal s}^{-1}$.

On the basis of method B, the "normal" heat flow is assumed to be $2 \times 10^{-6} \text{ cal cm}^{-2} \text{ s}^{-1}$. The "normal" heat discharge is then

$$(2 \times 10^{-6} \text{ cal cm}^{-2} \text{ s}^{-1})(20.3 \times 10^{10} \text{ cm}^2) = 0.41 \times 10^6 \text{ cal s}^{-1}.$$

The estimate of net heat discharge by method B is therefore equal to the total heat discharge, $5.8 \times 10^6 \text{ cal s}^{-1}$, minus the "normal" conductive heat discharge, $0.41 \times 10^6 \text{ cal s}^{-1}$, or $5.4 \times 10^6 \text{ cal s}^{-1}$.

Water Discharge

Water discharge from the Gerlach hydrothermal system is estimated by the water-budget and the heat-budget methods described in the section "Estimates of water discharge"

Water-budget method.—Outflow items in the water-budget method are ground-water evapotranspiration and lateral ground-water outflow from the thermal area. Ground-water evapotranspiration, which constitutes almost all the outflow, is estimated to be about $1.7 \times 10^6 \text{ m}^3 \text{ yr}^{-1}$. Derivation of the estimate is given in table 15. Lateral ground-water outflow, computed using the horizontal components of the confined potential gradient along segments beneath the 15°C isotherm at 30 m depth and an estimated average transmissivity of $30 \text{ m}^2 \text{ day}^{-1}$, is less than $0.1 \times 10^6 \text{ m}^3 \text{ yr}^{-1}$. Thus, the total outflow is estimated to be the sum of ground-water evapotranspiration and lateral ground-water outflow, or $1.8 \times 10^6 \text{ m}^3 \text{ yr}^{-1}$. This total includes both thermal and nonthermal water discharge.

Table 15.--Estimate of ground-water evapotranspiration within the Gerlach thermal area.

Type of vegetation	Area (x 10 ³ m ²)	Annual evapotranspiration Depth (cm)	Volume (x 10 ³ m ³)
Lush grass and tules; includes areas of spring-supported vegetation and warm ground.	850	100	850
Saltgrass	770	45	350
Greasewood and saltgrass	1,700	18	310
Saltgrass, pickleweed, and bare soil.	69	24	17
Greasewood	1,900	6	110
Playa	260	9	23
Total (rounded)	5,500	31 ^{1/}	1,700

^{1/} Average

Inflow items in the water budget are recharge from local precipitation and runoff, imported water, and upflow of thermal water from deep sources. Recharge from local precipitation and runoff, computed by methods described by Eakin and others (1951) and Sinclair (1963), is about $0.2 \times 10^6 \text{ m}^3 \text{ yr}^{-1}$. Imported water, which consists of water piped to Gerlach from Granite and Graden Springs in the Granite Range to the north, is about $0.1 \times 10^6 \text{ m}^3 \text{ yr}^{-1}$. Upflow of thermal water is computed by balancing inflow and outflow in the hydrologic equation:

$$\begin{aligned}
 (\text{Thermal-water upflow}) &= (\text{total outflow}) - (\text{recharge} + \text{imported water}) \\
 &= (1.8 \times 10^6 \text{ m}^3 \text{ yr}^{-1}) - (0.2 + 0.1) \times 10^6 \text{ m}^3 \text{ yr}^{-1} \\
 &= 1.5 \times 10^6 \text{ m}^3 \text{ yr}^{-1}
 \end{aligned}$$

Heat-budget method.--The upflow of thermal water is computed using the heat-budget method as follows. Temperature of the thermal water leaving the deep sources is assumed to be 171°C , the average of the temperatures indicated by the silica-quartz geothermometer (167°C) and the sodium-potassium geothermometer (175°C) (Mariner and others, 1974, table 3). Average surface temperature is assumed to be 11°C , so the net heat content of the thermal water is $(171^\circ - 11^\circ\text{C})(1.0 \text{ cal g}^{-1} \text{ }^\circ\text{C}^{-1}) = 160 \text{ cal g}^{-1}$. Net discharge from the thermal area is $6.4 \times 10^6 \text{ cal s}^{-1}$ on the basis of the estimate by method A and $5.4 \times 10^6 \text{ cal s}^{-1}$ by method B. Thus, the discharge of thermal water computed by method A is:

$$\frac{6.4 \times 10^6 \text{ cal s}^{-1}}{1.6 \times 10^2 \text{ cal g}^{-1}} = 4.0 \times 10^4 \text{ g s}^{-1}, \text{ or } 1.3 \times 10^6 \text{ m}^3 \text{ yr}^{-1},$$

at an average discharge temperature of 80°C , and by method B is

$$\frac{5.4 \times 10^6 \text{ cal s}^{-1}}{1.6 \times 10^2 \text{ cal g}^{-1}} = 3.4 \times 10^4 \text{ g s}^{-1}, \text{ or } 1.1 \times 10^6 \text{ m}^3 \text{ yr}^{-1}.$$

The estimate of $1.1 \times 10^6 \text{ m}^3 \text{ yr}^{-1}$ by method B is believed to be the more reliable of the two estimates. Both estimates are somewhat less than the estimate of $1.5 \times 10^6 \text{ m}^3 \text{ yr}^{-1}$ by the water-budget method. The reason for the difference is uncertain. The water budget is dominated by the discharge of thermal water by evapotranspiration from areas of phreatophytic vegetation. Errors in estimated rates of use by the more heavily water-using types such as salt grass and tules (table 15) could result in an overestimate by the water-budget method. Alternatively, the estimated rates of heat flow used in the heat-budget method could be too small. Further studies are needed to resolve the discrepancy.

Inferred Nature of Hydrothermal System

Although the three-dimensional distribution of temperature, lithologic characteristics, and fluid potential is not known in detail for the Gerlach hydrothermal system, some of the broad features of the system may be inferred with reasonable confidence.

Exposed bedrock is almost entirely Mesozoic granodiorite, and similar rock underlies most, if not all, of the thermal area. Thickness of the overlying basinfilling deposits of Tertiary (?) and Quaternary age is not known; the thickness may exceed 2 km near the center of the basin, but the deposits probably are much thinner beneath the spring area. The nearest exposures of Tertiary volcanic rocks are 7 km from the spring area, and none of the rocks is known to be less than 15 m.y. in age. Geochemical data indicate a water-rock equilibrium temperature of about 170°C (table 1, Mariner and others, 1974). Data from test holes in fine-grained lacustrine deposits outside the area affected by convective upflow of thermal water indicate "normal" heat flow for the northern Basin and Range province (about

1-1/2 - 2 HFU). A local shallow-crustal heat source therefore appears unlikely but cannot be completely ruled out from present information.

With "normal" heat flow, the equilibrium temperature, and the geology inferred above, the depth of circulation of the thermal ground water probably is on the order of 3-6 km, well within the granodiorite basement rock. Primary porosity of this kind of rock is virtually zero. Instead, the water probably circulates through secondary openings, such as open fractures in the fault zones or in open joints. The nature and extent of the deep thermal reservoir cannot be inferred with reasonable certainty from available data.

The thermal water moves through faults, joints, and other fractures, and probably is recharged from precipitation in the higher parts of the Granite Range north of Gerlach, and rises along fault-controlled conduits in the granodiorite into the overlying sediments. The rising water moves rapidly enough to maintain a temperature close to that of its deep source until it begins to boil at a hydrostatic depth of approximately 55-60 m beneath the main outlets of Great Boiling Springs. Upward movement is slower through the fault zones northwest and southeast of Great Boiling Springs, and boiling may not occur in these conduits. The discharge-conduit system appears to be of the leaky type. Thermal water probably leaks laterally from the upper parts of all the conduits into sandy aquifers in the basin-fill sediments, where it moves laterally in the direction of the potential gradient. The hot water may mix with shallow nonthermal water in some of the aquifers. The thermal gradients below some aquifers is reversed, as observed in several test holes down the

potential gradient from faults. Heat is discharged chiefly by conduction through the predominantly fine-grained sediments near the land surface, by springflow, and by steam or hot air escaping from boiling pools, vents, and cracks in the ground.

SULPHUR HOT SPRINGS THERMAL AREA

Location

The Sulphur Hot Springs thermal area is in northwestern Ruby Valley and in south-central Elko County (fig. 5). The springs are in sec. 11, T. 31 N., R. 59 E., at an altitude of about 1,845 m. Elko, the principal center of population and trading in the region, is 97 km by road to the northwest. The thermal areas has not been classified as a KGRA, but is within lands classified as valuable prospectively for geothermal resources.

Test Drilling

The U. S. Geological Survey drilled or bored 11 test holes at Sulphur Hot Springs as part of this study. Additional shallow holes were augered at three of the sites to determine depth to the water table and vertical potential gradient. Six of the test holes were bored with hollowstem auger during the spring of 1973; five holes were drilled by the hydraulic-rotary method during the fall of the same year. All but two of the holes have screen or perforated pipe at the bottom and are therefore used for water-level measurements as well as for temperature measurements. Test holes AH-6 and DH-11 are capped at the bottom and filled with water for temperature measurements. Data for the test holes are presented in table 16.

Table 16 -- Data for U. S. Geological Survey test holes in Sulphur Hot Springs thermal area

Type of completion: Casing type is indicated by "St" (steel) or "P" (PVC).

Wells capped at bottom and filled with water are indicated by "C". Wells

with well-point screens at bottom are indicated by "Sc". Plastic well

casing (PVC) that is slotted or perforated at the bottom are indicated by "Sl".

Depth to water table: Source of data; "G" indicates geophysical logs and

"M" indicates measured.

Geophysical logs available: Gamma ("G"), gamma-gamma ("G²"), neutron ("N"), and temperature ("T").

Well number	Location	Depth (Metres below land surface)	Casing		Land-surface altitude (m)	Depth to water table			Static confined water level		Geophysical logs available	Remarks
			Inside diameter (cm)	Type of completion		Metres below land surface	Source of data	Date	Metres below land surface	Date		
EH-1	31/59-11ccc	15.58	5.1	P, Sl	1846.5	8.2	G	73 05 04	10.17	73 10 18	G, G ² , N, T	Near gravel pit
AH-2A	2ced1	43.98	5.1	P, Sl	1852.9	4.3	G	73 05 04	4.61	73 10 18	G, G ² , N, T	Inside fence, SE
AH-2B	2ced2	9.51	3.8/5.1	St/P, Sc	1852.9	3.8	G	73 05 04	4.45	73 10 18	G, G ² , N, T	Same site as 2A
AH-3A	11abd1	35.66	5.1	P, Sc	1838.3	--	-	-	0.91 0.97	73 10 18 73 05 03	G, G ² , N, T	On N back of
AH-3B	11abd2	1.51	5.1	P, Sl	1838.3	--	-	-	1.44	73 10 31	-	Same site as 3A
AH-4	11abd	38.86	5.1	P, Sc	1833.7	--	-	-	1.87 2.46	73 05 03 73 10 16	G, G ² , N, T	Nr. S edge of trail
AH-5	11bdc	38.80	3.8	St, Sc	1841.0	>1.22	M	73 10 31	1.18 0.46	73 10 16 73 10 31	G, G ² , N, T	Nr. W edge of trail
AH-6	10ada	14.75	5.1	P, C	1858.4	Dry	-	-	-	-	G, G ² , N, T	In field, 20 m N of driveway.
EH-7	11acd	6.80	5.1	P, Sl	1833.4	--	-	-	0.89	73 10 18	G, G ² , N, T	On sinter outcrop, 40 M W of fence.
EH-8A	12cba1	45.42	3.8	St, Sc	1827.0	--	-	-	0.08	73 11 05	G, G ² , N	S of fence, 37 m
AH-8B	12cba2	3.05	5.1	P, Sl	1827.0	--	-	-	1.44	73 11 05	-	Same site as 8A
EH-9	2dab	34.35	5.1	P, Sc	1846.8	2.3	G	73 11 05	3.02	73 10 22	G, G ² , N	S of fence line, 10
EH-10	11acd	43.89	5.1	P, Sc	1830.0	4.3	G	73 11 05	4.97	73 10 22	G, G ² , N	N of trail jet, 3 m
EH-11	3ada	12.80	5.1	P, C	1869.0	Dry	M	73 10 20	-	-	G, G ² , N	SE of fence 6 m. Possible water table at 7.5 m.

(see remarks)

Geology

The rocks in the vicinity of Sulphur Hot Springs include unconsolidated rocks of pre-Tertiary age, several kinds of unconsolidated deposits of late Tertiary and Quaternary age, and sinter. The surface distribution of the various kinds of rocks and deposits is shown on figure 25.

Consolidated rocks are exposed in the Ruby Mountains about 1 km west of Sulphur Hot Springs. According to Hope (1970), the rocks as far west of the springs as the top of the mountain ridge are entirely metamorphosed limestone of Paleozoic age. However, granitic boulders on the alluvial fan of Lutts Creek, just north of the hot springs, indicate nearby exposures of this type of rock. Much of the coarse sand and gravel in the alluvial-fan and lake deposits near the springs contains feldspars and micas, which suggests possible derivation of these deposits from a granitic terrane.

The unconsolidated deposits include pediment deposits, slope wash, and colluvium, alluvial-fan deposits, and lake deposits.

The pediment deposits are chiefly coarse sand and gravel which form a veneer on a pediment between the principal Basin and Range fault along the east margin of the Ruby Mountains and the steep fault-line escarpment west of the fault.

The slope wash and colluvium lie to the east of the principal fault. These deposits consist of a poorly sorted, crudely stratified mixture of gravel, sand, and silt, deposited on a gently sloping alluvial apron above the highest shoreline of a Pleistocene lake (above an altitude of about 1,850 m above mean sea level).

The alluvial-fan deposits underlie the alluvial fan of Lutts Creek, about 0.5 to 2.5 km north of Sulphur Hot Springs. These deposits are typically coarse grained and include boulders as much as 1 m in diameter, but they are poorly sorted and include so much silt and clay that their permeability is generally low. The lake deposits lie below the highest

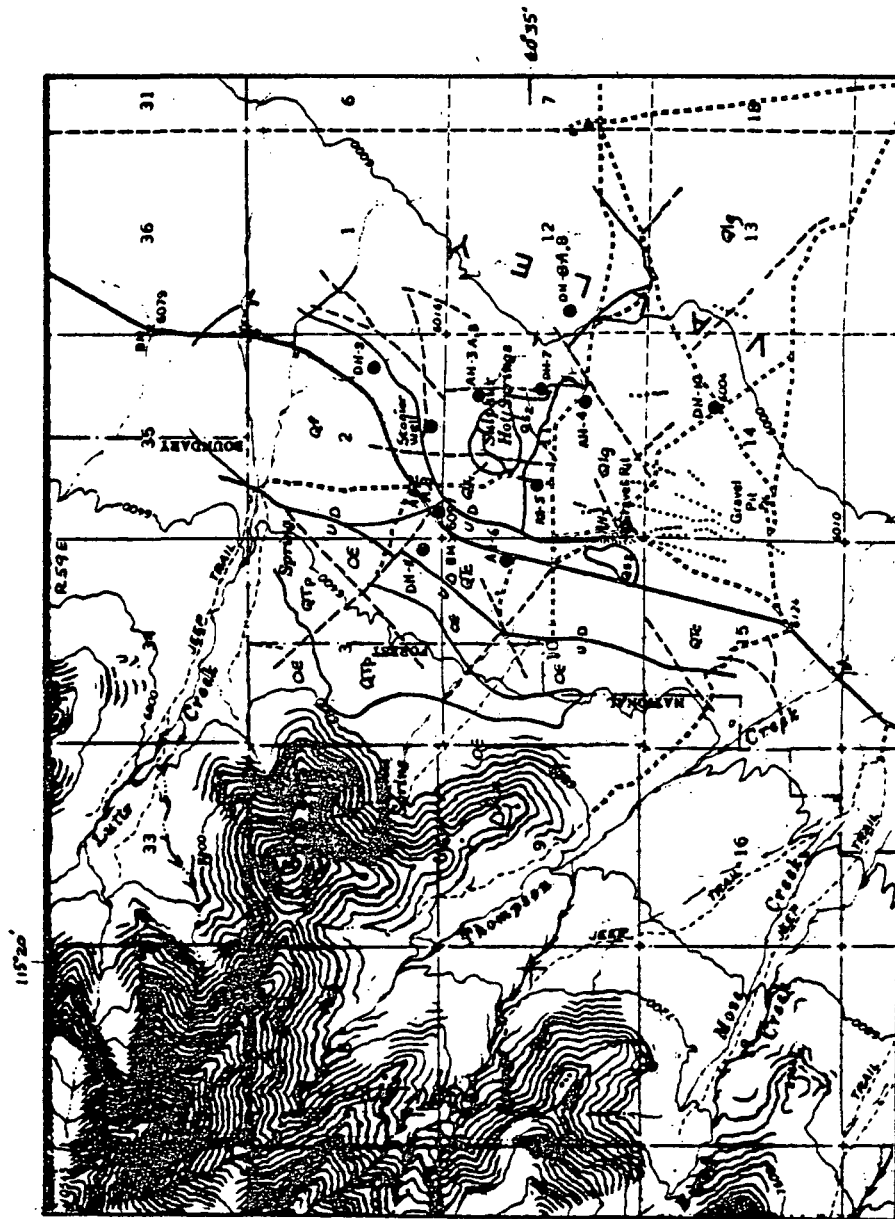


Figure 25.--Geologic map of Sulphur Hot Springs thermal area showing location of test holes.

EXPLANATION

Qs1 Qs2

Sinter

Chiefly white to light-gray opaline sinter at Sulphur Hot Springs and at sites of former hot springs to the southwest

Qs1, consolidated phase covered by sod in northwest part of present spring mound.

Qs2, consolidated and fragments of gravel and sand size. On present spring mound, forms irregular terraces decreasing in altitude to the southeast

Qlc Qlg

Lake deposits

Deposited in a shallow lake occupying valley floor and lower slopes of alluvial apron at base of Ruby Mountains.

Qlc, clay, silt, sand; poorly sorted; mostly soft and wet because of shallow water table

Qlg, Gravel and sand, well sorted; forms bar 3-15 m higher than adjacent valley floor and oriented generally perpendicular to mountain front

Qf

Alluvial fan deposits

Gravel, sand and boulders; some silt and clay; poorly sorted, chiefly unconsolidated. Surface slope decreases from about 0.08 at apex of fan to about 0.04 at distal margin

QTc

Slope wash and colluvium

Gravel, sand and silt; poorly sorted; deposited on a gently sloping alluvial apron above level of a Pleistocene lake

QTp

Pediment deposits

Sand and gravel veneering a pediment underlain by limestone

O6

Consolidated rocks, undifferentiated

Probably chiefly metamorphosed limestone within area shown on map; granitic intrusive rocks probably-present outside mapped area

Contact

QUATERNARY

TERTIARY AND QUATERNARY

CAMBRIAN AND (OR) ORDOVICIAN

of several shorelines of lakes which occupied Ruby Valley during pluvial stages in the late Pleistocene. The deposits are classified on figure 25 in two major facies: (1) fine-grained lake-bottom deposits, chiefly clay, silt, and fine sand; and (2) coarse sand and fine gravel, which form a near-shore bar 3-15 m above the surface of the lake-bottom deposits.

The sinter consists of white to light gray earthy amorphous silica (probably opal) deposited by both present and ancestral hot springs. The sinter at Sulphur Hot Springs forms a conspicuous mound about 450 m in diameter and 2-10 m above the adjacent alluvial apron. The northwest part of the mound is covered by sod generally less than 1 m thick and is identified separately on figure 25.

A major Basin and Range normal fault forms the contact of the unconsolidated rocks and unconsolidated deposits at the mountain front (fig. 25). Another fault was mapped in the unconsolidated deposits, parallel to the major fault and about half the distance between Sulphur Hot Springs and the major fault. The trace of the second fault is concealed by the lake gravel bar on the south and the alluvial-fan deposits of Lutts Creek on the north. Other linear features are apparent on aerial photographs and are shown on figure 25. These features may be minor faults.

Hydrology

Most of the ground water and streamflow in the Sulphur Hot Springs area originates as snowmelt in the Ruby Mountains. The snowmelt runs off chiefly in the spring and early summer and is used for irrigation. The area north and northeast of the hot springs (fig. 25) receives irrigation water from Lutts Creek, some of which percolates downward to the water table. The depth of circulation of the locally derived water is not known but probably does not exceed a few hundred metres. The deep-circulating thermal water is almost certainly derived from recharge

in the Ruby Mountains to the west, but the exact location and extent of the recharge area or areas are not known.

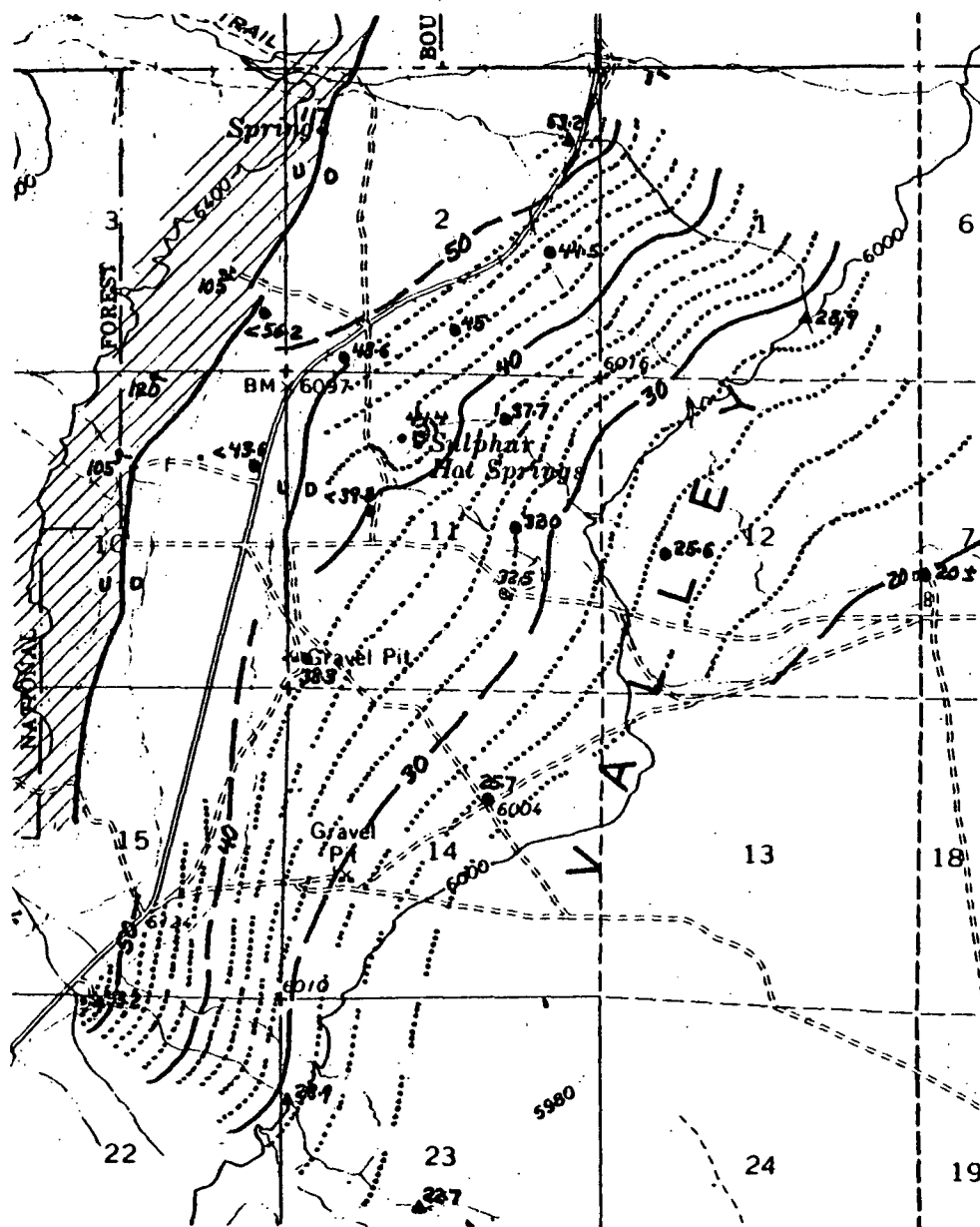
Ground water occupies intergranular pore spaces of the unconsolidated deposits and fractures and solution openings of the limestone bedrock and the sinter. Throughout most of the lowlands the water table is within a few metres of the land surface. Depths to the water table increase westward, toward the mountains. The ground water is generally unconfined but is confined locally by poorly permeable lenses of lacustrine clay and silt.

Ground-water movement in the vicinity of the hot springs is generally southeastward, as shown in figure 26. Movement is from the alluvial apron, where streamflow and irrigation water percolate downward to the water table, toward the discharge area on the valley floor. Most of the discharge area that receives flow from the thermal area is southeast of the area shown in figure 26. However, water is also discharged by evapotranspiration on the spring mound and surrounding area, as shown in figure 27.

A mound of hot water underlies the spring mound of Sulphur Hot Springs (fig. 26). A part of the mounding is a result of the thermo-artesian effect (low-density hot water "floating" in the surrounding cooler denser water), but an unknown proportion of the mounding probably results also from true artesian conditions. Because many of the spring pools overflow, the potentiometric surface of the ground-water body that supplies the springflow is higher than the pools.

The Hot Springs

Sulphur Hot Springs, probably named for their odor of hydrogen sulfide, flow from a sinter mound above a southeastward sloping alluvial apron which separates the valley floor to the east from the mountains to the west. The mound is roughly circular and has a diameter of about 450 m (fig. 26). It rises 2-10 m above the surrounding alluvial apron.



EXPLANATION



Unconsolidated valley fill



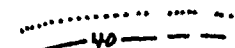
Consolidated rocks



Fault

U, upthrown side

D, downthrown side



Water-level contours

Altitude in metres above a datum 1,800 m above mean sea level. Solid lines indicate 10-m-interval contours; dotted lines, 2-m-interval contours. Contours dashed where location is uncertain.

● 37.7

Test hole and altitude of water table

Altitude in metres above a datum 1,800 m above mean sea level.

~ 105

Spring and altitude

Altitude in metres above a datum 1,800 m above mean sea level.

▲ 28.9

Stream site and altitude of water table

Altitude in metres above a datum 1,800 m above mean sea level.

Figure 26.--Map of Sulphur Hot Springs thermal area showing configuration of water table, April 1973.

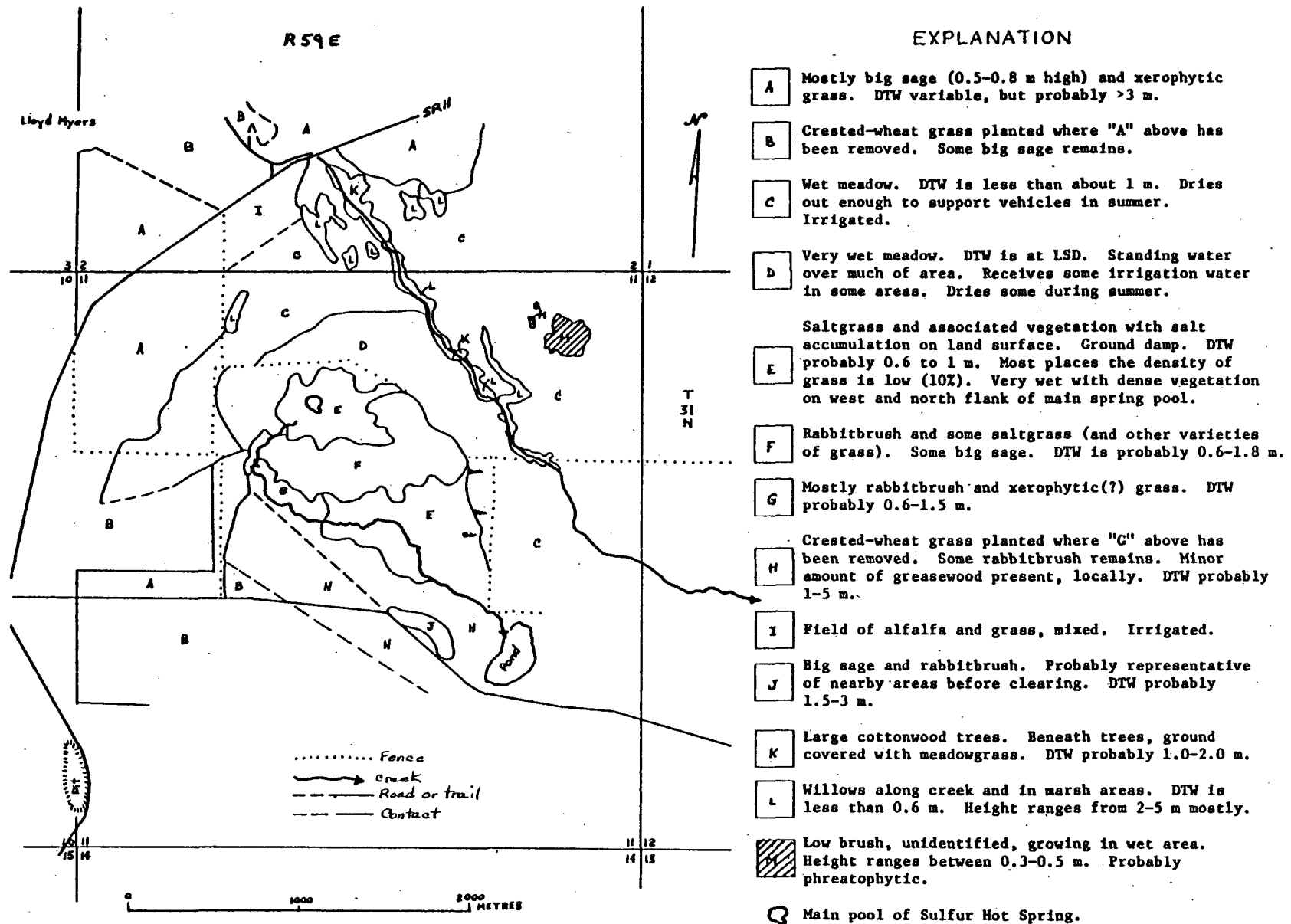


Figure 27.--Map of Sulphur Hot Springs thermal area showing distribution of vegetation types.

The southeast side of the mound is terraced, but the remainder is a smooth low dome.

The sinter extends to unknown depths within the valley-fill deposits. Thickness of the underlying and surrounding valley-fill deposits also is unknown. The geologic setting suggests, however, that the fill is much thinner beneath the springs than it is farther east, toward the axis of the valley.

A total of 101 spring pools was inventoried in this study. The spring data are presented in table 17. Maps showing configuration of the water table, distribution of spring-pool overflow, discharge temperatures at spring orifices, and specific conductance of spring-water samples are given on figures 28 a-d. Many other pools and orifices were not included in the inventory because of their small size.

Thirty-two pools overflow. Maximum flow is from the so-called "main pool," the largest of the pools. This pool has a surface area of about $1,200 \text{ m}^2$; the overflow rate is estimated to have been about 3.8 l s^{-1} in April 1973. The combined surface area of all the remaining pools is about half that of the main pool. Flow from all pools, including the main pool, is estimated to have been 8.2 l s^{-1} in April 1973. The smaller overflowing pools surround the main pool, except to the east, where they are generally absent, as shown in figure 28b.

Altitudes of the pool surfaces are shown on figure 28a. Although the main pool is near the center of the mound, water levels are higher in 11 smaller pools to the north and south. The highest pool was 3.04 m higher than the lowest pool in April 1973.

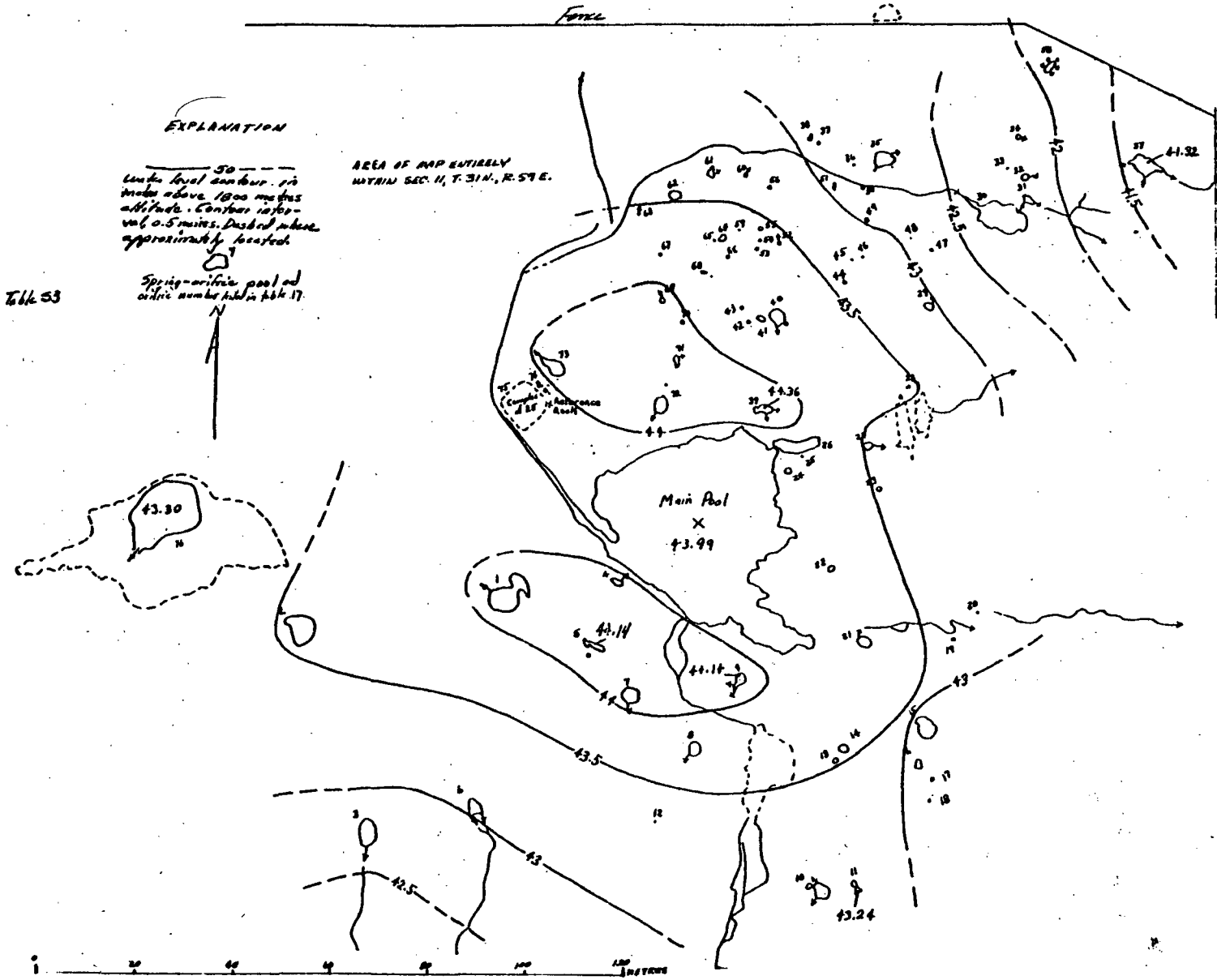


Figure 28a.--Maps of Sulphur Hot Springs mound showing configuration of water table.

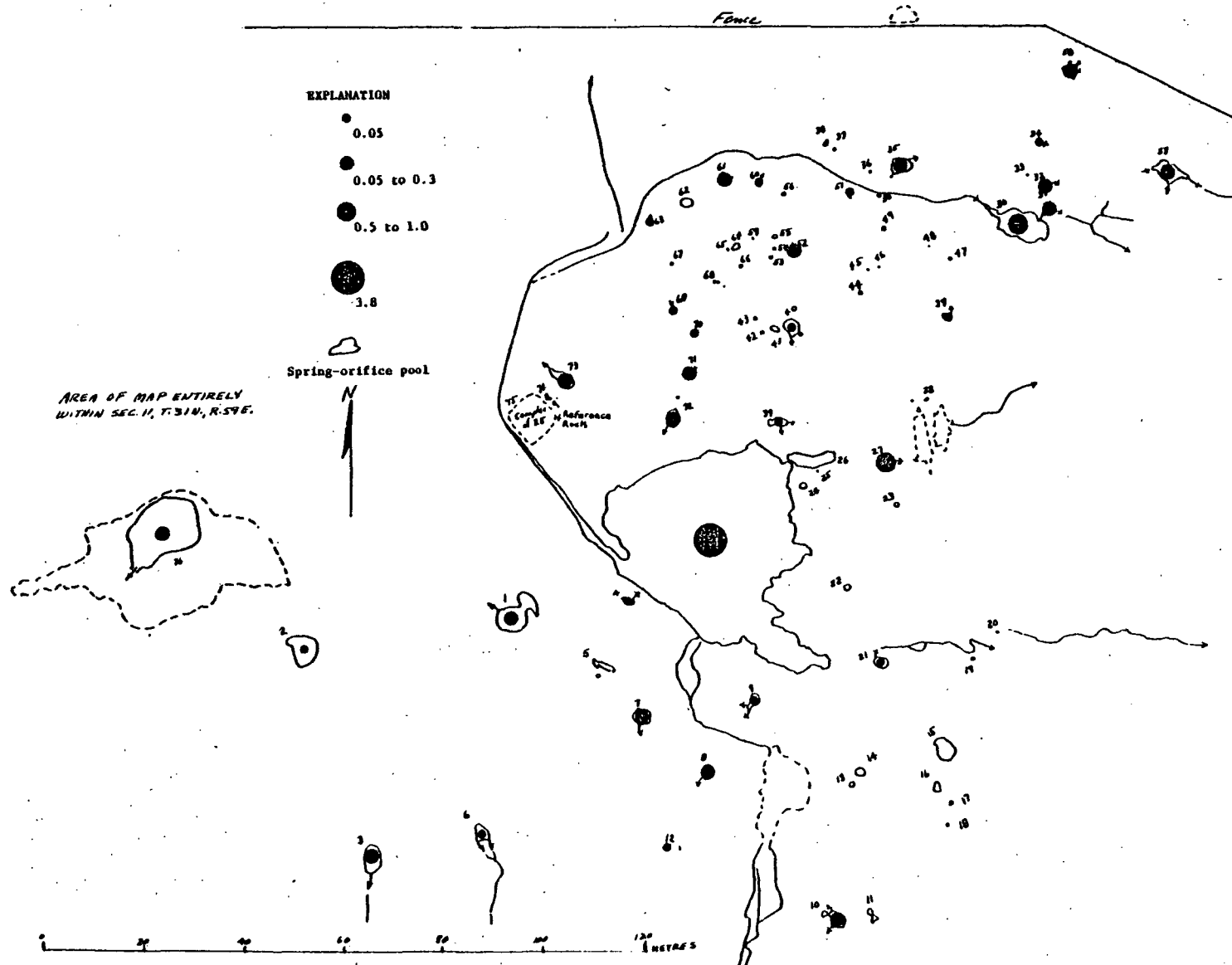


Figure 28b.--Map of Sulphur Hot Springs mound showing distribution of spring-pool overflow.

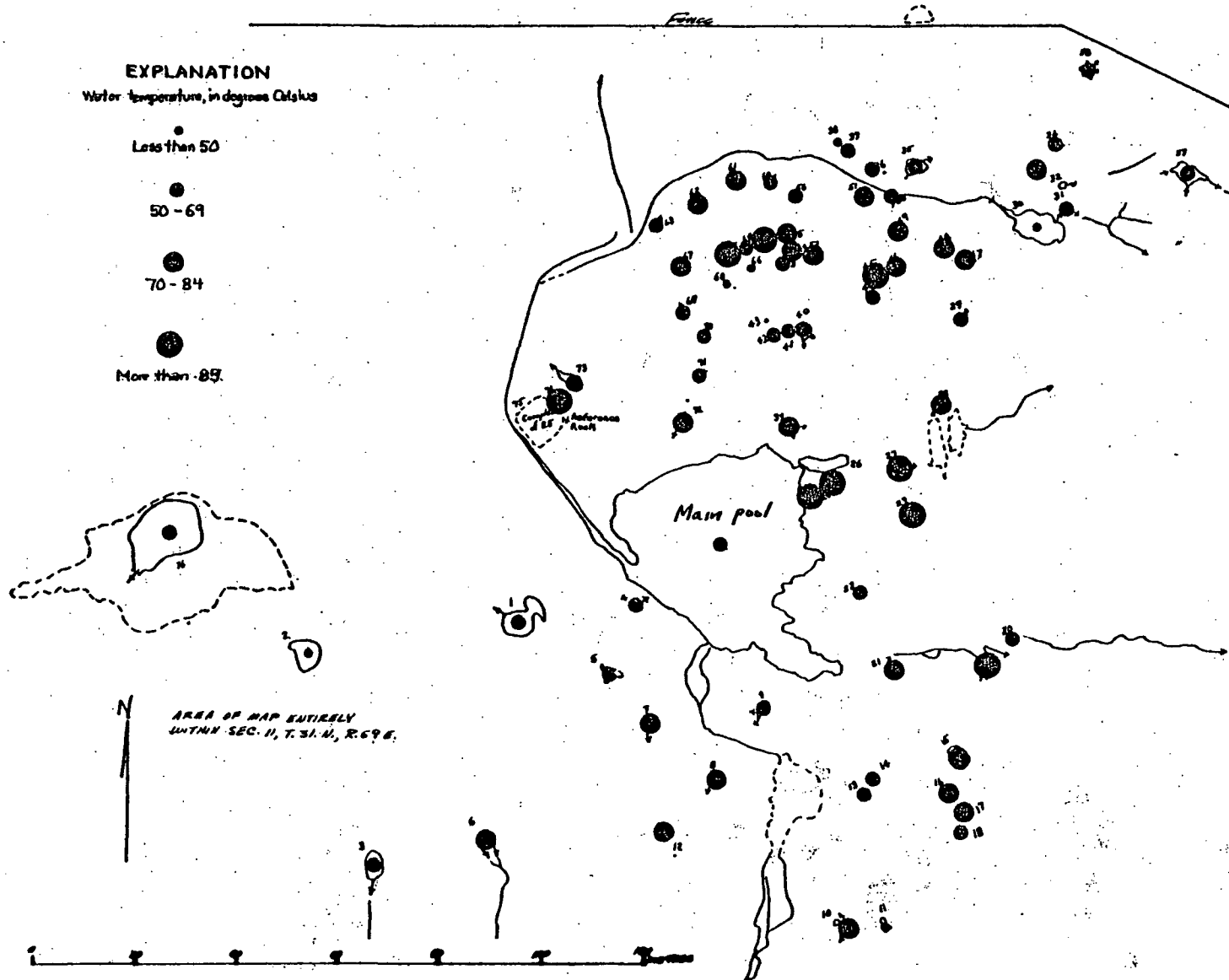


Figure 28c.--Maps of Sulphur Hot Springs mound showing discharge temperatures at spring orifices.

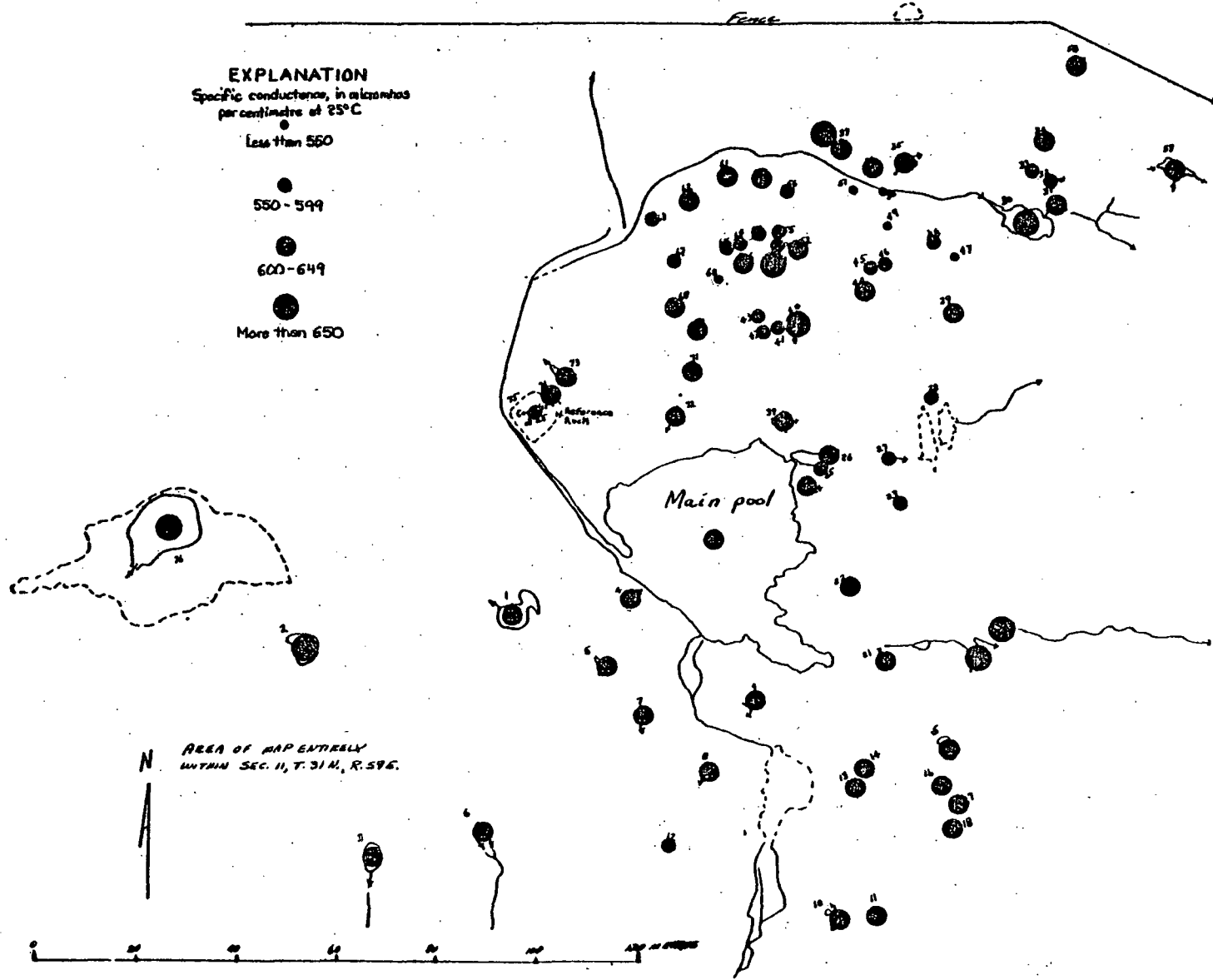


Figure 28d.--Maps of Sulphur Hot Springs mound showing specific conductance of spring-water samples.

The temperatures in the pool orifices ranged from 28° to 96° (superheated) in April 1973 (fig. 28c.). The hottest pools are in an east-west basin array north of the main pool and in a second group east of the main pool. No relations are apparent between temperature and altitude, discharge (overflow), or specific conductance of the pools (fig. 28d). Data for Sulphur Hot Springs are listed in table 17.

Chemical Character of Springflow

Water from one of the hottest overflowing pools at Sulphur Hot Springs was analyzed by Mariner and others (1974). The silica-quartz geothermometer (Fournier, White and Truesdell, 1974) indicates a reservoir temperature of 183°-190°C, one of the highest of all the hot springs sampled in northern and central Nevada (table 1; fig. 2). The abundance of sinter corroborates the high indicated temperature.

Subsurface Temperature Distribution

The distribution of temperature at a depth of 30 m below the land surface is shown on figure 29. The temperature pattern in the central, northern, eastern, and southern parts of the thermal area may be inferred with reasonable confidence on the basis of the test-hole data. However, no data are available for the western part of the area. Abnormally high temperature and thermal gradient at shallow depth in test hole DH-11 suggest that the major fault 175 m to the west is a secondary source of heat, but the extent of the high temperatures associated with the source is unknown. Additional test holes would be required to delineate the thermal area associated with the fault.

The thermal area surrounding the springs is crudely circular, but the hottest part, at the hot springs, is somewhat northeast of the center of the cooler isotherms. Comparison of the water-table contours (fig. 26)

Table 17.—Data for Sulphur Hot Springs, 1973

Heading remarks:

1. Numbered counterclockwise starting at ditch outlet from SW side of main pool
2. Approximate
3. Approximate
4. Above an altitude of 1,800 m (73 07 18)
5. Above (+) or below (-) main pool water level of 1844.46 (73 07 08)
6. Approximate; first number is length; second is width | to length
7. b=bowl, s=shoal, n=neck
8. Approximate
9. Measured generally at deepest point (April 1973)
10. Estimated (April 1973)
11. Sampled 73 07 19

Orifice number	Direction to center of main pool	Distance from near edge of main pool (metres)	Altitude of water surface (metres)	Elevation of pool in reference to main pool (metres)	Pool dimensions (metres)	Pool shape	Maximum depth of pool (metres)	Temperature (°C)	Orifice discharge l s ⁻¹	Specific conductance	Remarks
Main pool	—	—	43.99	—	55 x 35	s,n	—	58	3.8	647	
1	N73E	22.9	44.08	+0.08	7.6 x 4.6	b	2.1	60	0.1-0.2	636	
2	N81E	64.2	43.34	-.45	6.1 x 3.0	b,s	1.5	28	<.1	700	
3	N53E	78.0	42.63	-1.37	7.6 x 3.0	b	1.8	66	.25-.3	612	Undercut .3-9 m on most sides.
4	N52E	3.7	44.02	+ .02	2.7 x 1.2	b	.6	67	<.1	625	Discharge flows into main pool.
5	N44E	22.9	44.14	+ .15	5.5 x .9	s	.6	64	0	629	Scall orifice .9 m away, .15 m ft deep; discharge is <1 .1 l/s flowing when sampled.
6	N41E	64.2	43.01	-.99	2.7 x 1.8	s	.3	81	<.1	614	Distance 22.0 m
7	N27E	22.9	44.06	+ .07	3.0 x 2.1	b	.9	74	.1	625	Channel to E. Distance 11.9.
8	N6E	27.5	43.64	-.36	2.7 x 2.4	b,s	1.2	70	.1	614	Water channels on all sides. Distance 8-7 = 18.3 m. Steel pipe, 5.1 cm diameter in orifice.
9	N10W	11.9	44.14	+0.15	2.1 x 2.1	b	.8	60	<.1	625	
10	N15W	59.6	43.29	-.70	2.1 x 1.8	b,s	.6	70	.1	609	
11	N15W	59.6	43.24	-.75	2.7 x .9	b,s	.3	39	0	632	Altitude is slightly higher than no. 10. Distance 7.3 m. Roll of wire near.
12	N0E	41.3	43.40	-.59	.6 x .6	b,s	.5	79	<.1	550	Distance 12-8= 18.3 m. Not flowing when sampled.
13	N25W	36.7	43.55	-.45	1.2 x .9	b	.2	58	0	621	Distance 13-14= .92 m
14	N28W	36.7	43.56	-.44	1.8 x 1.5	b	.9	58	0	621	Six-inch vertical wall above water surface.
15	N43W	45.9	42.88	-1.12	4.6 x 3.7	b,s	1.7	81	0	607	.6 m vertical wall above water surface.
16	N39W	45.9	42.87	-1.12	1.8 x 1.5	b	.3	76	0	621	Distance 16-15= 4.88 m
17	N40W	50.5	42.87	-1.13	.9 x .6	b,s	1.1	80	0	600	Distance 17-16= 2.44 m
18	N34W	55.0	42.77	-1.23	.5 x .3	s	.1	67	0	614	Distance 18-17= 3.96 m
19	N63W	45.9	43.19	-.80	.21 x .21	b	.1	86	0	669	Receiving flow when sampled.
20	N71W	50.5	43.35	-.64	.3 x .3	b	.2	58	0	667	Distance 20-19= 8.3 m when sampled.
21	N56W	27.5	43.90	-0.10	3.0 x 2.4	b	1.2	76	<.1	632	
22	N71W	13.8	43.88	-.12	1.2 x 1.2	b,s	.5	54	0	625	

Table 17.—Continued

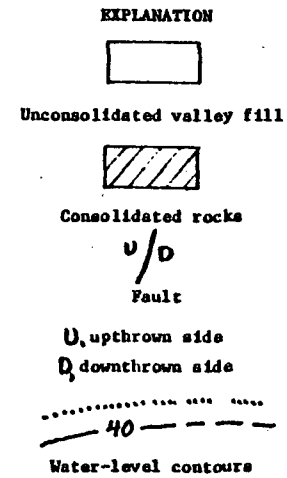
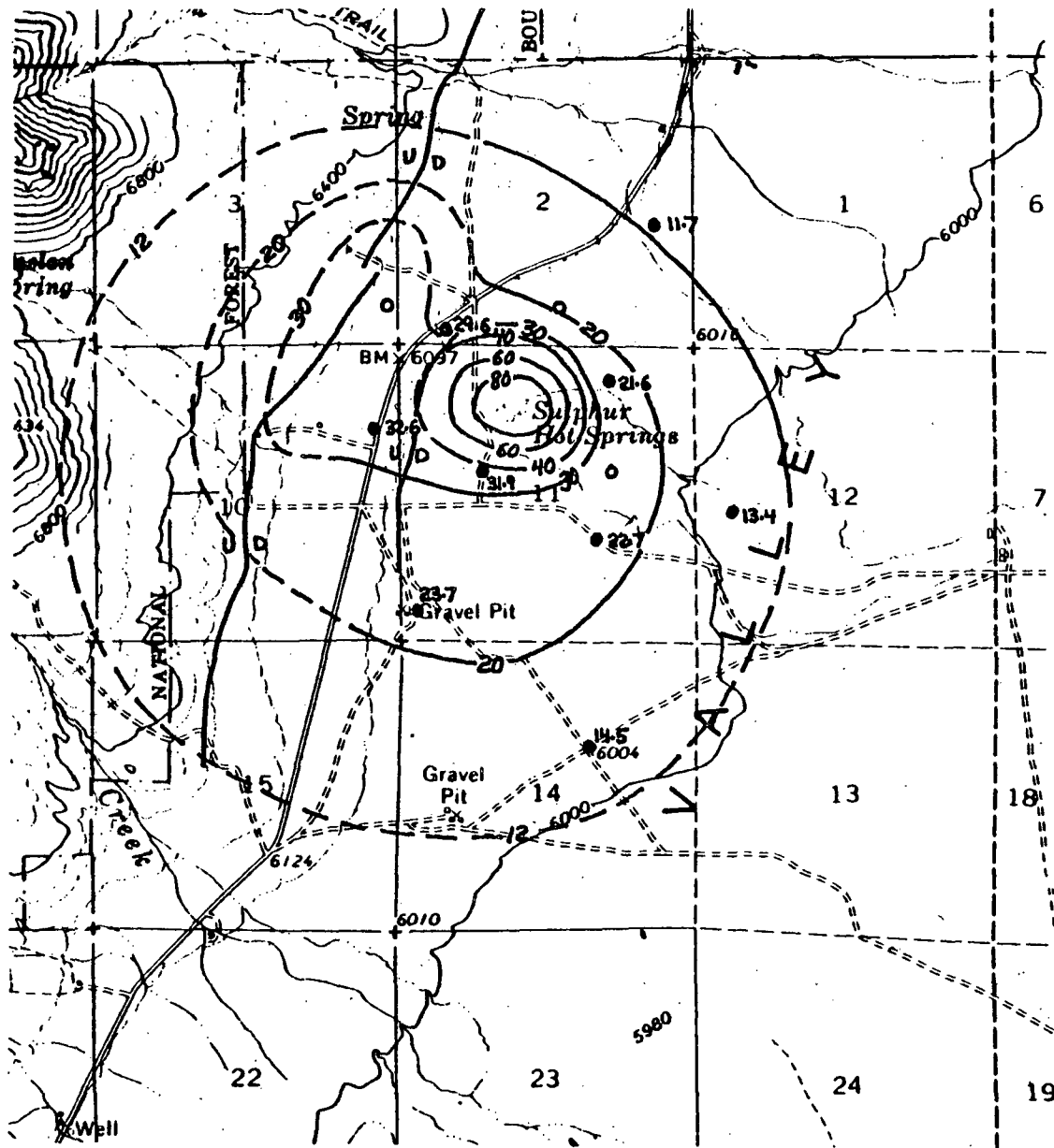
1	2	3	4	5	6	7	8	9	10	11	12
Orifice number	Direction to center of main pool	Distance from near edge of main pool (metres)	Altitude of water surface (metres)	Elevation of pool in reference to main pool (metres)	Pool dimensions (metres)	Pool shape	Maximum depth of pool (metres)	Temperature (°C)	Orifice discharge (l s ⁻¹)	Specific conductance	Remarks
23	S82W	22.9	43.48	-.52	.6 x .6	b,s	1.2	96	0	590	Steel pipe in orifice
24	S64W	2.8	43.97	-.02	1.2 x .9	b,s	.6	86	0	632	
25	S59W	6.4	43.92	-.08	.05 x .15	n	.1	96	0	586	Boiling hard. Distance 25-24 = 4.6 m.
26	S58W	0.3	43.73	-.26	10.7 x 2.4	b,s	.9	—	0	632	.3 m rim separates main pool from no. 26
27	S65W	21.1	43.47	-.53	1.5 x 1.5	b,s	2.4	95	.6 -1.3	598	Distance between 27 and 26 = 10.1 m Lumber in orifice.
28	S62W	36.7	43.53	-.46	.6 x .3	b	.2	80	0	580	Distance 28-27 = 17.4 m
29	S46W	50.5	43.05	-.95	1.8 x 1.2	b,s	.6	69	<.1	610	
30	S53W	82.6	42.19	-1.80	10.7 x 6.1	b	1.5	47	See remarks	656	Receives inflow of .32 l/s (T=32°) Outflow is 1.58 l/s Pool used for swimming.
31	S53W	89.9	42.15	-1.85	3.0 x 1.5	b	.9	68	See remarks	636	Receives inflow of .32 l/s (T=35°). Outflow is .63 l/s Inflow is from no. 30. Distance between 31 and 30 = 2.8 m.
32	S48W	91.7	42.15	-1.85	1.2 x 1.2	b,s	.6	91	.1	577	Distance between 32 and 31 = 3.7 m. Not flowing when sampled.
33	S47W	90.8	42.20	-1.80	.3 x .2	b	.2	73	0	568	Distance between 33 and 32 = 1.8 m.
34	S45W	98.17	42.19	-1.80	1.2 x .9	b	1.5	64	<.1	632	9.2 m N of no. 32. Undercut.
35	S39W	75.2	42.76	-1.23	3.7 x 3.0	b,s	2.1	65	.1	629	2.8 m N of ditch running to no. 30. Temperature in embayment = 71°C. Two small orifices 2.44 m S and 2.74 m NSW.
36	S32W	71.56	42.81	-1.19	.9 x .9	b,s	2.4	75	0	600	1.8 m N of ditch.
37	S27W	71.56	42.89	-1.10	.46 x .46	b	1.5	59	0	618	4.6 m N of ditch. Water turbid.
38	S26W	71.56	42.92	-1.08	1.2 x .6	b,s	1.5	46	0	729	4.6 m N of ditch. Water turbid.
39	S35W	6.4	44.36	+.37	4.6 x 2.4	b,s	1.2	82	<.1	638	At measuring point of T, .9 m deep. Distance between 39 and 26 = 6.4 m.
40	S28W	30.28	43.88	-.11	3.7 x 2.7	b	1.8	59	<.1	682	
41	S23W	29.36	43.78	-.21	1.8 x .9	b	1.5	53	0	560	
42	S23W	27.5	43.79	-.20	.46 x .46	b	.3	65	0	550	Distance between 42 and 41 = 1.8 m.
43	S23W	29.36	43.80	-.20	—	—	—	—	0	550	

Table 11—Continued

1	2	3	4	5	6	7	8	9	10	11	12
Orifice number	Direction to center of main pool	Distance from near edge of main pool (metres)	Altitude of water surface (metres)	Elevation of pool in reference to main pool (metres)	Pool dimensions (metres)	Pool shape	Maximum depth of pool (metres)	Temperature (°C)	Orifice discharge (l s ⁻¹)	Specific conductance	Remarks
44	S38W	44.95	43.25	-0.73	.9 x .6	b,s	0.9	52	0	636	Distance 44-40=20 18.3 m distance 44-29=20.2 m.
45	S37W	50.46	43.30	-.70	.15 x .18	n	.9	89	0	574	
46	S38W	52.29	43.28	-.71	.09 x .09	n	.3	82	0	561	Slightly larger diameter neck, .2m S, 1.22 m deep, No. 45 is 2.8 m SW.
47	S46W	62.39	42.75	-1.24	.27 x .27	n	1.2	76	0	512	In grass, SW of No. 47
48	S46W	61.47	42.93	-1.06	.3 x .27	b	.2	76	0	598	5.5 m W of no. 47
49	S40W	61.47	42.95	-1.04	.9 x .6	b	.5	71	0	517	11.0 m W of no. 48 and 9.2 m N of no. 46.
50	S35W	66.97	42.84	-1.16	.6 x .6	b,s	1.8	63	0	467	.92 m S of ditch to no. 30.
51	S30W	65.14	42.93	-1.07	.46 x .3	b,s	.6	71	0+	458	1.8 m S of ditch. Not flowing when sampled.
52	S23W	47.71	43.57	-.42	.9 x .6	b,s,n	2.4	81	.1	602	
53	S18W	44.95	43.45	-.45	.6 x .3	b,n	1.8	53	0	673	4.6 m W of 52; south end of line of 3.
54	S18W	47.71	43.57	-.42	.24 x .18	n	1.5	76	0	590	4.6 m W of no. 52 and 1.8 m S of no. 53.
55	S18W	50.46	43.57	-.42	.9 x .6	n	2.4	75	0	593	North end of line of 3 (nos. 53-55).
56	S18W	60.55	43.37	-.63	.27 x .27	n	.2	57	0	575	10.1 m N of no. 55. Flowing when sampled.
57	S55W	155.96	41.32	-2.67	7.3 x 4.9	b,s	1.8	55	See remarks	648	NE of no. 30. Temperature not at maximum depth. Inflow to orifice = .95 l/s (37°). Outflow = 1.26 l/s.
58	S40W	155.96	41.86	-2.14	4.6 x 2.4	s	—	87	2.3	600	4.6 m S of fence
59	S19W	47.71	43.60	-.39	.24 x .24	s,n	.6	92	0	583	
60	S19W	61.47	43.35	-.65	.9 x .6	b,s,n	1.8	69	0+	629	5.5 m S of ditch to no. 30.
61	S14W	60.55	43.36	-.63	2.4 x 1.5	b,s,n	1.2	70	.3	600	5.5 m W of no. 60. Lumber (4"x8") in orifice.
62	S7W	57.80	43.44	-.55	2.1 x 1.8	b,s,n	1.5	74	0	609	9.2 m W of no. 61
63	S2E	53.21	43.53	-.46	.27 x .21	s,n	.3	69	0+	559	2.8 m S of ditch to no. 30. 4.6 m to N-S ditch alignment.
64	S10W	50.46	43.57	-.42	1.2 x .9	b,s	.6	66	0	568	3.7 m W of no. 59
65	S10W	49.54	43.60	-.40	.12 x .12	n	.9	95	0	561	.6 m W of no. 64
66	S10W	46.79	43.61	-.39	.46 x .3	n	1.5	45	0	618	3.7 m S of no. 65
67	S1E	44.04	43.77	-.23	.43 x .43	b	.2	70	0	564	15.6 m W of no. 66
68	S12W	36.70	43.62	-.38	.76 x .43	b	1.5	38	0	507	8.3 m SW of no. 65 and 9.2 m SE of no. 67. Small orifice (.15 m x .05 m) 2.8 m SE, slightly warm. Small orifice (.06 m x .05 m) 6.4 m SSE.

Table 17.—Continued

1	2	3	4	5	6	7	8	9	10	11	12
Orifice number	Direction to center of main pool	Distance from near edge of main pool (metres)	Altitude of water surface (metres)	Elevation of pool in reference to main pool (metres)	Pool dimensions (metres)	Pool shape	Maximum depth of pool (metres)	Temperature (°C)	Orifice discharge (l s ⁻¹)	Specific conductance	Remarks
69	S1E	33.03	44.25	+0.26	1.2 x .9	b	.9	64	0+	629	
70	SSW	25.69	44.03	+ .04	.9 x .9	n	1.5	56	0+	648	5.5 m SSE of no. 69. Not flowing when sampled.
71	S2E	17.43	44.31	+ .32	2.1 x 1.2	b	1.2	61	1	632	8.3 m S of no. 70
72	S12E	9.17	44.30	+ .31	3.7 x 3.0	b	1.5	72	.2 - .3	625	11.0 m SW of no. 71. Discharge flows into main pool. Small orifice 1.8 m N.
73	S38E	24.77	44.16	+ .16	4.0 x 3.0	b,s	.9	66	.2 - .3	621	
74	S47E	22.94	43.88	- .11	1.2 x 6	b,n	.9	90	0	600	Distance between no. 73 and 74 = 2.8 m. Complex of 5 orifices over a distance of 3.7 m.
75	S49E	22.02	43.88	- .12	—	—	—	—	0-	596	Complex of about 25 small orifices within a circle having a diameter of 7.3 m. All are small.
76	N86E	87.16	43.30	- .70	15 x 9	s,b	.9 - 1.5	60	.1 - .3	723	Turbid and swampy



Show altitude in metres above a datum 1,800 m above mean sea level. Solid lines indicate 10-m-interval contours; dotted lines, 2-m-interval contours. Dashed where uncertain.

● 37.7
Test hole. Number is altitude of water table, in metres above a datum 1,800 m above mean sea level.

○ 10.5
Spring. Number is altitude, in metres above a datum 1,800 m above mean sea level.

▲ 28.9
Stream site. Number is altitude of water table, in metres above a datum 1,800 m above mean sea level.

Figure 29.--Map of Sulphur Hot Springs thermal area showing temperature at a depth of 30 m, fall 1973.

and the isotherms (fig.29) does not indicate rapid transport of heat by lateral flow of ground water in very shallow aquifers like that in the Soda Lakes-Upsal Hogback area in the Carson Desert. The southerly extension of above-normal temperatures may be related to the occurrence of earlier hydrothermal activity south of the present hot springs, as reflected by sinter deposits just west of test hole AH-1 (fig.25). Another possible explanation of the wide spacing of the isotherms south of the hot springs is that thermal water rises into and flows laterally in aquifers at depths greater than 30 m in that part of the area.

Heat Discharge

Most of the heat discharge from the Sulphur Hot Springs hydrothermal system is by conduction through near-surface materials and by convection in springflow and steam discharge. Boundaries of the thermal area are drawn so as to minimize heat discharge by lateral ground-water outflow. Heat discharged as evaporation from hot-water surfaces is included in that measured as springflow. Radiative heat discharge from warm soil or water surfaces may be significant locally, but the areas of high radiative discharge are only a small fraction of the entire thermal area. The total heat discharge by radiation is believed to be small and is not estimated as a separate item in the heat budget.

Conductive heat discharge.--Discharge of heat by conduction through near-surface materials at Sulphur Hot Springs is estimated by method A described in the section, "Estimates of heat discharge." The total conductive heat discharge is estimated to be 1.43×10^6 cal s⁻¹. Derivation of the estimate is given in table 18.

Table 18.--Estimate of conductive heat discharge from Sulphur Hot Springs hydrothermal system on the basis of method A described in the text.

Temperature range (°C)	Geometric mean temperature (°C)	Thermal gradient ^{1/} ($\times 10^{-3}$ °C cm ⁻¹)	Heat flow ^{2/} ($\times 10^{-6}$ cal cm ⁻² s ⁻¹)	Area ($\times 10^{10}$ cm ²)	Heat discharge ($\times 10^6$ cal s ⁻¹)
12-20	15.5	2.5	6.5	7.31	0.48
20-30	24.5	5.5	14	3.02	.42
30-40	34.6	8.9	23	1.16	.27
40-60	49.0	14	36	.29	.10
60-80	69.3	20	52	.16	.08
> 80	98.0	30	78	.10	.08
Total				12.0	1.43

(1) Based on 8.0 °C mean annual temperature at the land surface.

(2) Based on harmonic-mean thermal conductivity of 2.6×10^{-3} cal cm⁻¹ s⁻¹ °C⁻¹.

An attempt was made to estimate conductive heat discharge by method B, but data are insufficient to define heat-flow isograms in the western part of the area, along the major fault 1 km west of the springs. Computed heat flow at test hole DH-11, about 175 m east of the fault, is 58 HFU, which is higher than the heat flow at any of the other test holes and probably about as high as that on the margins of the spring mound. A heat-flow high is very likely associated with the fault as well as with the hot springs, but the extent and configuration of this second high cannot be determined with present data.

Method B does, however, provide the most reliable data that indicate the magnitude of the heat flow near the margin of the thermal area. Computed heat-flow values at test holes DH-8A and DH-10 are respectively 4.8 and 3.9 HFU. Both sites are a short distance within the thermal area, as defined by the 12°C isotherm on figure 29. Therefore, the so-called "normal" heat flow on the margin of the thermal area may be about 3 HFU. Using this heat flow over the thermal area, the "normal" heat discharge is estimated to be

$$(12.0 \times 10^{10} \text{ cm}^2)(3.0 \times 10^{-6} \text{ cal cm}^{-2} \text{ s}^{-1}) = 0.36 \times 10^6 \text{ cal s}^{-1}$$

Therefore, the net conductive heat discharge that results from the rising thermal water is estimated to be total conductive heat discharge minus "normal" heat discharge for the area,

$$(1.43 - 0.36) \times 10^6 \text{ cal s}^{-1} = 1.07 \times 10^6 \text{ cal s}^{-1}.$$

Heat discharge by springflow.--Convective heat discharge by springflow is estimated to be $0.48 \times 10^6 \text{ cal s}^{-1}$ on the basis of an average flow of 8.9 l s^{-1} from the spring orifices (spring-pool overflow plus evaporation from pool surfaces), an average discharge temperature of 63°C, and a mean annual air temperature of 8°C.

Heat discharge by steam.-- As discussed in the sections, " Estimates of heat discharge" and "Estimates of water discharge," only a part of the heat loss between the thermal reservoir and the land surface is represented by steam discharge. The discharge of steam from boiling pools (as equivalent water) is estimated to be $0.006 \times 10^6 \text{ m}^3 \text{ yr}^{-1}$, as explained in the section, "Estimates of water discharge" . The heat discharged by this steam is computed as the product of the mass flow rate and the enthalpy of the steam:

$$\begin{aligned} (6 \times 10^9 \text{ g yr}^{-1})(5.43 \times 10^2 \text{ cal g}^{-1}) &= 3.3 \times 10^{12} \text{ cal yr}^{-1} \\ &= 0.10 \times 10^6 \times 10^6 \text{ cal s}^{-1} \end{aligned}$$

The remainder of the heat loss between the thermal reservoir and the land surface is believed to be included in that measured as conduction and as springflow augmented by the steam condensed in and near the conduit system.

Net heat discharge.--The net heat discharge from the hydrothermal system that results from the convective upflow of the thermal water is computed as the sum of the net conductive heat discharge, the convective heat discharge by springflow, and the convective heat discharge by steam:

	($\times 10^6 \text{ cal s}^{-1}$)
Net conductive heat discharge	1.07
Convective heat discharge by springflow	.48
Convective heat discharge by steam	.10
<hr/>	
Total (rounded)	1.6

Water Discharge

Ground water discharges from the Sulphur Hot Springs thermal area by springflow, evapotranspiration from the spring-mound area, and lateral subsurface outflow. Total ground-water discharge, which may include nonthermal as well as thermal water, is estimated by the water-budget method. Thermal-water discharge is estimated by the heat-budget method.

Water-budget method.--Discharge from the spring mound includes overflow from the orifice pools, evaporation from the pool surfaces, evapotranspiration, and lateral subsurface flow.

Thirty-two pools overflow. The estimated total overflow discharge is 8.2 l s^{-1} ($0.26 \times 10^6 \text{ m}^3 \text{ yr}^{-1}$). About half the total originates from the main pool. The above conclusions are based on observations made in April 1973. Slightly different flow rates were observed at other times.

Average annual evaporation from the surface of the orifice pools is estimated to be between 17,000 and 25,000 m^3 , or about 20,000 m^3 of water. This estimate is based on a water-surface area of 1,700 m^2 , an average water temperature of 40°-45°C, and an average annual evaporation rate of 10-15 m.

Evapotranspiration of ground water from the spring mound is by two processes: (1) evapotranspiration by phreatophytes rooted in a shallow water table and (2) plant use of water that reaches the surface by upward seepage from the western and northern flanks of the spring mound. On these two flanks of the mound, dense low vegetation covers an area of about 8,000 m^2 . The discharge rate in this area is probably about 120 cm yr^{-1} . In the remainder of the area, about 45,000 m^2 , the principal phreatophyte is saltgrass, but some rabbitbrush is also present. The discharge rate is probably about 10 cm yr^{-1} . Thus, from the entire area of the mound, the evapotranspiration discharge is about 14,000 $\text{m}^3 \text{ yr}^{-1}$.

Lateral flow in the subsurface from the hydrothermal system to the regional ground-water system is likely because of the higher fluid potentials in the hydrothermal system. The rate of flow probably is small, however, owing to the low permeability of the sinter and cemented deposits surrounding the spring conduits. No estimate of the lateral subsurface outflow is attempted.

Ground-water discharge from the hydrothermal system in the spring-mound area is summarized as follows:

	Discharge ($\times 10^6 \text{ m}^3 \text{ yr}^{-1}$)
Spring-pool overflow	0.26
Evaporation from pool surfaces	.020
Evapotranspiration	.014
	<hr/>
Total (rounded)	.29

Heat-budget method.--Upflow of thermal water from the deep part of the hydrothermal system is computed, using the heat-budget method, as follows. Temperature of the water leaving the deep reservoir is assumed to be 186°C on the basis of the silica-quartz geothermometer (table 1; Mariner and others, 1974, table 3). Mean annual temperature at the land surface is assumed to be 8°C on the basis of data from the Ruby Lake weather station (table 6). Net enthalpy of the water is

$$(188 - 8) \text{ cal g}^{-1} = 180 \text{ cal g}^{-1}$$

Net heat discharge from the hydrothermal system is estimated to be $1.6 \times 10^6 \text{ cal s}^{-1}$, as described in the preceding section. Thermal-water discharge is therefore

$$\frac{1.6 \times 10^6 \text{ cal s}^{-1}}{1.8 \times 10^2 \text{ cal g}^{-1}} (1.018 \times 10^{-6} \text{ m}^3 \text{ g}^{-1})(3.16 \times 10^7 \text{ s}^{-1} \text{ yr}^{-1})$$

$$= 0.29 \times 10^6 \text{ m}^3 \text{ yr}^{-1}$$

at an average discharge temperature of 63°C.

Comparison of two estimates.--The two estimates of thermal-water discharge are in good agreement, which suggests that virtually all the discharge estimated by the water-budget method represents thermal water having a source temperature indicated by the silica-quartz geothermometer. If any admixed waters from shallower sources are included in the discharge, the temperature of the deep source must be higher than the 183°-190°C indicated temperature.

Inferred Nature of Hydrothermal System

The depth, extent, and nature of the thermal reservoir are unknown. It seems likely, however, that carbonate rocks like those exposed in the Ruby Mountains west of Sulphur Hot Springs contain secondary openings formed or (and) enlarged by solution which provide channelways through which ground water circulates to depths of several kilometres.

Presence or absence of a local crustal heat source cannot be determined from present data. Ambiguous data from the shallow test holes drilled in this study indicate above-average heat flow (~ 3 HFU) outside the thermal area, but deeper drilling is needed to confirm or deny this interpretation.

Sources of recharge to the hypothermal system likewise are not known specifically, but the most likely general area is the higher part of the Ruby Mountains, several kilometres west of the hot springs.

Distribution of temperatures at depths less than 50 m suggests that the thermal water rises nearly vertically in a conduit system under the spring mound.

The configuration of the conduit system is not known, but the principal Basin and Range fault at the east base of the Ruby Mountains probably contains the principal deep conduits for the rising thermal water. Other faults, toward the east, may be branches of the main fault and may provide avenues for the

thermal water to rise into the present spring mound, which is 1 km east of the main fault.

The upflow of thermal water may be sufficiently rapid so that the deep reservoir temperature of 180° - 190°C indicated by the silica-quartz geothermometer (table 1; Mariner and others, 1974) is maintained until the boiling point is reached at a hydrostatic depth of about 100 - 110 m beneath the spring mound.

Little heat may be lost until this point is reached, except by conduction laterally through the walls of the conduit system.

Distribution of shallow temperatures suggests that discharge of water from the conduit system into near-surface aquifers in the Tertiary and Quaternary sediments is small. Leakage into zones deeper than about 50 m is not precluded by available data, however.

LEACH HOT SPRINGS THERMAL AREA

Location

Leach Hot Springs are in Grass Valley, in Pershing County, about 45 km by road south of Winnemucca, Nevada (fig. 5). The springs are at the base of a low fault escarpment near the east side of the valley, in the SE $\frac{1}{4}$ sec. 36, T. 32 S., R. 38 E., Mount Diablo baseline and meridian. The surrounding area is used intermittently for cattle grazing, and the spring-flow is used for watering stock and for irrigation at a ranch just west of the springs. An area of 3,612 ha surrounding the springs has been classified as the Leach Hot Springs KGRA.

Test Drilling

Eleven test holes were drilled near Leach Hot Springs as a part of this study. The holes were drilled by the hydraulic-rotary method and range in depth from about 17 to about 50 m. The first seven holes were drilled in the spring of 1973 by the U.S. Bureau of Reclamation, the last four holes,

Table 19.--Data for U.S. Geological Survey test holes in
the Leach Hot Springs thermal area

Well number: Wells 1-7 drilled during June 12-19, 1973, using rotary rig and "Revert" mud. Wells 8-11 drilled during October 29 - November 2, 1973, using rotary rig and "Revert" mud.

Type of completion: Casing type is indicated by "St" (3.8-cm nominal inside diameter steel) or "P" (5.1-cm nominal inside diameter PVC, topped by 2-m length of 5.1-cm steel casing). Wells capped and filled with water are indicated by "C". Wells with well-point screens at bottom are indicated by "Sc".

Depth to water table: Depth below land-surface datum, obtained from neutron (N) log.

Static water level: Depth below land-surface datum.

Geophysical log available: Gamma ("G"), gamma-gamma ("G²"), neutron ("N"), resistivity ("R"), and temperature ("T").

Well number	Location	Depth (metres below land surface)	Casing		Land-surface altitude (m)	Depth to water table			Static confined water level		Geophysical logs available	Approximate depth to Tertiary sedimentary rocks (m)
			Inside diameter (cm)	Type of completion		Metres below land surface	Source of data	Date	Metres below land surface	Date		
QVDM-1	33/38-1dbs	45.17	5.1	P, Sc	1,407.3	12.6	N	73 11 15	12.38	73 12 14	G, G ² , N, T	>44.8 ^a
DH-2	32/39-30acc	50.05	5.1	P, C	1,468.5	40.8	N	73 11 14	-	-	G, G ² , N, T	18.4 (?)
DH-3	-31cbb	49.99	5.1	P, C	1,452.4	22.2	N	73 11 13	-	-	G, G ² , N, T	8.0
DH-4	32/38-25dcd	49.83	5.1	P, C	1,429.5	23.6	N	73 11 14	-	-	G, G ² , N, T	18.6 (?)
DH-5	32/39-31ead	27.10	5.1	P, C	1,481.9	>27.1	N	73 11 13	-	-	G, G ² , N, T	7.3
DH-6	31/38-1aac	45.02	3.8	St, Sc	1,426.2	16.7	N	73 11 15	16.37	73 12 14	G, G ² , N, T	9.4
DH-7	32/38-25ecd	50.90	5.1	P, Sc	1,396.0	26.4	N	73 11 09	26.33	73 12 15	G, G ² , N, T	47.2
DH-8	-35dba	44.8	5.1	P, Sc	1,394.2	23.2	N	73 11 09	23.16	73 12 13	G, G ² , N, R, T	>44.8
DH-9	-36deb	45.02	3.8	St, Sc	1,417.9	36.2	N	73 11	30.48	74 08 07	G, G ² , N, T	>45.0
DH-10	-36ada	17.34	3.8	St, Sc	1,432.6	-	-	-	5.77	73 12 15	G, T	3.7
DH-11	-36bdb	44.81	3.8	St, Sc	1,401.2	29.5	N	73 11 13	29.32	73 12 15	G, G ² , N, R, T	30.6 (?)

a. May not have reached equilibrium water level.

Table 20 .--Data for selected water wells near Leach Hot Springs^{a/}

Location	Depth (metres)	Perforated interval (metres)	Land- surface altitude (metres)	Static water level Metres	Date	State log number
31/38-26abb	60	52-56	1,472	46	47 07 12	309
31/39-32abc	90	53-88	1,460	42	58 05 22	4082
32/38-18acc	41	40-41	1,378	24	55 09 22	270
-33bcc	76	43-76	1,401	<u>b/</u> 39	73 10 29	8621
-36cba	45	30-45	1,398	<u>b/</u> 25	73 06 14	6424
33/38-32bab	18	17-18	1,352	9	61 10 03	269

a/ Data from Cohen (1964, table 8) and files of Nevada State Engineer.

b/ Depth below land-surface datum; datum for other water levels unknown.

in the fall of 1973 by the U.S. Geological Survey. Because of the substantial depths to water in parts of the area, four of the holes were furnished with pipes capped and filled with water rather than with pipes fitted with well points. The test-hole data are given in table 19.

Data for selected water wells near Leach Hot Springs are presented in table 20. Static water levels were measured in two of these wells during this study.

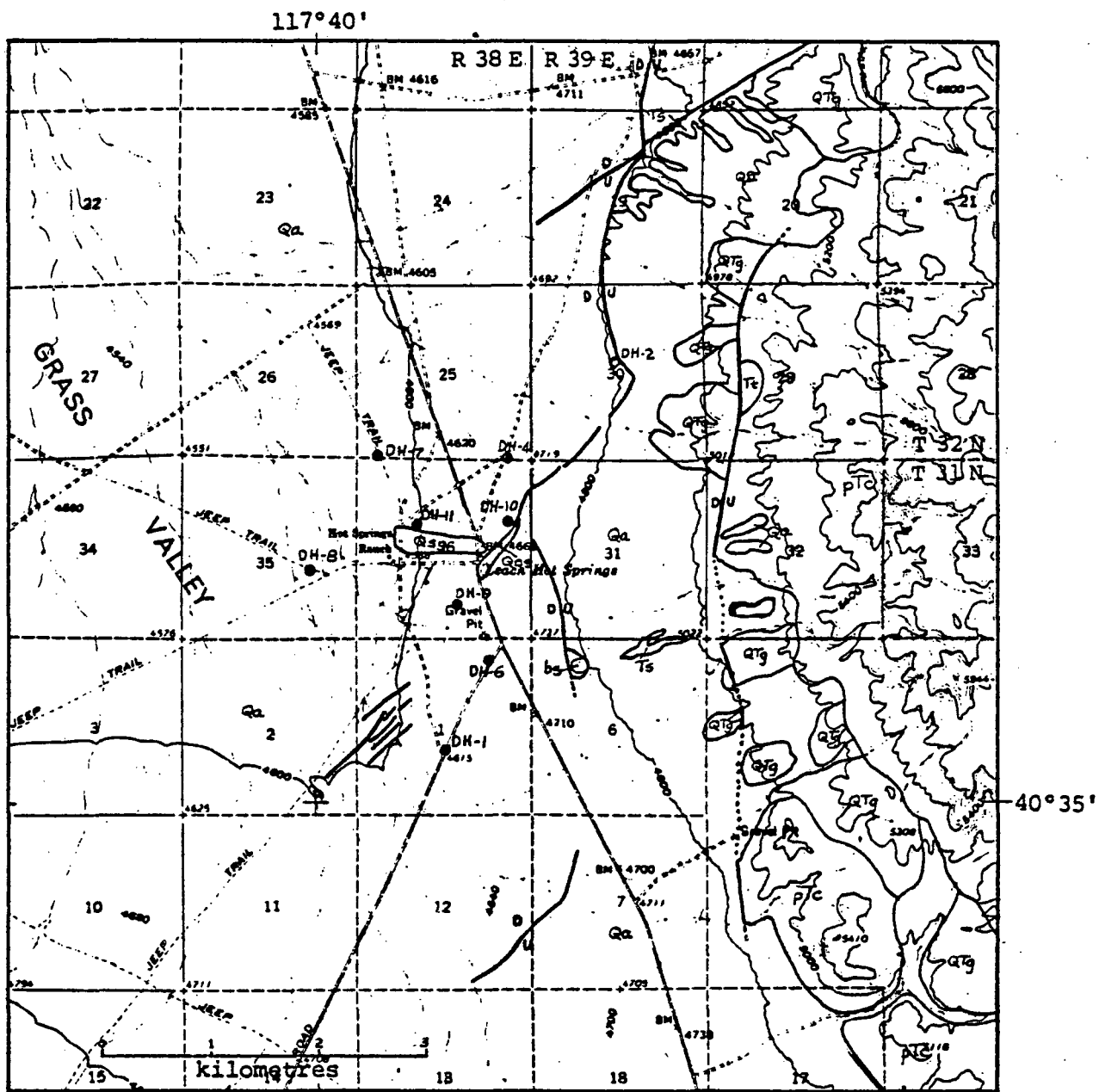
Geology

Rocks exposed near Leach Hot Springs range from consolidated rocks of Paleozoic age to unconsolidated alluvial and colluvial deposits of Holocene age. Areal distribution of units classified in this study is shown on figure 30. The springs issue from late Pleistocene or Holocene alluvial deposits, but the thermal water undoubtedly has flowed through older rocks like those exposed nearby to the east.

The consolidated rocks of pre-Tertiary age are grouped into one unit on figure 30. Included in this unit are the Pumpnickel Formation, the Havallah Formation, the Koipato Group, and the China Mountain Formation (Tatlock, 1969).

The Pumpnickel Formation, of Pennsylvanian and Permian age, is the most extensively exposed unit on the west flank of the mountains east of Leach Hot Springs. The exposed rocks include greenstone (altered lavas), dark-gray chert, argillite, and minor sandstone and limestone, all of probable eugeosynclinal affinities.

The Pumpnickel Formation is overlain by, or is in fault contact with, the Havallah Formation of Pennsylvanian and Permian age. Within the area of figure 30, the Havallah consists chiefly of chert, quartzite, and somewhat calcareous slate.

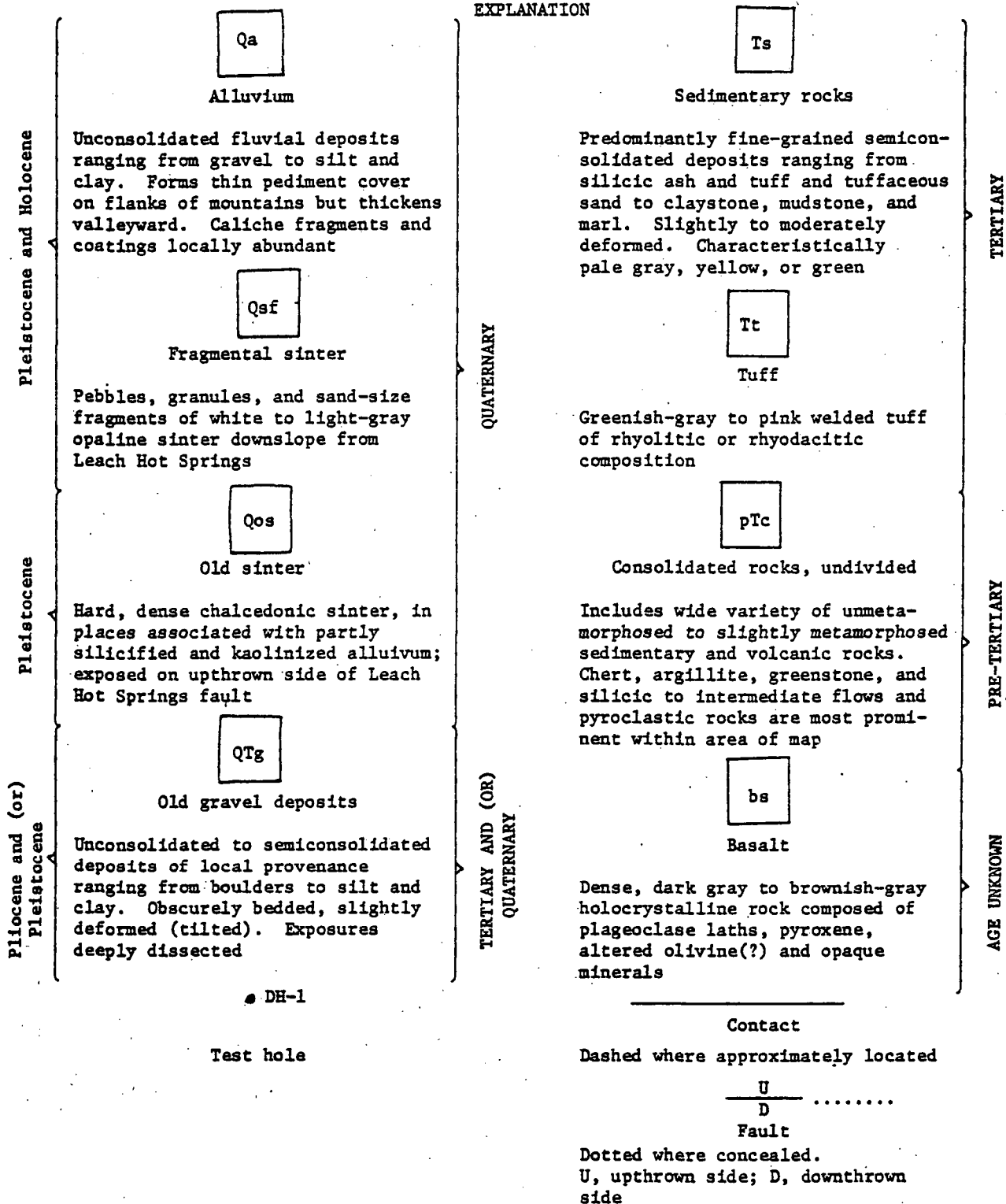


Geology by F. H. Olmsted, 1973

Figure 30.--Geologic map of Leach Hot Springs thermal area showing location of test holes.

LEACH HOT SPRINGS AREA

EXPLANATION



The Koipato Group, of Permian age, is exposed in the bedrock outlier near the southeast corner of figure 30. There it consists chiefly of slightly metamorphosed lavas or ignimbrites of silicic to intermediate composition.

The Koipato Group is overlain unconformably by, or is in fault contact with, the China Mountain Formation of Triassic age. Within the area of figure 30, the China Mountain Formation includes light-colored chert or fine-grained quartzite, limestone, dolomite, and argillite.

Basalt of unknown age crops out in a low hill on the upthrown side of a fault 1.2 km southeast of the hot springs. The basalt is dark gray, weathers to brown or brownish gray, and contains abundant plagioclase, pyroxene, altered olivine, and opaque minerals.

Tuff of Tertiary age (Tatlock, 1969) crops out in a small area on the west margin of the bedrock exposures, about 3 km northeast of the hot springs. The rock is greenish gray to pink and appears to be a welded tuff of rhyolitic or dacitic composition.

Overlying the consolidated rocks of pre-Tertiary and Tertiary age are unconsolidated to semiconsolidated sedimentary rocks which range in age from late Tertiary to Holocene. These rocks comprise the following units, shown on figure 30: sedimentary rocks (Tertiary); old gravel deposits (Tertiary and (or) Quaternary); and alluvium. In addition, two units, designated as old sinter and fragmental sinter, are exposed near the hot springs.

The sedimentary rocks of Tertiary age underlie buried pediment surfaces, are exposed in several ravines in the eastern and northeastern parts of the area, and are penetrated by several of the test holes beneath alluvium of Quaternary age. The rocks are semiconsolidated and include claystone, mudstone, marl, tuffaceous sand, silicic ash, and tuff. The beds are slightly to moderately deformed; dips of as much as 30° were

observed in the northeastern part of the area. The near-surface parts of the conduits that carry the flow of the hot springs are probably within the Tertiary sedimentary rocks.

The old gravel deposits form hilly exposures on the west flank of the mountains east of the hot springs and may underlie the alluvium farther west. These deposits are unconsolidated to semiconsolidated, obscurely bedded, and form an ill-sorted assemblage of debris-flow, colluvial, and fluvial deposits which range from boulders to silt and clay. The deposits are mildly deformed; gentle easterly dips were observed at a few localities.

Unconsolidated deposits, classified on figure 30 as alluvium, blanket the older rocks throughout most of the thermal area. The alluvium ranges from gravel to silt and clay and at most places is poorly sorted and obscurely bedded. Caliche forms fragments and coatings on pebbles in many exposures and was observed in test-hole cuttings. In the eastern parts of the area, the alluvium forms a pediment veneer only a few metres thick, but the thickness increases westward, toward the axis of Grass Valley, particularly west of the hot springs fault.

The old sinter is exposed on the upthrown side of the hot springs fault scarp from just south of the hot springs to a point about 0.6 km northeast of the hot springs (fig. 30). The sinter is composed chiefly of dense chalcedony rather than the opaline sinter now being deposited and is commonly associated with partly silicified and kaolinized alluvium. The sinter may have been reconstituted from opal to chalcedony considerably after the time of original deposition.

The fragmental sinter is composed of pebble-, granule-, and sand-size fragments of white to light-gray opaline sinter downgradient from Leach Hot Springs. The fragments obviously have been distributed by the runoff from the springs.

The Leach Hot Springs area is traversed by numerous faults. Faults within the pre-Tertiary rocks are not shown on figure 30. The faults shown are Basin and Range normal faults on which the downthrown sides are toward the west or northwest.

Most significant to this study is the somewhat sinuous fault that extends generally northward from the hot springs. The trace of this fault is concealed south of the hot springs, but several prominent cracks in the alluvium 1.5 km south-southwest of the springs (fig.30) may represent response of near-surface materials to displacement along the buried southerly continuation of the hot springs fault.

A fault marked by a low escarpment in the alluvium about 0.6 km east of the hot springs may be a branch of the main hot springs fault, although the traces of the two faults do not appear to join northeast of the springs. The trace of the eastern fault is concealed south of the exposure of basalt on the upthrown side, but the fault 3-4 km south of the hot springs very likely is the same fault (fig. 30).

A third Basin and Range fault marks the west edge of the bedrock exposures from a point east of the hot springs northward for about 3 km. Farther south, the fault trace is concealed by pediment gravel (alluvium), but the older gravel deposits and the sedimentary rocks of Tertiary age apparently are cut by the fault.

Hydrology

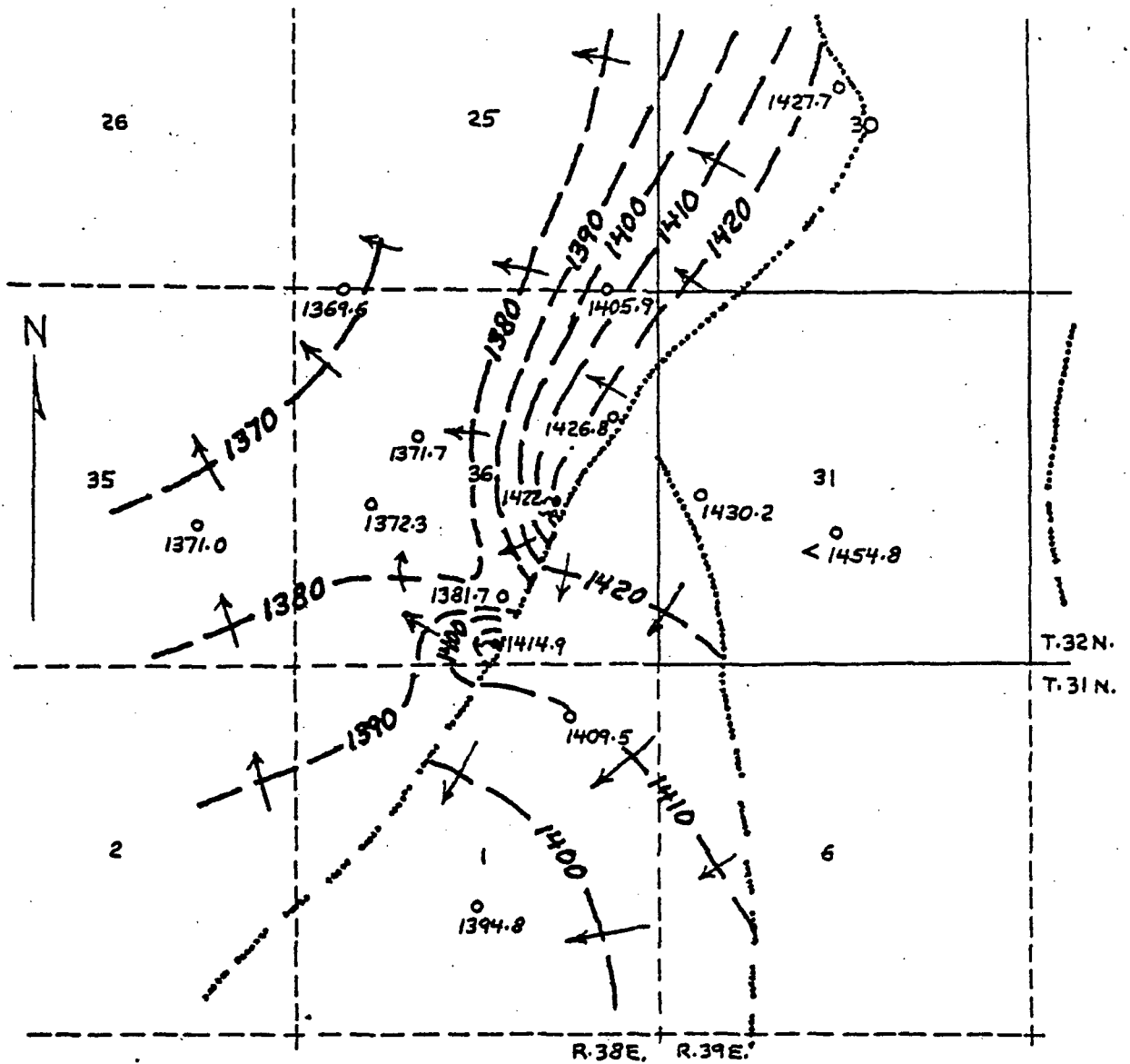
Precipitation is the source of virtually all ground water in the Leach Hot Springs area. The quantity of thermal water discharged by the springs is much greater than the quantity of recharge in the approximately 5 km² drainage area tributary to the hot springs. However, precipitation in the adjacent mountainous area is capable of generating much of the flow. For example, the recharge in the 106 km² area that includes the

drainage basin of Sheep Ranch Canyon about 10 km northeast of the springs and Panther Canyon 14 km southeast of the springs is about $1.2 \times 10^6 \text{ m}^3 \text{ yr}^{-1}$ on the basis of the relation of recharge to altitude and precipitation used by Cohen (1964; p. 19). The quantity is about three times the estimated discharge of thermal water. Thus, although the specific recharge areas that feed the deep-circulating thermal system are unknown, no great lateral distance of ground-water movement seems necessary. The most probable source areas are generally east of the hot springs, in the Sonoma Range.

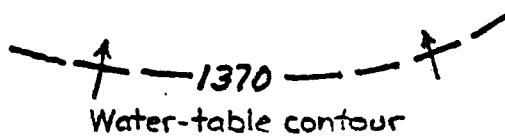
The sedimentary deposits are unsaturated to depths of more than 20 m in most of the area surrounding the hot springs. However, depths to the water table are less than 20 m immediately adjacent to the springs and in the area southeast of the ground-water barrier that extends south-southwest of the hot springs, in sec. 1, T. 31 N., R. 38 E. Ground water is both confined and unconfined throughout the thermal area. Because of widespread lenses of clay and silt, ground water may be confined at depths only a few metres below the water table.

The general ground-water-flow pattern and the configuration of the water table are shown in figure 31. Ground-water barriers (along faults) and upwelling thermal water exert important controls on directions of movement. The barriers and the thermal water appear to redirect the flow of nonthermal ground water, particularly south and east of the springs.

Vertical components of ground-water flow apparently are small in most of the area. Where the water level in the pipe and the water table indicated by the neutron log approximately coincide, as in holes DH-1, 7, 8, and 11 (table 19), ground-water flow presumably has little if any



EXPLANATION



Shows altitude of water table. Contour interval 10 metres. Datum is mean sea level. Arrows indicate horizontal component of ground-water flow

○
1371.7
Test hole
Number is altitude of water table, in metres above mean sea level

○
1414.9
Spring
Number is altitude, in metres above mean sea level

.....
Fault
Interrupted dots where concealed

Figure 3L.—Map of Leach Hot Springs thermal area showing configuration of water table, fall 1973.

vertical component. However, at the site of DH-9, between the two areas of emerging thermal water, the potential gradient indicates a predominantly upward flow, whereas at DH-6, downgradient from the hot springs, a downward component of flow is indicated. Unfortunately, vertical potential gradients are not known at DH's 2-5 and 10, so the picture of vertical ground-water movement is incomplete.

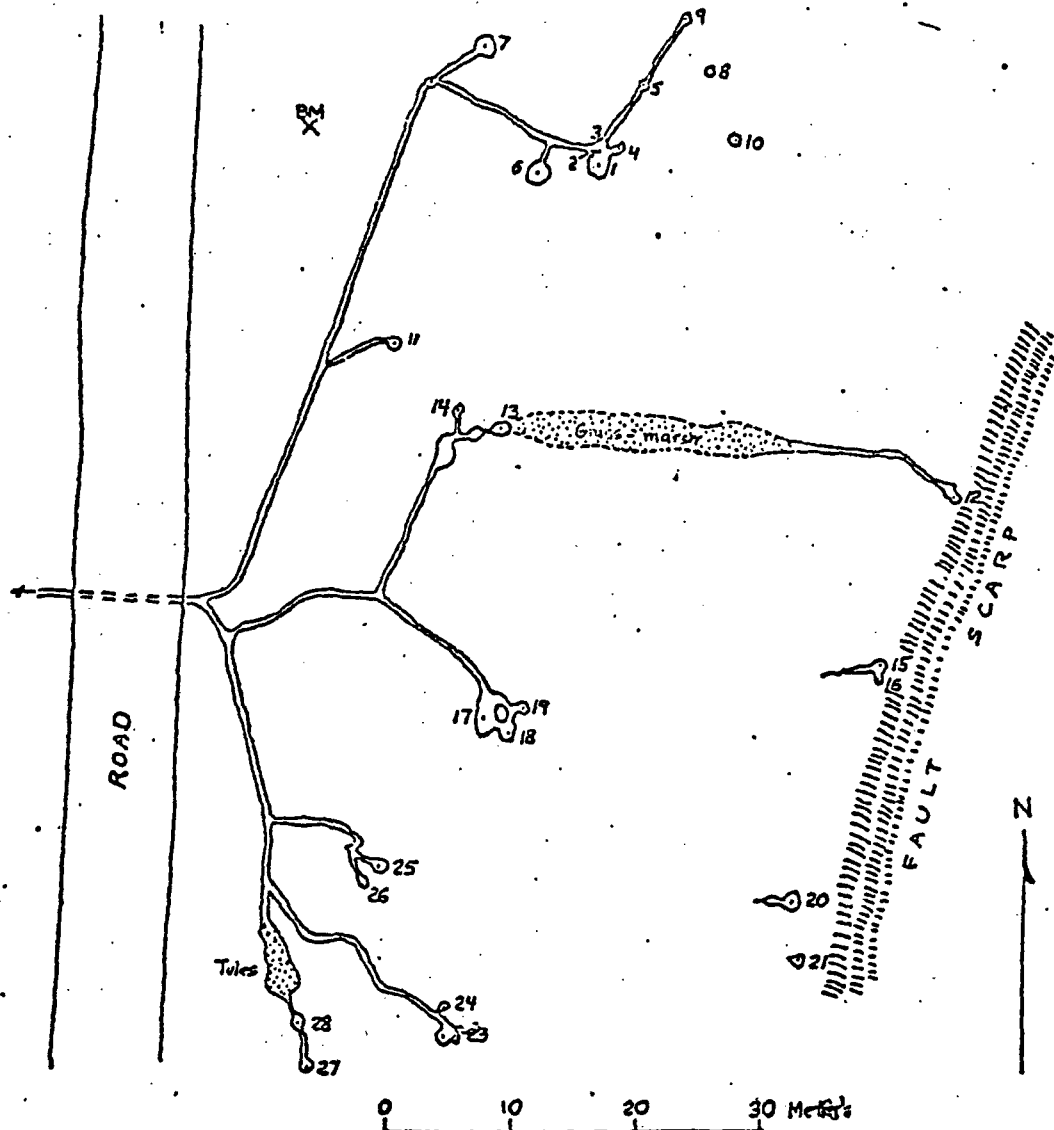
Water-level and temperature data (figs. 31 and 33) suggest that areas of upwelling thermal water are related to the hot springs fault. Although the thermal water emerges as springflow at only two places, the area of upwelling apparently extends at least 600 m northeast of the springs.

Ground water discharges at the land surface as springflow and evapotranspiration. Some thermal ground water may also leave the hot-spring area as subsurface outflow. Estimates of ground-water discharge are given in a later section.

The Springs

Leach Hot Springs are at the base of a fault escarpment about 6-10 m in height. Materials exposed near the springs consist of ill-sorted alluvial and colluvial gravel, hydrothermally altered gravel deposits, chalcedonic old sinter, opaline young sinter, and tufa. The springs include at least 29 identifiable orifices within an area of about 3,000 m². A warm spring about 670 m south-southwest of the main spring cluster appears to be controlled by the same fault, but the trace of the fault is concealed there by unaffected alluvium.

The main spring cluster consists essentially of two linear arrays of orifices, both oriented about N. 20° E., parallel to the trace of the fault (See fig. 32.) The western array forms a narrow linear zone about 30 m



EXPLANATION


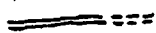
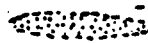
- 
 Spring pool and orifice
 Number indicates orifice referred to in table 21; dot indicates location of orifice
- 
 Channel carrying hot-spring discharge
 Dashed where in culvert beneath road
- 
 Pool or marsh with grass or tules

Figure 32.--Sketch map of Leach Hot Springs

west of the fault trace, which is inferred to be at the base of the escarpment and along the western edge of the exposures of old sinter shown on figure 30. The eastern array lies along the fault trace.

The spring orifices are characterized by a broad range of flow rates and temperatures (table 21). Total discharge from orifices 1-29 in November 1973 was about $11\text{-}1/2 \text{ l s}^{-1}$, of which almost 80 percent was from six major orifices in the western linear array. The 30-m offset of these orifices from the fault trace suggests that the zone of principal discharge has migrated westward with time as former conduits became clogged and finally sealed near the land surface by mineral precipitation (principally sinter). The limited data in table 22 suggest that total spring discharge may not vary much with time. The average discharge, used later in estimates of discharge of heat and water from the hydrothermal system, is estimated to be $12\text{-}1/2 \text{ l s}^{-1}$, or $0.40 \times 10^6 \text{ m}^3 \text{ yr}^{-1}$. Weighted-average temperature of the spring discharge, computed from table 21, is 79.6°C for orifices 1-29 and 77.5°C for all orifices (1-30).

Table 21.--Temperature, discharge, and chemical character of flow from individual orifices at Leach Hot Springs

Orifice	Temperature (°C) ^{1/}		Discharge (litres per second) ^{1/}	Specific conduct- ance ^{3/} (micromhos per cm at 25°C)	Chloride (Cl) (mg l-1) ^{3/}
	1938	1973-74			
1	85	83.3-85.0	1.7	796	28
2	--	83.3-85.0		--	--
3	--	77.5-78.8	2.1d	--	--
4	--	81.9-83.6	.42	--	--
5	83-1/2	82.2-83.6	<.01	--	--
6	75-1/2	72.5-80.8	.34	--	--
7	73	62.8-70.0	.34	773	28
7A	--	73.6	--	--	--
8	--	33.9	<.01	--	--
9	59-1/2	34.4	<.01	--	--
10	67	43.3	<.01	--	--
11	73-1/2	65.3-66.4	.06	797	--
12	94	91.1-92.3	.06	833	32
13	95-1/2b	86.9-93.6	.71d	784	28
14	--	70.3-72.8	.01	--	--
14A	--	75.0-75.4	.23d	--	--
15	91	94.2-95.6b	<.01	613	15
16	--	91.7-95.0	<.01	--	--
17	78	74.2-77.8	.59d	803	--
17A	--	77.8			
18	--	80.8-82.8	.06	--	--
19	--	71.9-83.4	.06	--	--
20	--	38.1-47.2	<.01	819	--
21	--	47.2	<.01	--	--
22	79-1/2	80.6-81.4	2.0d	788	28
23	--	78.6-80.6	2.0d	--	--
24	--	78.1-79.2	.11	--	--
25	72	67.2-70.3	.08	797	--
26	--	66.9-68.1	<.01	--	--
27	71	47.2-56.1	<.01	--	--
28	--	70.6-71.4	.03d	796	--
29	--	41.5-48.6	.40	890	30
Total flow, orifices 1-29			11.3	--	--
30	--	34.5-39.0	.59	812	28
Total flow, all orifices			11.9	--	--

Footnotes

1. Temperatures for 1938 measured by Dreyer (1940,p.22) sometime between 1 Sep. and 15 Oct., and may be accurate to nearest 0.6°C (1°F).
Temperatures for 1973-74 measured one or more times from 6 May 1973 to 24 September 1974. Boiling indicated by "b". Measurements in 1973-74 were made using a single maximum thermometer, lowered as deeply as possible into orifice. Accuracy probably about $\pm 0.3^{\circ}\text{C}$.
2. Discharges are measured, estimated, or calculated by difference (the latter values are indicated by "d"). Data collected Nov. 1973. Accuracies generally range from ± 50 percent or more for the smallest quantities to ± 10 percent or less for the largest quantities. Recorded values do not include an allowance for loss by evaporation but such a loss probably represents a very small part (perhaps 1-2 percent) of the total flow.
3. Samples collected 2 Nov. 1973 except: Orifice 29, 14 Nov.

Table 22.--Total discharge of Leach Hot Springs orifices 1-29,
1947 and 1973-74

Discharge		
Date	(l/s)	Source of data
47 05 05	11	Current-meter measurement, files of U.S. Geol. Survey
73 11 13-14	11-1/2	Table orifices 1-29
74 01 22	12	Estimate based on staff-gage reading
74 04 05	13-1/4	Do.
74 05 31	14	Do.
74 07 05	13-1/2	Do.
74 08 06	13	Do.
74 09 24	12	Do.

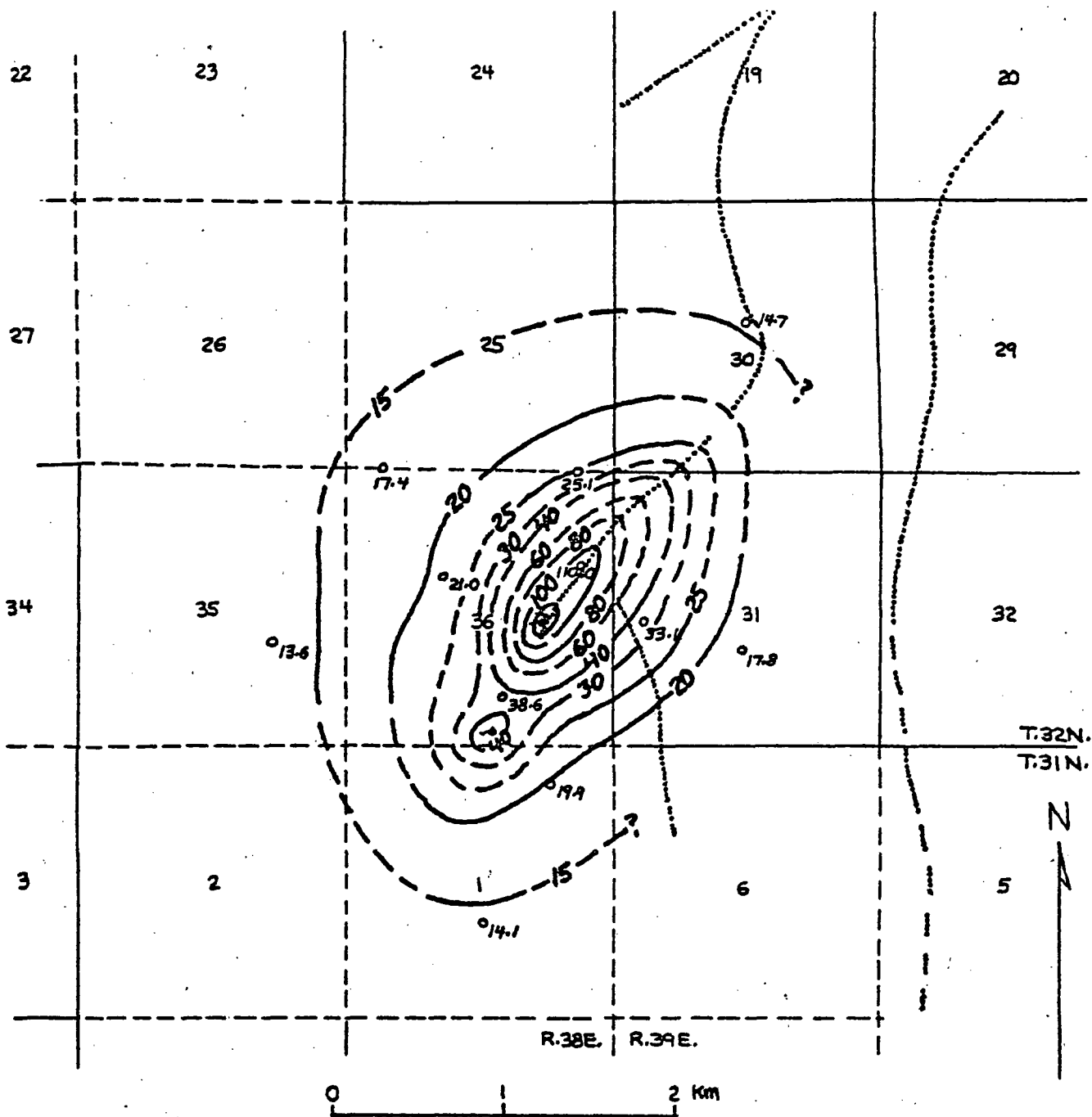
Chemical Character of Springflow

The general chemical character of water from Leach Hot Springs is indicated by the analysis from Mariner and others (1974, p.13) listed in table 1. (The sample was collected from orifice 13 but may have included a small amount of overland flow from orifice 12; see fig. 32 and table 21.) The dissolved solids, which are dominated by sodium, bicarbonate, and silica, total about 580 mg l^{-1} . Estimated reservoir temperature is 155°C by the silica-quartz geothermometer, or 176°C by the sodium-potassium-calcium geothermometer (table 1, Mariner and others, 1974, table 3).



Determinations of specific conductance and chloride for selected orifices (table 21) provide an index of chemical variability from spring to spring. Specific conductance ranges from 613 to 890 micromhos per cm, although samples from major orifices (flow-rate more than 0.5 l s^{-1}) have a smaller range, from 784 to 812 mmhos cm^{-1} . No systematic variation in chemical character with orifice location or discharge temperature is apparent.

Subsurface Temperature Distribution

The extent and configuration of the thermal area are indicated by the distribution of temperature at a depth of 30 m below the land surface, as shown on figure 33. The isotherms have a roughly elliptical pattern centered at the hot springs. The long axis of the ellipse trends north-eastward, in the direction of the fault that controls the position of the hot springs. The 15°C isotherm approximately defines the outer limit of the thermal area. The area is about 3.0 by 3.9 km and has an extent of about 8.5 km^2 .



EXPLANATION

 20
 Line of equal temperature, in degrees Celsius, at a depth of 30 metres below land surface
 Dashed where uncertain. Interval 5, 10, and 20 degrees Celsius
 Hot spring



 19.9
 Test hole
 Number is temperature, in degrees Celsius, at a depth of 30 m below land surface
 Fault
 Interrupted dots where concealed

Figure 33. — Map of Leach Hot Springs thermal area showing temperature at a depth of 30 m, December 1973

The hottest area extends from the springs northeastward about 600 m, along exposures of old sinter and hydrothermally altered alluvium. Temperatures at a depth of 30 m within the narrow, elongate area probably exceed 100°C--somewhat above the land-surface boiling temperature of about 95.5°C.

Comparison of the temperature pattern (fig. 33) with the configuration of the water table (fig. 31) suggests that transport of heat by lateral ground-water flow is not nearly as significant as that at the Soda Lakes-Upsal Hogback or Gerlach thermal areas. If appreciable quantities of thermal water discharged into shallow aquifers instead of at the spring orifices, the lateral transport of heat in the direction of the ground-water potential gradient would produce a thermal anomaly elongated toward the west or northwest instead of toward the northeast. It is inferred that, if any significant amount of thermal water discharges laterally from the spring-system conduit or conduits, it does so at depths greater than the 40-50 m penetrated by most of the test holes.

Heat Discharge

Heat is discharged from the Leach Hot Springs hydrothermal system chiefly by conduction through near-surface materials, by convection as springflow, and by convection as steam. Each of these modes of heat discharge is discussed briefly below.

Conductive heat discharge.--Conductive heat discharge from the thermal area is estimated by both methods described in the section, "Estimates of heat discharge." The estimate by method A is considered less reliable than that by method B because of the considerable thickness of unsaturated material in the depth range 0-30 m in which the estimated thermal conductivity is more uncertain than it is in saturated material.

The following values are used in the derivation of the estimated Total conductive heat discharge by method A:

Mean annual temperature at the land surface = 9°C

Harmonic-mean thermal conductivity, 0-30 m = 2.1×10^{-3} cal cm⁻¹ s⁻¹°C⁻¹

Boundary of thermal area = 15°C isotherm at 30 m depth (8.45 km²)

Using these values, the estimated total conductive heat discharge from the thermal area by method A is 0.99×10^6 cal s⁻¹. Derivation of the estimate is given in table 23.

Net conductive heat discharge from the thermal area is computed using an estimated "normal" conductive heat flow of 2 HFU:

$$\begin{aligned} & [0.99 \times 10^6 \text{ cal s}^{-1}] - [(2.0 \times 10^{-6} \text{ cal cm}^{-2} \text{ s}^{-1})(8.45 \times 10^{10} \text{ cm}^2)] \\ & = 0.82 \times 10^6 \text{ cal s}^{-1} \end{aligned}$$

Total conductive heat discharge from the thermal area is estimated by method B at 1.00×10^6 cal s⁻¹, about the same as the estimate by method A. The distribution of heat flow within the thermal area, as interpreted from the heat-flow values computed at the test-hole sites, is shown on figure 34. Derivation of the estimate is given in table 24.

Net conductive heat discharge is estimated by method B, using a "normal" heat flow of 2 HFU and a thermal area of 8.03 km²:

$$\begin{aligned} & [(1.00 \times 10^6 \text{ cal s}^{-1})] - [(2.0 \times 10^{-6} \text{ cal cm}^{-2} \text{ s}^{-1})(8.03 \times 10^{10} \text{ cm}^2)] \\ & = 0.84 \times 10^6 \text{ cal s}^{-1} \end{aligned}$$

Table 23.--Estimate of conductive heat discharge from Leach Hot Springs hydrothermal system on the basis of method A described in the text.

Temperature Range (°C)	Geometric-mean temperature (°C)	Thermal gradient ^{1/2} ($\times 10^{-3}$ °C cm ⁻¹)	Heat flow ^{2/} ($\times 10^{-7}$ cal cm ⁻² s ⁻¹)	Area ($\times 10^{10}$ cm ²)	Heat discharge ($\times 10^6$ cal s ⁻¹)
15 - 20	17.3	2.8	5.9	5.24	0.32
20 - 30	24.5	5.2	11	1.53	.17
30 - 40	34.6	8.5	18	.51	.092
40 - 60	49.3	13	27	.42	.11
60 - 80	69.3	20	42	.24	.10
80 - 100	89.4	27	57	.18	.10
100 - 120	109.5	34	71	.11	.078
> 120	121	37	75	.02	.016
Total				8.45	0.99

^{1/} Based on 9°C mean-annual temperature at land surface

^{2/} Based on harmonic-mean thermal conductivity of 2.1×10^{-3} cal cm⁻¹ s⁻¹ °C⁻¹

Table 24.--Estimate of conductive heat discharge from Leach Hot Springs hydrothermal system on the basis of method B described in the text.

Range in heat flow (HFU)	Geometric-mean heat flow (HFU)	Area ($\times 10^{10}$ cm ²)	Heat discharge ($\times 10^6$ cal s ⁻¹)
2 - 10	4.5	4.85	0.22
10 - 20	14.1	1.99	.28
20 - 50	31.6	.88	.28
50 - 100	70.7	.30	.21
100	100	.01	.01
Total		8.03	1.00

EXPLANATION

---10---

Line of equal heat flow in HFU ($\times 10^{-6} \text{ cal cm}^{-2} \text{ s}^{-1}$)

°23

Test hole

Number is estimated heat flow in HFU ($\times 10^{-6} \text{ cal cm}^{-2} \text{ s}^{-1}$)

----- Fault

Interrupted dots where concealed

N

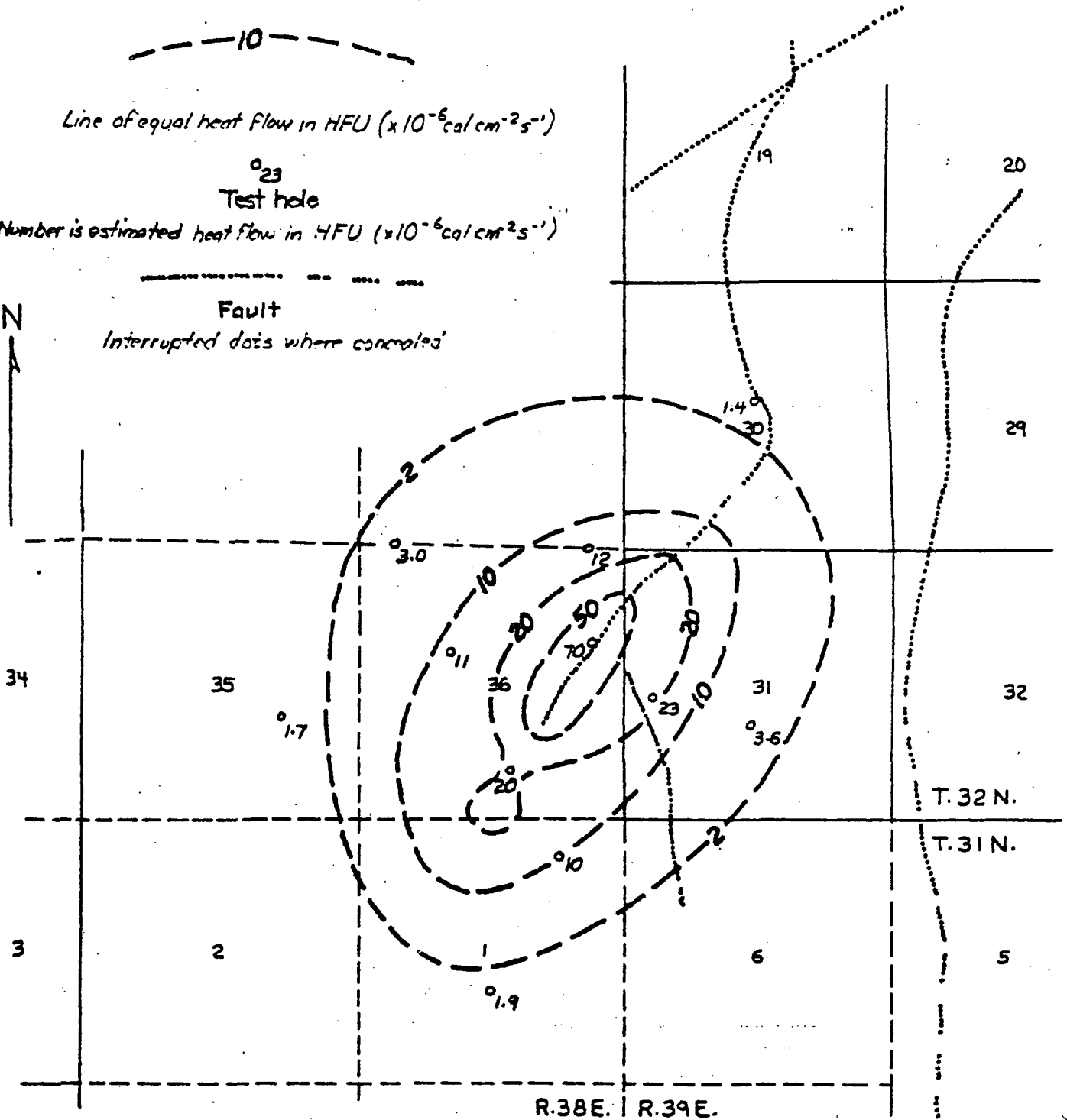


Figure 34.—Map of Leach Hot Springs thermal area showing estimated near-surface heat flow.

Convective heat discharge by springflow.--Heat discharge by springflow is estimated using the following data:

$$\text{Average springflow} = 12\text{-}1/2 \text{ l s}^{-1} = 12.5 \times 10^3 \text{ cm}^3 \text{ s}^{-1}$$

$$\text{Weighted-average temperature of springflow} = 77.5^\circ\text{C};$$

$$\text{enthalpy} = 77.5 \text{ cal g}^{-1}$$

$$\text{Mean-annual temperature at land surface} = 9^\circ\text{C};$$

$$\text{enthalpy} = \underline{9 \text{ cal g}^{-1}}$$

$$\text{Net enthalpy of springflow} = 68.5 \text{ cal g}^{-1}$$

$$\text{Density of water at } 77.5^\circ\text{C} = 0.973 \text{ g cm}^{-3}$$

$$\begin{aligned} \text{Heat discharge} &= (12.5 \times 10^3 \text{ cm}^3 \text{ s}^{-1})(68.5 \text{ cal g}^{-1})(0.973 \text{ g cm}^{-3}) \\ &= 0.83 \times 10^6 \text{ cal s}^{-1} \end{aligned}$$

Convective heat discharge by steam.-- Heat discharged as steam from boiling springs is estimated using the following data:

$$\text{Boiling-spring discharge (volume rate)} = 0.78 \text{ l s}^{-1} = 0.025 \times 10^6 \text{ m}^3 \text{ yr}^{-1}$$

$$\text{Density of water at } 95^\circ\text{C} = 0.962 \text{ g cm}^{-3}$$

$$\text{Boiling-spring discharge (mass rate)} = (0.962 \times 10^6 \text{ g m}^{-3})$$

$$(0.025 \times 10^6 \text{ m}^3 \text{ yr}^{-1}) = 2.4 \times 10^{10} \text{ g yr}^{-1}$$

$$\text{Reservoir temperature (SiO}_2) = 155^\circ\text{C}; \text{ enthalpy of water} = 156 \text{ cal g}^{-1}$$

$$\text{Boiling temperature at surface} = 95^\circ\text{C}; \text{ enthalpy of water} = 95 \text{ cal g}^{-1}$$

$$\text{Net enthalpy available for steam} = 61 \text{ cal g}^{-1}$$

$$\text{Enthalpy of steam-water mixture at } 95^\circ\text{C} = 542 \text{ cal g}^{-1}$$

$$\text{Weight percent of steam in discharge} = 61/542 = 11.3 \text{ percent}$$

$$\begin{aligned} \text{Heat discharge by steam} &= (0.113)(2.4 \times 10^{10} \text{ g yr}^{-1})(5.42 \times 10^2 \text{ cal g}^{-1}) \\ &= 1.47 \times 10^{12} \text{ cal yr}^{-1} = 0.05 \times 10^6 \text{ cal s}^{-1} \end{aligned}$$

Net heat discharge from hydrothermal system.--The net heat discharge from the Leach Hot Springs hydrothermal system is computed as the sum of the net conductive heat discharge, the heat discharge by spring-flow, and the heat discharge by steam:

	<u>Heat discharge (x 10⁶ cal s⁻¹)</u>
Net conduction through near-surface materials	0.84
Convection by springflow	.83
Convection by steam	<u>.05</u>
Total	1.7

Water Discharge

Discharge of thermal ground water from the system includes spring-flow, steam (as equivalent water), evapotranspiration, and subsurface outflow. The magnitude of the discharge is estimated by both the water-budget and the heat-budget methods.

Water-budget method.--The dominant mode of discharge is springflow. On the basis of measurements made from November 1973 to September 1974, the average springflow is estimated to be 12-1/2 l s⁻¹, or 0.40 x 10⁶ m³ yr⁻¹. (See tables 21 and 22.)

Discharge of steam (as equivalent water) probably is very small. On the basis of data given in the preceding section, the discharge is

$$\frac{(0.113)(2.4 \times 10^{10} \text{ g yr}^{-1})}{(0.962 \times 10^6 \text{ g m}^{-3})} = 0.0028 \times 10^6 \text{ m}^3 \text{ yr}^{-1}$$

or less than 1 percent of the discharge as springflow,

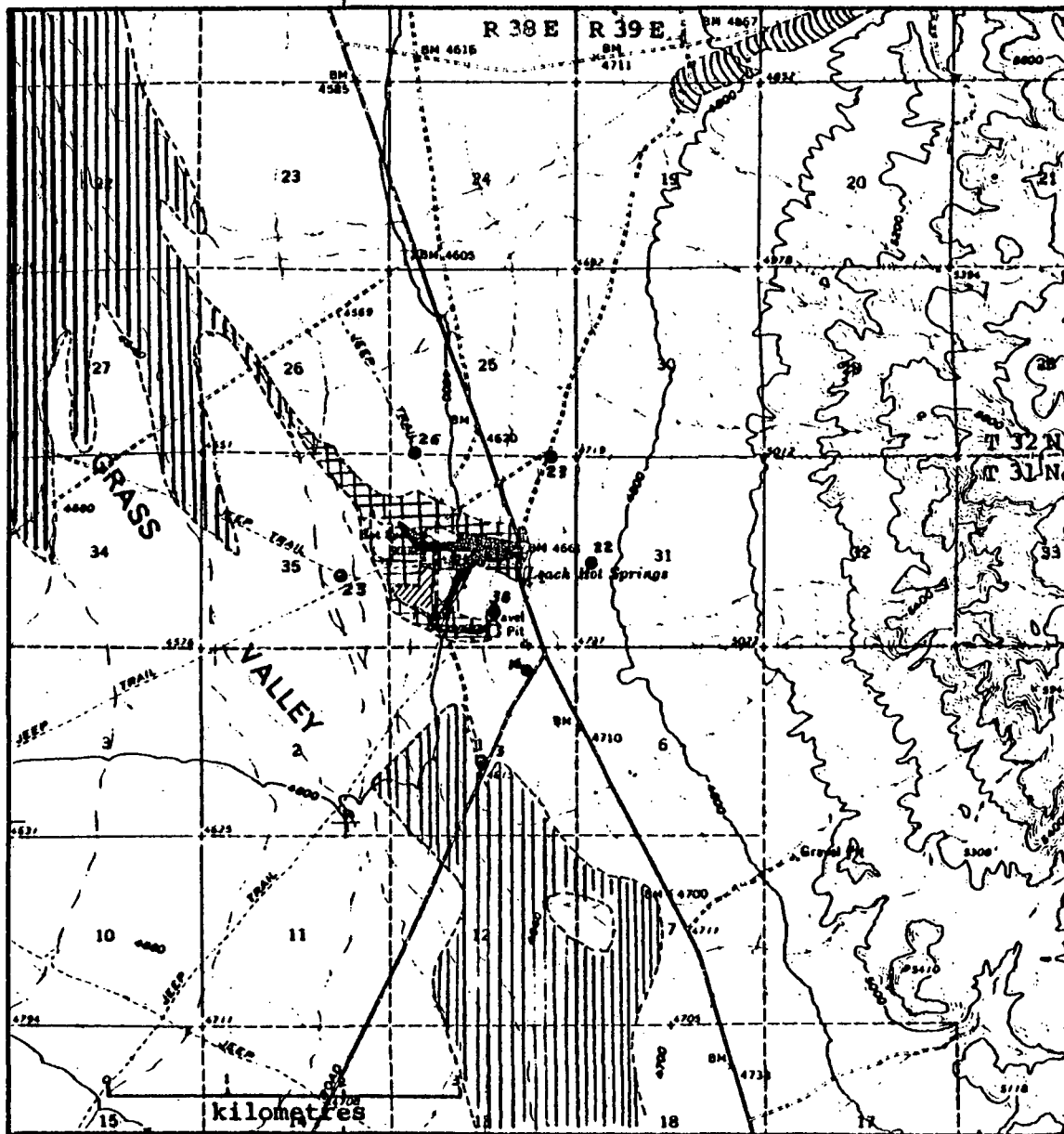
The discharge of thermal ground water by evapotranspiration is difficult to estimate. Some of the thermal area is occupied by phreatophytes and irrigated cropland (compare figs. 33 and 35), but most of this vegetation probably is supported by percolating springflow rather than by thermal ground water that has not previously emerged at the land surface. This inference is supported by the fact that the depth to water is greater than 20 m throughout most of the area downslope from the springs occupied by phreatophytes or irrigated crops (fig. 35). Evapotranspiration of thermal ground water occurs only near the springs and may amount to no more than about $0.012 \times 10^6 \text{ m}^3 \text{ yr}^{-1}$ on the basis of an area of $60,000 \text{ m}^2$ and an estimated water use of 20 cm yr^{-1} . Total evapotranspiration of thermal water, most of which is probably infiltrated springflow, is estimated to be about $0.056 \times 10^6 \text{ m}^3 \text{ yr}^{-1}$ on the basis of areas and use rates given in table 25.

Lateral subsurface outflow of thermal water cannot be estimated within narrow limits from present data. A very rough estimate of $0.06 \times 10^6 \text{ m}^3 \text{ yr}^{-1}$ is made on the basis of an assumed width of transmitting section of 1,000 m, an average potential gradient of 0.017, and an average transmissivity of $10 \text{ m}^2 \text{ day}^{-1}$.

Total discharge of thermal water is then estimated by the water-budget method as:

	<u>$\times 10^6 \text{ m}^3 \text{ yr}^{-1}$</u>
Springflow	0.40
Steam discharge (water equivalent)	.003
Evapotranspiration	.012
Lateral subsurface outflow	<u>.06</u>
Total	0.48

117°40'



EXPLANATION

Phreatophytes Associated with Dominantly Thermal Ground Water



Dense saltgrass



Saltgrass with greasewood and (or) rabbitbrush



Greasewood, with or without rabbitbrush



Presently irrigated lands (1973)

Phreatophytes Associated with Dominantly Nonthermal Ground Water



Greasewood, rabbitbrush, and some saltgrass



Greasewood



Well, number is depth to water table, in metres

40°35'

202

Figure 35.—Map of Leach Hot Springs area showing distribution of phreatophytes.

Table 25 .--Estimated average annual evapotranspiration of dominantly thermal water at Leach Hot Springs, for natural conditions.

Phreatophytes	Area (x 10 ³ m ²)	Depth to water (m)	Evapotranspiration (m/yr) (x 10 ³ m ³ /yr)	
Dense saltgrass, with or without greasewood and (or) rabbitbrush.	28	0.3?	0.25	7
Dense to scattered saltgrass with greasewood or rabbitbrush.	73	1 ¹ / ₂ -4 ¹ / ₂	.18	13
Greasewood, with or without rabbitbrush.	310	(a)	.06	19
Scattered greasewood	580	(a)	.03	17
Total	990	--	--	56

(a) Depth to water table exceeds 20 m throughout most of area; phreatophytes apparently use thermal ground water percolating in unsaturated zone above water table.

Heat-budget method.--Discharge of thermal water is computed by the heat-budget method, using the following data:

Reservoir temperature (table 1) = 155°C; enthalpy of water = 156 cal g⁻¹

Mean-annual temperature at surface = 9°C; enthalpy of water = 9 cal g⁻¹

Net enthalpy of water at source = 147 cal g⁻¹

Net heat discharge = $1.7 \times 10^6 \text{ cal s}^{-1} = 5.4 \times 10^{13} \text{ cal yr}^{-1}$

Density of discharge water at 77.5°C = $0.973 \times 10^6 \text{ g m}^{-3}$

$$\text{Water discharge} = \frac{5.4 \times 10^{13} \text{ cal yr}^{-1}}{1.47 \times 10^2 \text{ cal g}^{-1}} \div 0.973 \times 10^6 \text{ g m}^{-3}$$

$$= 0.38 \times 10^6 \text{ m}^3 \text{ yr}^{-1}$$

If the reservoir temperature of 176°C from the sodium-potassium-calcium geothermometer (table 1) is used instead of the silica-quartz temperature of 155°C, the estimated water discharge is

$$\frac{5.4 \times 10^{13} \text{ cal yr}^{-1}}{1.69 \times 10^2 \text{ cal g}^{-1}} \div 0.973 \times 10^6 \text{ g m}^{-3}$$

$$= 0.33 \times 10^6 \text{ m}^3 \text{ yr}^{-1}$$

Discussion of water-budget and heat-budget estimates.--The

estimate of thermal-water discharge by the water-budget method, $0.48 \times 10^6 \text{ m}^3 \text{ yr}^{-1}$ exceeds the estimates by the heat-budget method, 0.38 and $0.33 \times 10^6 \text{ m}^3 \text{ yr}^{-1}$, by perhaps significant margins. The reason for the differences in the estimates is uncertain. Possibly, the estimated heat discharge used in the heat-budget method is too small. Alternatively, the estimates of evapotranspiration and lateral subsurface outflow and the measurements of springflow used in the water-budget method may be too large. Or, the springflow may include admixed shallow ground water of nonthermal origin. More data are required to refine the estimates of discharge of both water and heat from the hydrothermal system.

Hypothetical Model of Hydrothermal-Discharge System

No test drilling to depths greater than 50 m has been done at Leach Hot Springs. For this reason, only the general nature of the hydrothermal-discharge system, can be inferred with reasonable assurance.

If no local shallow source of heat is present beneath the thermal area depth of circulation of the thermal water may be estimated within broad limits from the quotient of the heat flow outside the area affected by convective upflow and the thermal conductivity of the rocks. The Leach Hot Springs area lies within the "Battle Mountain high" (heat-flow high) of Sass and others (1971, p.6407,6409) where heat-flow values ranging from 2.5 to 3.8 HFU were determined at several test-hole sites. The highest heat flow was, in fact, measured at Panther Canyon, only 7 1/2 km southeast of the hot springs. However, less reliable data from test holes drilled immediately outside the thermal area during this investigation indicate heat flows of perhaps no more than 2 HFU. Thermal conductivities of the Tertiary and pre-Tertiary rocks probably range from about 4 to $8 \times 10^{-3} \text{ cal cm}^{-1} \text{ s}^{-1} \text{ }^{\circ}\text{C}^{-1}$. (See tables 2 and 3 for Tertiary sedimentary rocks; also Birch, and others, 1942, table 17.) Thus, thermal gradients outside the thermal area may range from:

$$2.5 \times 10^{-4} \text{ }^{\circ}\text{C cm}^{-1} (25^{\circ}\text{C km}^{-1}) \quad \frac{2 \times 10^{-6} \text{ cal cm}^{-2} \text{ s}^{-1}}{8 \times 10^{-3} \text{ cal cm}^{-1} \text{ s}^{-1} \text{ }^{\circ}\text{C}^{-1}} =$$

$$\text{to } 3.8 \times 10^{-6} \text{ cal cm}^{-2} \text{ s}^{-1} \quad =$$

$$9.5 \times 10^{-4} \text{ }^{\circ}\text{C cm}^{-1} (95^{\circ}\text{C km}^{-1}) \quad \frac{\quad}{4 \times 10^{-3} \text{ cal cm}^{-1} \text{ s}^{-1} \text{ }^{\circ}\text{C}^{-1}}$$

9.5 x 10⁻⁴ °C cm⁻¹ (95°C km⁻¹). On the basis of the quartz-silica geothermometer, the reservoir or equilibrium temperature of the thermal water is about 155°C (table 1; Mariner and others, 1974, table 3.) The depth of circulation would therefore be within the range of 155° - 9 °C to

$$\frac{155^{\circ} - 9^{\circ} \text{ }^{\circ}\text{C}}{25^{\circ}\text{C km}^{-1}}, \text{ or } 1.5 \text{ to } 5.9 \text{ km.}$$

$$\frac{\quad}{95^{\circ}\text{C km}^{-1}}$$

The thermal water probably rises along a steeply inclined conduit or conduit system associated with the hot springs fault. As in most of the other systems discussed in this report, the rate of rise may be sufficiently rapid so that the temperature of the water decreases but slightly until it boils at a hydrostatic depth of perhaps 40-50 m beneath the springs.

As discussed previously distribution of temperatures at depths of less than 50 m suggests that most of the thermal water discharges from the spring orifices, rather than from the conduit system laterally into shallow aquifers. Heat is lost by conduction through the walls of the conduit or conduit system, and shallow ground water of nonthermal origin is heated as it approaches the spring area. Some of the water boils all the way to the surface and steam is discharged from a few boiling spring pools.

The fault immediately east of the hot springs fault may also transmit thermal water upward, but data are insufficient to confirm or deny this possibility. Additional test drilling may indicate that faults other than the main hot springs fault also are the loci of near-surface high-temperature anomalies.

BRADY'S HOT SPRINGS THERMAL AREA

Location and Geologic Setting

The Brady's Hot Springs thermal area is on the northwest flank of the Hot Springs Mountains, in the western part of Hot Springs Flat, in Churchill County, Nevada. The area is about 27 km northeast of Fernley, Nevada, and is traversed by U. S. Interstate Route 80. A large part of the area has been classified as the Brady Hot Spring KGRA, which encompasses about 2,346 ha.

The hot springs, no longer flowing since several deep geothermal test holes were drilled and tested in the early 1960's, are along a fault or fault zone that traverses a pediment and alluvial apron at the foot of the Hot Springs Mountains. Alluvial-fan and pediment deposits predominate at the surface, but many other rock types are exposed or occur beneath these deposits (fig. 36).

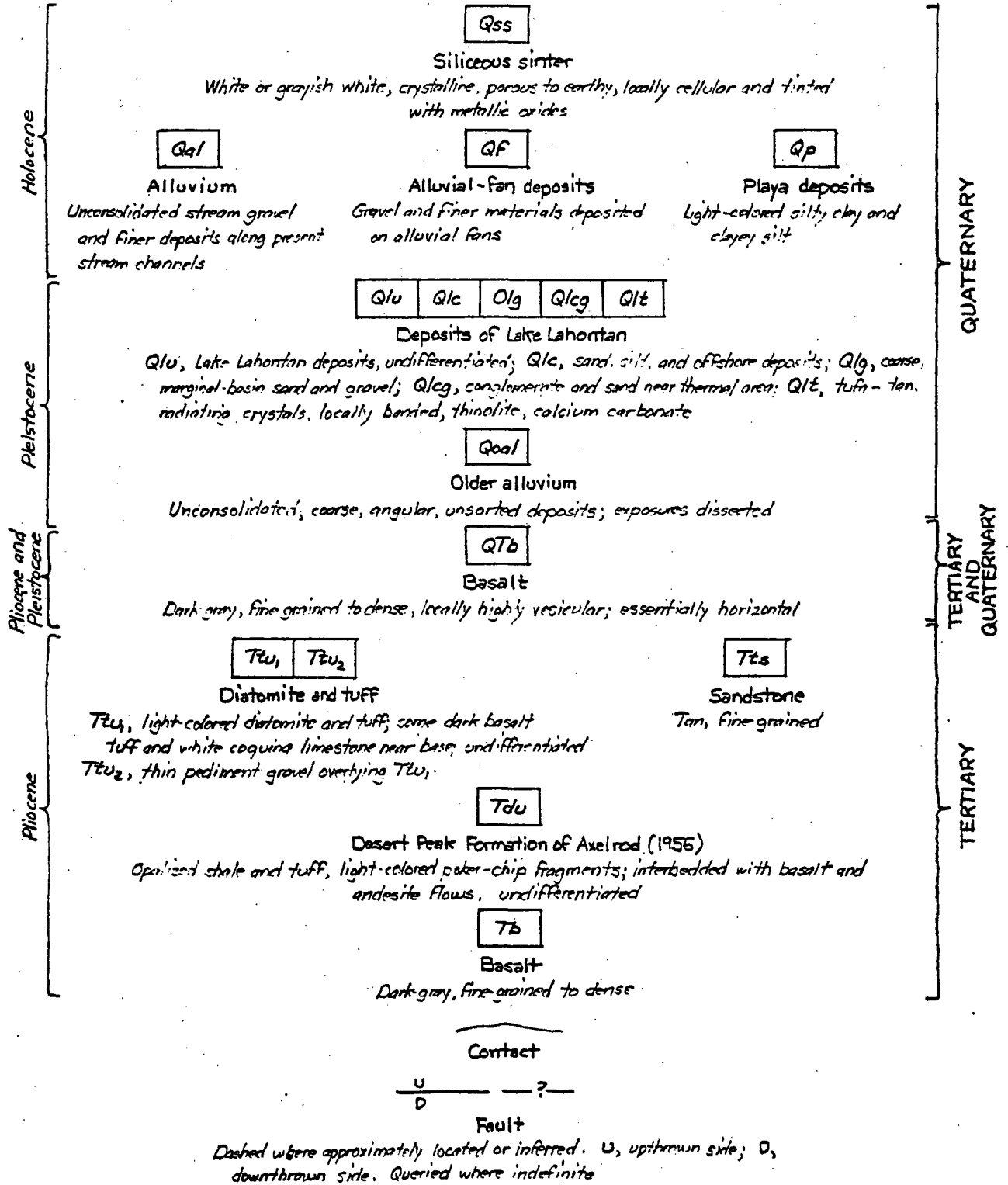
Four main types of rocks are exposed near the thermal area:

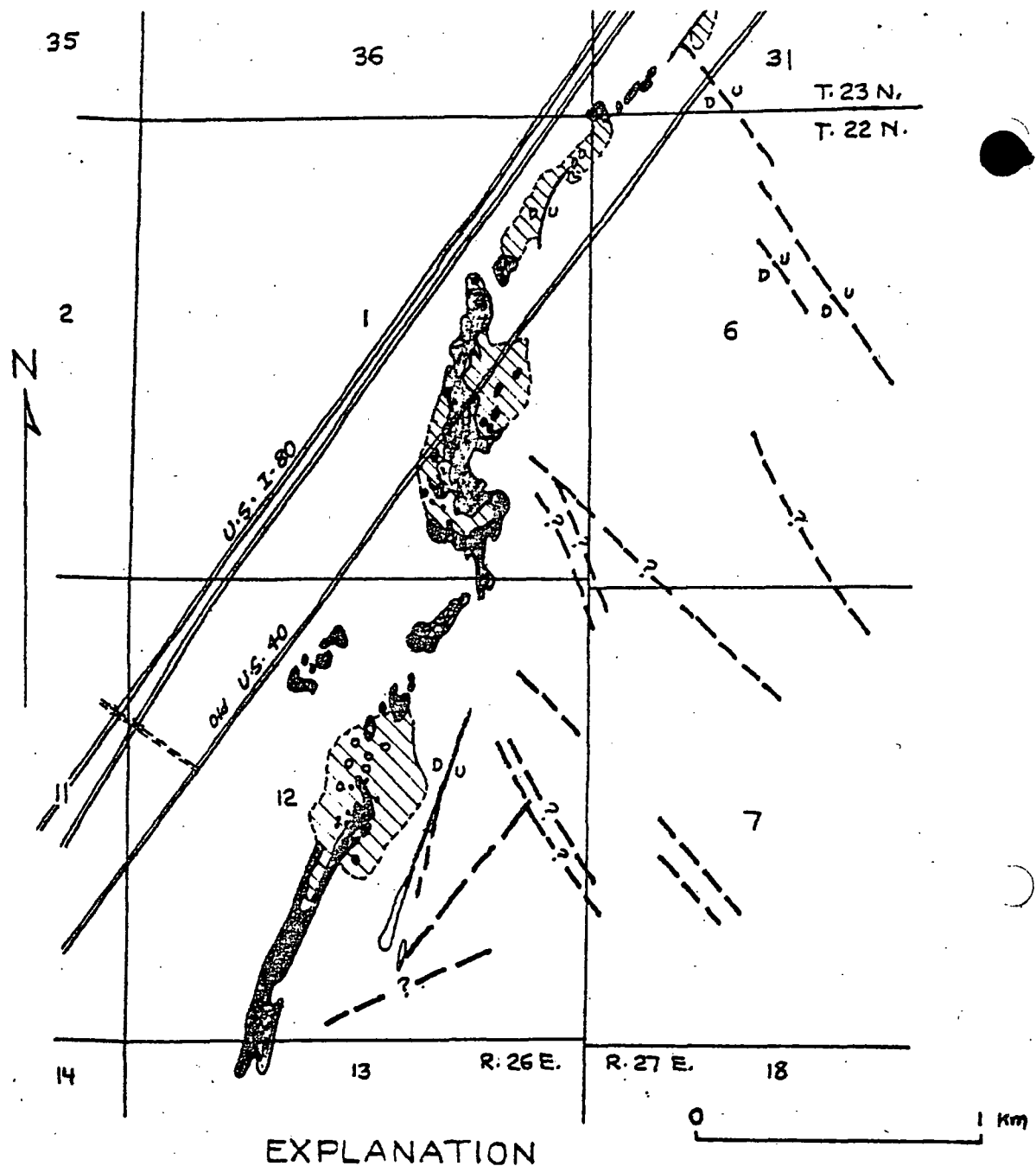
(1) volcanic rocks of Tertiary and possibly early Quaternary age, chiefly basalt, in the mountains east of the springs; (2) sedimentary rocks of Tertiary age consisting of sandstone, shale, tuff, diatomite, and minor limestone; (3) lake deposits, mostly clay, silt, and sand, and tufa coatings, all of late Pleistocene Lake Lahontan; and (4) coarse alluvial-fan and pediment deposits. In addition, the rocks and deposits along the major fault, referred to for convenience as the Hot Springs fault, have been altered to many different minerals, and sinter has been deposited by hydrothermal activity. Distribution of the mapped units is shown on figure 36.

The former hot springs, warm ground, hydrothermally altered deposits, and other manifestations of hydrothermal activity all are controlled by the Hot Springs fault. The fault is a normal fault of unknown displacement, dipping steeply westward, with the downthrown side to the west. Other faults and linear features were mapped by Anctil and others (1960) and were mapped from aerial photographs during the present study (figs. 36 and 37).

The Hot Springs fault zone within the thermal area was mapped in detail during this study (fig. 37). Mapped features include steam vents,

EXPLANATION





EXPLANATION





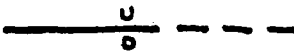
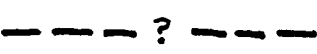
- | | |
|--|---|
| 
Area of observed snowmelt
Observed on 3 January 1974 | 
Area of hydrothermal alteration
Includes snowmelt areas |
| 
Well
Exploratory well drilled before 1973 | 
Vent or fumarole
Site where discharge of vapor or heat
is observed at the land surface |
| 
Fault
Dashed where approximately located
U, upthrown side; D, downthrown side | 
Lination
Linear feature of unknown origin.
May be fault or fracture |

Figure 37. — Reconnaissance surface hydrothermics of the Brady's Hot Springs thermal area.

extinct spring orifices, areas of snowmelt caused by geothermal flux observed during February 1974, and areas where the hydrogeologic environment has been altered by hydrothermal discharge associated with the springs. The alteration includes deposition of tufa, sinter, and salts, silicification of rocks, oxidation of metallic elements to orange, yellow, and white deposits, formation of kaolinite, and the noticeable discharge at the land surface of either heat or vapor. In addition, figure 37 shows the sites of large-diameter exploratory wells.

Test Drilling

Twenty-two test holes were bored or drilled at 21 sites by the U. S. Geological Survey and the U. S. Bureau of Reclamation in order to determine shallow subsurface temperatures and thermal gradients and to evaluate the movement of ground water. Locations of the test holes are shown on figure 36, and selected data for the test holes are listed in table 26.

Hydrologic Setting

Discharge of thermal water in the Brady's Hot Springs area is small enough to be derived from local ground-water recharge. However, deep circulation is suggested by the high water temperatures. Boundaries of the deep circulating system were not delineated by this study. The recharge area of the thermal system could be outside the local drainage area.

Ground water occurs in alluvial and lacustrine deposits at shallow to moderate depth in the western part of the thermal area. Depth to the water table generally increases farther east, toward the Hot Springs Mountains, where most ground water occurs in joints and other fractures in the sedimentary and volcanic rocks of Tertiary age. An exception to the eastward deepening of the water table is a narrow zone along the Hot

Table 28.--Data for U. S. Geological Survey test holes in Brady's Hot Springs thermal area.

Type of completion: Casing type indicated by "St" (steel) or "P" (PVC).

Wells capped and filled with water are indicated by "C". Wells with well-point screens or perforations at bottom are indicated by "Sc".

Depth to water table: Depth below land-surface datum. Obtained from neutron log. Accuracy about 10.5 metre except in clays where capillary fringes may cause larger errors.

Static water level: Depth below land-surface datum.

Geophysical logs available: Gamma ("G"), gamma-gamma ("G²"), neutron ("N"), resistivity ("R"), and temperature ("T").

217

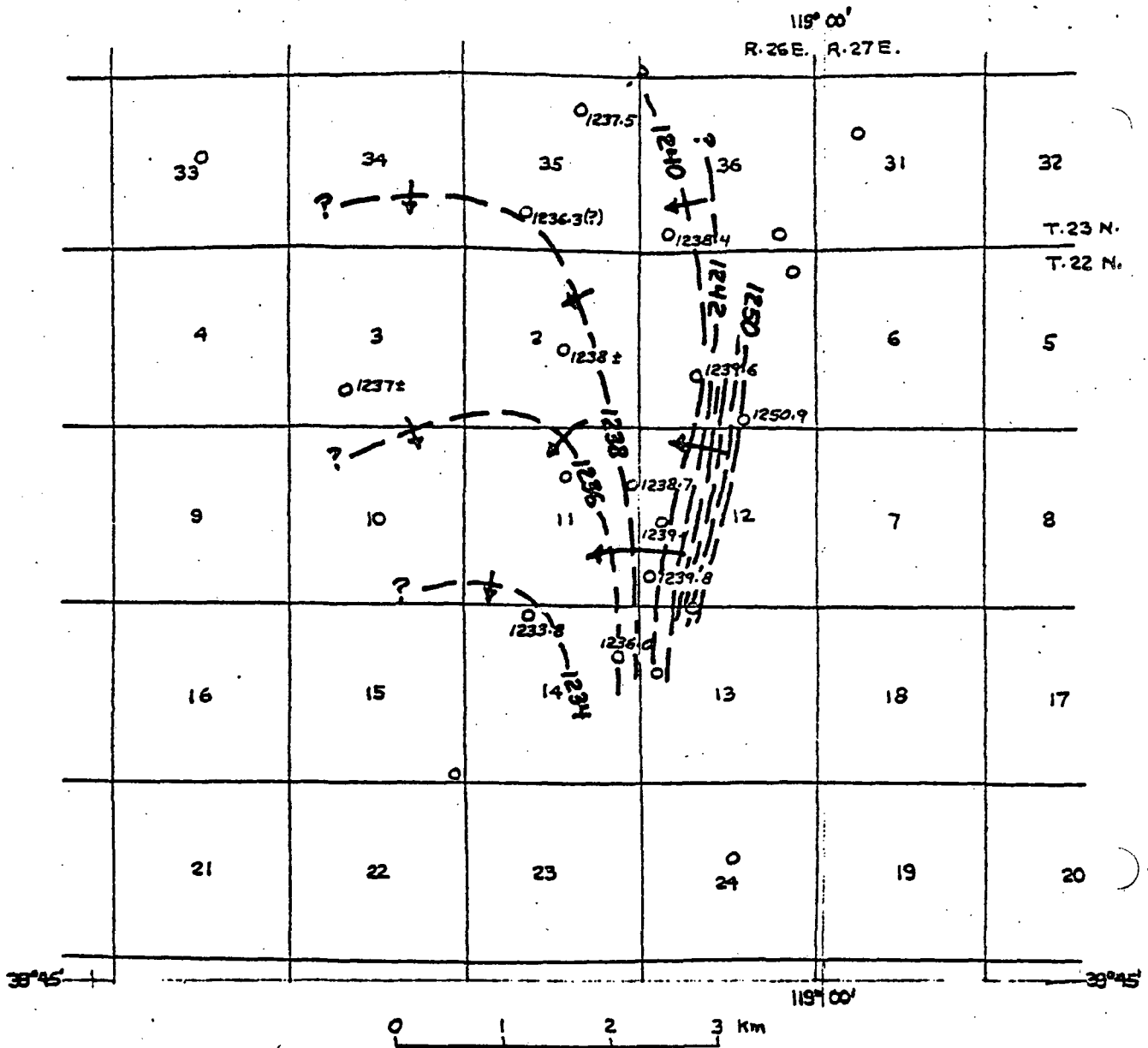
Well number	Location	Depth (metres) below land surface	Casing		Land-surface altitude (m)	Depth to water table			Static confined water level		Geophysical logs available	Remarks
			Inside diameter (cm)	Type of completion		Metres below land surface	Source of data	Date	Metres below land surface	Date		
BHAB-1A	22/26-11cbb1	27.3	3.8	St, Sc	1,241.4	2.0	G ²	73 11 29	2.38	73 12 15	G, G ² , T	
BHAB-1B	22/26-11cbb2	5.5	5.1	P, Sc	1,241.4	2.20	N	74 05 20	--	--		Water-table well
BHAB-2	22/26-11cbb	47.5	3.8	St, Sc	1,242.4	2.3	G ²	73 11 29	2.52	73 12 15	G, G ² , T	
BHAB-3	22/26-11cbb	28.3	3.8	St, Sc	1,239	3.2	G ²	73 11 28	3.26	73 11 28	G, G ²	
BHAB-4	22/26-11cbb	21.4	3.8	St, Sc	1,237	--	--	--	2.94	73 12 01	G	
BHAB-5	23/26-11cbb	30.2	3.8	St, Sc	1,251	13.1	N	73 11 19	13.53	73 12 01	G, G ² , N, T	
BHAB-6	23/26-11cbb	16.6	3.8	St, Sc	1,251.8	14.5	G ²	73 12 03	14.72	73 12 01	G, G ² , N	
BHAB-7	23/26-2dcb	35.4	3.8	St, Sc	1,243	3.7	N	73 11 28	4.28	73 11 28	G, G ² , N	
BHAB-8	22/26-11cbb	36.0	3.8	St, Sc	1,244	7.7	N	73 11 19	8.42	73 12 01	G, G ² , N, T	
BHAB-9	22/26-15cdd	18.6	3.8	St, Sc	1,235	6.3	G ²	73 12 04	1.83	73 12 01	G, G ²	
BHAB-10	22/26-12cab	43.3	5.1	P, C	1,292	43.9	N	73 ?	--	--	G, G ² , N	
BHAB-11	23/26-11cbb	31.1	3.8	St, Sc	?	6.1	N	73 11 19	6.58	73 12 01	G, G ² , N	
BHAB-12	23/27-11cbb	50.6	5.1	P, C	1,284	>50.3 (?)	N	73 11 29	--	--	G, G ² , N	
BHAB-13	22/26-11cbb	34.7	3.8	St, Sc	1,242	4.1	N	73 11 28	4.49	73 11 28	G, G ² , N	
BHAB-14	22/26-21cbb	20.4	3.8	St, C	1,261	>29.0	N	73 11 28	--	--	G, G ² , N	
BHAB-15	22/26-11cbb	18.6	3.8	St, Sc	1,256	--	--	--	4.37	73 11 29	--	Water table as measured in annulus.
BHAB-16	22/26-11cbb	14.3	3.8	St, Sc	1,250	--	--	--	4.35	74 05 20	--	
BHAB-17	22/26-11cbb	44.5	3.8	St, Sc	1,242	3.8	N	73 12 01	3.49	73 11 30	G, G ² , N, T	
BHAB-18	22/26-11cbb	15.2	3.8	St, Sc	1,245.7	5.9	N	73 12 03	6.45	73 12 16	G, G ² , T	
BHAB-19	22/26-11cbb	15.8	3.8	St, C	1,267	>15.8	N	73 11 30	--	--	G, G ² , N	
BHAB-20	22/26-11cbb	26.8	3.8	St, Sc	1,250	?	--	--	11.21	73 11 30	--	
BHAB-21	22/26-11cbb	12.8	3.8	St, C	1,265	>13.0	N	73 11 30	--	--	G, G ² , N	

219

Springs fault, where an elongate mound of thermal water is present at shallow depths. The fault seems to function as a long, narrow steeply-inclined aquifer, nearly perpendicular to the gently dipping aquifers in the alluvial and lacustrine deposits.

The general direction of ground-water movement in the shallow rocks and deposits is indicated by the configuration of the water table (fig. 38). Two flow patterns are suggested. One is the movement of nonthermal water toward the west and south. The other pattern is upward movement of thermal water along the Hot Springs fault, as indicated by a steep-sided water-table mound.

Except for the upward flow in the vicinity of the Hot Springs fault and also in the narrow gap at the south end of Hot Springs Flat, vertical components of ground-water flow are not well understood. Static confined water levels in wells not near the fault are generally somewhat lower than the water table indicated by the neutron or gamma-gamma logs (table 26). However, in almost all the wells, the difference could represent the thickness of the saturated part of the capillary zone rather than a water table higher than the confined potentiometric surface. For example, the water table indicated by the gamma-gamma log in test hole BHAH-1A in the late fall of 1973 was about 0.1 m higher than the static confined water level, but the water table actually measured in shallow test hole BHAH-1B in the late spring of 1974 was about 0.1 m lower than the static confined water level in AH-1A (table 26). Vertical potential gradients are believed to be small except near the Hot Springs fault and in the gap south of Hot Springs Flat, at the site of BHAH-9, where sizable upward gradients are indicated.



EXPLANATION



Water-table contour

Shows attitude of water table. Contour interval 2 metres. Datum is mean sea level. Arrows show horizontal component of ground-water flow

○ 1233-8

Test hole

Number is attitude of water table, in metres above mean sea level

Figure 38.—Map of Brady's Hot Springs thermal area showing configuration of water table, fall 1973.

Ground water discharge from the thermal area is in part by evapo-transpiration and in part by lateral subsurface outflow toward the south. Prior to attempts to develop thermal water, discharge from Brady's Hot Springs was reported to be about 3.2 l s^{-1} (Waring and others, 1965, p.34). D.E. White (written commun., 1974) estimated a springflow of about 1.3 l s^{-1} before the geothermal test drilling but after diversion of the flow to a swimming pool; he believes that the estimate of Waring and others (1965) is too large. In 1973, only a small amount of steam discharged from several mud fumaroles and vents along the fault trace.

Effects of Initial Development on Hydrologic Conditions

Test drilling by Magma Power Company caused some change in the hydrologic regimen of the thermal flow system. These changes were described by Osterling and Anctil (1960, p.3-5). Their description is as follows:

"An interesting result of Magma Power Company's drilling has been the gradual spreading of geothermal activity along the Brady Thermal fault. Prior to the drilling of Magma #2 steam well, the only thermal activity at the surface was the hot springs pool (180°F) located 130 feet $\text{S}23^{\circ}\text{W}$ from the well #2, two fumaroles (204°F) immediately north of the hot springs, and one fumarole a short distance south of the Springs (Allen, 1960, oral communication).

"Allen (1960) stated that after the #2 steam well blew in, steam vents gradually worked open to the north and the original hot springs pool was desiccated. Some mud pots located 220 feet $\text{N}23^{\circ}\text{E}$ of the #3 well were born with explosive force. Numerous areas of hot, moist ground developed, most with some steam escaping from cracks. At a depth of one or two inches at

these latter areas, the ground is too hot to touch. Where the Brady Thermal fault crosses U. S. Highway 40 in Section 1, the zone of thermal activity is about 200-300 feet wide. On the east side of the highway, the creosote is boiling out of the base of a telephone pole. A few feet to the north, where an access trail enters the highway, there is an area about 4-5 feet in diameter where, on May 24, 1960, the ground was hot and moist but steam would escape only after the passing of a vehicle on the highway. Apparently the ground vibration was sufficient to squeeze out some steam through small cracks and holes."

"The formation of many new thermal areas at the surface seems to follow a set pattern, various stages of which were observed. Initially, the ground becomes moist and dark, then the lower few inches of sagebrush become burnt and brown. Next, large circular cracks develop and the ground slumps in the center of the area to depths of up to 2 or 3 feet. Sagebrush, as pointed out by Allen, is commonly located in the center of the newly formed hot spots, apparently because the steam finds more permeability along the root system. Some of these areas are dangerous ground to cross because of the possibility of caving into a steam-filled hole or crevice. Many show evidence of undercutting after the slumping. At some sites, sulphur crystals are forming on the ground. There were some 105 of these surface phenomena as of May 24, 1960, most of which were induced as a result of the tapping of a main steam-filled fissure (Brady Thermal fault) by Magma #2 and #3 steam wells.

"The increased activity may be due to the progressive lowering of the water table by the blowing wells or simply to steam escaping through the uncased portions of the well bores into the adjacent fault zone.

"By mid-1961, all but a half dozen or so of these new phenomena were dormant."

Because of these effects the exact subsurface distribution of temperature and the precise pattern of ground-water flow prior to development cannot be determined. Data collected during 1973 include residual effects of the above described phenomena.

Chemical Character of Ground Water

No data on chemical character of the ground water in the Brady's Hot Springs area were obtained in this study. Harrill (1970) reports analyses of waters from three wells and a spring in or near the thermal area.

One of the wells, a steam well near the center of the area (22/26-12c), produced thermal water having a dissolved-solids concentration of 2,600 mg l⁻¹, chiefly sodium chloride, and a silica concentration of 242 mg l⁻¹ (Harrill, 1970, table 9). The silica concentration indicates a reservoir temperature of about 182°C, according to the silica-quartz equilibrium curve shown by Fournier and Rowe (1966, fig. 5).

Water from stock well 23/26-33ac, in western Hot Springs Flat about 5.8 km west-northwest of the center of the thermal area, had a specific conductance of 1,800 μhos cm⁻¹ (Harrill, 1970, table 9)--which indicates a dissolved-solids concentration substantially lower than that of the sample from the steam well.

A sample from well 22/27-30c, a stock well 5 km south of the center of the thermal area, had a specific conductance of 13,200 μhos cm⁻¹; chief dissolved constituents were sodium and chloride (Harrill, 1970, table 9). Spring 22/26-35a, about 2 km west of the stock well, produced water having a specific conductance of 12,000 μhos cm⁻¹; almost as high as that from the stock well. The high concentration of dissolved solids (chiefly sodium chloride) in the ground water in this area probably results from high rates of evaporation from a shallow water table; salt was produced in earlier times from numerous evaporation ponds near the spring cited above.

Subsurface Temperature Distribution

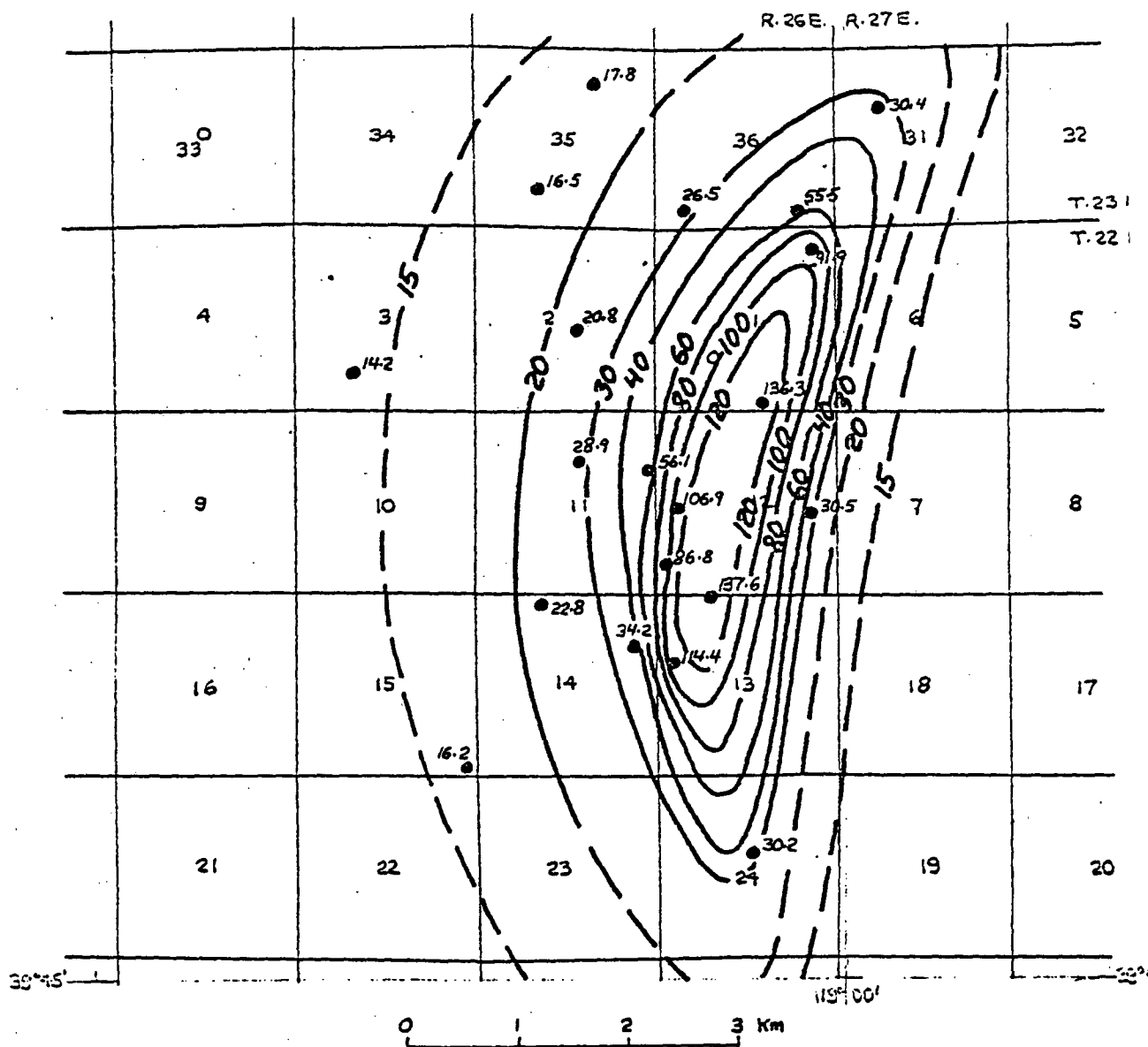
The Brady's Hot Springs thermal area has an elongate, banana-like shape, as indicated by temperatures at a depth of 30 m in the test holes (figure 39). The pattern is obviously related to the Hot Springs fault. Although test holes were bored or drilled at 21 sites, control is not sufficient to determine the northward or southward extent of the cooler parts of the thermal area, and the inferred temperature pattern on the eastern side is based on only one test hole, DH-10. Hot water may rise along some of the faults other than the main Hot Springs fault, but the available data are insufficient to confirm or deny this possibility.

Temperatures near the fault in sec. 12, T. 22 N., R. 26 E. and in parts of the adjacent sections to the north and south probably exceed 120°C at a depth of 30 m. Boiling probably occurs within much of this area. (Owing to high temperatures, most of the test holes in the hottest area were not bored or drilled to as deep as 30 m, and the temperatures shown on figure 39 are extrapolated to 30 m, using either the gradients near the bottom of the holes or the boiling point vs. hydrostatic-depth curve where appropriate.)

Temperature profiles in several test holes west of the hottest part of the thermal area indicate that hot water moves westward from the Hot Springs fault through shallow aquifers. This pattern of movement is much more prominent in the northern part of the area, north of the southern edge of sec. 12, T. 22 N., R. 26 E., than it is to the south.

Heat Discharge

Before attempts at development by geothermal test wells in the early 1960's, heat was discharged from the Brady's Hot Springs hydrothermal system by convection as springflow, as well as by conduction through near-surface materials, convection as steam discharge, radiation from warm ground, and evaporation from pool surfaces and moist ground. Springflow



EXPLANATION



Line of equal temperature at a depth of 30 m below the land surface
Dashed where uncertain. Interval 5, 10, and 20 degrees Celsius

● 30.2

Test hole

Number is temperature, in degrees Celsius, at a depth of 30 m below the land surface

Figure 39.---Map of Brady's Hot Springs thermal area showing temperature at a depth of 30 metres, 1973.

has now ceased, but discharge of steam and heated air continues. In the computation of heat discharge from the thermal area, it is assumed that all heat is discharged by conduction through near-surface materials and by convection as steam. Radiative heat discharge may be substantial, as suggested by snowmelt patterns (fig. 37), but data are not available to make a reasonable estimate of this quantity. The estimate of net heat discharge from the system is therefore believed to be conservatively low.

Conductive heat discharge.-- Conductive heat discharge is estimated by both methods described in the section, "Estimates of heat discharge". Both estimates are highly uncertain, because the eastward, northward, and southward extent of the cooler parts of the thermal area is unknown. Unlike most of the other thermal areas described in this report, the estimate of heat discharge by method B is believed to be no more reliable than that by method A at Brady's Hot Springs, principally because of the great extent of the hottest area, where conductive heat flow is difficult to estimate.

Total conductive heat discharge is estimated by method A, using the following data:

Boundary of thermal area is 15°C isotherm at 30 m depth (42.9 km²)

Mean-annual temperature at land surface = 11°C (about the average of the long-term mean-annual air temperatures at Fallon (table 6) and Lahontan Dam in the nearby Carson Desert)

Harmonic-mean thermal conductivity 0-30 m = 2.5×10^{-3} cal cm⁻¹ s⁻¹

°C⁻¹ (the average of the values computed from the logs of 20 test holes).

Using the values above, the total conductive heat discharge estimated by method A is 7.8×10^6 cal s⁻¹. Derivation of the estimate is given in table 27.

Table 27.--Estimate of conductive heat discharge from Brady's Hot Springs hydrothermal system on the basis of method A described in the text.

Temperature range (°C)	Geothermal mean temperature (°C)	Thermal gradient ^{1/} ($\times 10^{-3} \text{ } ^\circ\text{C cm}^{-1}$)	Heat flow ^{2/} ($\times 10^{-6} \text{ cal cm}^{-2} \text{ s}^{-1}$)	Area ($\times 10^{10} \text{ cm}^2$)	Heat discharge ($\times 10^6 \text{ cal s}^{-1}$)
15-20	17.3	2.1	5.3	21.83	1.16
20-30	24.5	4.5	11	9.95	1.09
30-40	34.6	7.9	20	2.49	.50
40-60	49.0	13	32	2.73	.87
60-80	69.3	19	48	1.82	.87
80-100	89.4	26	65	1.63	1.06
100-120	109.5	33	82	1.28	1.05
> 120	128.5	39	98	1.20	1.18
Totals (rounded)				42.9	7.8

^{1/} Based on 11.0°C mean annual temperature at the land surface

^{2/} Based on harmonic-mean thermal conductivity of $2.5 \times 10^{-3} \text{ cal cm}^{-1} \text{ s}^{-1} \text{ } ^\circ\text{C}^{-1}$

Net conductive heat discharge is computed as the difference between the total and the "normal" conductive heat discharge. The "normal" heat flow is assumed to be 2 HFU on the basis of data developed for method B. The net heat discharge is then

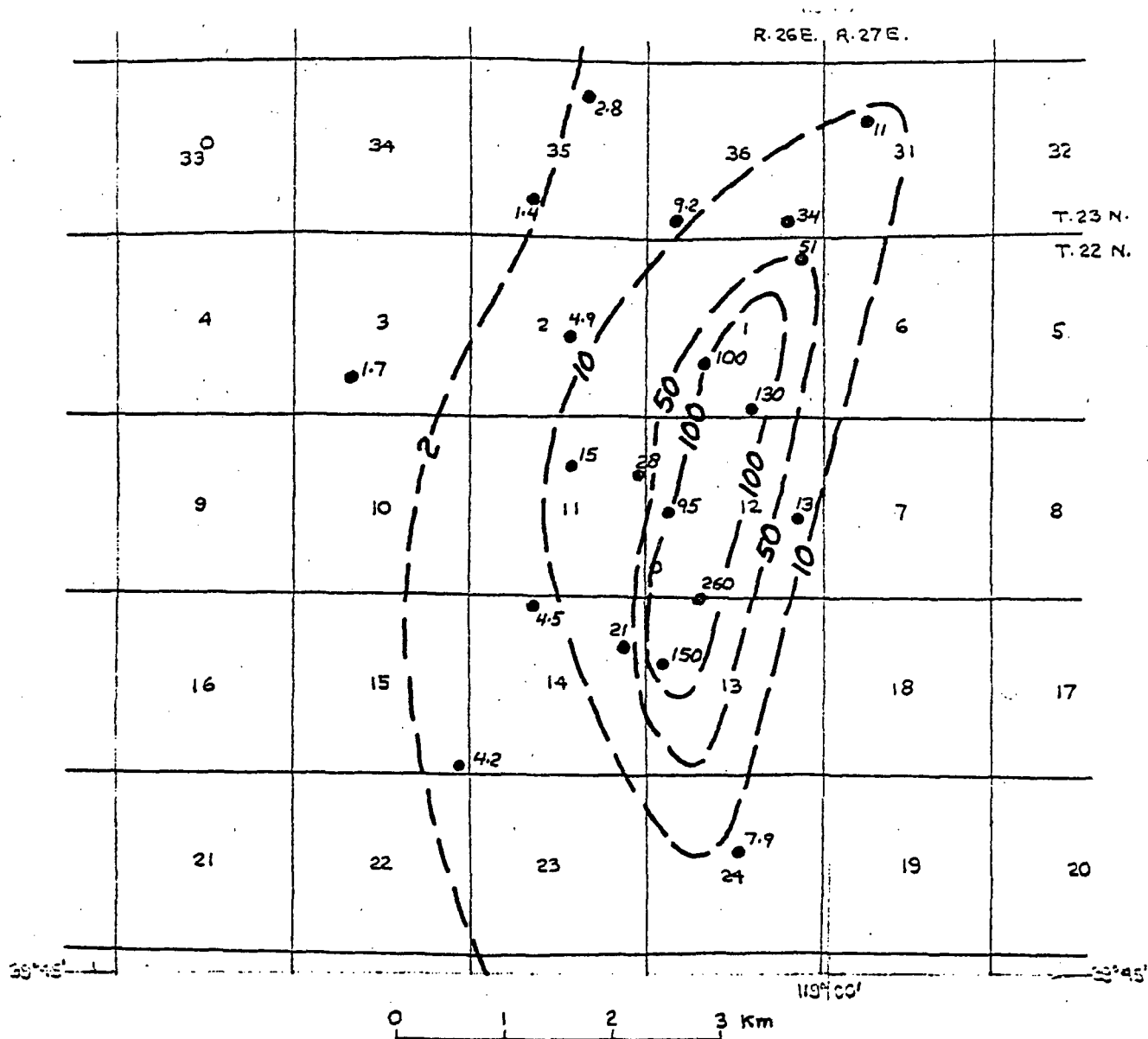
$$[7.8 \times 10^6 \text{ cal s}^{-1}] - [(2 \times 10^{-6} \text{ cal cm}^{-2} \text{ s}^{-1})(42.9 \times 10^{10} \text{ cm}^2)] = 6.9 \times 10^6 \text{ cal s}^{-1}$$

Total conductive heat discharge estimated by method B amounts to $8.5 \times 10^6 \text{ cal s}^{-1}$, slightly more than the estimate by Method A. Heat-flow values used in the estimate are shown on figure 40, and the derivation of the estimate is given in table 28.

Net conductive heat discharge by method B is estimated using an assumed "normal" heat flow of 2 HFU, slightly more than the heat flow computed for two of the test holes believed to be outside the thermal area (fig. 40). The estimate of net conductive heat discharge is then

$$[8.5 \times 10^6 \text{ cal s}^{-1}] - [(2 \times 10^{-6} \text{ cal cm}^{-2} \text{ s}^{-1})(55.3 \times 10^{10} \text{ cm}^2)] = 7.4 \times 10^6 \text{ cal s}^{-1}$$

Largest elements of uncertainty in the estimate are the extent of the area of relatively low heat flow (2-10 HFU) and the heat flow in the hottest area. In deriving the estimate, it is assumed that the total area having a heat flow of 2-10 HFU is three times the area between the 2 and 10 HFU isograms on the west side of the thermal area between the north edge of secs. 35 and 36, T. 23 N., R. 26 E. and the south edge of secs. 22 and 23, T. 22 N., R. 26 E., where data are available. It is also assumed that the average heat flow in the area enclosed by the 100 HFU isogram is 141 HFU--the geometric mean of 100 and 200 HFU. However, extent of the snowmelt observed in January 1974 suggests that the average heat flow within this area may be much greater than that used in deriving the estimate.



EXPLANATION

-----50-----

Line of equal heat flow in HFU ($\times 10^{-6} \text{ cal cm}^{-2} \text{ s}^{-1}$)

• 28
Test hole

Number is estimated heat flow, in HFU ($\times 10^{-6} \text{ cal cm}^{-2} \text{ s}^{-1}$)

Figure 40.--Map of Brady's Hot Springs thermal area showing estimated near-surface conductive heat flow.

Table 28 .--Estimate of conductive heat discharge from Brady's Hot Springs hydrothermal system on the basis of method B described in the text

Range in heat flow (HFU)	Geometric-mean heat flow (HFU)	Area ($\times 10^{10}$ cm ²)	Heat discharge ($\times 10^6$ cal s ⁻¹)
2 - 10	4.5	42.5	1.9
10 - 50	22.4	8.5	1.9
50 - 100	70.7	1.9	1.3
> 100	141 ^{1/}	2.4	3.4
Total		55.3	8.5

^{1/} Assumed range, 100 - 200 HFU

Convective heat discharge as steam.--The rate of convective heat discharge as steam cannot be estimated within narrow limits. However, a crude estimate can be made by assuming that all the pre-development springflow (mass flow rate) is now discharged as steam. The actual rate of steam discharge probably is less than this estimate, but the error introduced may be offset, at least in part, by the omission of heat discharge by radiation and evaporation from the estimates of net heat discharge.

As discussed earlier, the springflow before development may have been about 1.3 l s^{-1} (20 gpm). Heat discharge as steam is then estimated using the following data:

$$\begin{aligned} \text{Steam discharge (mass flow rate)} &= (1.3 \times 10^3 \text{ cm}^3 \text{ s}^{-1})(0.972 \text{ g cm}^{-3}) \\ &= 1.26 \times 10^3 \text{ g s}^{-1} = 4.0 \times 10^{10} \text{ g yr}^{-1} \end{aligned}$$

$$\text{Enthalpy of steam-water mixture at } 95^\circ\text{C} = 542 \text{ cal g}^{-1}$$

Heat discharge as steam is computed to be

$$\begin{aligned} (4.0 \times 10^{10} \text{ g yr}^{-1})(5.42 \times 10^2 \text{ cal g}^{-1}) &= 2.17 \times 10^{13} \text{ cal yr}^{-1} \\ &= 0.69 \times 10^6 \text{ cal s}^{-1} \end{aligned}$$

Net heat discharge from system.--Net heat discharge from the Brady's Hot Springs hydrothermal system is computed as the sum of the net conductive discharge and the convective discharge as steam

	($\times 10^6 \text{ cal s}^{-1}$)	
	<u>Method A</u>	<u>Method B</u>
Net conductive heat discharge	6.9	7.4
Convective heat discharge as steam	<u>.69</u>	<u>.69</u>
Total (rounded)	7.6	8.1

As explained above, the actual rate of net heat discharge probably exceeds both of these estimates, perhaps by a significant margin.

Water Discharge

Data are insufficient to estimate the discharge of water from the Brady's Hot Springs hydrothermal system, except by the heat-budget method.

The following data are used in deriving the estimate:

$$\text{Net heat discharge (method B)} = 8.1 \times 10^6 \text{ cal s}^{-1} = 2.56 \times 10^{14} \text{ cal yr}^{-1}$$

Reservoir temperature (test well data) = 200°C ; enthalpy of water =

$$204 \text{ cal g}^{-1}$$

Mean-annual surface temperature = 11°C ;
enthalpy of water =

$$\underline{11 \text{ cal g}^{-1}}$$

Net enthalpy of water in reservoir

$$193 \text{ cal g}^{-1}$$

Density of water at assumed discharge temperature
of 80°C = 0.972 g cm^{-3}

Density of water at assumed discharge temperature of 80°C = 0.972 g cm^{-3}

Water discharge is then

$$\frac{2.56 \times 10^{14} \text{ cal yr}^{-1}}{1.93 \times 10^2 \text{ cal g}^{-1}} \div (0.972 \times 10^6 \text{ g m}^{-3})$$
$$= 1.4 \times 10^6 \text{ m}^3 \text{ yr}^{-1}$$

Hypothetical Model of Hydrothermal-Discharge System

Presently available data indicate that all thermal-water discharge in the Brady's Hot Springs thermal area moves upward along a conduit system associated with the principal (Hot Springs) fault. Other faults in the area may transmit some thermal water, but data points are not spaced closely enough to confirm or deny this possibility. (See fig. 39) No water presently discharges at the land surface along the Hot Springs fault, although some steam escapes from fumaroles and irregular vents in secs. 1 and 12, T. 22 N., R. 26 E.

The temperature pattern (fig.39), the heat-flow pattern (fig.40), the configuration of the water table (fig.38), and vertical potential gradients all suggest that thermal water rises along the Hot Springs fault, in the segment approximately from the northeast corner of sec. 1 southward to the west-central part of sec. 13, T. 22 N., R. 26E.; then moves laterally (chiefly westward) in aquifers in unconsolidated deposits and in joints and other fractures in the underlying consolidated rocks. Temperature profiles in some of the test holes installed during this study show that much of the lateral movement of thermal water is within a few tens of metres of the water table, in the most permeable alluvial and lacustrine deposits.

As discussed earlier, data are insufficient to determine whether any of the faults east of the Hot Springs fault carry thermal-water upflow. If they do, temperatures east of the Hot Springs fault probably would be higher than those shown on figure 39. Near-surface conductive heat flow in this area also would be greater than that shown on figure 40.

Temperature of the rising thermal water is assumed to be at least 200°C on the basis of geothermal test-well data obtained in the early 1960's. Depth of circulation and source of the thermal water are not known. However, thermal gradients measured in shallow test holes west of the thermal area during this study suggest that conductive heat flow outside the area affected by thermal-water upflow and discharge into shallow aquifers may be no more than about 2 HFU (fig.40)--about average for the northern Basin and Range province. The implication is therefore clear that, unless a local crustal heat source is present beneath the eastern part of the thermal area, the thermal water must circulate to depths of several kilometres in order to attain the observed temperatures.

BUFFALO VALLEY HOT SPRINGS THERMAL AREA

Location

Buffalo Valley Hot Springs are in sec. 23, T. 29 N., R. 41 E., in western Lander County, Nev. The springs are in southeastern Buffalo Valley, 47 km by road southwest of Battle Mountain. They occupy a low mound near the foot of the slope on the southeast side of the valley at an altitude of about 1410 m above mean sea level. The springflow is undeveloped except as a source of drinking water for livestock. The area surrounding the springs has not been classified as a KGRA but is within lands classified as being valuable prospectively for geothermal resources.

Test Drilling

In the fall of 1973, the U. S. Geological Survey placed six drill holes and three auger holes in the hot springs area in order to determine the extent of the thermal area and to estimate discharge of heat and water from the hydrothermal system. All the test holes are within 1.8 km of the center of the spring mound. They range in depth from 24.8 to 47.9 m, and all but one, DH-9, are fitted with well points. Test hole DH-9 is entirely above the water table and is capped at the bottom and filled with water for temperature measurements. Data for all the test holes are given in table 29.

Geology

Exposed rocks and deposits near Buffalo Valley Hot Springs include tuff of middle Tertiary age, basalt of late Tertiary or early Quaternary age in the form of cinder cones and lava flows, and unconsolidated valley fill and spring deposits of Quaternary age. Areal extent of the geologic units mapped in this study is shown on figure 41

Table 29.--Data for U.S. Geological Survey test holes in the Buffalo Valley Hot Springs thermal area

Well number: Test holes 1-5 drilled during 9-12 October 1973, test holes 6-9 drilled during 25-27 October, 1973. Test holes 1 and 6-9 drilled using rotary rig; "Revert" mud used in wells 1 and 6-9; bentonite mud used in well 5. Test holes 2-4 drilled using solid-stem auger.

Depth: Depth completed, in feet below land-surface datum. Test holes 2-8 encountered only unconsolidated sedimentary deposits. In test holes 1 and 9, these deposits are underlain by basalt at 29.9 and 21.0 m, respectively.

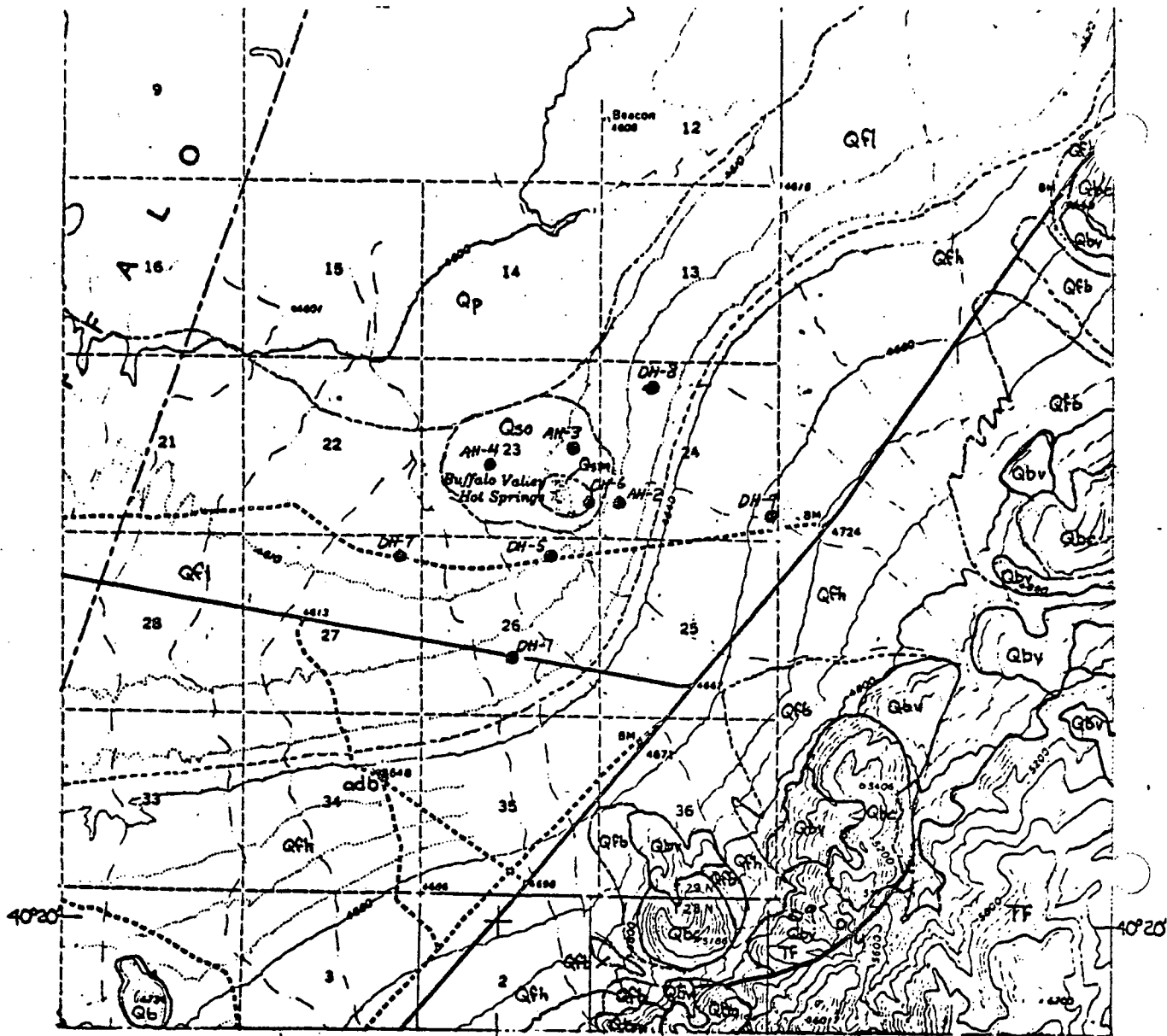
Type of completion: Casing type is indicated by "St" (3.8-cm nominal inside diameter steel) or "P" (5.1-cm nominal inside diameter PVC, topped by 2-m length of 5.1-cm steel casing). Casing capped and filled with water is indicated by "C". Casings with well-point screens at bottom are indicated by "Sc".

Depth to water table: Obtained from neutron (N) or gamma-gamma (G²) log.

Geophysical logs available: Gamma ("G"), gamma-gamma ("G²"), neutron ("N"), resistivity ("R"), and temperature ("T").

Well number	Location	Depth	Type of completion	Land-surface altitude (m)	Depth to water table			Static confined water level		Geophysical logs available
					Metres below land-surface datum	Source or data	Date	Metres below land-surface datum	Date	
BVDH-1	29/41-26dbc	32.55	P,Sc	1,409.4	4.4	N	73 11 08	5.44	73 11 08	G,G ² ,N,R,T
AH-2	-24cca	44.71	St,Sc	1,409.1	3.0	N	73 11 07	>+1.01	73 11 09	G,G ² ,N,T
AH-3	-23add	26.88	St,Sc	1,406.0	<1.2	G ²	73 11 06	.51	73 11 06	G,G ² ,N
AH-4	-23caa	35.05	St,Sc	1,404.2	4.3(?)	G ²	73 11 06	.51	73 11 06	G,G ² ,N
DH-5	-26aba	42.31	P,Sc	1,405.1	1.1	N	73 11 07	1.11	73 11 07	G,G ² ,N,T
DH-6	-23dda	47.85	St,Sc	1,408.2	<1 (?)	-	73 11 07	>+2.68	73 11 07	G
DH-7	-27aaa	45.11	P,Sc	1,404.5	<1 (?)	-	73 11 08	.52	73 11 08	G,G ² ,N
DH-8	-24bab	44.77	St,Sc	1,409.7	2.8	N	73 11 06	2.72	73 11 06	G,G ² ,N,T
DH-9	-24dda	24.78	St,C	1,429.5	(?)	-	--	--	--	G,G ² ,N,T

238



Base from U.S. Geological Survey Buffalo Springs 15-minute sheet

117°20' 0 2 3 km

Geology by F.H. Olmsted, 1973

Contour interval 40 feet. Dashed lines represent 10-foot contours. Datum is mean sea level

EXPLANATION



- | | | | |
|---|--|---|---|
| Qfh Qfb | Qfi | Qp | Qso Qsm |
| Alluvial-fan deposits
Qfh, heterogeneous deposits
Qfb, basalt detritus | Alluvial fan and lacustrine deposits | Playa deposits | Spring deposits
Qso, older deposits
Qsm, modern spring mound |
| Qbc | Qbv Qbn Qb | | |
| Basalt cinders | Basalt
Qbv, vesicular flows associated with cinder cones
Qbn, nonvesicular flows
Qb, vesicular to nonvesicular rock of uncertain association | | |
| TF |  |  | |
| Fish Creek Mountains Tuff | TERTIARY
U, upthrown side
D, downthrown side | Contact | |

Figure 41.—Geologic map of Buffalo Valley Hot Springs thermal area showing location of test holes.

The oldest unit exposed within the area of figure 41 is the Fish Creek Mountains Tuff of early Miocene age. Fission-track and potassium-argon ages indicate an age of 24.3 ± 0.7 m.y. (McKee, 1970). Outside the area of study, the Fish Creek Mountains Tuff unconformably overlies the Caetano Tuff of Oligocene age, various dark lavas and tuffaceous sedimentary rocks of Oligocene(?) age, and a granitic pluton of Jurassic(?) age. The granite is exposed within the drainage areas of intermittent streams that enter the mapped area from the east; boulders of granite are locally abundant on the alluvial fans east of the hot springs.

The Fish Creek Mountains Tuff is a large ash-flow sheet which erupted from the central part of the Fish Creek Mountains southeast of Buffalo Valley. As determined by McKee (1970), the tuff is rhyolitic, with recognizable phenocrysts of sanidine and quartz, ranges in thickness from about 30 m near the margins to about 900 m near the center of the mountains, and probably has a total volume of more than 300 km^3 . Along the southeast side of the mapped area, the tuff is light pink, gray, or yellowish-brown, contains abundant lithic and pumice fragments as well as crystals of quartz, sanidine, and biotite, is slightly to moderately welded, and is generally porous and vesicular.

Extruded from vents cutting the Fish Creek Mountains Tuff and older rocks are several basaltic cinder cones and associated lava flows. The cones appear fairly fresh and uneroded, but some are tens to hundreds of metres above the present western base of the Fish Creek Mountains. They probably predate the last faulting that elevated the Fish Creek Mountains relative to Buffalo Valley. The general northeasterly alignment of the cones, parallel to the base of the mountains and to at least one high-angle normal fault in the Fish Creek Mountains Tuff (see fig. 41), suggests extrusion of the basalt along a Basin and Range fault or fault zone.

Potassium-argon dating has recently established the age of the basalt as about 3 m.y. (E.D. McKee, oral commun., 1974),--either latest Pliocene or earliest Pleistocene, according to various time scales currently accepted.

The basalt is typically dark gray, or red where oxidized, highly vesicular, and locally contains abundant zeolites. Olivine is present, as well as pyroxene and plagioclase. Most samples examined in the field contain xenoliths of rhyolite tuff and xenocrysts of quartz and sanidine derived from the underlying Fish Creek Mountains Tuff and older tuffs and flows. Not all the basalt is vesicular. A dense, platy flow rock crops out at the southern edge of the mapped area (fig. 41). An isolated exposure of somewhat vesicular basalt at the southwest corner of the area, 6 km southwest of the hot springs, may be related to the cinder cones and flows to the east, but the correlation is uncertain. Vesicular basalt penetrated in two of the test holes, BV DH's 1 and 9, at depths of 29.9 and 21.0 m, respectively, probably represents the westward subsurface extension of flows exposed to the east. The thin alluvial cover on the flows at these sites attests to the slow rate of deposition along the east side of Buffalo Valley during the past 3 million years.

The unconsolidated valley fill consists of alluvial-fan deposits, lacustrine deposits, playa deposits, and spring deposits. Total thickness of these deposits is unknown, but gravity data (U.S. Geol. Survey, unpublished data, 1973) suggest that the fill is much thicker beneath central and west-central Buffalo Valley than it is on the east side, near the hot springs.

The alluvial fan deposits are grouped into two facies on figure 41: heterogeneous deposits, and basaltic detritus. Both facies are generally an ill-sorted mixture of gravel, sand, silt, and clay, which represent deposition by muddy water or mud flows during short-lived storm runoff from the Fish Creek Mountains. The heterogeneous deposits include abundant

tuff and some nonvolcanic detritus, as well as fragments of basalt derived from the cinder cones and flows on the east side of the valley. The basaltic detritus consists entirely or almost entirely of basalt clasts of various sizes in a matrix of sandy silt and clay.

At times during the late Pleistocene, Buffalo Valley was occupied by lakes, which have left their record as shorelines at several levels up to about 1,417 m above mean sea level. Below the top shoreline the alluvial-fan deposits have been reworked by lacustrine processes, which have left beach ridges, gravel bars, and fine sands and muds of the lake bottom. Lake-bottom deposits are recognized in some of the test holes as gray or greenish-gray chemically reduced clay and silt.

Playa deposits of Holocene age overlie the lacustrine deposits in central Buffalo Valley. The deposits resemble the lacustrine deposits, and the subsurface contact of the two units is vague and arbitrary. Salts have accumulated in the near-surface playa deposits, owing to evaporation of ground water, but wind has removed much of the salt crust in parts of the playa.

The spring deposits consist of clay, silt, and fine sand on the mound of Buffalo Valley Hot Springs, and a surrounding larger area of older spring deposits. The deposits are in large part calcareous; some of the hotter spring orifices are rimmed by travertine. No sinter has been observed in the spring deposits.

No fault is obviously associated with the hot springs, although a northeast-trending Basin and Range normal fault was mapped in the mountains to the east (fig. 41), and the linear pattern of the basaltic cinder cones and associated lava flows suggests a northeast-trending fault or fault zone. A fault or faults having a similar trend may be present beneath the springs or between the springs and the mountains to the east. Delineation of such possible features would require the use of various surface geophysical techniques and test drilling.

Hydrology

The relatively small discharge of thermal water in the Buffalo valley Hot Springs area doubtless is fed by precipitation. The deep-circulating thermal ground water may have originated as recharge in the Fish Creek Mountains, east and southeast of the thermal area. No great distance of lateral movement seems necessary for the thermal water.

Sedimentary deposits on the valley floor adjacent to the hot springs are saturated at depths of 3 m or less. As land-surface altitude increases to the east and south, water depths increase also: at well DH-9, 1.7 km east of the springs, the depth to water exceeds 25 m; and at stock well 29/41-34adb, 3.2 km southwest of the springs, the depth to water is about 11 m.

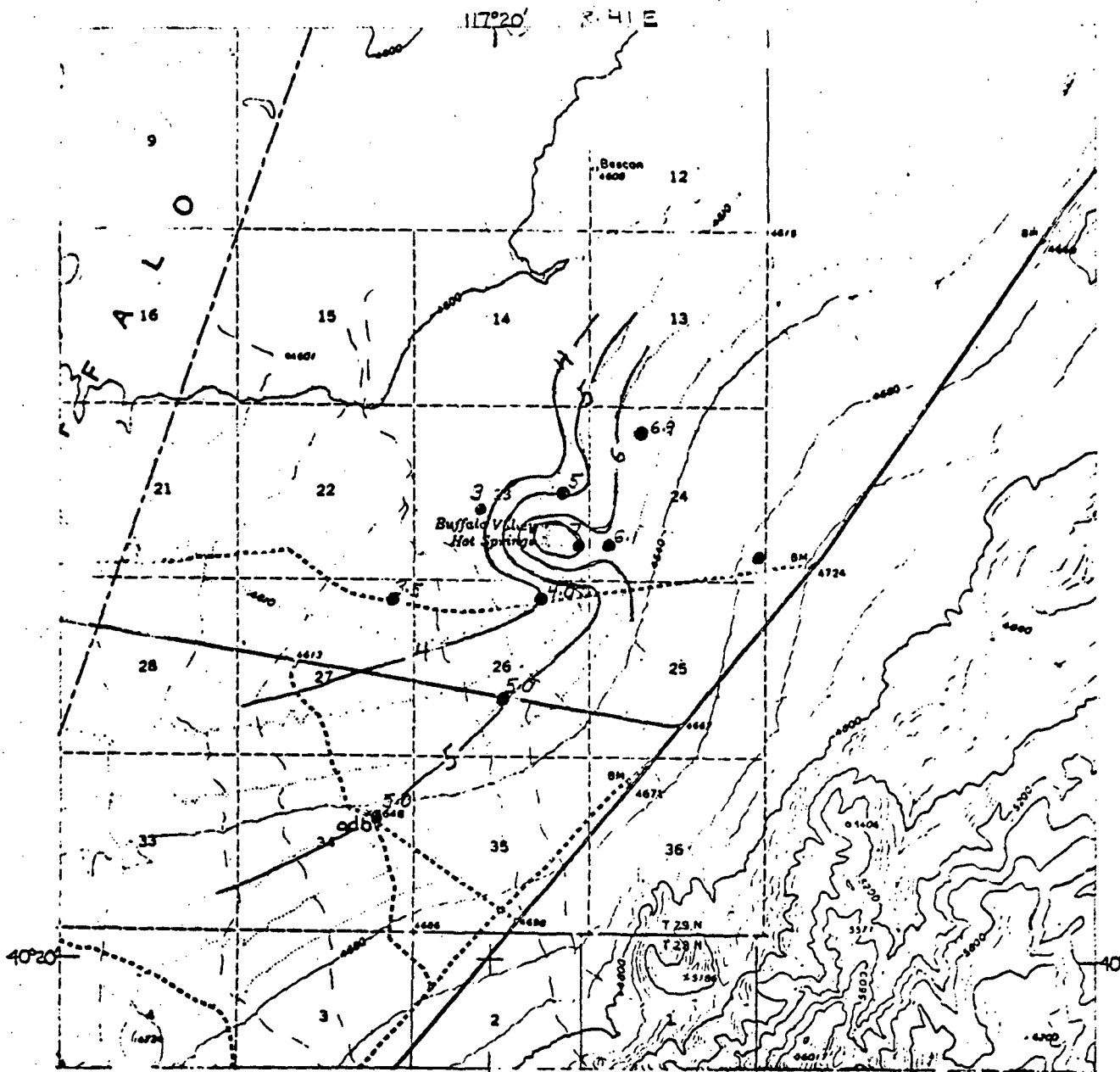
Adjacent to the springs, the regional water table is almost flat, as shown in figure 42. Directions of movement for the nonthermal ground water are generally northwestward, from the upland recharge areas toward the valley floor. Superimposed on this regional flow system is an area of upwelling thermal water evidenced at land surface by the springs. The resulting mound of hot water is due in part to true artesian conditions, and in part to thermo-artesian conditions, but the relative magnitude of the two components is unknown.

Nonthermal ground water discharges at the land surface by evaporation and transpiration. Thermal water also is dissipated by these mechanisms, and in addition it discharges as springflow. Estimates of total thermal-water discharge are given in a later section.

The Hot Springs

Buffalo Valley Hot Springs occupy a low mound about 450 m in diameter and about 3.5 m in altitude above the surrounding valley floor.

The number of active or recently active springs exceeds 200. The springs differ considerably in appearance: some are merely damp, grass-filled depressions; others feed pools as large as 2 m in diameter



Base from U. S. Geological Survey Buffalo Springs 15-minute sheet. Contour interval 40 feet. Dashed lines represent 10-foot contours. Datum is mean sea level.



EXPLANATION

— 4 —
Water-table contour

Shows altitude above a datum 1,400 m above mean sea level. Contour interval 1 metre

● 6.9

Test hole

Number is altitude of water table, in metres, above a datum 1,400 m above mean sea level

Figure 42.--Map of Buffalo Valley Hot Springs thermal area showing configuration of water table, fall 1973.

(the average pool diameter may be about 0.5 m); and others issue from travertine mounds. Few of the springs yield much water. Only one orifice yields more than about 0.1 l s^{-1} , and most yield less than 0.01 l s^{-1} . The combined flow of all springs in October 1973 may have been on the order of only 0.6 l s^{-1} . Measured orifice-throat temperatures of flowing springs range from 31° to 79°C .

Chemical Character of Springflow

The general chemical character of water from Buffalo Valley Hot Springs is indicated by the analysis from Mariner and others (1974, p. 12) listed in table 1. The dissolved solids, which are dominated by sodium and bicarbonate, total about 960 mg l^{-1} . The silica geothermometer indicates a reservoir temperature of 125°C (table 1; from Mariner and others, 1974, p. 18).

Specific-conductance data for the flow from four of the principal orifices (table 30, fig. 43) indicate only a small range in salinity from spring to spring.

The thermal ground water is chemically different from the non-thermal water of nearby well 29/41-34adb (3.2 km southwest of the springs; $16\frac{1}{2}$ m deep; water temperature 14.4°C after 30 minutes pumping). The chemical contrast is shown by the following data:

Source	Specific conductance (micromhos)	Chloride (mg/l)
Hot spring	$\sim 1,500$	29
Well 29/41-34adb	914	161

Table 30.--Temperature, discharge, and specific conductance of flow
from individual orifices at Buffalo Valley Hot Springs,
5 August, 1974.

Orifice (fig. 52)	Temperature (°C)	Estimated discharge (litres per second)	Specific conductance (micromhos per cm at 25°C)
1	78.8	<0.006	1,460
9	70.0	< .006	1,480
31	71.6	< .013	1,470
177	71.8	< .003	1,440

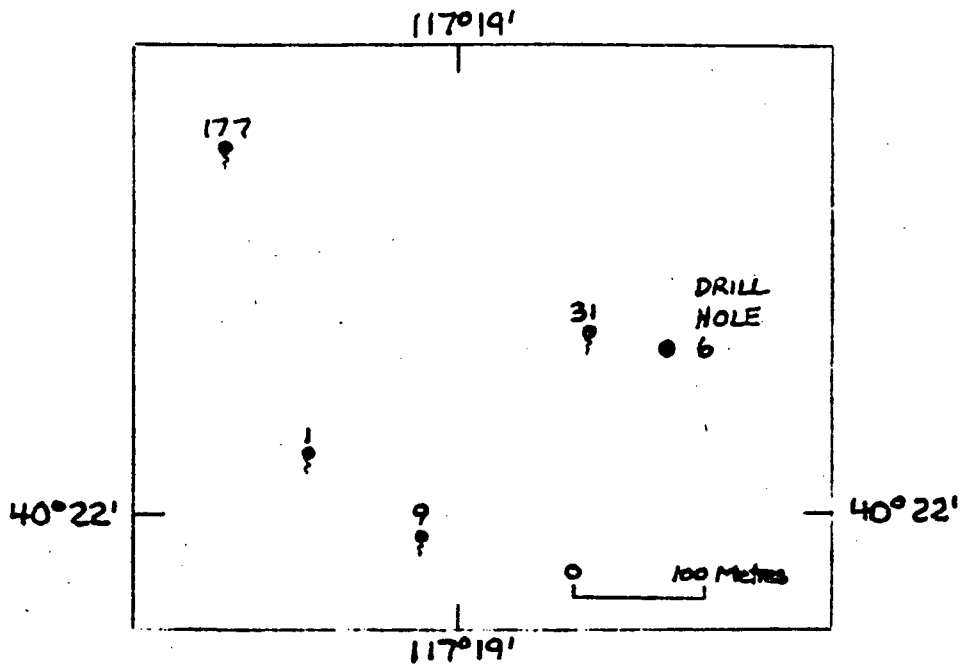


Figure 43.--Sketch map of part of Buffalo Valley Hot Springs mound
 showing location of orifices sampled in August 1974.

Subsurface Temperature Distribution

The distribution of temperature at a depth of 30 m below the land surface, as measured in the test holes in the fall of 1973, is shown in figure 44. The general shape of the thermal area is fairly well defined, but the configuration of the 15°C isotherm is uncertain, except southwest of the hot springs. More data especially are needed to determine the northerly and easterly extent of the thermal area.

The striking feature of the temperature pattern is the small extent of the nearly circular area centered at the hot springs where the temperatures are above 30°C, and the general asymmetry of the cooler part of the thermal area where temperatures are between 15°C and 30°C. Alternative explanations of the observed temperature patterns are given later, in the section "Hypothetical model of hydrothermal-discharge system."

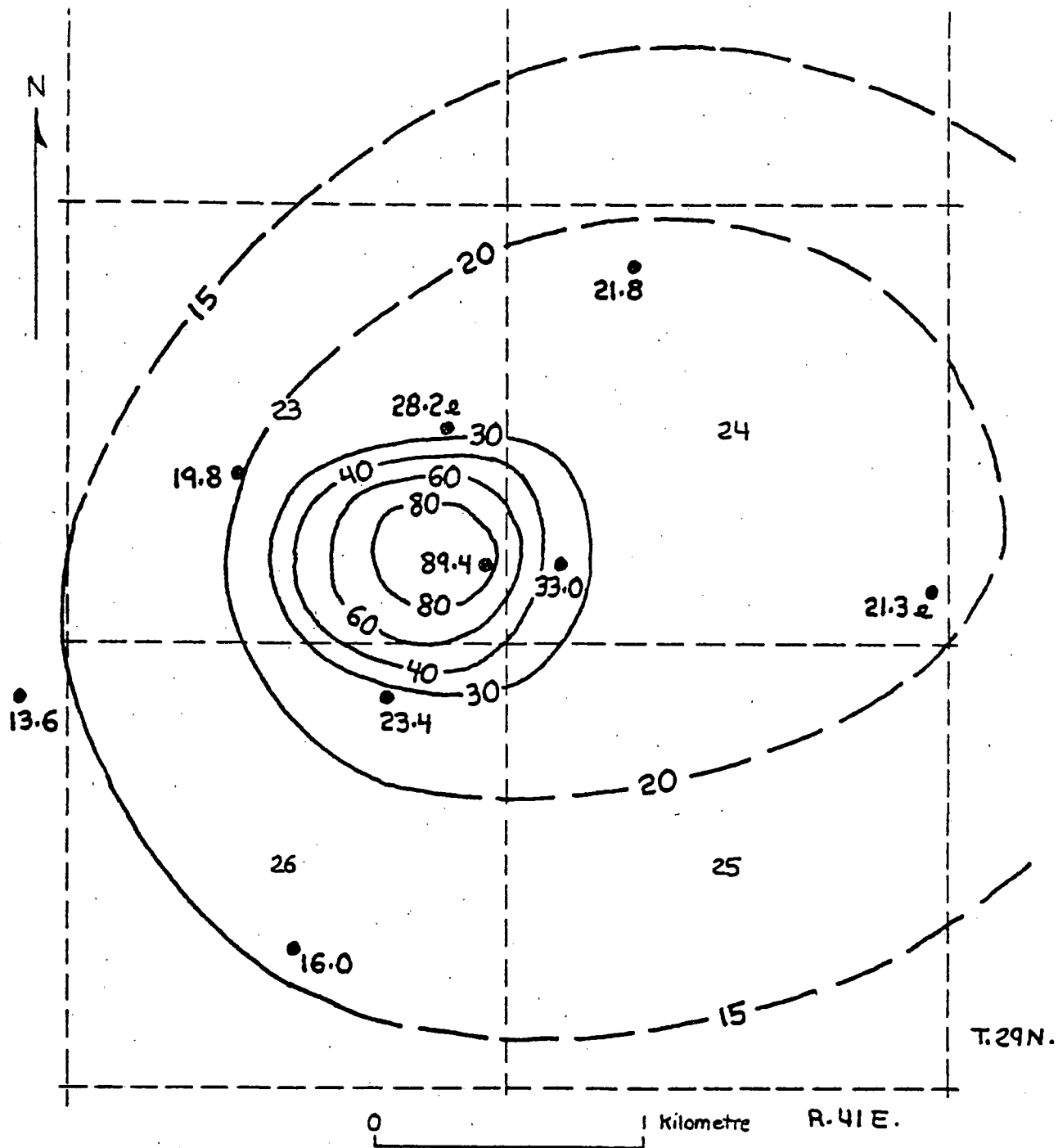
Heat Discharge

Heat discharge from the Buffalo Valley hydrothermal system is chiefly by conduction through near-surface materials; convective discharge as springflow is small, and little or no heat is discharged as steam.

Conductive heat discharge.--The conductive heat discharge that results from convective upflow of thermal water is estimated by methods A and B described in the section, "Estimates of heat discharge." Both estimates are uncertain because of the paucity of temperature and thermal-gradient data in most of the outer part of the thermal area. The magnitude of conductive heat discharge near the hot springs also is difficult to estimate because the relative importance of conductive and convective heat discharge in the top 30 m is poorly understood in this area.

The following data are used in the estimate of total conductive heat discharge by method A:

Boundary of thermal area is 15°C isotherm at 30 m depth (12.2 km²)



Line of equal temperature at a depth of 30 metres
below the land surface
Interval 5, 10, and 20 degrees Celsius. Dashed where uncertain

● 16.0

Test hole

Number is temperature, in degrees Celsius, at a depth of 30 metres.
2, temperature extrapolated from thermal gradient above 30 metres

Figure 44.---Map of Buffalo Valley Hot Springs thermal area showing
temperature at a depth of 30 metres, fall 1973.

Mean-annual temperature at land surface = 9°C, about equal to the long-term mean-annual temperature at Winnemucca (table 6)

Harmonic-mean thermal conductivity 0-30 m = $2.5 \times 10^{-3} \text{ cal cm}^{-1} \text{ s}^{-1} \text{ } ^\circ\text{C}^{-1}$

(the average of values computed from the logs of 9 test holes)

Using the values above, the total conductive heat discharge estimated by method A is $1.38 \times 10^6 \text{ cal s}^{-1}$. Derivation of the estimate is given in table 31.

Net conductive heat discharge is computed as the difference between the total and the "normal" conductive heat discharge. The "normal" heat flow is assumed to be 4 HFU on the basis of data developed for method B. The net conductive heat discharge is then

$$\begin{aligned} [1.38 \times 10^6 \text{ cal s}^{-1}] - [(4 \times 10^{-6} \text{ cal cm}^{-2} \text{ s}^{-1})(12.2 \times 10^{10} \text{ cm}^2)] \\ = 0.89 \times 10^6 \text{ cal s}^{-1} \end{aligned}$$

Total conductive heat flow estimated by method B is $1.16 \times 10^6 \text{ cal s}^{-1}$, somewhat less than the estimate by method A. Heat-flow values used in the estimate are shown on figure 45, and the derivation of the estimate is given in table 32.

Net conductive heat discharge is estimated by method B, using an assumed "normal" heat flow of 4 HFU, slightly more than the heat flow computed for BV DH-7, believed to be just outside the thermal area (fig. 45). The estimate of net conductive heat discharge is then

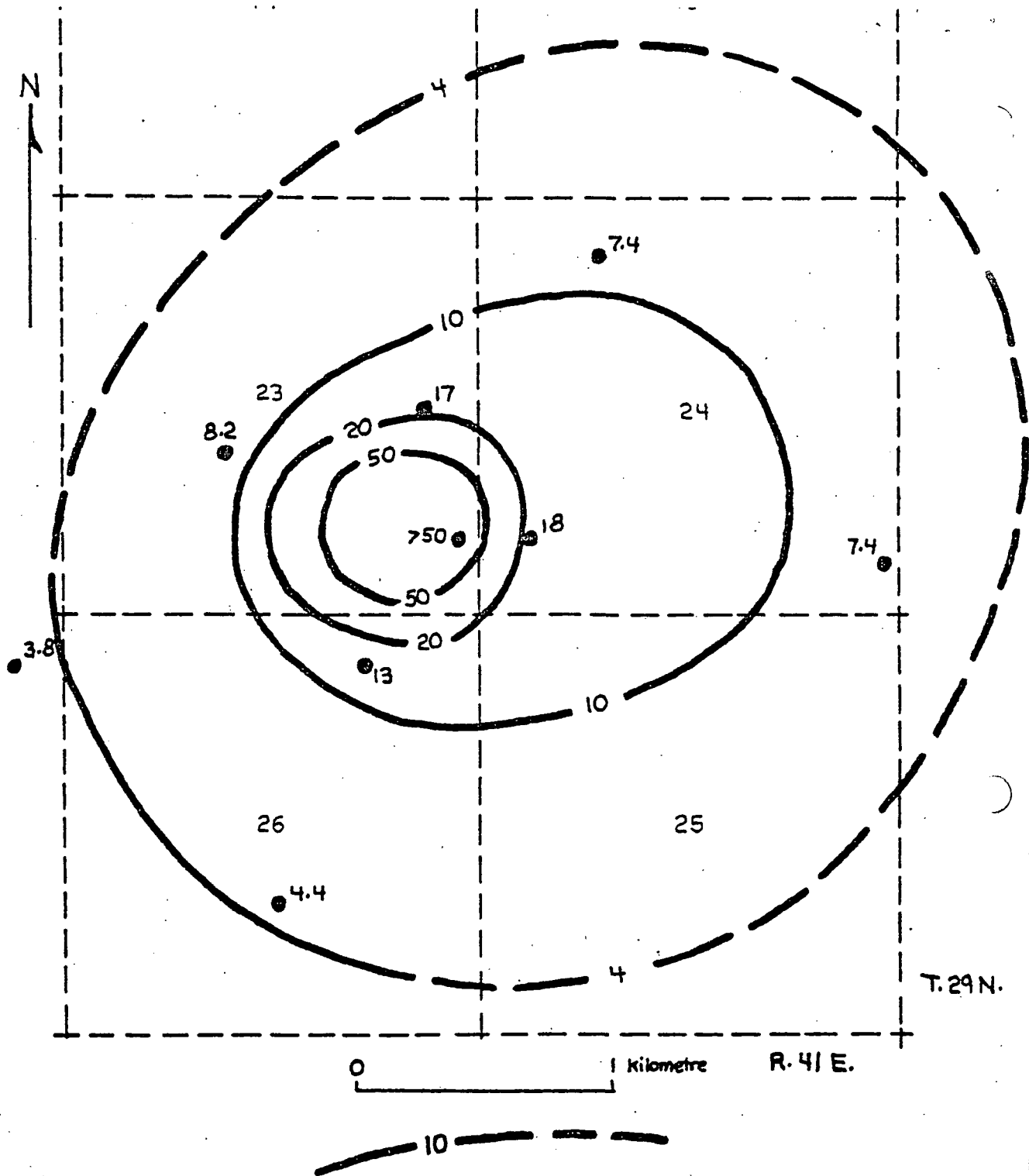
$$\begin{aligned} [1.16 \times 10^6 \text{ cal s}^{-1}] - [(4 \times 10^{-6} \text{ cal cm}^{-2} \text{ s}^{-1})(11.1 \times 10^{10} \text{ cm}^2)] \\ = 0.72 \times 10^6 \text{ cal s}^{-1}. \end{aligned}$$

Table 31. -- Estimate of conductive heat discharge from Buffalo Valley Hot Springs hydrothermal system on the basis of method A described in the text.

Temperature range (°C)	Geometric mean temperature (°C)	Thermal gradient ($\times 10^{-3}$ °C cm ⁻¹)	Heat flow ($\times 10^{-6}$ cal cm ⁻² s ⁻¹)	Area ($\times 10^{10}$ cm ²)	Heat discharge ($\times 10^6$ cal s ⁻¹)
15 - 20	17.3	2.8	7.0	7.24	0.51
20 - 30	24.5	5.2	13	3.97	.52
30 - 40	34.6	8.5	21	.35	.074
40 - 60	49.0	13	32	.26	.083
60 - 80	69.3	20	50	.20	.10
> 80	87.2	26	65	.15	.098
Totals (rounded)				12.2	1.38

1/ Based on 90°C mean annual temperature at the land surface

2/ Based on harmonic-mean thermal conductivity of 2.4×10^{-3} cal cm⁻¹ s⁻¹ °C⁻¹.



Line of equal conductive heat flow, in HFU ($\times 10^{-6} \text{ cal cm}^{-2} \text{ s}^{-1}$)

● 7.4

Test hole

Number is conductive heat flow, in HFU ($\times 10^{-6} \text{ cal cm}^{-2} \text{ s}^{-1}$)

Figure 45.—Map of Buffalo Valley Hot Springs thermal area showing near-surface conductive heat flow.

Table 32 ---Estimate of conductive heat discharge from Buffalo Valley Hot Springs hydrothermal system on the basis of method B described in text.

Range in heat flow (HFU)	Geometric-mean heat flow (HFU)	Area ($\times 10^{10} \text{ cm}^2$)	Heat discharge ($\times 10^6 \text{ cal s}^{-1}$)
4 - 10	6.3	8.18	0.52
10 - 20	14.1	2.23	.31
20 - 50	31.6	.41	.13
> 50	63.2 ^{1/}	.31	.20
Total		11.1	1.14

^{1/} Assumed range, 50 - 80 HFU

Convective heat discharge as springflow.--As stated earlier, the springflow in October 1973 may have been about 0.6 l s^{-1} . Weighted-average temperature is not known within narrow limits. The temperatures of the springs having the largest flows average about $70^\circ - 80^\circ\text{C}$. (See table 30.) For the purpose of the estimate of heat discharge, the following values are assumed:

Weighted average temperature of springflow = 72°C . Enthalpy = 72 cal g^{-1}

Mean-annual temperature at land surface = 9°C Enthalpy = 9 cal g^{-1}

Net enthalpy of springflow 63 cal g^{-1}

Spring discharge = $0.6 \text{ l s}^{-1} = 0.02 \times 10^6 \text{ m}^3 \text{ yr}^{-1}$

Density of water at $72^\circ = 0.977 \times 10^6 \text{ g m}^{-3}$

Heat discharge is then

$$\begin{aligned} & (0.02 \times 10^6 \text{ m}^3 \text{ yr}^{-1})(0.977 \times 10^6 \text{ g m}^{-3})(63 \text{ cal g}^{-1}) \\ & = 1.2 \times 10^{12} \text{ cal yr}^{-1} \\ & = 0.038 \times 10^6 \text{ cal s}^{-1} \end{aligned}$$

Net heat discharge from system.--Net heat discharge from the Buffalo Valley Hot Springs hydrothermal system is equal to the sum of the net conductive heat discharge and the convective heat discharge as springflow:

	$(\times 10^6 \text{ cal s}^{-1})$	
	Method A	Method B
Net conductive heat discharge	0.89	0.72
Conductive heat discharge as springflow	.038	.038
Total (rounded)	0.93	0.76

Water Discharge

Thermal ground water discharges from Buffalo Valley Hot Springs system as springflow, evaporation, transpiration, and perhaps as lateral subsurface flow away from the spring area. The magnitude of the discharge is estimated by both the water-budget and the heat-budget methods.

Water-budget method .-- Springflow may total about 0.6 l s^{-1} , or about $0.02 \times 10^6 \text{ m}^3 \text{ yr}^{-1}$. The estimation of evaporation plus transpiration is difficult, primarily because the areas actually fed by thermal ground water are unknown. Figure 45 shows the distribution of phreatophytes in the hot springs area. For lack of positive information, it is assumed that the spring mound and the area of dense to very scattered saltgrass and rabbitbrush surrounding it are fed by dominantly thermal ground water. Table 33 gives estimates of evaporation and transpiration based on this assumption.

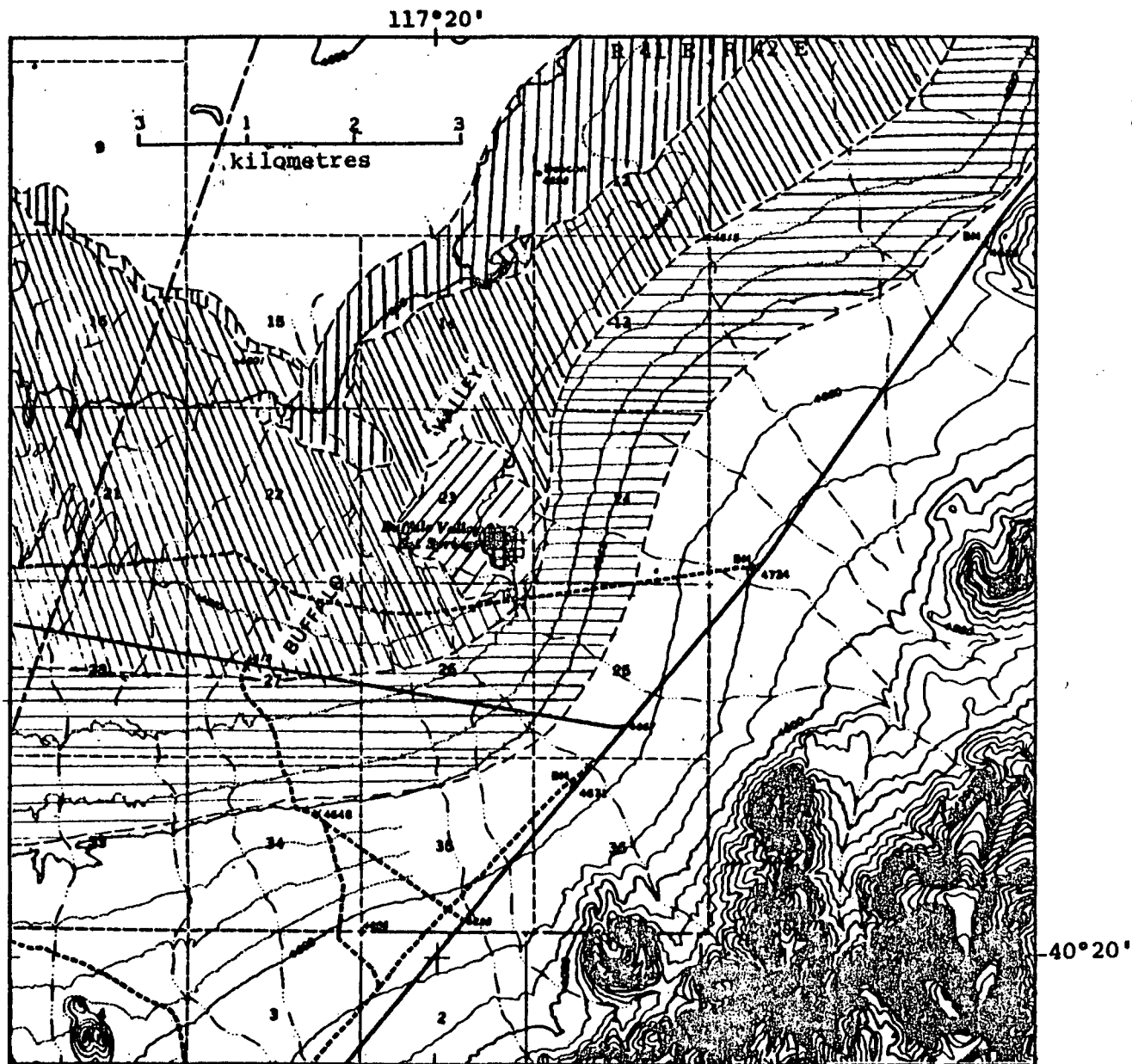
Because no springflow leaves the mound, and because estimated water-surface evaporation is a small quantity, most of the springflow must percolate back into the ground and dissipate subsequently by phreatophytic transpiration and soil-surface evaporation. Therefore, the total in table 33, $0.17 \times 10^6 \text{ m}^3 \text{ yr}^{-1}$, represents the actual amount of thermal water believed to be discharged as springflow and evapotranspiration.

The quantity of thermal water that flows away from the hot-spring area in the subsurface cannot be estimated with available information.

Heat-budget method.--The following data are used in deriving the estimate of water discharge from the Buffalo Valley Hot Springs hydrothermal system by the heat-budget method:

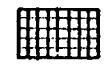
$$\text{Net heat discharge (method A)} = 0.93 \times 10^6 \text{ cal s}^{-1} = 2.94 \times 10^{13} \text{ cal yr}^{-1}$$

$$\text{(method B)} = 0.76 \times 10^6 \text{ cal s}^{-1} = 2.40 \times 10^{13} \text{ cal yr}^{-1}$$

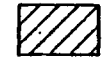


EXPLANATION

Phreatophytes Associated Wholly or in Large Parts with Thermal Ground Water



Saltgrass

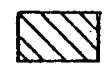


Saltgrass, with rabbitbrush

Phreatophytes Associated with Dominantly Nonthermal Ground Water



Saltgrass



Saltgrass with greasewood and (or) rabbitbrush



Greasewood

Phreatophyte mapping by
A. S. VanDenburgh, 1973

Figure 46.-- Map of Buffalo Valley Hot Springs are showing distribution of phreatophytes.

Table 33.--Estimated average annual evaporation and transpiration of
dominantly thermal ground water at Buffalo Hot Springs

Type of water loss	Area ($\times 10^3 \text{ m}^2$)	Depth to water (m)	<u>Evapotranspiration</u>	
			(m yr ⁻¹)	($\times 10^6 \text{ m}^3 \text{ yr}^{-1}$)
Water-surface evaporation	0.04	0	<u>a</u> /12	<0.001
Transpiration by dense to scattered saltgrass, plus soil-surface evaporation	120	0-1	.18	.022
Transpiration by moderately dense to very scattered saltgrass with or without scattered rabbitbrush, plus soil-surface evaporation	1,260	$\frac{1}{2}$ -3	.12	.15
Total (rounded)	1,380	--	--	.17

a. Adjusted for elevated temperature, assuming an average water-surface temperature of 40°C.

Reservoir temperature (table 1) = 125°C Enthalpy of water = 125 cal g⁻¹

Mean-annual surface temperature = 9°C Enthalpy of water = 9 cal g⁻¹

Net enthalpy of thermal water at source = 116 cal g⁻¹

Density of water at assumed discharge temperature of 72°C = 0.977 g cm⁻³

Water discharge is then

$$\left(\frac{2.94 \times 10^{13} \text{ cal yr}^{-1}}{1.16 \times 10^2 \text{ cal g}^{-1}} \right) \div (0.977 \times 10^6 \text{ g m}^{-3}) = 0.26 \times 10^6 \text{ m}^3 \text{ yr}^{-1}$$

using the heat-discharge estimate by method A, or

$$\left(\frac{2.40 \times 10^{13} \text{ cal yr}^{-1}}{1.16 \times 10^2 \text{ cal g}^{-1}} \right) \div (0.977 \times 10^6 \text{ g m}^{-3}) = 0.21 \times 10^6 \text{ m}^3 \text{ yr}^{-1}$$

using the heat discharge estimate by method B.

Comparison of heat-budget and water-budget estimates.--The estimates of thermal-water discharge by the heat-budget method, $0.26 \times 10^6 \text{ m}^3 \text{ yr}^{-1}$ (using heat-discharge estimate by method A) and $0.21 \times 10^6 \text{ m}^3 \text{ yr}^{-1}$ (using heat-discharge estimate by method B), exceed that by the water-budget method, $0.17 \times 10^6 \text{ m}^3 \text{ yr}^{-1}$, by perhaps significant margins. The heat-budget estimate based on method B is believed to be the most reliable of the three estimates. The water-budget estimate is believed to be too small for two principal reasons: (1) lateral outflow of thermal ground water is not included; (2) the area of phreatophytes supported by thermal water probably is greater than used in the estimate. Alternatively, other errors in all three estimates could account for the differences. More data are needed to resolve the discrepancies.

Inferred Nature of Hydrothermal System

The nature of the Buffalo Valley Hot Springs hydrothermal system is even more enigmatic than that of the other systems studied. Heat flow outside the thermal area seems to be greater than normal for the northern

Basin and Range province. Temperature of the thermal reservoir indicated by the silica-quartz geothermometer, 125°C, is substantially less than that of the other systems; depth of circulation of the thermal water is correspondingly less if, as seems likely, the average thermal conductivity of the rocks overlying the reservoir is no greater than that of the other systems. Assuming an average thermal conductivity of $2\frac{1}{2}$ to $3\frac{1}{2} \times 10^{-3}$ cal cm⁻¹s⁻¹°C⁻¹ and an average heat flow of $3-4 \times 10^{-6}$ cal cm⁻¹s⁻¹ outside the thermal area, the depth of circulation would be only about 0.7-1.4 km. Materials at such depths might consist of valley fill or of Tertiary volcanic or sedimentary rocks of moderate porosity and permeability.

The hot springs are not obviously related to a fault having surface expression. However, the deep part of the conduit system that feeds the springs probably is along a fault or fault system. Distribution of temperatures at depths less than 50 m suggests a conduit system dipping steeply eastward or southeastward or, possibly, a conduit system that leaks laterally into aquifer toward the east or southeast. The upflow of thermal water from the reservoir is not rapid enough to maintain high temperature until the water boils. Heat of the rising water is lost by both conduction through the walls of the conduit system and mixing of thermal and nonthermal waters, but the relative magnitude of the two processes cannot be determined from present data.

INTERPRETATION AND EVALUATION OF FINDINGS

Recapitulation of Objectives

As outlined in the introduction, the objectives of the study were to (1) delineate areas of high heat flow associated with rising thermal ground water, (2) determine the nature of the discharge parts of the hydrothermal systems, (3) estimate heat discharge from the hydrothermal

systems, (4) estimate thermal-water discharge from the hydrothermal systems, and (5) obtain rough estimates of conductive heat flow outside areas of hydrothermal discharge, and (6) evaluate several investigative techniques that would yield the required information quickly and at relatively low cost..

Not all the techniques required for a comprehensive study of hydrothermal systems were evaluated or used. For example, recharge areas for the systems were not delineated; nor were determined the patterns of ground-water circulation through the systems, the location, extent and nature of the thermal reservoirs, or the complex chemical reactions of rocks and thermal fluids. Instead, attention was focused on the discharge parts of the systems, particularly on the natural discharge of heat and water. Not only is this last type of information easier to obtain than the other types mentioned above, but the findings of this study tend to confirm the inference made from geologic studies by Hose and Taylor (1974) that the natural rates of discharge of both heat and fluid may place severe constraints on the scale of economic development of the systems.

Delineation of Areas of High Heat Flow

Areas of high heat flow associated with rising thermal ground water were reasonably well delineated during the study. The following thermal areas were outlined by shallow test drilling: Stillwater; Soda Lakes-Upsal Hogback; Gerlach; Brady's Hot Springs; Leach Hot Springs; Buffalo Valley Hot Springs; and Sulphur Hot Springs. In addition, some information was obtained about thermal areas at Fly Ranch, Granite Ranch, and Double Hot Springs in the Black Rock Desert, and about parts of southern and central Carson Desert outside the Stillwater and Soda Lakes-Upsal Hogback thermal areas.

Not all the thermal areas were equally well delineated, however, The western extent of the Gerlach thermal area was not explored, owing to the difficulty of drilling in the rugged exposures of granodiorite in that part of the area. The north and south ends of the thermal area associated with Brady's Hot Springs were not defined, and the eastward extent also is poorly known. The thermal area associated with Sulphur Hot Springs was defined with fair accuracy, but the extent of a nearby subsurface hydrothermal-discharge system associated with the major Basin and Range fault west of the springs is unknown.

Shallow-temperature data appear to be adequate to identify and delineate hydrothermal systems in which the fluid discharges at the land surface or into shallow aquifers, at depths of less than, say, 100 m. However, information obtained from the southern Carson Desert suggests that test drilling much deeper than 50 m may be required to identify systems in which the near-surface thermal effects of convection of thermal water at depths of perhaps several hundred metres are masked by rapid circulation of overlying nonthermal ground water and by changes in the thermal regime caused by application of large amounts of irrigation water for many decades.

The extent of the thermal areas studied is given in table 34. A thermal area is defined as an area in which the near-surface conductive heat flow that results from convective upflow of thermal water is significantly greater than the conductive heat flow in the surrounding area unaffected by the upflow of thermal water. Different criteria for the boundaries are used for the various thermal areas, depending on the kind of data available. Boundaries based on heat-flow values used in estimates of heat discharge by method B described in the section, "Estimates

Table 34.--Extent of thermal areas studied in northern and central Nevada

Thermal area	Extent (km ²)	Assumed boundary
Stillwater	59.1	20°C isotherm at 30 m
Brady's Hot Springs	55.3	2 HFU isogram
Soda Lakes-Upsal Hogback	21.1	20°C isotherm at 30 m
Gerlach	20.3	4 HFU isogram
Sulphur Hot Springs	12.0	15°C isotherm at 30 m
Buffalo Valley Hot Springs	11.1	4 HFU isogram
Leach Hot Springs	8.0	15°C isotherm at 30 m

of heat discharge" are believed to be more reliable than boundaries based on temperature at 30 m depth used in estimates by method A. Thermal areas estimated by method A are generally too small.

Nature of Discharge Parts of Hydrothermal Systems

Only partial success was achieved in attaining the second objective of the investigation -- the determination of the nature of the discharge parts of the hydrothermal systems. Some of the systems studied--those at Gerlach, Brady's Hot Springs, Leach Hot Springs, Fly Ranch, and Double Hot Springs--clearly are associated with Basin and Range faults. These discharge systems appear to be steeply inclined conduits in or near the fault zones. Other systems--those at Stillwater, Soda Lakes-Upsal Hogback, and Sulphur Hot Springs--probably are associated with faults, but the faults are not obviously exposed at the springs or in the center of the thermal anomalies. Buffalo Valley Hot Springs are even less obviously related to a fault.

All the systems studied thus far appear to contain steeply inclined discharge conduits. Some conduits are very leaky, such as those at Stillwater, Soda Lakes-Upsal Hogback, Brady's Hot Springs, and Gerlach. Others such as those at Leach, Sulphur, and Buffalo Valley Hot Springs, appear to leak at only small to moderate rates, at least in the upper 50 m.

Further studies of discharge systems are needed, using surface geophysical methods, additional chemical sampling, additional test drilling (both shallow and deep), very shallow temperature measurements, aerial photography, and remote sensing.

Summary of Heat-Discharge Estimates

The net heat discharge--that is, the heat discharge that results from convective upflow of thermal water--was estimated for all the systems for which sufficient shallow subsurface temperature and hydrogeologic data were obtained. The surface or near-surface heat discharge from most of the systems includes three major components; (1) conduction through near-surface materials; (2) convection by springflow; and (3) convection by steam discharge.

Relatively crude estimates of near-surface conductive heat discharge were made by method A, which uses the temperatures measured at a depth of 30 m in the test holes. In four of the seven areas, more refined estimates were also made by method B, which uses the conductive thermal gradients in the saturated zone. Virtually all the net heat discharge is conductive in the Stillwater and Soda Lakes-Upsal Hogback systems, which have no springs associated with them.

The net heat discharge includes convection by springflow in the Gerlach, Leach Hot Springs, Sulphur Hot Springs, and Buffalo Valley Hot Springs hydrothermal systems and by steam discharge in the Brady's Hot Springs, Gerlach, Leach Hot Springs, and Sulphur Hot Springs systems.

The estimates of net heat discharge are summarized in table 35. Heat discharge from the Steamboat Springs hydrothermal system, estimated by White (1968), is included for comparison. The values range from less than 10^6 cal s⁻¹ to more than 10^7 cal s⁻¹. Because of errors inherent in the estimates, the actual heat discharges of the systems listed in table 35 may be within the range of one-half to twice as large as the estimates.

Table 35.--Estimates of net heat discharge from hydrothermal systems studied in northern and central Nevada.

(See text for explanation of methods of estimates.)

	Net heat discharge ($\times 10^6$ cal s ⁻¹)	Method of estimate of conductive heat discharge
Stillwater	14	A
Steamboat Springs (White, 1968)	11.8	
Brady's Hot Springs	7.6	A
	8.1	B
Gerlach	6.4	A
	5.4	B
Soda Lakes-Upsal Hogback	--	A
Leach Hot Springs	1.7	A
	1.7	B
Sulphur Hot Springs	1.6	A
Buffalo Valley Hot Springs	.93	A
	.76	B

Most of the hydrothermal systems studied are fairly small in terms of the total heat discharge. For example, Wairakei, a well-known hot-water geothermal system in New Zealand has a natural heat discharge of about 1 to 1.5×10^8 cal s⁻¹, according to several estimates summarized by White (1965). Fournier, White, and Truesdell (1967) estimated a heat discharge of 4.7×10^8 cal s⁻¹ from the Upper, Midway, and Lower Geyser Basins of Yellowstone National Park. Heat discharge from the Long Valley, California, geothermal system is about 4×10^7 cal s⁻¹, according to a recent estimate (M. L. Sorey, oral communication, 1974)

Summary of Water-Discharge Estimates

Estimates of thermal-water discharge were made for six of the seven systems for which heat discharge was estimated. Total water discharge (thermal and nonthermal) was also estimated for one of the systems (Gerlach). The results are summarized in table 36. Methods used in the derivation of the estimates are explained in the section, "Estimates of water discharge". An estimate of the water discharge from the Steamboat Springs hydrothermal system by White (1968) is included in table 36 for comparison.

Estimated discharge of thermal water from the systems studied ranges from about 0.2×10^6 m³ yr⁻¹ to about 3×10^6 m³ yr⁻¹. Errors in the estimates based on the heat-budget method probably are about the same proportionately as those of the heat discharge--that is, the true values may lie within the range of about one-half to double the estimated values. Where independent estimates by the water-budget were made, and the figures are in reasonably close agreement, as they are for Gerlach and Brady's Hot Springs systems, the range of probable values is believed to be smaller than it is for the estimates by the heat budget only.

Table 36.--Estimates of water discharge from hydrothermal systems studied in northern and central Nevada.

(See text for explanation of methods of estimates. Estimated reservoir temperatures based on the silica-quartz geothermometer)

System	Estimated reservoir temperature (°C)	Water discharge (x 10 ⁶ m ³ yr ⁻¹)		Method of estimate
		Total	Thermal	
Stillwater	159	--	3.1	Heat budget, A
Steamboat Springs (White, 1968)	>200	--	2.2	Water budget
Gerlach	171	1.8	1.5	Water budget
		--	1.3	Heat budget, A
		--	1.1	Heat budget, B
Brady's Hot Springs	>200	--		
		--	1.4	Heat budget, B
Leach Hot Springs	155	--	.46+	Water budget
		--	.38	Heat budget, A
		--	.38	Heat budget, B
Sulphur Hot Springs	186	--	.29	Water budget
		--	.29	Heat budget, A
Buffalo Valley Hot Springs	125	--	.17	Water budget
		--	.26	Heat budget, A
		--	.21	Heat budget, B

Interpretation of Estimates of Regional Conductive Heat Flow

Results obtained during this study from test holes 154-274 m deep in the Black Rock and Carson Deserts indicate that estimates of regional conductive heat flow may be obtained at low cost at sites in fine-grained lacustrine and playa deposits. At such sites, upflow of ground water is so slow that the effect of convection on the thermal gradient is minimal, and the observed gradients are essentially conductive.

Results to date also indicate that holes deeper than about 50 m probably are not required; valid heat-flow estimates can be made using thermal gradients in the depth range 15-50 m. However, corrected estimates require data on the rate of deposition of materials in this depth range.

On the basis of rather sparse data obtained to date, heat flow in both the Black Rock Deserts outside thermal areas appears to be about 1.5 - 2 HFU. Crude data from shallow (<50m) test holes outside the Brady's Hot Springs and Leach Hot Springs thermal areas indicate similar values. However, heat flow outside the thermal area at Buffalo Hot Springs may be about 3.5-4 HFU, and the heat flow outside the Sulphur Hot Springs thermal area in northern Ruby Valley may be about 3 HFU. The estimates for Buffalo Valley are within the upper range of more accurate values obtained in deep test holes near Battle Mountain, about 30 km to the northeast (See fig. 1; Sass and others, 1971). As interpreted by Sass and others (1971, fig. 4), Buffalo Valley is within the area of the Battle Mountain (heat-flow) high. Leach Hot Springs also is within the Battle Mountain high; the relatively low heat-flow values indicated in the shallow test holes outside the thermal area therefore are difficult to interpret. Deeper test drilling near Leach Hot Springs is needed to resolve this problem.

Significance of Estimates of Heat and Water Discharge

Allowing for the uncertainties in the estimates, most of the systems studied in northern and central Nevada appear to have small to moderate rates of discharge of heat and fluid (chiefly water). In the developed geothermal systems of the world, the quantity of heat and fluid stored in the thermal reservoir, and other reservoir characteristics such as depth, permeability, and temperature, are of far greater significance in terms of productive capacity than is the flux of heat and fluid through the system. In most of the Nevada systems, however, the scale of potential commercial development for production of electricity or for other uses may be constrained by the natural discharge of heat and water. The reason for this is that, in most of the systems, developments within economic drilling depths probably would be restricted to small tracts surrounding the conduits carrying the upflowing thermal water, and the rates at which fluid could be withdrawn by wells for long periods probably could not exceed the natural upflow. Greater rates of production almost certainly would result in decreases in both temperatures and pressures in the system. Hose and Taylor (1974) report that venting of test wells in the Beowawe, Nevada, system during the early 1960's caused large decreases in temperature and pressure, which provides dramatic empirical support of the conclusion above.

Theoretically, it would be possible, of course, to drill production wells outside the discharge systems. However, as discussed in the section, "Conceptual models of hydrothermal systems," depths of thermal reservoirs in areas of near-normal regional heat flow (≈ 2 HFU) might be as great as 5 or 6 km--beyond present economic drilling depths--and the permeability at these depths might be insufficient to allow adequate rates of fluid production.

Exceptions to the seemingly unfavorable prospects described above might occur at favorable sites within broad areas of high heat flow, such as the Battle Mountain heat-flow high. For example, Buffalo Valley Hot Springs, a system within the Battle Mountain heat-flow high, the natural discharge of heat and water is small. However, owing to the above-average heat flow over a considerable area, depth of circulation of thermal water might be one half or less that in areas of "normal" regional heat flow. The thermal reservoir might therefore be within shallower, more permeable rocks or deposits. Furthermore, the reservoir would more likely be within economic drilling depths.

Thus, it would appear that, in northern and central Nevada, the most favorable targets for exploration are within broad areas of high heat flow, such as the Battle Mountain high, rather than the relatively restricted convective thermal systems in areas of "normal" regional heat flow.

References

- Anctil, R. S., and others, 1960, Geology of the Brady Hot Springs and vicinity, Churchill County, Nevada: Southern Pacific Co. unpublished Mineral Resources Survey map.
- Axelrod, D. I., 1956, Mio-Pliocene floras from west-central Nevada: California Univ. Pubs. in Geol. Sci., v. 33, 321 p.
- Birkeland, P.W., Crandell, D.R., and Richmond, G.M., 1971, Status of correlation of Quaternary stratigraphic units in the western coterminous United States: Quaternary Research, v.1, no. 2, p.208-227
- Cohen, Philip, 1964, Preliminary results of hydrogeologic investigations in the valley of the Humboldt River near Winnemucca, Nevada: U.S. Geol. Survey Water-Supply Paper 1954, 59 p.
- Dinwiddie, G. A., and Schroder, L. J., 1971, Summary of hydraulic testing in and chemical analysis of water samples from deep exploratory holes in Little Fish Lake, Monitor, Hot Creek, and Little Smoky Valleys, Nevada: Central Nevada-40, U.S. Geol. Survey 474-90, prepared under Agreement no. AT(29-2)-474 for Nevada Operations Office, U.S. Atomic Energy Commission, 70 p.
- Dreyer, R. M., 1940, Goldbanks Mining District, Pershing County, Nevada: Univ. Nevada Bull., v. 34, no. 1, 38 p.
- Eakin, T. E., 1966, A regional interbasin ground-water system in the White River area, southeastern Nevada: Water Resources Research, v. 2, no. 2, p. 251-271.

Eakin, T. E., and Maxey, G. B., 1951, Ground water in Ruby Valley, Elko and White Pine Counties, Nevada, in Eakin, T. E., and others, Contributions to the hydrology of eastern Nevada: Nevada State Engineers Office, Water Resources Bull. 12.

Fournier, R. O., and Rowe, J. J., 1966, Estimation of underground temperatures from the silica content of water from hot springs and wet-stream wells: Am. Jour. Sci., v. 264, p. 685-697.

Fournier, R. O., White, D. E., and Truesdell, A. H., 1967, Discharge of thermal water and heat from Upper, Midway, and Lower Geyser Basins, Yellowstone Park [abs]: Geol. Soc. America Program 1967 Ann. Mtgs., p. 70.

Fournier, R. O., White, D. E., and Truesdell, A. H., 1974, Geochemical indicators of subsurface temperature, Part I, Basic assumptions: U.S. Geol. Survey Jour. Research, v.2, no.3, p. 259-262.

Hardman, George, 1936, Nevada precipitation and acreages of land by rainfall zones: Nevada Univ. Agr. Exp. Sta. mimeo. rept. and map, 10 p.

Hardman, George, and Mason, H. G., 1949, Irrigated lands of Nevada: Nevada Univ. Agr. Sta. Bull. 183, 57 p.

Harrill, J. R., 1969, Hydrologic response to irrigation pumping in Hualapai Flat, Washoe, Pershing, and Humboldt Counties, Nevada, 1960-67: Nevada Dept. Conserv. and Nat. Res., Water Res., Bul, No. 37, 75 p.

- Harrill, J. R., 1970, Water-resources appraisal of the Granite Springs Valley area, Pershing, Churchill, and Lyon Counties, Nevada: Nevada Dept. Conservation and Natural Resources, Water Resources-Reconnaissance Ser. Rept. 55, 36 p.
- Hose, R. K., and Taylor, B. E., 1974, Geothermal systems of northern Nevada: U.S. Geol. Survey Open-File Rept.
- Hunt, C. S., and Robinson, T. W., 1960, Possible interbasin circulation of ground water in the southern part of the Great Basin: Art. 123 in U.S. Geol. Survey Prof. Paper 400-B, p. B273-B274.
- Kohler, M. A., Nordenson, T. J., and Baker, D. R., 1959, Evaporation maps for the United States: U.S. Weather Bur. Tech. Paper 37. 13 p.
- Lee, C. H., and Clark, W. O., 1916, Report in Soda Lakes investigation, Truckee--Carson Project near Fallon, Nevada: U.S. Geol. Survey Rept., p. 657-706.
- Mariner, R. H., Rapp, J. B., Willey, L. M., and Presser, T. S., 1974, The chemical composition and estimated minimum thermal reservoir temperatures of the principal hot springs of northern and central Nevada: U.S. Geol. Survey open-file report, 32 p.

- Mathias, Ken E., 1974, Preliminary results of geothermal wells Mesa 6-1 and Mesa 6-2, East Mesa KGRA, Imperial Valley, California: Am. Geophys. Union Trans., v. 55, no. 4, p. 489.
- McKee, E.H., 1970, Fish Creek Mountains Tuff and volcanic center, Lander County, Nevada: U.S. Geol. Survey Prof. Paper 681.
- McKee, E.H., and Marvin, R.F., 1974, Summary of ages of Tertiary volcanic rocks in Nevada, Part IV; northwestern Nevada: Isochron West, no. 10, p. 1-6.
- Mifflin, M.D., 1968, Delineation of ground-water flow systems in Nevada: Desert Research Inst., Hydrol. and Water Res., Pub. no. 4, 111 p.
- Morrison, 1964, Lake Lahontan: geology of the southern Carson Desert, Nevada: U.S. Geol. Survey Prof. Paper 401, 156 p.
- Osterling, W.A., and Anctil, R.J., 1969, Geological and economic appraisal of geothermal steam resources at Brady Hot Springs, Nevada: Southern Pacific Co. rpt.
- Olmsted, F.H., and others, 1973, Sources of data for evaluation of selected geothermal areas in northern and central Nevada: U.S. Geol. Survey, Water-Resources Investigations 44-73, 78 p.
- Parasnis, D.S., 1971, Temperature extrapolation to infinite time in geothermal measurements: Geophys. Prospecting, v. 19, p. 612-614.
- Rush, F.E., 1972, Hydrologic reconnaissance of Big and Little Soda Lakes, Churchill County, Nevada: Nevada Dept. Conser. and Water Res., Water Resources - Information Ser. Rept. 11.

- Sammel, E. A., 1968, Convective flow and its effect on temperature logging in small-diameter wells: *Geophysics*, v. 33, no. 6, p. 1004-1011.
- Sass, J. H., Lachenbruch, A. H., Munroe, R. J., Greene, G. W., and Moses, T. H., Jr., 1971, heat flow in the Western United States: *Jour. Geophys. Research*, v. 76, no 26, p. 6376-6413.
- Scott, B. R., and others, 1971, Nevada's water resources: Nevada Water Planning Report 3, 87 p. and map.
- Sekioka, Mitsuru, Yuhara, Kozo, 1974, Heat flux determination in Geothermal Areas based on the heat balance of the ground surface: *Jour. of Geol. Phys. Research*, v. 79, no. 14, p. 2053-2058.
- Sinclair, W. C., 1963, Ground-water appraisal of the Black Rock Desert area, northwestern Nevada: Nevada Dept. Cons. and Nat. Resources, Ground-Water Resources-Reconnaissance Ser., Rept. 20, 32 p.
- Stabler, Herman, 1904, Report on ground waters of Carson Sink: U.S. Geol. Survey open-file rept., 49 p.
- Stacey, F. D., 1969, *Physics of the earth*: New York, John Wiley & sons, 324 p.
- Stewart, J. H. 1971, Basin and Range structure: A system of horsts and grabens produced by deep-seated extension: *Geol. Soc. America Bull.*, v. 82, p. 1019-1044

Tatlock, D. B., 1969, Preliminary geologic map of Pershing County, Nevada:
U.S. Geol. Survey open-file map, 1:200,000.

Thompson, G. A., and Burke, D. B., 1973, Rate and direction of spreading
in Dixie Valley, Basin and Range province, Nevada: Geol. Soc.
America Bull., v. 84, p. 627-632.

Toth, J., 1963, A theoretical analysis of ground water flow in small
drainage basins: Jour. Geophys. Research, v. 68, no. 16, p.
4795-4812.

U.S. Bureau of Reclamation, 1971, Geothermal resource investigations,
Imperial Valley, California: U.S. Bur. Recl.. Region 3, Status
Report, 47 p.

Waring, G. A. and others, 1965, Thermal springs of the United States
and other countries of the world--a summary: U.S. Geol. Survey Prof.
Paper 492, 383 p.

White, D. E., 1965, Geothermal energy: U.S. Geol. Survey Circ. 519, 17 p.

White, D. E., 1968, Hydrology, activity, and heat flow of the Steamboat
Springs thermal system, Washoe County, Nevada: U.S. Geol. Survey
Prof. Paper 458-C, 109 p.

White, D. E., Fournier, R. O., Muffler, L.J.P., and Truesdell, A. H.,
1974, Physical results of research drilling in thermal areas of
Yellowstone National Park, Wyoming: U.S. Geol. Survey Prof. Paper,
in press.

Winograd, I. J., 1962, Interbasin movement of ground water at the
Nevada Test Site, Nevada: U.S. Geol Survey Prof. Paper 450-C,
p. C108-C111.

Winograd, I. J., and Thordarson, William, 1968, Structural control of
groundwater movement in migeosynclinal rocks of southcentral Nevada,
in Nevada Test Site, Mem. 110, Ed. by E. B. Eckel, Geol. Soc. of
Am., Boulder, Colo., p. 35-48.